การสังเคราะห์และการสร้างแบบจำลองโมเลกุลของมัลติซินนาโมอิลแอนะล็อกชนิดใหม่เพื่อเป็นสารยับยั้งเอชไอวี-1 อินทิเกรส

นางสาววิภา ทัพเชียงใหม่

วิทยานิพนธ์นี้เป็นส่วนหนึ่งของการศึกษาตามหลักสูตรปริญญาวิทยาศาสตรดุษฎีบัณฑิต
สาขาวิชาเคมี ภาควิชาเคมี
คณะวิทยาศาสตร์ จุฬาลงกรณ์มหาวิทยาลัย
ปีการศึกษา 2553

SYNTHESIS AND MOLECULAR MODELING OF NEW MULTI-CINNAMOYL ANALOGS AS HIV-1 INTEGRASE INHIBITORS

Miss Wipa Tupchiangmai

A Dissertation Submitted in Partial Fulfillment of the Requirements
for the Degree of Doctor of Philosophy Program in Chemistry
Department of Chemistry
Faculty of Science
Chulalongkorn University
Academic Year 2010

Thesis Title	SYNTHESIS AND MOLECULAR MODELING OF NEW MULTI-CINNAMOYL ANALOGS AS HIV-1 INTEGRASE INHIBITORS
By	Miss Wipa Tupchiangmai
Field of Study	Chemistry
Thesis Advisor	Assistant Professor Yongsak Sritana-anant, Ph.D.
Thesis Co-advisor	Assistant Professor Somsak Pianwanit, Ph.D.
Thesis Co-advisor	Associate Professor Supinya Tewtrakul, Ph.D.

Accepted by the Faculty of Science, Chulalongkorn University in Partial Fulfillment of the Requirements for the Doctoral Degree

…….. Dean of the Faculty of Science
(Professor Supot Hannongbua, Dr.rer.nat.)

THESIS COMMITTEE

…….. Chairman
(Assistant Professor Warinthorn Chavasiri, Ph.D.)

…….. Thesis Advisor
(Assistant Professor Yongsak Sritana-anant, Ph.D.)

…….. Thesis Co-advisor
(Assistant Professor Somsak Pianwanit, Ph.D.)

…….. Thesis Co-advisor
(Associate Professor Supinya Tewtrakul, Ph.D.)

…….. Examiner
(Assistant Professor Aroonsiri Shitangkoon, Ph.D.)

…….. Examiner
(Sumrit Wacharasindhu, Ph.D.)

…….. External Examiner
(Professor Apichart Suksamrarn, Ph.D.)

วิภา ทัพเชียงใหม่ : การสังเคราะห์และการสร้างแบบจำลองโมเลกุลของมัลติซินนาโมอิลแอนะล็อกชนิดใหม่เพื่อเป็นสารยับยั้งเอชไอวี-1 อินทิเกรส. (SYNTHESIS AND MOLECULAR MODELING OF NEW MULTI-CINNAMOYL ANALOGS AS HIV-1 INTEGRASE INHIBITORS) อ.ที่ปรึกษาวิทยานิพนธ์หลัก: ผศ.ดร.ยงศักดิ์ ศรีธนาอนันต์, อ.ที่ปรึกษาวิทยานิพนธ์ร่วม: ผศ.ดร.สมศักดิ์ เพียรวณิช, รศ.ดร. สุภิญญา ติ๋วตระกูล, 142 หน้า.

ได้สังเคราะห์สารมัลติซินนาโมอิลแอนะล็อกบนฐานโครงสร้างเบนซีนที่มีหมู่แทนที่ 6 หมู่ จำนวน 21 ชนิด และทดสอบฤทธิ์ในการยับยั้งเอชไอวี-1 อินทิเกรส สารทั้งหมดเตรียมได้จากปฏิกิริยาควบแน่นแบบ Claisen-Schmidt ระหว่างสาร **335** กับอนุพันธ์เบนซาลดีไฮด์ที่มีหมู่แทนที่ในตำแหน่งที่สอดคล้องกับโครงสร้างบนผลิตภัณฑ์ที่ต้องการ ได้สารผลิตภัณฑ์ในปริมาณต่างๆ ในช่วง 3-49% จากนั้นกำจัดหมู่เมทิลออกจากหมู่เมทอกซีในส่วนของวงเบนซีนของหมู่ซินนาโมอิลด้านข้าง ได้หมู่ฟีนอล หรือโครงสร้างแคทิคอล สารที่มีฤทธิ์ดีที่สุดในการยับยั้งเอชไอวี-1 อินทิเกรส จากการทดสอบด้วยวิธีมัลติเพลตอินทิเกรชัน (MIA) คือสาร **353** ซึ่งมีค่า IC_{50} เท่ากับ 3.5 ไมโครโมลาร์ เพื่อให้เข้าใจถึงการเข้าจับกันของสารยับยั้งกับเอนไซม์เอชไอวี-1 อินทิเกรส ได้ทำการคำนวณการเข้าจับกันของโครงสร้างสารมัลติซินนาโมอิลแอนะล็อก 21 ชนิดกับส่วนคอร์ของเอชไอวี-1 อินทิเกรส ด้วยโปรแกรมออโต้ด๊อก 4.0 ตัวแปรการเข้าจับที่ได้จากการคำนวณสามารถใช้อธิบายฤทธิ์ทางชีวภาพของสารได้เป็นส่วนใหญ่โดยใช้พันธะไฮโดรเจนและพลังงานการเข้าจับเป็นหลัก โดยทั่วไปพบว่าสารยับยั้งที่มีฤทธิ์สูงจะเกิดพันธะไฮโดรเจนกับอินทิเกรสได้มากกว่าสารที่มีฤทธิ์ต่ำ

ภาควิชา.....เคมี…….. ลายมือชื่อนิสิต.....

สาขาวิชา.....เคมี..... ลายมือชื่อ อ.ที่ปรึกษาวิทยานิพนธ์หลัก.....

ปีการศึกษา.....2553..... ลายมือชื่อ อ.ที่ปรึกษาวิทยานิพนธ์ร่วม .....

ลายมือชื่อ อ.ที่ปรึกษาวิทยานิพนธ์ร่วม .....

5073928923 : MAJOR CHEMISTRY
KEYWORDS : CINNAMOYL ANALOGS / HIV-1 INTEGRASE /
MOLECULAR MODELING

WIPA TUPCHIANGMAI: SYNTHESIS AND MOLECULAR MODELING OF NEW MULTI-CINNAMOYL ANALOGS AS HIV-1 INTEGRASE INHIBITORS. ADVISOR: ASST. PROF. YONGSAK SRITANA-ANANT, Ph.D., CO-ADVISOR: ASST. PROF. SOMSAK PIANWANIT, Ph.D., ASSOC. PROF. SUPINYA TEWTRAKUL, Ph.D., 142 pp.

Twenty one multi-cinnamoyl-based analogs on the hexasubstituted benzene platform were synthesized and tested as a new group of synthetic inhibitors of HIV-1 integrase (IN). They were prepared from the Claisen-Schmidt condensations of **335** and the corresponding substituted benzaldehydes in various ranges of yields (3-49%). Partial demethylations of the methoxy groups on the flanking phenyl rings gave the free phenolic or catecholic moieties. The most potent compound **353** showed the inhibition activity against HIV-1 integrase in multiplate integration assay (MIA) with IC_{50} value of 3.5 μM. To understand the binding of these inhibitors to HIV-1 IN, the flexible models of selected 21 multi-cinnamoyl compounds were computationally docked into the catalytic core domain of HIV-1 IN using Autodock 4.0 program. The obtained docking parameters, mainly hydrogen bonding and binding energy, can be used to explain biological activity of most compounds. In general, it is found that active inhibitors forms more hydrogen bonds with IN than inactive analogs.

Department : Chemistry	Student's Signature .....
Field of Study : Chemistry	Advisor's Signature .....
Academic Year : 2010	Co-advisor's Signature .....
	Co-advisor's Signature .....

ACKNOWLEDGEMENTS

My appreciation goes to my thesis advisor, Assistance Professor Yongsak Sritana-anant, and co-advisors, Assistance Professor Somsak Pianwanit and Associate Professor Supinya Tewtrakul for their intensive supervision, guidance, valuable instruction and hearty encouragement throughout the course of this work.

I would also like to thank Assistance Professor Warinthorn Chavasiri, Assistance Professor Aroonsiri Shitangkoon, Sumrit Wacharasindhu, and Professor. Apichart Suksamrarn, for their valuable suggestions and constructive comments.

I would like to thank Center for Petroleum, Petrochemicals and Advanced Materials, Chulalongkorn University for part of financial and instrumental support.

The scholarship support for doctoral study and research from Suan Dusit Rajabhat University is also acknowledged.

I would also be grateful to Dr. Thitinun Karpkird for providing some of raw chemical starting materials, Miss Saowanaporn Choksakulporn for recording the NMR technique, suggestion about synthesis of 1,3,5-triacetyl-2-4-6-trihydroxybenzene and 1,3,5-triacetyl-2,4,6-trimethoxybenzene, Mr. Thanatip Ruksilp for recording MS technique, Mr. Kiattisak Lugsanangarm for basic computer molecular docking suggestion, Miss Sawdah Makklai and Miss Kingkan Bunluepuech for suggestion and testing of HIV-1 integrase assay.

I would like to thank the members of research groups on the fourteenth floor, Mahamakut building for their companionship and friendship.

Finally, none of this work would have been possible without love, encouragement and understanding from my family, friends and colleagues.

CONTENTS

Page

Page

Page

Page

LIST OF TABLES

LIST OF FIGURES

Figure Page

Figure Page

LIST OF SCHEMES

LIST OF ABBREVIATIONS

AcCl	: acetyl chloride
AIDS	: acquired immune deficiency syndrome
Ala	: alanine
$AlCl_3$	: aluminum chloride
AP	: alkaline phosphatase
Asn	: asparagine
Asp	: aspartic acid
^{13}C-NMR	: carbon-13 nuclear magnetic resonance spectroscopy
$CDCl_3$	: deuterated chloroform
CH_2Cl_2	: dichloromethane
5CITEP	: 1-(5-chloroindol-3-yl)-3-hydroxy-3-(2*H*-tetrazol-5-yl)-propenone
Cys	: cysteine
Da	: Dalton
DIG	: digoxigenin
DKA	: diketone acid
DMSO	: dimethylsulfoxide
DNA	: deoxyribonucleic acid
DTT	: dithiothritol
ELISA	: enzyme-linked immunosorbent assay
EtOAc	: ethyl acetate
EtOH	: ethanol
FT-IR	: Fourier-transform infrared spectrophotometer
Gln	: glutamine
Glu	: glutamic acid
^{1}H-NMR	: proton nuclear magnetic resonance spectroscopy
Hz	: Hertz
h	: hour
HIV-1	: human immunodeficiency virus type 1
His	: histidine
IN	: integrase enzyme

INI	: integrase inhibitor
IC_{50}	: inhibitory concentration at 50% inhibition
KOH	: potassium hydroxide
LTR	: long terminal repeat
Lys	: lysine
MeOH	: methanol
min	: minute
MIA	: multiplate integration assay
MOPS	: 3-(*N*-morpholino)propanesulfonic acid
mU	: multi unit
nm	: nanometre
NMR	: nuclear magnetic resonance spectroscopy
OD	: absorbance detected
PBS	: phosphate buffer saline
PIC	: pre-integration complex
PRI	: protease inhibitor
RNA	: ribonucleic acid
RTI	: reverse transcriptase inhibitor
Ser	: serine
Thr	: threonine
TLC	: thin layer chromatography
tris-HCl	: 2-amino-2-(hydroxymethyl)-1,3-propanediol, hydrochloride
J	: coupling constant
d	: doublet (NMR)
s	: singlet (NMR)
t	: triplet (NMR)
μL	: microlitre
μM	: micromolar
τ	: torsion angle

CHAPTER I

INTRODUCTION

1.1 The human immunodeficiency virus-type 1 (HIV-1)

Acquired Immune Deficiency Syndrome (AIDS) was first found in 1981 by Gottlieb and coworkers [1]. AIDS caused by human immunodeficiency virus type 1 (HIV-1). The First human retroviruses (HTLV-I) were first reported in 1983 by Montagnier, Gallo and Levy [2]. AIDS remains a serious global health problem worldwide. World Health Organization (WHO) reported that there were 33.3 million people lived with HIV infections at the end of 2009 [3]. HIV-1 has three important enzymes in its replication processes, namely reverse transcriptase, protease and integrase enzymes. After viral entry, the viral RNA is transcribed into double strand DNA during reverse transcription. Next step integrase binds to specific sequences in long terminal repeat (LTR) region of viral DNA that results in a stable viral DNA integrase binding complex or pre-integration complex (PIC) which is transported to the nucleus wherein it is integrated the viral DNA into host cell DNA by the integrase enzyme. Transcription generates messengers RNAs as well as progeny virion RNA. Some viral RNA were synthesized viral protein and protease enzyme cut longchain protein to individual protein (**Figure 1.1**) [4].

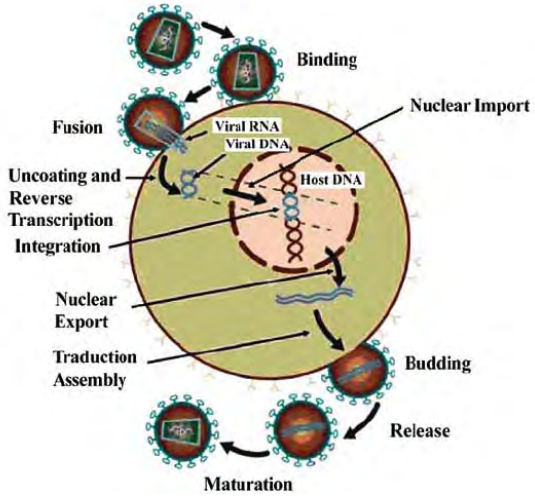

Figure 1.1 Pharmacological targets during HIV-1 replication

Viral protein and genomic RNA and three importance enzymes are assembled and released by budding. Current AIDS treatments involve mixture of drugs targeting different binding sites of proteins essential in the viral life cycle [5, 6]. Three different classes of chemotherapeutic agents are available to block such replication: reverse transcriptase inhibitors (RTI) [7], protease inhibitors (PRI) [8] and, more recently, inhibitors of the viral fusion or integrase inhibitors (INI) [9]. RTI and PRI are well known for drug therapy. However, wide usage of these drugs rendered the appearance of resistant HIV-1 virus. Consequently, new targets and new mechanisms are needed to combat these emerging strains of HIV-1. The target potentially amenable to a selective chemotherapeutic intervention is the HIV-1 integrase (IN), an enzyme which has no counterpart in the host cell and catalyzes an essential step in the retroviral life cycle. HIV-1 IN is a 32 kDa enzyme that has 288 amino acid residues in three distinct domains. The N-terminal domain was analyzed by NMR technique, which includes residues 1-50 and contains a conserved Zinc binding motif including two histidine and two cysteine residues. The catalytic domain was analyzed by X-ray technique, which is responsible for catalytic activity as well as specific contact with viral DNA. It contains residues 50-212 that has three important residues such as D64, D116 and E152 (the so-called D, D-(35)E motif) which are required for catalysis. The C-terminal domain was analyzed by NMR technique, residues 212-288 participate binding in DNA strongly but is not specifically (**Figure 1.2**) [4].

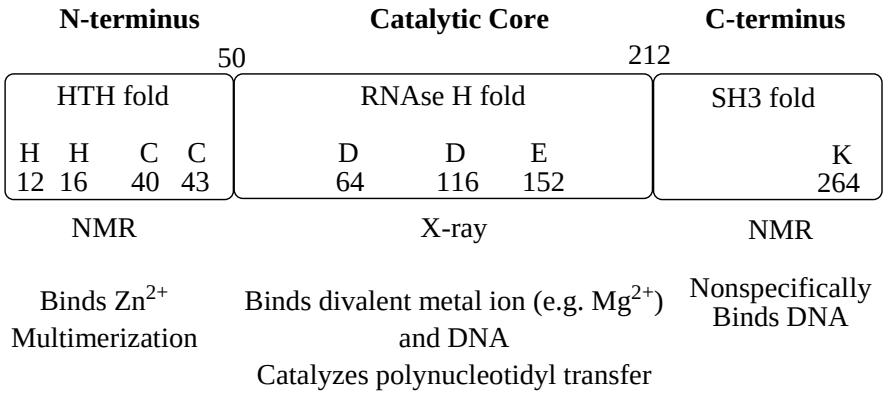

Figure 1.2 Domain structure of HIV-1 integrase

The retroviral DNA integrase has its main function divided into two steps (**Figure 1.3**) [4]. 3'-Processing reaction step, two nucleotides are removed from each 3' terminus of the blunt-ended viral DNA. The second step (strand transfer) integrates viral DNA into host cell DNA with Mg^{2+} or Mn^{2+} as a co-factor [9-16].

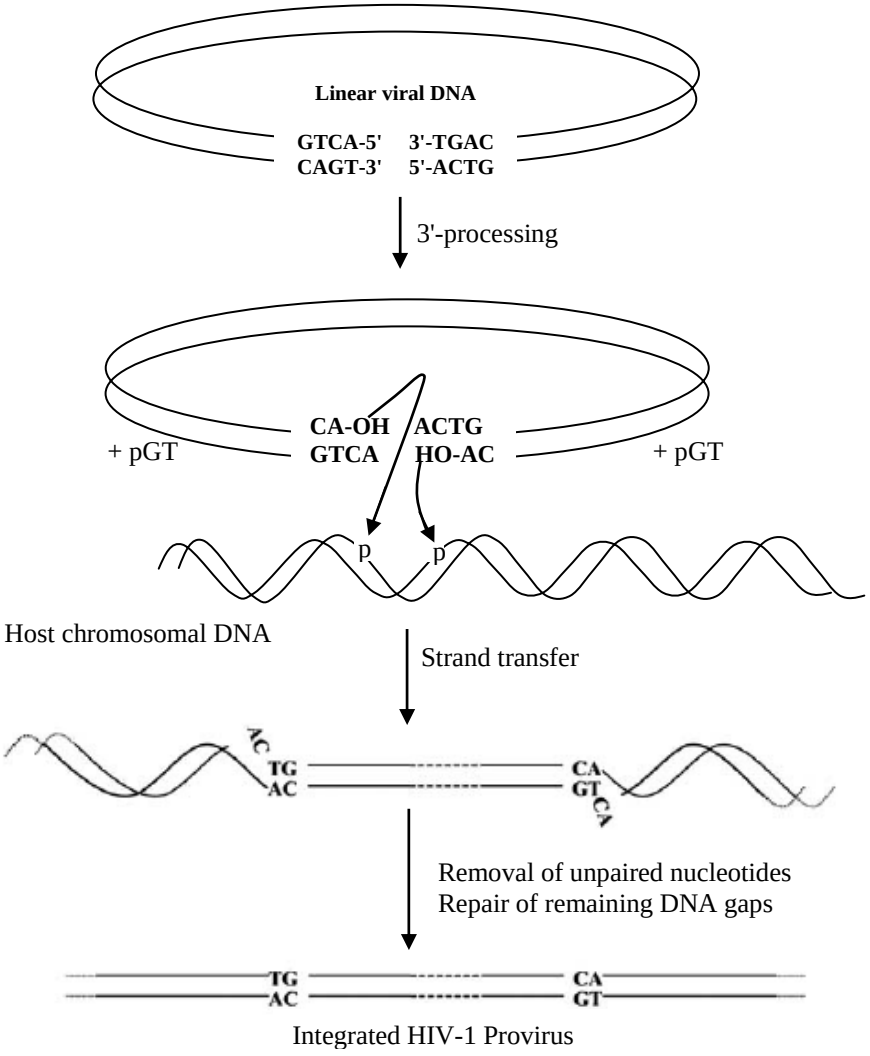

Figure 1.3 The different steps of integration

In 1987, zidovudine (AZT) was the first drug for the treatment of HIV-1/AIDS. Since then, more than 21 drugs have been approved by FDA of USA. These drugs could be divided into four classes: nucleoside reverse transcriptase inhibitors (NRTIs), non-nucleoside reverse transcriptase inhibitors (NNRTIs), protease inhibitors (PIs) and fusion inhibitors (**Table 1.1-1.4**) [4].

Table 1.1 Nucleoside reverse transcriptase inhibitors for anti-AIDS drugs

FDA approval	Brand Name	Generic name	Manufacturer
March 19, 1987	Retrovir	Zidovudine (AZT)	Glaxosmithkline
Oct. 9, 1991	Videx,	Didanosine (ddl)	Bristol-Myers Squibb
June 19, 1992	Hivid	Zalcitabine (ddC)	Roche Pharmaceuticals
June 24, 1994	Zerit	Stavudine (d4T)	Bristol-Myers Squibb
Nov. 17, 1995	Epivir	Lamivudine (3TC)	Glaxosmithkline
Dec. 17, 1998	Ziagen	Abacavir	Glaxosmithkline
Nov. 14, 2000	Trizivir	Abacavir, Lamivudine, Zidovudine	Glaxosmithkline
Oct. 21, 2001	Viread	Tenofovir DF	Gilead Sciences
July 2, 2003	Emtriva	Emtricitabine (FTC)	Gilead Sciences
Aug. 2, 2004	Truvada	Emtricitabine, Tenofovir DF	Gilead Sciences
Aug. 2, 2004	Epzicom	Abacavir, Lamivudine	Glaxosmithkline

Table 1.2 Non-nucleoside reverse transcriptase inhibitors for anti-AIDS drugs

FDA approval	Brand Name	Generic name	Manufacturer
June 21, 1996	Viramune	Nevirapine	Boehringer Ingelheim
April 4, 1997	Rescriptor	Delavirdine (DLV)	Pfizer
Sept. 17, 1998	Sustiva	Efavirenz	Bristol-Myers Squibb

Table 1.3 Protease inhibitors for anti-AIDS drugs

FDA approval	Brand Name	Generic name	Manufacturer
Dec. 6, 1995	Invirase	Saquinavir	Roche Pharmaceuticals
March 1, 1996	Norvir	Ritonavir	Abbott Laboratories
March 13, 1996	Crixivan	Indinavir (IDV)	Merck
March 14, 1997	Viracept	Nelfinavir	Pfizer
Nov. 7, 1997	Fortorase	Saquinavir Mesylate	Roche Pharmaceuticals
April 15, 1999	Agenerase	Amprenavir	Abbott Laboratories

Table 1.3 Continued

FDA approval	Brand Name	Generic name	Manufacturer
Sept. 15, 2000	Kaletra	Lopinavir, Ritonavir	Abbott Laboratories
June 20, 2003	Reyataz	Atazanavir	Bristol-Myers Squibb
Oct. 20, 2003	Lexiva	Fosamprenavir	Glaxosmithkline

Table 1.4 Fusion inhibitors for anti-AIDS drugs

FDA approval	Brand Name	Generic name	Manufacturer
March 13, 2003	Fuzeon	Enfuvirtide (T-20)	Roche Pharmaceuticals/ Trimeris

1.2 Anti-IN activities of HIV-1 IN inhibitors

Several families of HIV-1 IN inhibitors have been collected and identified into sixteen groups reported by Neamati and coworkers [17] such as nucleotides and guanosine quartets, topoisomerase poisons and other natural product inhibitors, DNA groove binders, lignanolides and related bis-catechols, caffeic acid phenyl ester (CAPE), CAPE-amides and other hydroxylated aromatics, tyrphostins, caffeoylquinic acid and related compounds, arylamides, bis-arylamides, hydrazides, coumarins, monomeric aurintricarboxylic acids, cosalane and cosalane analogs, depsides depsidones and related compounds, sulfonic acids and sulfonilamides and diarylsulfones [17].

Mazumder and coworkers studied on 3'-azido-3'-deoxythymidine (AZT) (**1**) and they found that AZT mono-, di- and tri-phosphate (**2-4**) exhibited strand transfer inhibition with IC_{50} value ranging from 100-150 μM while AZT was inactive (IC_{50} value = 400 μM) (**Table 1.5**) [17, 18], compounds **5-9** that inhibited HIV-1 replication [17, 19]. Many dinucleotides have been a platform for a sequence selectivity study of the IN inhibitors in which compounds **14**, **16** and **18** showed an IC_{50} values below 10 μM for both 3'-processing and strand transfer inhibition, whereas compounds **15**, **19** and **20** showed inactive an IC_{50} values of 100 μM (**Table 1.5**) [20]. Compounds **27**-**36** represented the increased nucleotide unit to three and

four but did not markedly increase potency [20]. Compounds **37**-**40** were oligonucleotides composed entirely of deoxyguanosine and thymidine, known as guanosine quartets [21]. They showed IC_{50} values increased activitiy than the mononucleotides (**Table 1.5**) [20, 21].

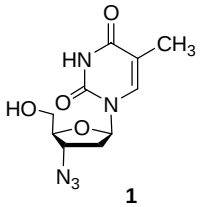

1
AZT

Table 1.5 Nucleotides and guanosine quartets as HIV-1 integrase inhibitors

Compound	No.	IC_{50} (μM)		Ref.
		3′-Processing	Strand transfer	
AZT	**1**	>400	>400	[18]
AZTMP	**2**	200	20	
AZTDP	**3**	150	120	
AZTTP	**4**	300	150	
D4TMP	**5**	110 ± 20	95 ± 15	[19]
FdTMP	**6**	95 ± 15	70 ± 12	
L-ddCMP	**7**	50 ± 8	45 ± 10	
L-5FddCMP	**8**	46 ± 6	39 ± 4	
L-5FddCTP	**9**	68 ± 2	48 ± 10	
5′-CA	**10**	>132	60	[20]
5′-pCA-3′	**11**	105 ± 20	13 ± 5	
5′-pCC-3′	**12**	15 ± 0.5	12 ± 5	
5′-pCG-3′	**13**	71 ± 11	12 ± 2	
5′-pCT-3′	**14**	8 ± 1	6 ± 1	
5′-pAA-3′	**15**	>100	100 ± 30	
5′-pAC-3′	**16**	6 ± 2	3 ± 1	
5′-pAG-3′	**17**	15 ± 7	9 ± 4	

Table 1.5 Continued

Compound	No.	IC_{50} (μM)		Ref.
		3′-Processing	Strand transfer	
5′-pAT-3′	**18**	7 ± 2	7 ± 3	[20]
5′-pGA-3′	**19**	>100	100 ± 40	
5′-pGC-3′	**20**	>100	100 ± 40	
5′-pGG-3′	**21**	54 ± 34	12 ± 4	
5′-pGT-3′	**22**	22 ± 1	7 ± 1	
5′-pTA-3′	**23**	85 ± 21	18 ± 10	
5′-pTC-3′	**24**	35 ± 17	37 ± 9	
5′-pTG-3′	**25**	65 ± 35	31 ± 4	
5′-pTT-3′	**26**	73 ± 27	53 ± 4	
5′-CAG-3′	**27**	57 ± 12	53 ± 11	
5′-CTA-3′	**28**	65 ± 15	25 ± 5	
5′-pCTA-3′	**29**	27 ± 6	6 ± 2	
5′-pCTT-3′	**30**	>100	13 ± 4	
5′-pCAT-3′	**31**	>100	20 ± 4	
5′-pCAC-3′	**32**	93 ± 19	27 ± 6	
5′-pCAA-3′	**33**	42 ± 9	22 ± 5	
5′-pCAG-3′	**34**	57 ± 11	15 ± 4	
5′-pGTC-3′	**35**	40 ± 5	9 ± 1	
5′-pGTCA-3′	**36**	32 ± 4	5 ± 1	
5′-GTGGTGGGTGGGTGGGT-3′	**37**	0.08 ± 0.02	0.05 ± 0.01	[21]
5′-GTGGTGGGTGGGTGGGT-3′b	**38**	0.11 ± 0.01	0.08 ± 0.07	
5′-GTGGTGGGTGTGGTGGGT-3′	**39**	0.15 ± 0.03	0.13 ± 0.02	
5′-GTGGTTGGTGTGGTTGGT-3′	**40**	0.76	0.61	

In 1993, Fesen and coworkers reported the topoisomerase poisonmerase poisons were DNA binders which act as inhibitors of IN such as compounds **41** and **43** (**Table 1.6**) [22]. These two compounds inhibited IN at low micromolar concentrations. The compounds **45** and **46**, natural products, were hydroxylated

aromatic compounds which also inhibited IN activity at low micromolar concentrations (**Table 1.6**) [22].

Table 1.6 Topoisomerase poisomerase poisons and other natural product as HIV-1 integrase inhibitors

Compound	No.	IC_{50} (μM)		Ref.
		3′-Processing	Strand transfer	
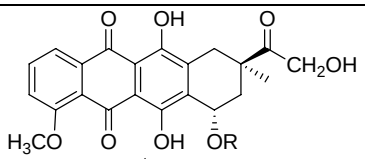 **41** R = 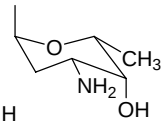 **42** R = H	**41**	0.9 ± 0.7	2.4	[22]
	42	>100	>100	
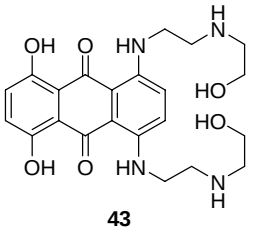 **43**	**43**	3.8 ± 0.6	8.0	
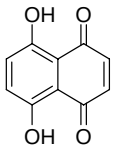 **44**	**44**	5.7 ± 2.7	2.5	
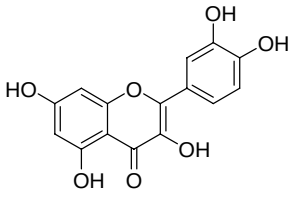 **45**	**45**	19.4 ± 9.9	11.0 ± 5.9	
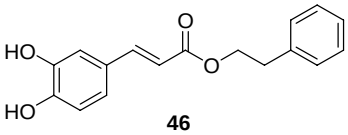 **46**	**46**	7	19	
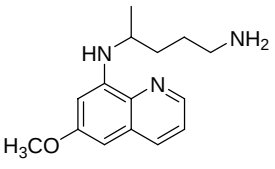 **47**	**47**	15.3 ± 3.6	3.6	

Table 1.6 Continued

Compound	No.	IC_{50} (μM)		Ref.
		3′-Processing	Strand transfer	
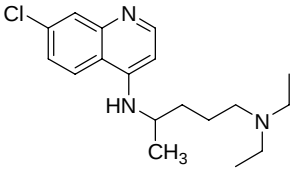 48	**48**	13.1 ± 10.0	5.7	[22]

Neamati and coworkers reported several bis-distamycins **55-58** identified as potent IN inhibitors at low nanomolar concentrations. They were DNA groove binders (**Table 1.7**) [23].

Table 1.7 DNA groove binders as HIV-1 integrase inhibitors

Compound	No.	IC_{50} (μM)		Ref.
		3′-Processing	Strand transfer	
Spermine	**49**	>100	>100	[23]
Spermidine	**50**	>100	>100	
Net-CO-Net[a]	**51**	42.8	29.0	
Net-$CO(CH_2)_2CO$-Net	**52**	5.8 ± 1.6	7.5 ± 2.5	
Net-$CO(CH_2)_9CO$-Net	**53**	37.6	10.0	
Net-$CO(CH_2)_{10}CO$-Net	**54**	33.8	8.7	
Dist-$CO(CH_2)_2CO$-Dist[b]	**55**	21 ± 8.5	9.5 ± 1.2	
Dist-$CO(CH_2)_6CO$-Dist	**56**	0.02	0.01	
Dist-$CO(CH_2)_8CO$-Dist	**57**	0.03	0.01	
Dist-$CO(CH_2)_{22}CO$-Dist	**58**	12.2 ± 0.3	8.0	
Distamycin	**59**	57	50	
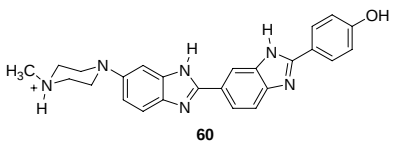 Hoechst 33258	**60**	>100	>100	

Table 1.7 Continued

Compound	No.	IC_{50} (μM)		Ref.
		3′-Processing	Strand transfer	
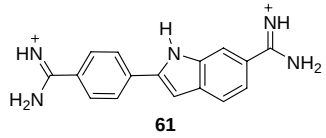 **61** DAPI	**61**	>100	>100	[23]
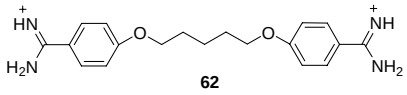 **62** Pentamidine	**62**	>100	>100	
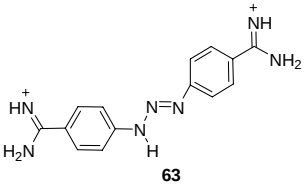 **63** Berenil	**63**	>100	>100	

[a]Net = Netropsin, [b]Dist = Distamycin

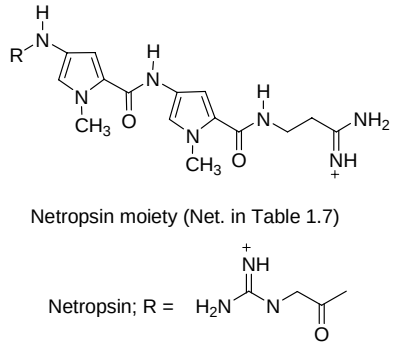

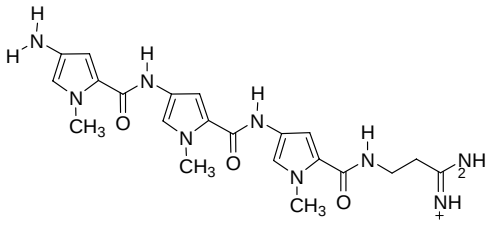
59 (Distamycin)

In 1996, Eich and coworkers isolated compound **64** from *Thuja plicata* DUNN., which were found to be in the class of lignans and lignaloids. Methoxy groups in *ortho* position of phenolic hydroxyls **64** can be demethylated by $AlCl_3$/pyridine in dichloromethane to obtain the catechol structures **65** and **66**. Compound **66**, a lignanolide with two catechol substructures, was characterized by total inhibition of the 3'-processing step as well as of strands transfer IC_{50} value showed in **Table 1.8**. Compound **64** decreased the activity because it lack of catechol moiety on benzene ring of the structure [24]. The bis-catechols, α- and β-conidendrol

inhibited IN at submicromolar concentrations in which the catechol group increased the activity was reported by LaFemina. (**Table 1.8**) [25].

Table 1.8 Lignanolides and related bis-catechols as HIV-1 integrase inhibitors

Compound	No.	IC_{50} (μM)		Ref.
		3′-Processing	Strand transfer	
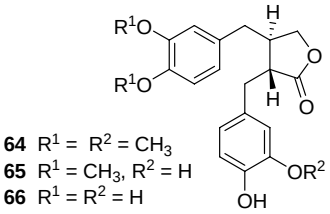 **64** $R^1 = R^2 = CH_3$ **65** $R^1 = CH_3$, $R^2 = H$ **66** $R^1 = R^2 = H$	**64**	>100	>100	[24]
	65	100	100	
	66	21.4 ± 15.0	5.4 ± 4.0	
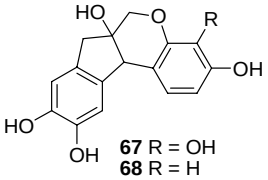 **67** R = OH **68** R = H	**67**	0.5	nd[a]	[25]
	68	1.7	nd[a]	
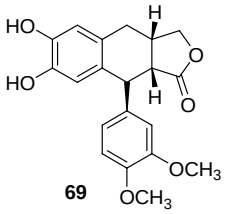 **69**	**69**	7	nd[a]	
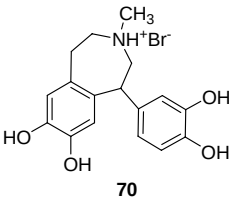 **70**	**70**	1.7	nd[a]	
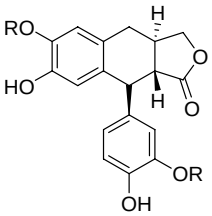 **71** R = CH_3 **72** R = H	**71**	>35	nd[a]	
	72	0.5	nd[a]	
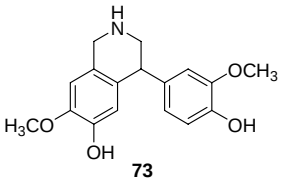 **73**	**73**	>35	nd[a]	

[a]nd = not determined

The caffeic acid phenyl ester (CAPE) **46** showed high activity in 3′-processing and strand transfer whereas CAPE amide, compounds **75**-**77**, were less potent than **46**. Such a high activity is perhaps appeared by hydroxyl moiety on phenyl ring increased hydroxylation of the phenyl ring such as compound **74** increased potency against IN activity (**Table 1.9**) [26].

Table 1.9 CAPE, CAPE-amides and other hydroxylated aromatics of HIV-1 integrase inhibitors

Compound	No.	IC_{50} (μM)		Ref.
		3′-Processing	Strand transfer	
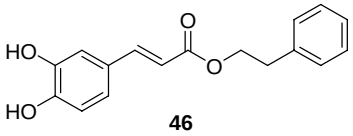 **46**	**46**	7	19	[22, 26]
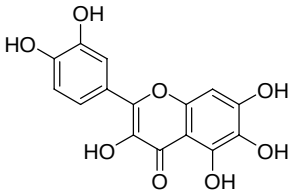 **74**	**74**	0.8 ± 0.3	0.1 ± 0.1	[22, 26]
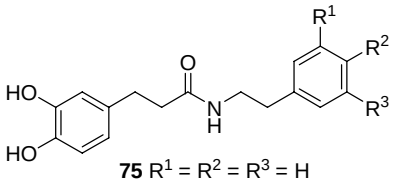 **75** $R^1 = R^2 = R^3 = H$ **76** $R^1 = H$, $R^2 = R^3 = OH$ **77** $R^1 = R^2 = R^3 = OH$	**75**	>100	>100	[27]
	76	33	33	
	77	nd[a]	4	

[a]nd = not determined

Several tyrphostins compounds **78**-**84** were synthetic analogs that inhibited IN at low micromolar concentration. These compounds have catechol moieties which are required for the activity. The various lengths of the linker and aromatic ring substitutions were less critical for activity (**Table 1.10**) [28].

Table 1.10 The tyrphostins as HIV-1 integrase inhibitors

Compound	No.	IC_{50} (μM)		Ref.
		3′-Processing	Strand transfer	
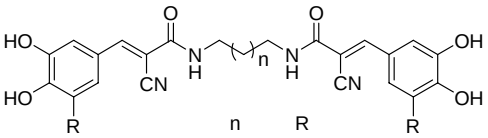	**78**	1.9	0.8	[28]
	79	0.4 ± 0.1	0.2	
	80	0.8 ± 0.4	0.4 ± 0.3	
	81	3.3	1.9	
	82	0.7 ± 0.5	0.6 ± 0.1	
	83	0.5 ± 0.1	0.2	
	84	1.4 ± 0.6	1.1 ± 0.5	

	n	R
78	0	H
79	0	OH
80	0	Br
81	0	NO_2
82	2	OH
83	3	OH
84	4	H

The hydroxylated aromatics containing catechol moieties such as L-chicoric acid **86** had been reported to have antiviral activity and inhibit purified IN (**Table 1.11**) [17, 29]. The dicaffeoylquinic acid derivatives **87**-**91** were considered potent inhibitors of IN, whereas the monomeric precursors, **85** and **93** as inactive (**Table 1.11**) [17, 29-30].

Table 1.11 Caffeoylquinic acids and related compounds as HIV-1 integrase inhibitors

Compound	No.	IC_{50} (μM)		Ref.
		3′-Processing	Strand transfer	
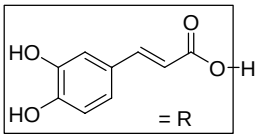 **85**	**85**	>200	>200	[17, 29]
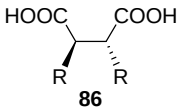 **86**	**86**	0.15 ± 0.02	0.13 ± 0.08	
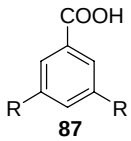 **87**	**87**	1.38 ±0.21	4.71 ± 0.96	
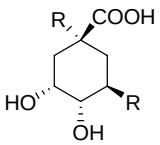 **88**	**88**	0.68 ± 0.08	1.08 ± 0.27	

Table 1.11 Continued

Compound	No.	IC_{50} (μM)		Ref.
		3′-Processing	Strand transfer	
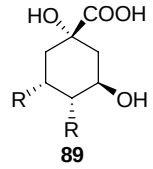 **89**	**89**	0.79 ± 0.17	0.54 ± 0.17	[17, 29]
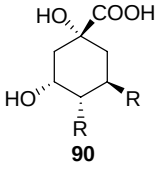 **90**	**90**	0.25 ± 0.04	0.46 ± 0.15	
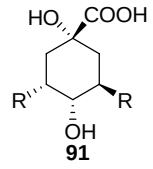 **91**	**91**	0.64 ± 0.2	0.66 ± 0.4	
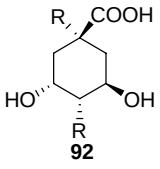 **92**	**92**	9.5 ± 2.0	7.8 ± 1.4	[30]
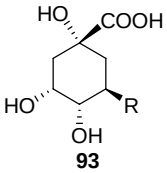 **93**	**93**	87.8	45.8	

Zhao and coworkers synthesized monohydroxylated arylamides compounds **94**-**101** and tested their activities. Only compound **94** with catechol moiety on both sides showed higher activity than none-bearing monohydroxyl derivatives or *ortho*-substituted analogs showed low activity with IC_{50} value up to 350 μM (**Table 1.12**) [31]. Moreover, compounds **103** and **105** containing protected hydroxyl groups showed no activity in 3′-processing and strand transfer compared to the free catecholic **105** and **107** (**Table 1.13**) [31].

Table 1.12 Arylamides as HIV-1 integrase inhibitors

Compound	No.	IC_{50} (μM)		Ref.
		3′-Processing	Strand transfer	
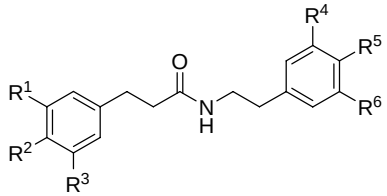	**94**	33.0	33.0	[31]
	95	>350	>350	
	96	>350	>350	
	97	>350	>350	
	98	>350	>350	
	99	>350	>350	
	100	>350	>350	
	101	>350	>350	

	R^1	R^2	R^3	R^4	R^5	R^6
94	OH	OH	H	H	OH	OH
95	H	OH	H	H	OH	H
96	OH	H	H	H	OH	H
97	H	OH	H	H	H	OH
98	OH	H	H	H	H	OH
99	OH	H	OH	H	OH	OH
100	OH	H	OH	OH	H	OH
101	OH	OH	H	OH	H	OH

Table 1.13 Bis-arylamides as HIV-1 integrase inhibitors

Compound	No.	IC_{50} (μM)		Ref.
		3′-Processing	Strand transfer	
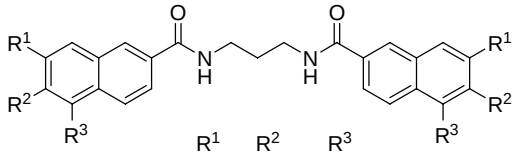	**102**	0.98±0.5	0.81±0.1	[31]
	103	>200	>200	
	104	0.23±0.05	0.11±0.07	
	105	>200	>200	

	R^1	R^2	R^3
102	OH	OH	H
103	OCH_3	OCH_3	H
104	H	OH	OH
105	H	OCH_3	OCH_3

Zhao and coworkers synthesized and studied activity relationship among *N*,*N*'-bis-salicylhydrazine analogs (**106**-**114**). The results of decreased activities were found when the 2-hydroxyl group was replaced by a mercapto group in compound **107** or removed 2-hydroxyl in compounds **110** and **111** (**Table 1.14**) [32].

Table 1.14 Hydrazides as HIV-1 integrase inhibitors

Compound	No.	IC_{50} (μM)		Ref.
		3′-Processing	Strand transfer	
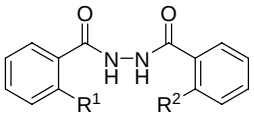 R¹ R² **106** OH OH **107** OH SH	**106**	2.07±0.75	0.73±0.13	[32]
	107	9.1±3.7	5.8±1.3	
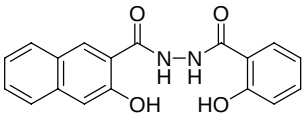 **108**	**108**	2.3±0.3	1.1±0.15	
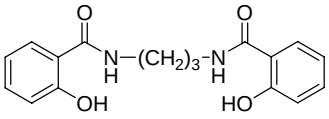 **109**	**109**	>200	>200	
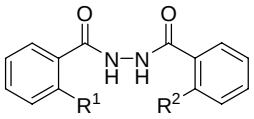 R¹ R² **110** H H **111** H OH	**110**	>100	>100	
	111	>100	>100	
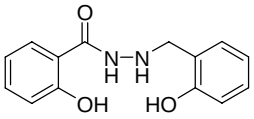 **112**	**112**	6.7±0.8	5.2±1.5	
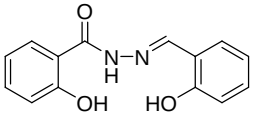 **113**	**113**	>100	>100	

Mazumder and coworkers reported the tetrameric 4-hydroxycoumarin **115**, coumarin group, has no catechol on benzene ring which showed IC_{50} value of 1.5 and 0.8 μM against 3′-processing and strand transfer, respectively [33]. Zao and coworkers synthesized over 30 coumarins that displayed a structure-activity relationship among this class of inhibitors [34]. They found that a coumarin dimmer gave increased activity when there was a hydroxyl group on the aromatic ring (**Table 1.15**) [33, 34].

Table 1.15 Coumarins as HIV-1 integrase inhibitors

Compound	No.	IC_{50} (μM)		Ref.
		3′-Processing	Strand transfer	
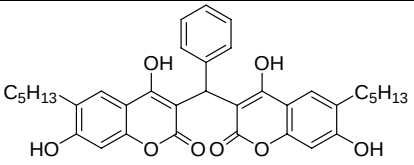 **114**	**114**	10.5	12.0	[33]
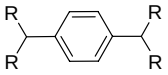	**115**	1.5±0.5	0.8±0.3	
115 **116** **117** 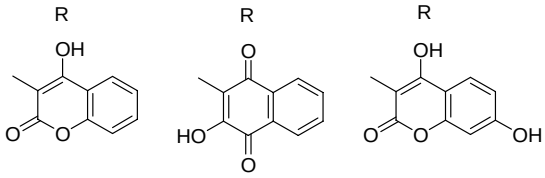	**116**	7.5±2.0	2.7±0.9	
	117	0.4±0.1	0.3±0.3	[34]
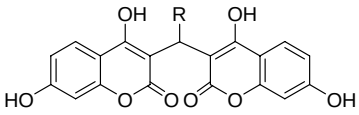	**118**	4.2±0.7	3.5±1.2	
R = 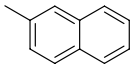 **118** R = 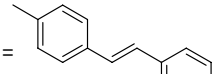 **119**	**119**	7.0±0.1	1.8±0.5	
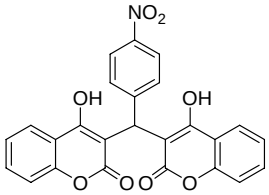 **120**	**120**	50	24	

Table 1.16 Monomeric aurintricarboxylic acids, cosalane and cosalane analogs as HIV-1 integrase inhibitors

Compound	No.	IC_{50} (μM)		Ref.
		3′-Processing	Strand transfer	
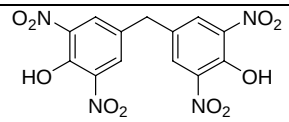 **121**	**121**	49.7	43.9	[30]
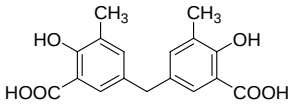 **122**	**122**	61.8 ±8.6	68.5±13.5	
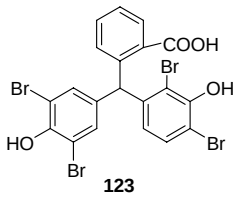 **123**	**123**	25.6	27.2	
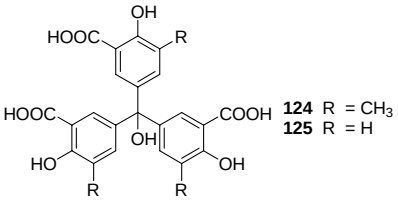 **124** R = CH_3 **125** R = H	**124**	32.8	23.0	
	125	10-50	nd[a]	[35]
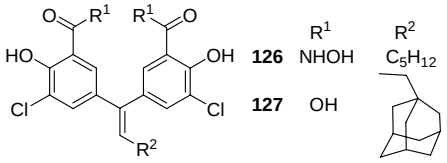 **126** R^1 = NHOH, R^2 = C_5H_{12} **127** R^1 = OH	**126**	4	nd[a]	[36]
	127	7	nd[a]	
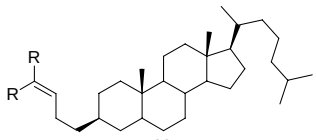 **128**	**128**	25	nd[a]	
R = 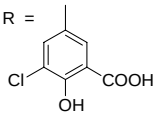 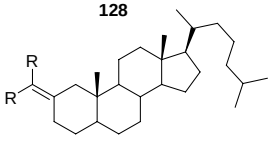 **129**	**129**	>100	nd[a]	
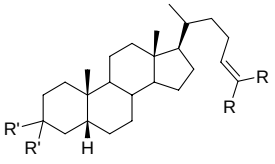 **130** R' = H **131** R' = F	**130**	2.2	nd[a]	[36]
	131	2.2	nd[a]	

[a]nd = not determined

Nemati and coworkers reported non-catechol-containing natural products such as compounds **132-139**, several lichen acids of the depsides and depsidones families, exhibited to inhibit IN activity at low micromolar concentrations. Compounds **132-134** exhibited IC_{50} values of 2-6 μM against IN. Compound **135** showed moderate activity. Compounds **136-139** were yielded a variety novel inhibitors that searched of the NCI 3D database, which showed IC_{50} values below 10 μM (**Table 1.17**) [30].

Table 1.17 Depsides, depsidones and related compounds as HIV-1 integrase inhibitors

Compound	No.	IC_{50} (μM)		Ref.
		3′-Processing	Strand transfer	
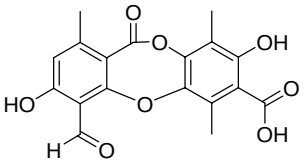 **132**	**132**	4.6±1.6	6.5±3.9	[30]
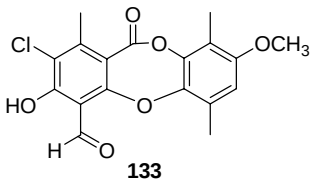 **133**	**133**	2.2	1.6	
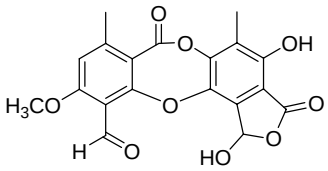 **134**	**134**	4.4	1.9	
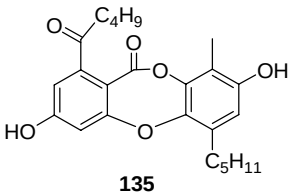 **135**	**135**	42.2	28.1	
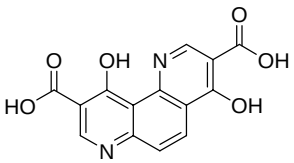 **136**	**136**	6.1	6.1	

Table 1.17 Continued

Compound	No.	IC_{50} (μM)		Ref.
		3′-Processing	Strand transfer	
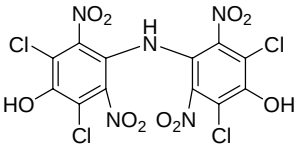 137	**137**	8.3	4.0	[30]
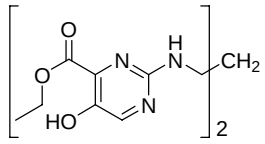 138	**138**	11.6	7.9	
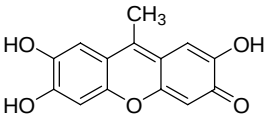 139	**139**	1.1	0.9	

Compound **140** was polyanionic sulfonate suramin, the first inhibitor of IN reported by Carteau group [37]. Sulfonamides compounds **141**-**147** were reported by Nicklaus and coworkers [38] and diarylsulfones **148**-**159** were reported by Nemati and coworkers [39] which these compounds **141**, **142**, **151**, **153** and **158** inhibited IN function at low micromolar concentrations as shown in **Table 1.18** and **Table 1.19**. Sulfonamides and sulfones are interesting classes of compounds because sulfa drugs are well known antimicrobial agents for *Pneumocystis carinii* pneumonia, a leading cause of morbidity and mortality in AIDS patients [17, 39].

Table 1.18 Sulfonic acids and sulfonilamides as HIV-1 integrase inhibitors

Compound	No.	IC_{50} (μM)		Ref.
		3′-Processing	Strand transfer	
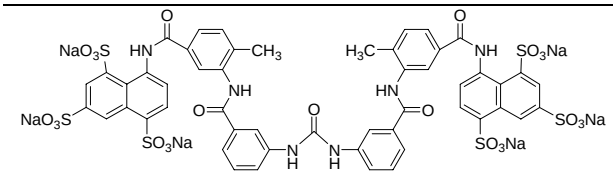 140	**140**	0.25	0.09	[37]

Table 1.18 Continued

Compound	No.	IC_{50} (μM)		Ref.
		3′-Processing	Strand transfer	
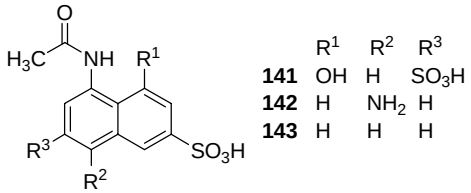 R1 R2 R3 **141** OH H SO_3H **142** H NH_2 H **143** H H H	**141**	0.47±0.02	0.29±0.04	[38]
	142	3.4 ±0.8	2.7±0.4	
	143	27.9±8.6	14.3±0.6	
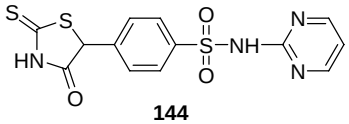 **144**	**144**	28.6±11.6	14.0±9.7	
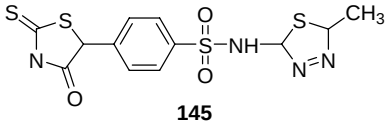 **145**	**145**	24.0±8.2	19.0±8.3	
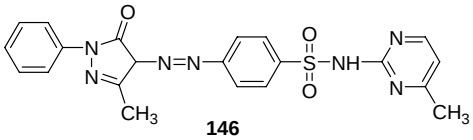 **146**	**146**	49.0±9.5	23.6±1.9	
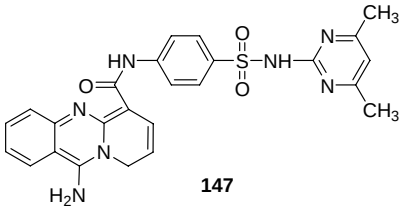 **147**	**147**	48.3±25.8	13.7±8.9	[38]

Table 1.19 Diarylsulfones as HIV-1 integrase inhibitors

Compound	No.	IC_{50} (μM)		Ref.
		3′-Processing	Strand transfer	
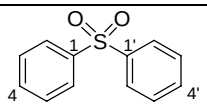				
3,3′-$(NO_2)_2$,4,4′-$(F)_2$	**148**	51.0±8.8	59.0±8.9	[39]
2,2′,4,4′-$(NO_2)_4$	**149**	60.0	76.5	
4,4′-$(N{=}NOH)_2$.2Na	**150**	6.5±3.0	6.1±0.9	
3,3′-$(NH_2)_2$,4,4′-$(OH)_2$	**151**	4.5±3.0	4.9±3.0	

Table 1.19 Continued

Compound	No.	IC_{50} (μM)		Ref.
		3′-Processing	Strand transfer	
4,4′-[(NHN=C(CN)$_2$]$_2$	**152**	25.9±6.7	21.9±1.9	[39]
3,3′-(CHO)$_2$,4,4′-(OH)$_2$	**153**	0.6±0.2	1.3±0.2	
3,4-(CO)$_2$O,3′,4′-(CO)$_2$O	**154**	20.9±1.7	18.6±2.0	
3,4-(COOH)$_2$,3′,4′-(COOH)$_2$	**155**	29.8±8.0	29.5±5.0	
3,3′-(NO$_2$)$_2$,4,4′-(COOH)$_2$	**156**	55	83	
3,3′,5-(NO$_2$)$_3$,4,4′-(Cl)$_2$	**157**	67.5±25.0	65.6±19.6	
3,3′-(NO$_2$)$_2$,4,4′-(SH)$_2$	**158**	2.9±0.7	2.5±0.5	
3,3′-(NO$_2$)$_2$,4,4′-(OCH$_2$COOH)$_2$	**159**	70.0±3.2	64.2±14.5	
2-NO$_2$,4-Cl	**160**	87.5	82.5	

Mazumder and coworkers synthesized eight curcumin analogs [40] following Pabon's method [41] and tested their bioactivity against HIV-1 integrase (**Table 1.20**). Curcumin derivatives **167** bearing catechol groups showed increased activity when compared to the parent curcumin **165**.

Table 1.20 Curcumin and related analogs as HIV-1 integrase inhibitors

Compound				No.	IC_{50} (μM)		Ref.
					3′-Processing	Strand transfer	
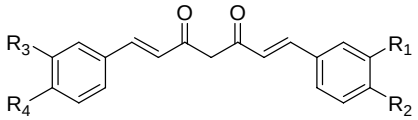							
R_1	R_2	R_3	R_4				
H	H	H	H	**161**	>300	>300	[40]
H	OH	H	OH	**162**	120	80±20	
H	OCH$_3$	H	OCH$_3$	**163**	>300	>300	
H	OH	OCH$_3$	OH	**164**	140	120	
OCH$_3$	OH	OCH$_3$	OH	**165**	150	140	
OCH$_3$	OH	OH	OH	**166**	18.0±9.0	9.0±3.0	
OH	OH	OH	OH	**167**	6.0±1.5	3.1±0.1	

Table 1.20 Continued

Compound	No.	IC_{50} (μM)		Ref.
		3′-Processing	Strand transfer	
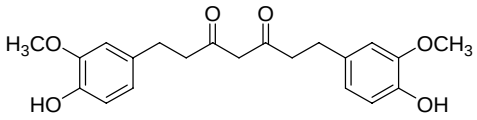 **168**	**168**	>300	>300	
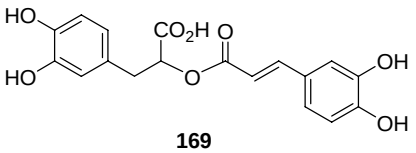 **169** Rosmarinic acid	**169**	9.0±7	4.0±1.5	

Artico and coworkers synthesized various cinnamoyl-based structures and tested their inhibitory effect against HIV-1 integrase. They studied effect of conformations of cyclovalone analogs **170**-**174** and indan derivatives **175**-**177** (**Table 1.21**). Compounds **178**-**181**, forced into a syn arrangement by conformation factors, were synthesized as open-chain counterpart of **167**-**174**. The effect of substitution pattern on chalcone derivatives **182**-**185** and the distance between two disubstituted benzenes were studied on 1,3-bis(cinnamoyl) benzene **193**-**194** compared to curcumin **165** and curcumin analogs **167**, **186**-**188**. They found that cyclovalone analogs **170**-**173** showed higher activity in 3'-processing due to the constrained and the presence of catechol of compared to curcumin analogs. Indane derivatives **175**-**177** both geometrically constrained in syn disposition, turned out to be active and moderately active, respectively. Chalcone derivatives **182** bearing 4-hydroxy on benzene of various ketones showed higher activity than dihydroxy groups **183** and non hydroxyl group bearing compounds **185**. The results of 1,3-bis(cinnamoyl)benzene **190** also comphasized the importance of catechol group over the distance between two disubstituted benzene ring compared to curcumin analogs [42].

Table 1.21 Cinnamoyl-base derivatives as HIV-1 integrase inhibitors

Compound	No.	IC_{50} (μM) 3′-Processing	Ref.
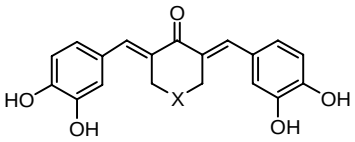			
X = CH_2	**170**	0.9±0.1	[42]
X = O	**171**	0.2±0.1	
X = S	**172**	0.2±0.1	
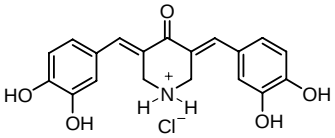 **173**	**173**	0.2±0.03	
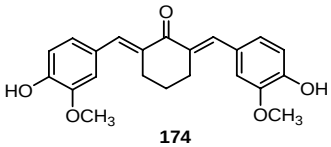 **174**	**174**	>100	
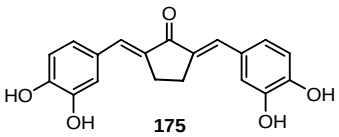 **175**	**175**	1±0.2	
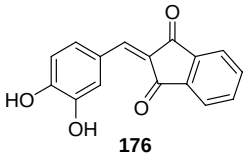 **176**	**176**	3±0.5	
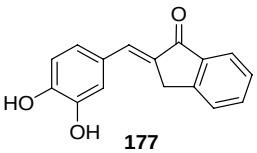 **177**	**177**	86±5	
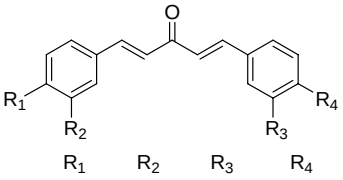	**178**	>100	
	179	37±1.5	
	180	0.6±0.3	
	181	>100	

	R_1	R_2	R_3	R_4
178	OCH_3	OCH_3	OCH_3	OCH_3
179	OH	OCH_3	OCH_3	OH
180	OH	OH	OH	OH
181	OH	H	H	OH

Table 1.21 Continued

Compound	No.	IC_{50} (μM) 3′-Processing	Ref.
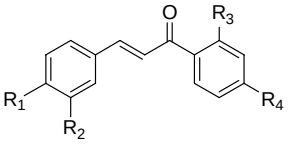	**182**	1.3±0.6	[42]
	183	20±4	
R1 R2 R3 R4 **182** OH OH H OH **183** OH OH OH OH **184** OH H OH OH **185** OH OH H H	**184**	>100	
	185	2.3±0.9	
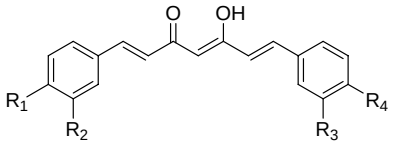	**186**	>100	
	187	>100	
R1 R2 R3 R4 **186** OCH_3 OCH_3 OCH_3 OCH_3 **187** OH H H OH **188** H H H H **165** OH OCH_3 OCH_3 OH **167** OH OH OH OH	**188**	>100	
	165	30±6	
	167	0.7±0.3	
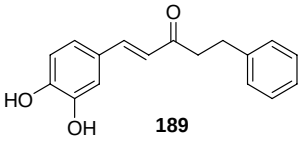 **189**	**189**	>100	
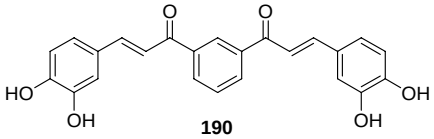 **190**	**190**	0.8±0.2	
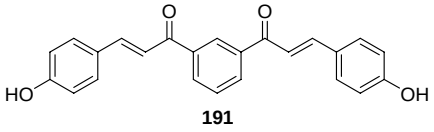 **191**	**191**	30±10	

Although compound **170** and related analogs endowed with potent inhibitory activity against IN enzyme assays, these compounds were found to be highly cytotoxic and totally ineffective in preventing the HIV-1 multiplication in acutely infected cells. In 2004, Costi and coworkers prepared and tested the biological activity of a series of catechol moiety that could be replaced by other 3,4-disubstituted systems (comprising with OH groups or without) (**Table 1.22**). They found that compound **230** showed the highest inhibitory activity in 3'-processing and strand transfer [43].

Table 1.22 Curcumin-like derivatives as HIV-1 integrase inhibitors

Compound	No.	IC_{50} (μM)		Ref.
		3′-Processing	Strand transfer	
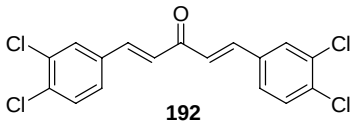 **192**	**192**	>100	>100	[43]
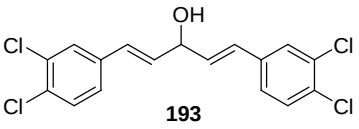 **193**	**193**	>100	>100	
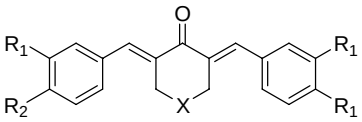	**194**	>100	>100	
	195	9±2	9±2	
	196	>100	>100	
	197	>100	>100	
	198	>100	>100	
	199	0.5±0.2	0.9±0.4	
	200	>100	>100	
	201	>100	>100	
	202	0.5±0.2	1.1±0.3	
	203	>100	>100	
	204	>100	>100	
	205	1.7±0.3	2.2±0.3	
	206	>100	>100	
	207	>100	>100	
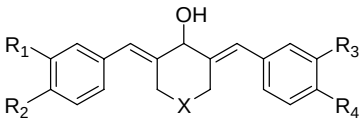	**208**	>100	>100	
	209	>100	>100	
	210	>100	>100	

	R_1	R_2	X
194	Cl	Cl	CH_2
195	Cl	Cl	O
196	Cl	Cl	S
197	NO_2	OH	NH
198	OH	NO_2	NH
199	OH	OH	NCH_3
200	NO_2	OH	NCH_3
201	OH	NO_2	NCH_3
202	OH	OH	NC_2H_5
203	NO_2	OH	NC_2H_5
204	OH	NO_2	NC_2H_5
205	OH	OH	NCH_2Ph
206	NO_2	OH	NCH_2Ph
207	OH	NO_2	NCH_2Ph

	R_1	R_2	X
208	Cl	Cl	CH_2
209	Cl	Cl	O
210	Cl	Cl	S

Table 1.22 Continued

Compound	No.	IC_{50} (μM)		Ref.
		3′-Processing	Strand transfer	
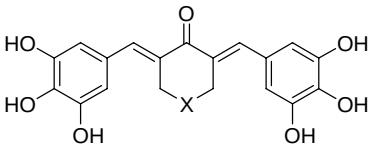 **211** X = NH **212** X = NCH_3 **213** X = NC_2H_5 **214** X = NCH_2Ph **215** X = CH_2 **216** X = O **217** X = S	**211**	0.3±0.1	0.5±0.2	[43]
	212	0.4±0.1	0.6±0.2	
	213	0.5±0.1	0.4±0.1	
	214	0.7±0.2	1.1±0.2	
	215	1.4±0.4	2.3±0.6	
	216	6.0±2.0	9.0±3.0	
	217	0.7±0.2	0.5±0.1	
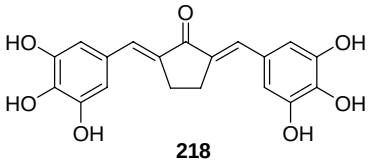 **218**	**218**	1.6±0.3	0.9±0.3	
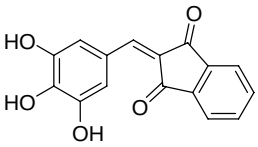 **219**	**219**	0.2±0.1	0.5±0.2	
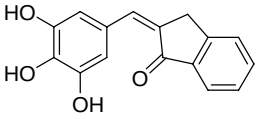 **220**	**220**	0.3±0.1	0.7±0.2	
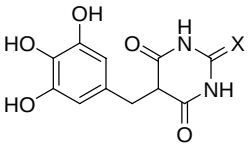 **221** X = O **222** X = S	**221**	3.0±0.5	4.0±1.0	
	222	1.0±0.3	1.6±0.2	
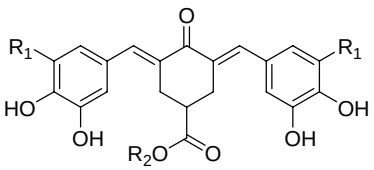	**223**	0.2±0.1	0.4±0.15	
	224	1.2±0.3	1.0±0.7	
	225	0.2±0.1	0.3±0.1	
	226	0.2±0.1	0.3±0.1	

R_1 R_2

223 H C_2H_5
224 H H
225 OH C_2H_5
226 OH H

Table 1.22 Continued

Compound	No.	IC_{50} (μM)		Ref.
		3′-Processing	Strand transfer	
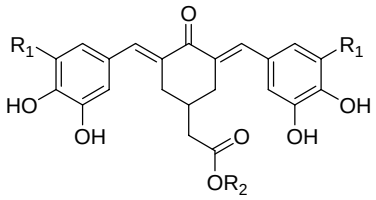	**227**	2.8±0.4	4.3±1.0	[43]
	228	0.7±0.3	1.2±0.4	
R_1 R_2	**229**	2.6±0.2	1.9±0.5	
227 H C_2H_5 **228** H H **229** OH C_2H_5 **230** OH H	**230**	0.2±0.1	0.2±0.1	

Comparing to curcumin, the boron complex **239** show much better inhibitory activity giving the IC_{50} value to be as low as 6 μM (**Table 1.23**) [44].

Table 1.23 Curcumin boron complexes as HIV-1 integrase inhibitors

Compound	No.	IC_{50} (μM)		Ref.
		HIV-1	HIV-2	
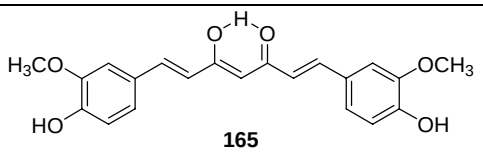 **165**	**165**	100	250	[44]
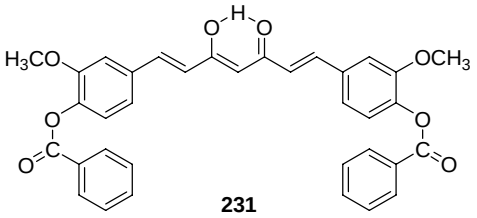 **231**	**231**	>50	>250	
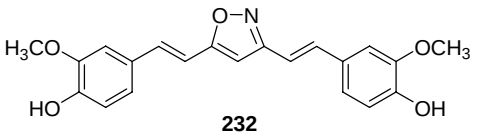 **232**	**232**	>100	300	
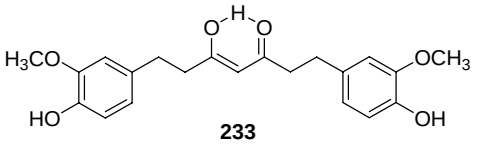 **233**	**233**	>100	600	

Table 1.23 Continued

Compound	No.	IC_{50} (μM)		Ref.
		HIV-1	HIV-2	
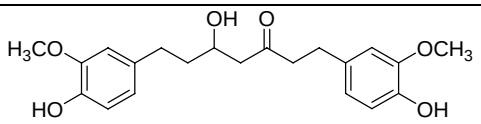 **234**	**234**	>100	nd[a]	[44]
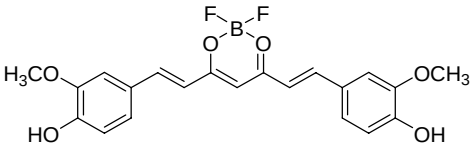 **235**	**235**	24	nd[a]	
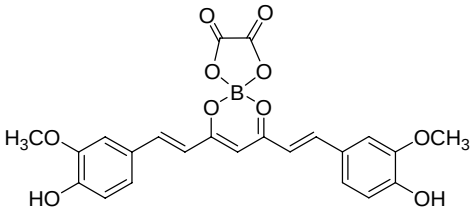 **236**	**236**	28	20	
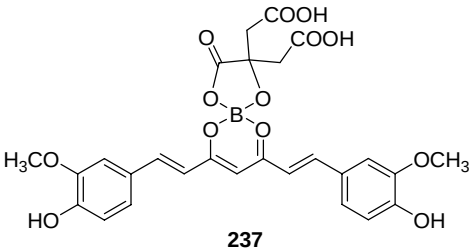 **237**	**237**	36	65	
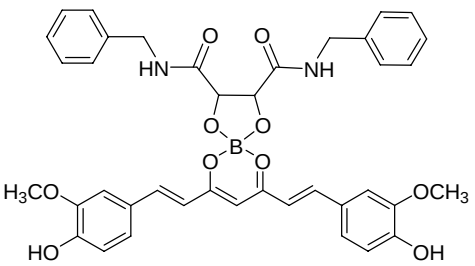 **238**	**238**	32	70	
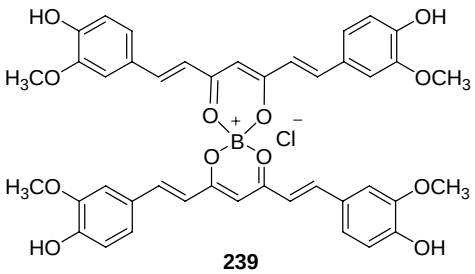 **239**	**239**	6	5.5	

Table 1.23 Continued

Compound	No.	IC_{50} (μM)		Ref.
		HIV-1	HIV-2	
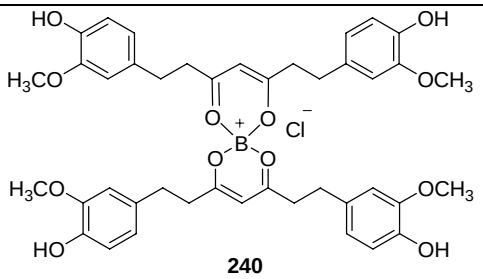 **240**	**240**	inactive	inactive	[44]
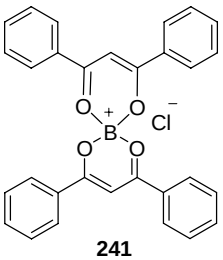 **241**	**241**	inactive	inactive	
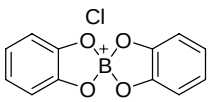 **242**	**242**	inactive	inactive	

[a]nd = not determined

Ramkumar and coworkers synthesized novel boron-containing compounds and tested their INI activities (**Table 1.24**) [45]. Some of the compounds such as **251** were found to increase the potency against HIV-1 IN and selective on integrase inhibition.

Table 1.24 3-Acetyl-4-hydroxy-2-pyranone derivatives and their difluoridoborate complexes as HIV-1 integrase inhibitors

Compound	No.	IC_{50} (μM)		Ref.
		3′-Processing	Strand transfer	
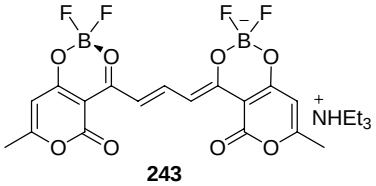 **243**	**243**	13±8	7±2	[45]

Table 1.24 Continued

Compound	No.	IC_{50} (μM)		Ref.
		3′-Processing	Strand transfer	
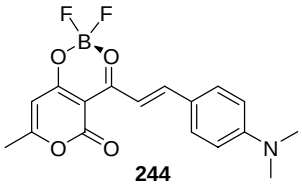 **244**	**244**	>100	56±1	[45]
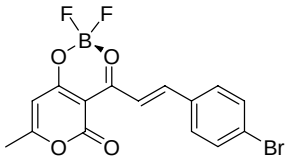 **245**	**245**	12±6	4±2	
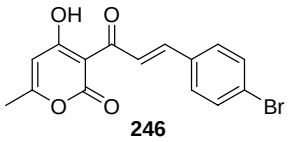 **246**	**246**	>100	>100	
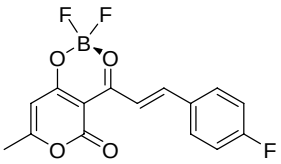 **247**	**247**	9±3	16±4	
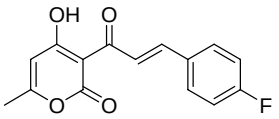 **248**	**248**	64	>100	
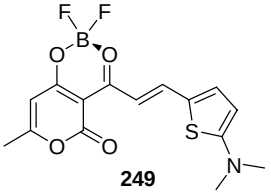 **249**	**249**	>100	>100	
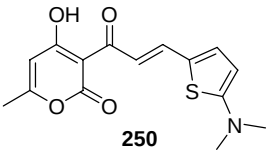 **250**	**250**	19±4	11±6	
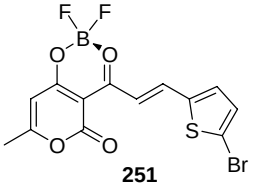 **251**	**251**	9±2	3±2	

Table 1.24 Continued

Compound	No.	IC_{50} (μM)		Ref.
		3′-Processing	Strand transfer	
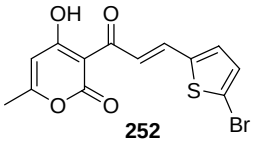 **252**	**252**	65±40	23±3	[45]
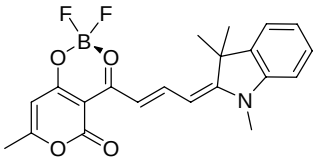 **253**	**253**	>100	>100	
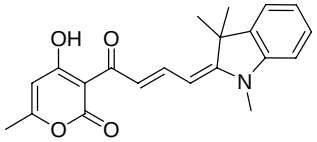 **254**	**254**	>100	>100	
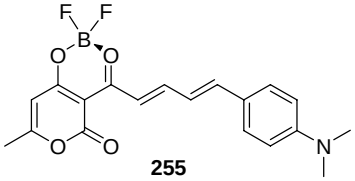 **255**	**255**	>100	100	
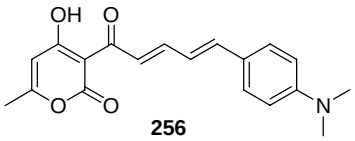 **256**	**256**	>100	>100	
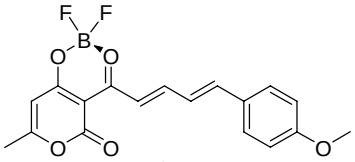 **257**	**257**	11±3	4±3	
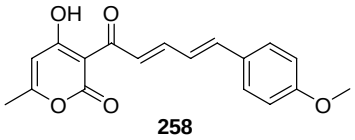 **258**	**258**	>100	39±14	
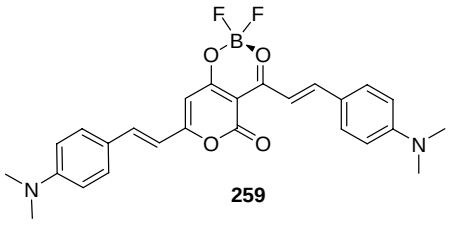 **259**	**259**	>100	>100	

Table 1.24 Continued

Compound	No.	IC_{50} (μM)		Ref.
		3′-Processing	Strand transfer	
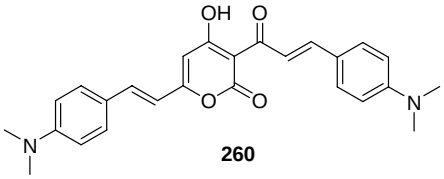 **260**	**260**	>100	>100	[45]
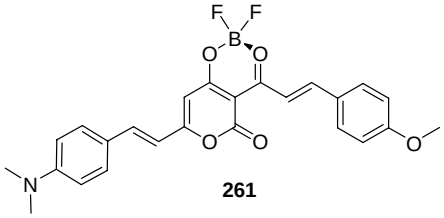 **261**	**261**	>100	>100	
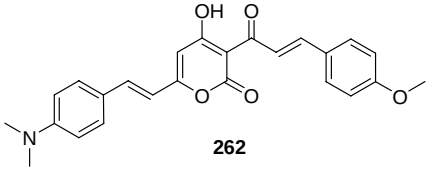 **262**	**262**	>100	>100	
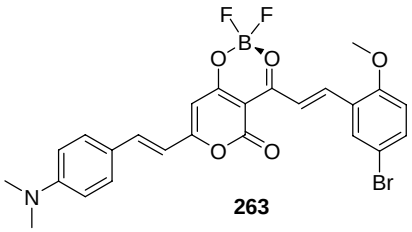 **263**	**263**	>100	>100	
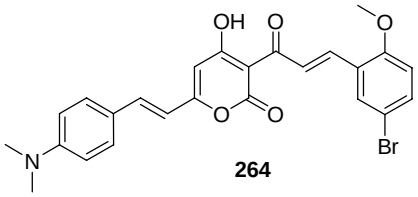 **264**	**264**	>100	100	

Compounds **265**-**282** were hydroxylated styrylquinolines. They showed potent activity by blocking the replication of HIV-1 in cell culture without significant cytotoxicity. Compounds **267**-**282** bearing carboxyl at C-7 and a hydroxyl at C-8 in the quinoline half gave the micromolar to submicromolar activities compared to the parent compounds **265** and **266** (**Table 1.25**) [46].

Table 1.25 Styrylquinolines as HIV-1 integrase inhibitors

Compound	No.	IC_{50} (μM)		Ref.
		3′-Processing	Strand transfer	
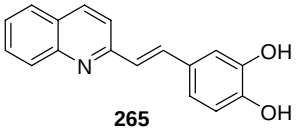 **265**	**265**	>100	nd	[46]
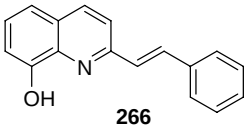 **266**	**266**	>100	>100	
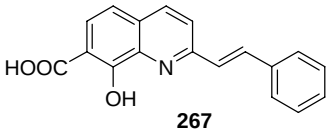 **267**	**267**	5.3	2.1	
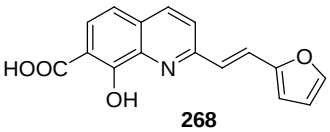 **268**	**268**	1.9	5.1	
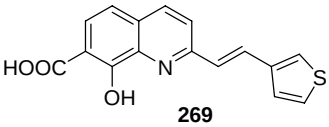 **269**	**269**	3.4	3.0	
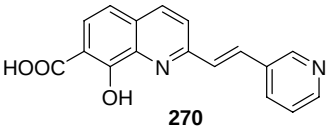 **270**	**270**	4.1	11	
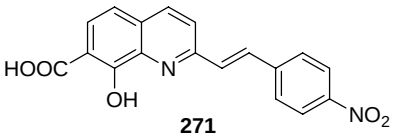 **271**	**271**	1.2	1.7	
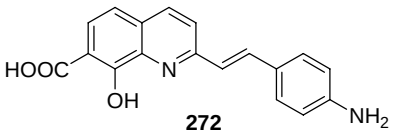 **272**	**272**	3.5	2.2	
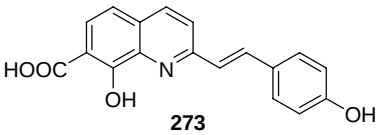 **273**	**273**	1.6	1.6	
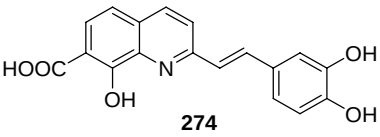 **274**	**274**	2.4	1.0	

Table 1.25 Continued

Compound	No.	IC_{50} (μM)		Ref.
		3′-Processing	Strand transfer	
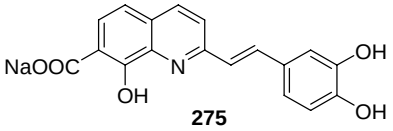 **275**	**275**	0.8	nd[a]	[46]
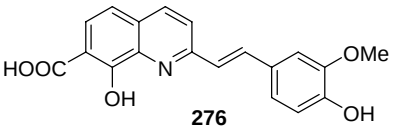 **276**	**276**	2.8	3.7	
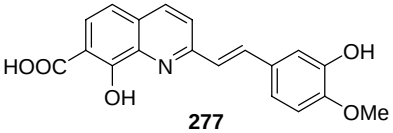 **277**	**277**	0.9	3.3	
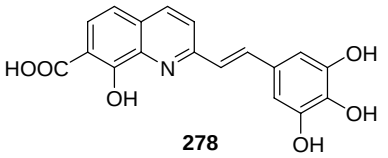 **278**	**278**	0.3	0.4	
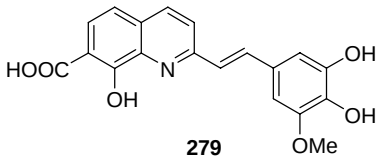 **279**	**279**	0.7	1.7	
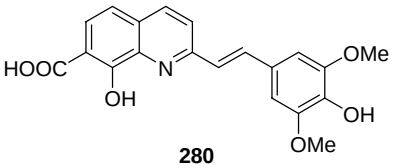 **280**	**280**	4.9	4.5	
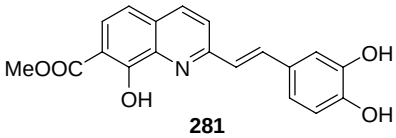 **281**	**281**	>100	>100	
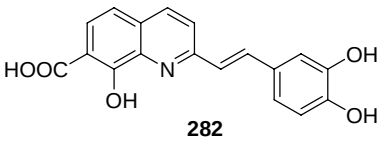 **282**	**282**	2.3	1.5	

[a]nd = not determined

Medicinal chemistry efforts based on an understanding of the mechanism of action of such diketone acid (DKA)-based compounds **283**-**288** (**Table 1.26**) and the required pharmacophore led to the identification of raltegravir **289**. Marchand and

coworkers studied the molecular interactions between DKA (**283** and **284**) and HIV-1 integrase [47]. They have compared 5CITEP (**285**) with one of the most potent DKAs reported by Merck group (L-708,906) and found that compound **285** inhibited 3'-processing and strand transfer with IC_{50} values of 35 μM and 0.65±0.19 μM respectively [47]. Moreover, compound **285** was successfully cocrystallized with the catalytic core domain of the enzyme. X-ray crystal structure of the complex showed that compound **285** was bound in the middle of the active site of the enzyme, lying between the three catalytic acidic residues, Asp64, Asp116 and Glu152, in the vicinity of the metal ion [14], whereas L-708,906 (**286**) is only active on strand transfer at 0.42±0.08 μM.

Hazuda and coworkers studied L-731988 (**287**) as inhibitors of strand transfer with IC_{50} value of 0.007 μM (**Table 1.26**) [48]. Embrey and coworkers reported that L-870812 (**288**) inhibited strand transfer with an IC_{50} value at 0.2 μM [49].

Table 1.26 Diketone acid as HIV-1 integrase inhibitors

Compound	No.	IC_{50} (μM)		Ref.
		3′-Processing	Strand transfer	
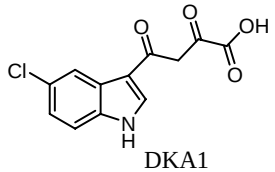 DKA1 **283**	**283**	65	0.52±0.10	[47]
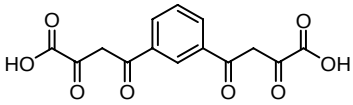 DKA2 **284**	**284**	7.8±2.2	1.83±0.32	
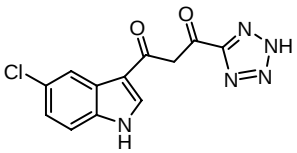 5CITEP **285**	**285**	35	0.65±0.19	

Table 1.26 Continued

Compound	No.	IC_{50} (μM)		Ref.
		3′-Processing	Strand transfer	
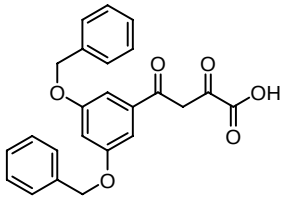 L-708,906 **286**	**286**	>100	0.42±0.08	[47]
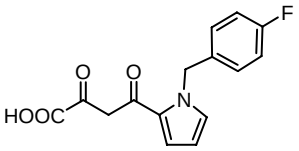 L-731988 **287**	**287**	>100	0.007	[48]
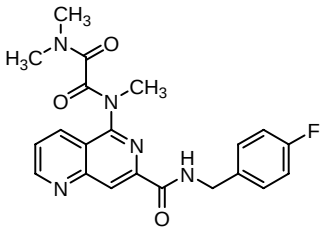 L-870812 **288**	**288**	nd[a]	0.2	[49]

[a]nd = not determined

In 2007, Raltegravir **289** (**Table 1.27**) was the first approved strand transfer inhibitor and is currently the only one drug against HIV-1 integrase for the treatment of HIV-1/AIDS. Miller and coworkers reported that compound **289** exhibited low nanomolar INI activity (IC_{50} of 2-7 nM) and strand transfer selectivity *in vitro*. It blocked HIV replication in a multiple-cycle replication assay with IC_{95} values of 19±14 nM and 33±23 nM in the presence of normal human serum (NHS) [50-53]. Elvitegravir **290** is another candidate presently in phase III clinical trials [53, 54].

Table 1.27 Raltegravir and elvitegravir as HIV-1 integrase inhibitors

Compound	No.	IC_{50} (μM) Strand transfer	Ref.
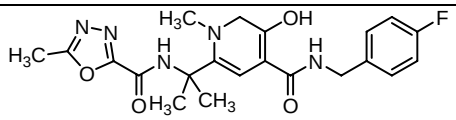 MK-0518 Raltegravir **289**	**289**	33 nM (IC_{95}) 10 nM (IC_{50})	[50-53]
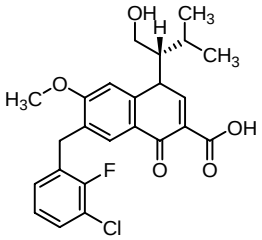 Elvitegravir **290**	**290**	1.2 nM (IC_{90})	[53, 54]

1.3 Synthetic method studies

Artico and coworkers synthesized various cinnamoyl-based structures and tested their inhibitory effect against HIV-1 integrase. For the synthesis of compounds **169-171, 181-184** and **189-190**, the catechol part of 3,4-dihydroxybenzaldehyde was protect by 3,4-dihydro-α-pyran in the presence of pyridinium *p*-toluenesulfonate to achieve 3,4-bis(tetrahydropyran-2-yloxy)benzaldehyde which reacted with various compounds having active methylene groups such as 2-propanone, cyclopentanone, cyclohexanone, 1,3-diacetylbenzene, 2,4-dihydroxyacetophenone, 2,3-dihydro-1-indanone, 2,3-dihydro-1,3-indandione, and others using Claisen-Schmidt condensation. The crude chalcone-like derivatives from condensation were subjected to deprotection by hydrolytic cleavage in the presence of *p*-toluenesulfonic acid (**Scheme 1.1-1.2**) [42].

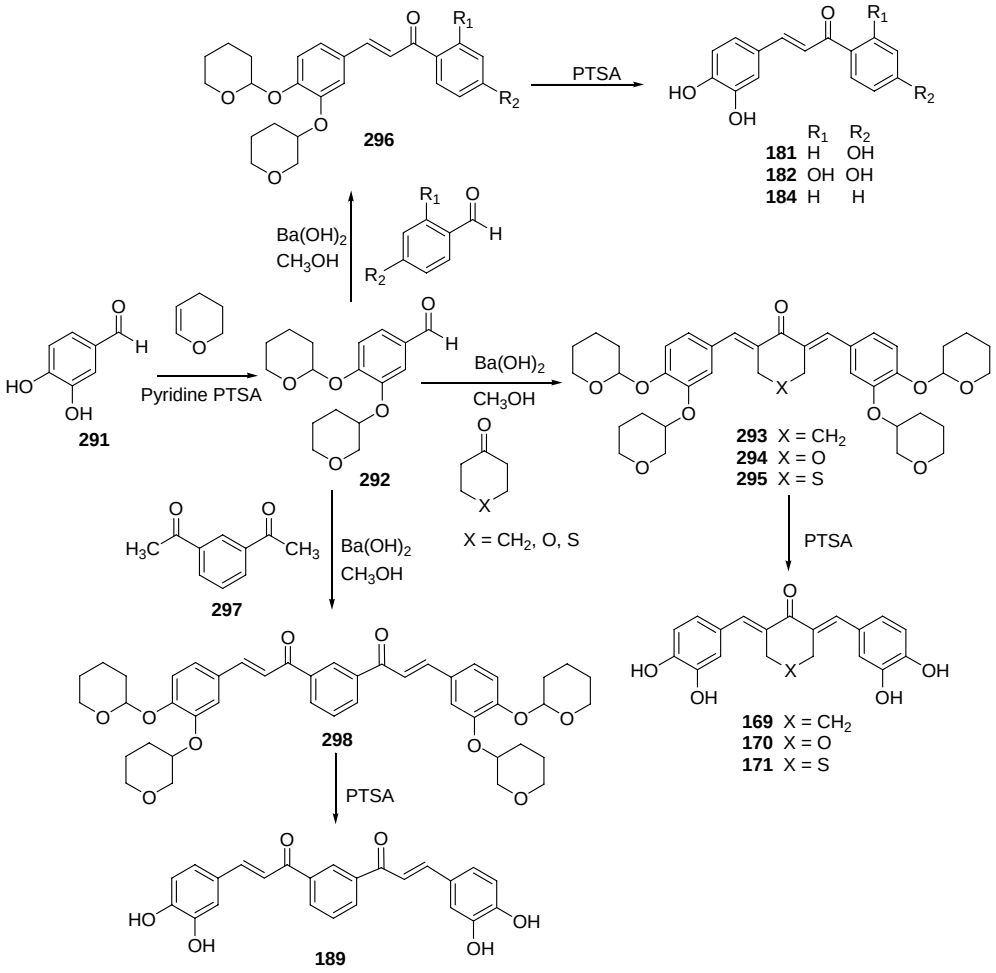

Scheme 1.1 Synthesis of various cinnamoyl-based structures

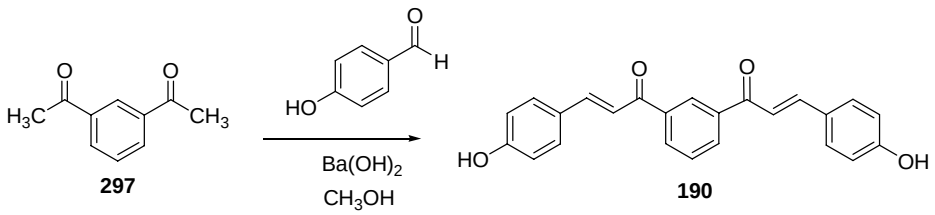

Scheme 1.2 Claisen-Schmidt condensation into a 1,3-bis(cinnamoyl)benzene derivative

Robinson and coworkers synthesized aromatic enones using Claisen-Schmidt condensation of various benzaldehydes condensed with various ketones under basic

condition which finally gave chalcone derivatives (**Scheme 1.3**) and tested via an established SVA cell proliferation assay [55].

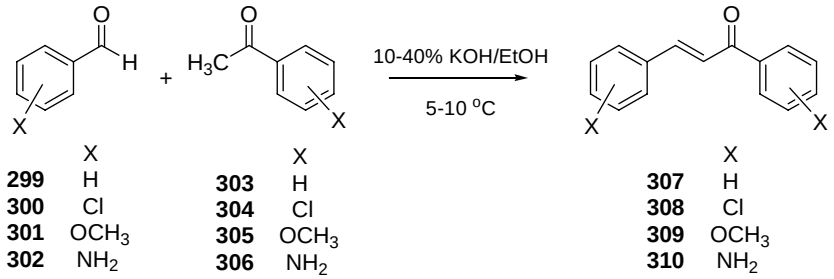

Scheme 1.3 Claisn-Schmidst condensation into enone derivatives

Jin and coworkers synthesized 2',4',6'-tris(methoxy) chalcone derivative **312** from 1-(2,4,6-trimethoxyphenyl) ethanone using KOH in methanol (**Scheme 1.4**). The compound showed anti-inflammatory activity [56].

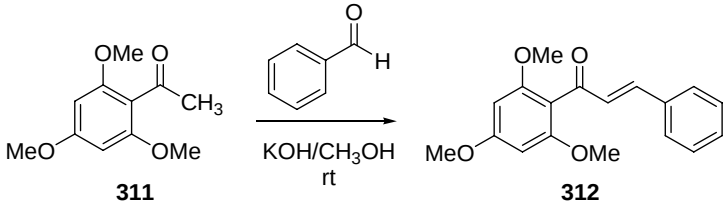

Scheme 1.4 Synthesis of 2',4',6'-tris(methoxy) chalcone derivative **312**

Aponte and coworkers synthesized compounds **315-318**, **321-325** from different series of acetophenones (**Scheme1.5**) [57]. 2,4,6-Trihydroxyacetophenone **313** was transformed into using dimethyl sulfate. Then, the methyl group at the *para*-methoxy group was remove using $AlCl_3$ to obtain 2,4-dihydroxy-6-methoxyaceptophenone **319** [58]. The hydroxyl groups were allyl bromide to give 2,4-allyloxy-6-methoxy-acetophenone **320** [59]. Claisen-Schmidt condensation with the corresponding aromatic aldehydes in the presence of aqueous KOH gave the chalcone products [60]. After a mild deprotection procedure to remove the allyl-protecting groups, using $Pd(PPh_3)_4$ and K_2CO_3, the resulting 2′4′-dihydroxy-6-methoxy chalcones [61] were finally reduced to produce the corresponding dihydrochalcones [62]. Compounds **315-318**, **321-325** were tested for *in vitro* anti-*T. cruzi* activity [57].

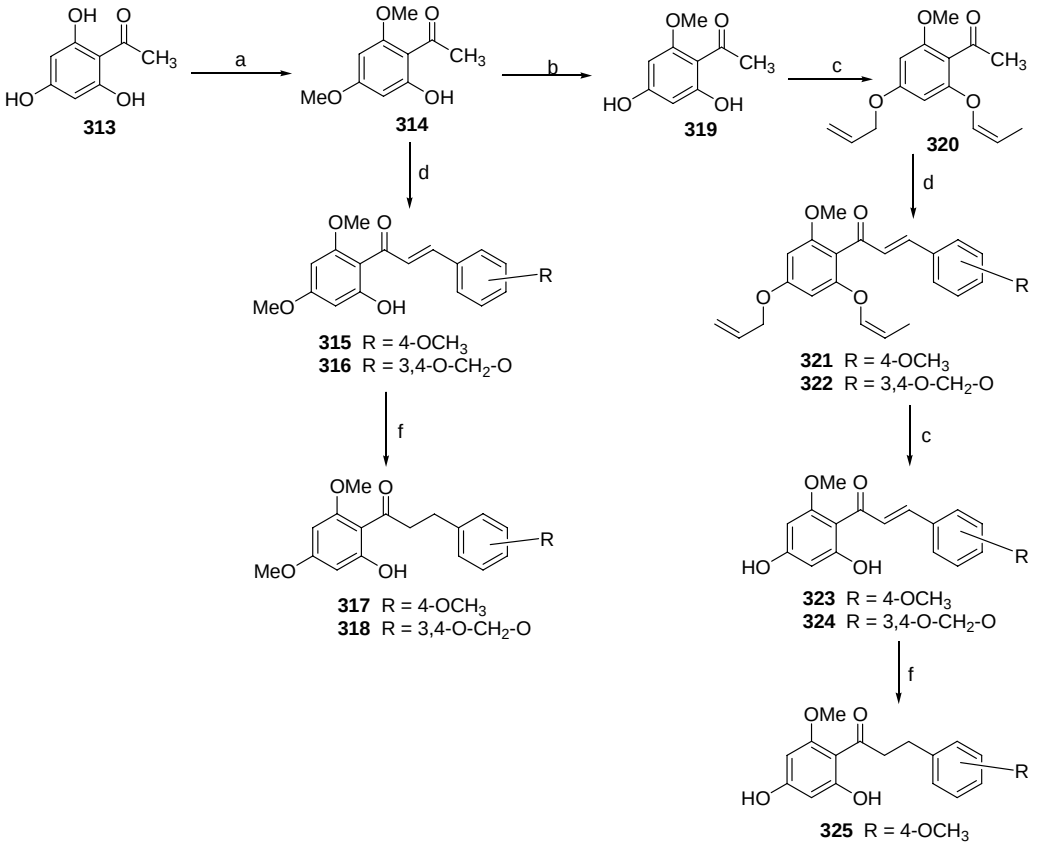

Scheme 1.5 Synthesis of compounds **315**-**318**, **321**-**325**; Reagent and conditions: (a) K_2CO_3, $(CH_3)_2SO_4$, $(CH_3)_2CO$, 65 °C, 6 h. (b) $AlCl_3$, benzene, reflux, 1 h. (c) K_2CO_3, allyl bromide, DMF, rt, overnight. (d) KOH, H_2O, CH_3OH, rt, 1-48 h. (e) K_2CO_3, catalytic $Pd(PPh_3)_4$, MeOH, 60 °C, 1 h. (f) catalytic Pd/C 5%, H_2 gas, 250 psi, EtOAc, rt, 1.5 h.

Maria and coworkers synthesized chalcones by Claisen-Schmidt condensation of various acetophenones and aromatic aldehydes (**Scheme 1.6**) and tested for anti-inflammatory activity [63].

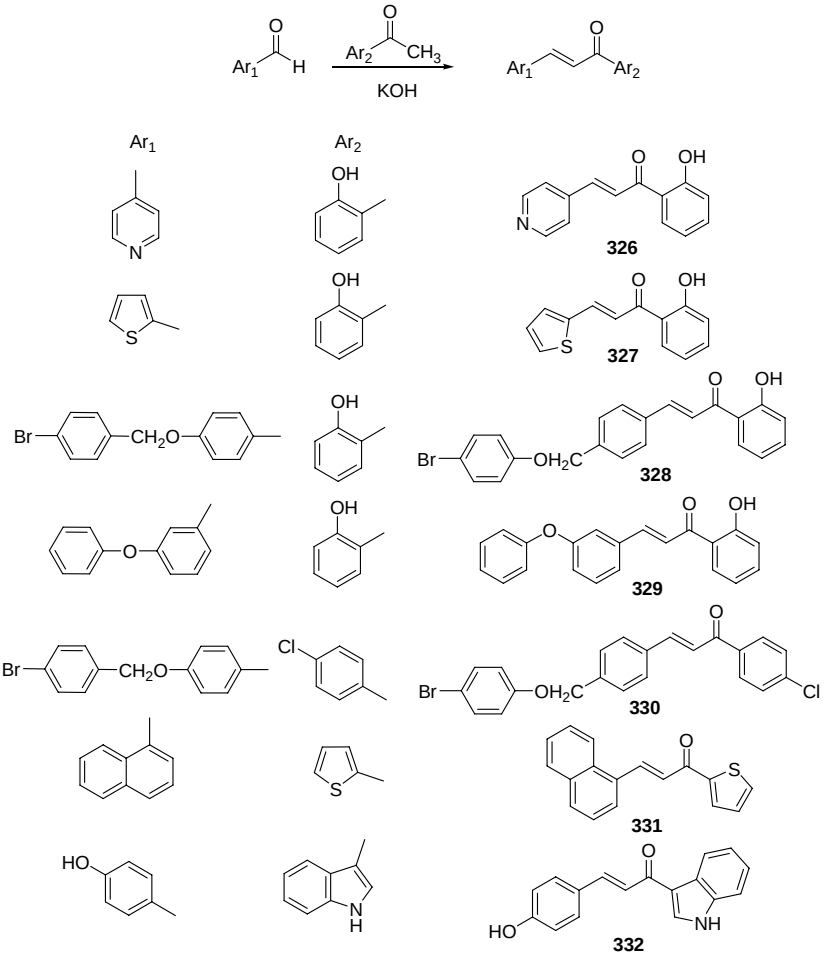

Scheme 1.6 Synthesis of chalcone derivatives

Mazumder and coworkers synthesized curcumin analogs by demethylation curcumin **165** using $AlCl_3$ as catalyst to obtain curcumin analogs that bearing catechol moieties and tested their bioactivity against HIV-1 integrase [40].

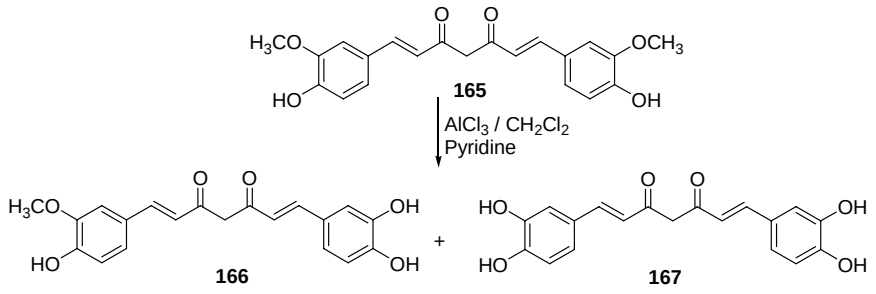

Scheme 1.7 Synthesis of compounds **166** and **167**

Choksakulporn synthesized 1,3,5-triacetyl-2,4,6-trihydroxybenzene from phloroglucinol dihydrate using acethylchloride and $AlCl_3$ under reflux condition to obtain 1,3,5-triacetyl-2,4,6-trihydroxybenzene **334** which was then methylateds into **335** (**Scheme 1.8**) [64, 65].

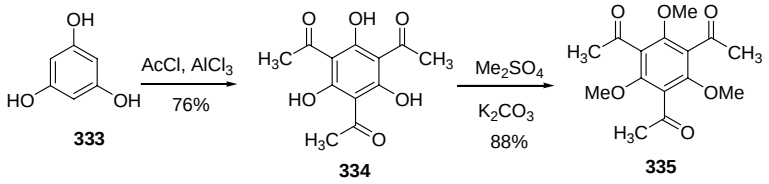

Scheme 1.8 Synthesis of compound **335**

1.4 Docking studies

Goldgur and coworkers studied the hydrogen bonding of 5CITEP 1-(5-chloroindol-3-yl)-3-hydroxy-3-(2*H*-tetrazol-5-yl)-propenone binding with HIV-1 integrase by X-ray crystallographic analysis (PDB code 1QS4) [14]. The essential amino acid residues of the enzyme, Gln148 and Glu152, interacted with nitrogen atom of the indole ring and enol hydroxyl of 5CITEP while Asn155, Thr66, Lys156 and Lys159 interacted with tetrazol by hydrogen bonding. Vajragupta and coworkers studied the interaction of curcumin with the active sites of HIV-1 integrase using molecular docking. The results showed hydrogen bonding between ligand and 9 amino acid residues, Asp116, Asp64, Glu92, Thr66, His67, Lys159, Asn120, Ser119 and Thr93 [66].

Healy and coworkers used Autodock 4.0 to study L-chicoric acid (L-CA), a bis-catechol that has been identified as a potent inhibitor of HIV-1 IN. The results for L-CA and its tetraacetylated derivatives with both 1QS4 and mutant Q148A are summarized in **Table 1.28** [67-69].

Table 1.28 The results of 100 independent docking runs for the ligands L-CA and its tetraacetylated derivative with proteins 1QS4 and the mutant Q148A

Ligand	IN Protein	Cluster Occ.[a]	ΔG_{bind} (kcal mol^{-1})	K_i (μM)	IC_{50} (relative)[b]	H-bonded residues
L-CA (s-*cis*/*s*-*cis*)	1QS4	44	-8.1	1.1	1	Asp116, Gln148, Lys156, Lys159
L -CA (s-*cis*/*s*-*trans*)	1QS4	29	-7.6	2.6	1	Thr66, His67, Asp92, Gln148, Lys156, Lys159
L -CA (s-*cis*/*s*-*cis*)	Q148A	27	-6.2	31.7	20	Asp116, Ala148, Lys156
L -CA tetraacetylated (s-*cis*/*s*-*cis*)	1QS4	33	-6.6	14.0	9	Thr66, His67, Gln148, Lys156, Lys159

[a] Number of individuals in the top-ranked cluster

[b] The relative values for L-CA with 1QS4 and Q148A are from [68] and the values for the tetraacetylated derivative of L-CA with 1QS4 are from [69]

1.5 HIV-1 integrase assay

There are many reports on HIV-1 integrase inhibitory assay such as isotope labeled substrate and denaturing gel separation of reaction products which were used for 3′-processing and strand transfer tested for HIV-1 integrase inhibitors [22] and non isotope technique is a method mimicking enzyme-linked immunosorbent assay (ELISA). This ELISA method is simple and can easily be adapted for high throughput screening of integrase inhibitors using DNA- coated plate [70].

In this work the integration activity was evaluated according to the multiplate integration assay (MIA) method previously described by Tewtrakul and coworkers [71, 72]. Digoxigenin-labelled target viral DNA (20 base pairs) is allowed to integrate with the immobilized host-cell donor DNA (34 base pairs) in the presence of integrase enzyme and a potential inhibitor. If the sample inhibits IN enzyme, the viral DNA would remain separated and being washed away. On the contrary, if the sample can not inhibit IN enzyme, the integrated viral DNA can bind to the alkaline phosphate

labeled anti-dioxigenin antibody which is subsequently added and followed by adding alkaline phosphatase containing *p*-nitrophenyl phosphate. The bound phosphatase release *p*-nitrophenol which exhibits a yellow color that absorbs visible light at λ_{max} 405 nm. The weakening or absence of this absorption comparing to the control indicates the higher degree of IN inhibition potency. This method is simple, convenient accurate and does not require the centrifugation, electrophoresis or other DNA denaturation steps. This assay screens for both 3'-processing and strand transfer inhibitors and can be used without any exposure to radioisotopes.

From the literature review, various structures of HIV-1 integrase inhibitors classes have been identified, including of hydroxylated aromatic or cinnamoyl analogues, such as bis-catechol (**67**), curcumin (**165**), curcumin analogues (**167**), various cinnamoyl-based structure groups (**190**, **191**) which these compounds have various ketones linker and various substituted benzenes. Computational structure-based design is a contributory tool for our understanding of the mechanism of integration, structural binding and identification of the action of the synthesized compounds. In this study, the effect on the activity of HIV-1 integrase inhibition from the number of cinnamoyl groups with various substitution patterns attached on the hexasubstituted benzene platform was probed. The anti HIV-1 integrase activity of the synthesized multi-cinnamoyl analoges were evaluated by the multiplate integration assay (MIA). Then, the molecular docking studies of selected compounds were performed to investigate the ligand-protein interactions responsible for the otained biological data.

1.6 Objectives

This work aimed to synthesize new multi-cinnamoyl analogs and test their biological activity against HIV-1 integrase and study the binding of new multi-cinnamoyl analogs to the active site of HIV-1 integrase by molecular modeling.

1.7 Scope of works

Synthesis of new multi-cinnamoyl analogs from 1,3,5-triacetyl-2,4,6-trihydroxybenzene and 1,3,5-triacetyl-2,4,6-trimethoxybenzene [64, 65] are performed using base with various substituted aldehydes and partial demethylation on flanking phenyl rings by $AlCl_3$ [40]. Their bioassay studies on HIV-1 IN inhibitory activity are carried out using the method reported by Tewtrakul and coworkers [71, 72]. The binding studies of new multi-cinnamoyl analogs to the active site of HIV-1 integrase enzyme are investigated by molecular modeling using molecular docking techniques (**Figure 1.4**).

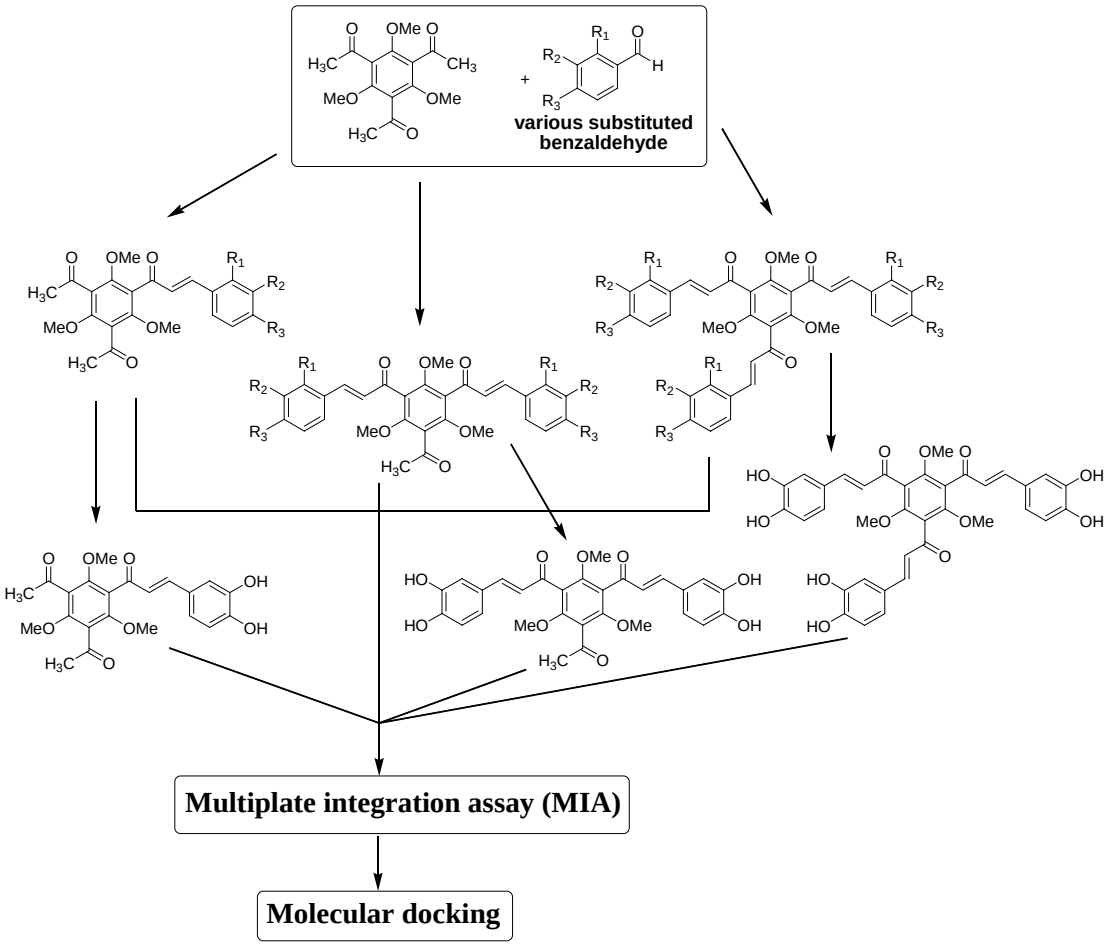

Figure 1.4 Synthesis strategies, bioactivity and molecular docking

CHAPTER II

EXPERIMENTAL

2.1 Instrumentation

The following analytical instruments were used throughout this work unless otherwise indicated.

The infrared (IR) spectra were recorded on FT-IR spectrometer model Nicolet 6700 using an ATR mode, Nicolet flourier transform infrared spectrophotometer: Impact 410 (Nicolet Instruments Technologies, Inc. WI, USA) and Perkin-Elmer FT-IR spectroscopy, spectrum RXI spectrometer (Perkin Elmer Instruments LLC., Shelton, USA).

^{1}H and ^{13}C NMR spectra were recorded on a Varian Mercury 400 spectrometer operating at 400 MHz for ^{1}H and 100 MHz for ^{13}C nuclei.

Mass spectra were determined on a mass spectrometer model VG TRIO 2000. Samples were dissolved in solvent and directly injected 100 μL of the solution into the mass spectrometer. Alternatively, mass spectrum of a high molecular weight sample was analyzed by matrix assisted laser desorption ionization-time of flight technique (MALDI-TOF): Microflex mass spectrometer (Bruker Daltonik GmbH, Germany). The instrument was equipped with nitrogen laser to desorb and ionize the samples, deposited on a stainless steel target. The sample was pre-dissolved in acetone and mixed with matrix solution.

2.2 Chemicals

Thin layer chromatography (TLC) was carried out using precoated silica gel on aluminum sheet (E. Merck Kieselgel 60 F254 with layer thickness 0.25 mm Merck KgaA, Darmstadt/Germany). Flash column chromatography was performed using Merck Kieselgel 60 Art 9385 (230/400 mesh) (Merck KgaA, Darmstadt, Germany). All solvents were used as purchased or were purified by distilled prior to use. All other chemicals were used as purchased unless noted otherwise.

2.3 Methods

2.3.1 Synthesis of 1,3,5-triacetyl-2,4,6-trihydroxybenzene (334)

Phloroglucinol dihydrate **333** (1,3,5-trihydroxybenzene dihydrate) (5.0 g, 30 mmol) was dissolved in excess acetyl chloride (50.0 mL) and anhydrous $AlCl_3$ (20.0 g, 15.0 mmol). The reaction was stirred under reflux for 1 h and was worked up with 10% HCl and then extracted with dichloromethane (3x100 mL). Evaporation of the solvent under vacuum gave crude product which was recrystallized in methanol to give colorless needle crystals of 1,3,5-triacetyl-2,4,6-trihydroxybenzene **334** (5.9 g, 76%). The reaction was showed in **Scheme 2.1**.

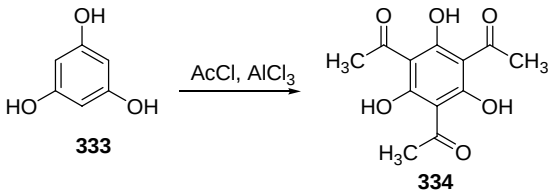

333 **334**

Scheme 2.1 Synthesis of compound **334**

^{1}H-NMR ($CDCl_3$) (δ, ppm): 2.72 (s, 9H, -COC<u>H</u>$_3$), 17.16 (s, 3H, -O<u>H</u>); ^{13}C-NMR ($CDCl_3$) (δ, ppm): 33.2, 103.3, 175.8, 205.2; IR (KBr pellet, cm^{-1}): 1579 (C=C), 1620 (C=O), 3426 (O-H); MS: [$M+H^+$]; m/z = 252.98.

2.3.2 Synthesis of 1,3,5-triacetyl-2,4,6-trimethoxybenzene (335)

1,3,5-Triacetyl-2,4,6-trihydroxybenzene **334** (5.9 g, 23 mmol) was dissolved in acetonitrile and added excess dimethyl sulfate (13.5 mL, 95.4 mmol) and K_2CO_3 (48.60 g, 352.0 mmol) and stirred under reflux for 13 h. The reaction was added with water 150 mL. The resulted precipitate was filtered, washed with cold water and crystallized from methanol to give 1,3,5-triacetyl-2,4,6-trimethoxybenzene **335** (6.0 g, 88%) The reaction was showed in **Scheme 2.2**.

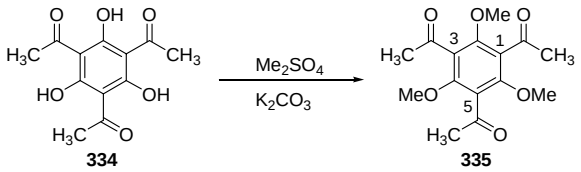

Scheme 2.2 Synthesis of compound **335**

^{1}H-NMR ($CDCl_3$) (δ, ppm): 2.54 (s, 9H, -COC<u>H</u>$_3$), 3.75 (s, 9H, -OC<u>H</u>$_3$); ^{13}C NMR ($CDCl_3$) (δ, ppm): 32.6, 64.7, 127.2, 155.4, 200.4; IR (KBr pellet, cm^{-1}): 1205 (C-O), 1582 (C=C), 1708 (C=O), 2947 (C-H);MS: [M+H$^+$]; m/z = 295.16.

2.3.3 Synthesis of 1-(2-hydroxycinnamoyl)-3,5-diacetyl-2,4,6-trimethoxy-benzene (336), 1,3-bis(2-hydroxycinnamoyl)-5-acetyl-2,4,6-trimethoxybenzene (337) and 1,3,5-tris(2-hydroxycinnamoyl)-2,4,6-trimethoxybenzene (338)

General procedure A: A mixture of 1,3,5-triacetyl-2,4,6-trimethoxybenzene **335** (590.0 mg, 2.0 mmol) and 2-hydroxybenzaldehyde (920.0 mg, 7.5 mmol) in methanol (20.0 mL) were added dropwise into a well stirred suspension of 80% aq KOH (5.0 mL). The mixture was stirred at room temperature for 7 h, then was worked up with 10% HCl and extracted with ethyl acetate (3x50 mL). The organic extracts were collected and washed with brine (3x50 mL), and dried by Na_2SO_4 anhydrous. Evaporation of the solvent gave the mixture of mono- **336**, bis- **337** and tris- **338** condensed products which were separated by gradient chromatography on silica gel column (hexane/ethyl acetate, 70:30, 60:40 and 20:80) to obtain pure **336** (228.0 mg, 28% yield), **337** (373.0 mg, 37% yield) and **338** (161.0 mg, 13% yield), respectively (**Scheme 2.3**).

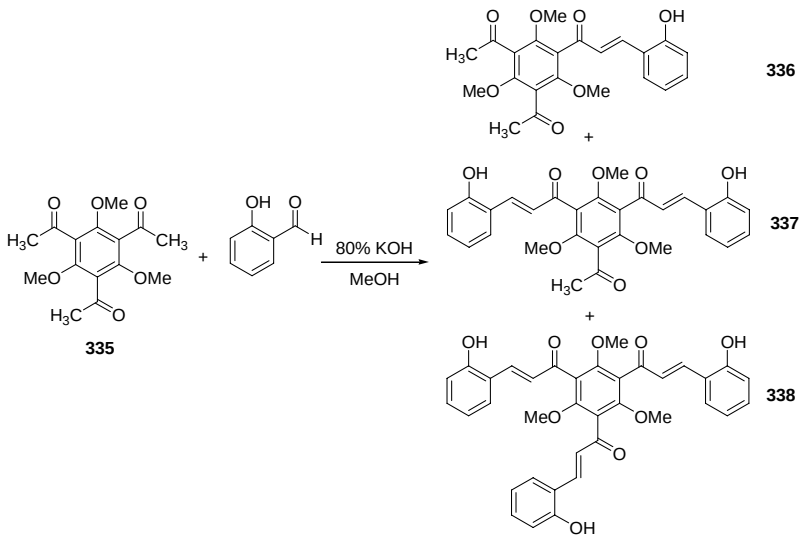

Scheme 2.3 Synthesis of compounds **336**, **337** and **338**

336: ^{1}H-NMR (Acetone-d_6) δ, ppm: 2.50 (s, 6H, -COC$\underline{H}_3$), 3.72 (s, 6H, -OC$\underline{H}_3$), 3.76 (s, 3H, -OC$\underline{H}_3$), 6.90 (t, 1H, H^{ar}, J = 8.0 Hz), 6.97 (d, 1H, H^{ar}, J = 8.0 Hz), 7.19 (d, 1H, -C$\underline{H}$, J = 16.0 Hz), 7.26 (t, 1H, H^{ar}, J = 8.0 Hz), 7.64 (d, 1H, H^{ar}, J = 4.0 Hz), 7.80 (d, 1H, -C$\underline{H}$, J = 16.3 Hz). ^{13}C-NMR (Acetone-d_6) δ, ppm: 31.7, 63.3, 63.7, 116.2, 120.1, 121.3, 124.9, 126.6, 127.7, 129.1, 132.3, 141.7, 154.9, 155.8, 156.9, 192.5, 199.8; IR cm^{-1}(ATR mode): 3456 (O-H st), 1682 and 1645 (C=O st); MS: [M+H^{+}]; m/z = 399.85

337: ^{1}H-NMR (Acetone-d_6) δ, ppm: 2.52 (s, 3H, -COC$\underline{H}_3$), 3.70 (s, 3H, -OC$\underline{H}_3$), 3.76 (s, 6H, -OC$\underline{H}_3$), 6.96 (t, 2H, H^{ar}, J = 8.0 Hz), 6.97 (d, 1H, H^{ar}, J = 8.0 Hz), 6.98 (d, 1H, H^{ar}, J = 8.0 Hz), 7.23 (d, 2H, -C$\underline{H}$, J = 16.0 Hz), 7.28 (t, 2H, H^{ar}, J = 8.0 Hz), 7.64 (d, 1H, H^{ar}, J = 8.0 Hz), 7.63 (d, 1H, H^{ar}, J = 8.0 Hz), 7.82 (d, 2H, -C$\underline{H}$, J = 16.0 Hz). ^{13}C-NMR (Acetone-d_6) δ, ppm: 31.7, 63.0, 63.3, 116.2, 120.1, 121.3, 124.8, 126.5, 127.9, 129.3, 132.2, 141.6, 155.7, 156.6, 156.9, 192.6, 199.8; IR cm^{-1} (ATR mode): 3159 (O-H st), 1706 and 1611 (C=O st). MS: [M+H^{+}]; m/z = 502.85

338: ^{1}H-NMR (Acetone-d_6) δ, ppm: 3.74 (s, 9H, -OC$\underline{H}_3$), 6.89 (t, 3H, H^{ar}, J = 8.0 Hz), 6.97 (d, 3H, H^{ar}, J = 8.0 Hz), 7.25 (d, 3H, -C$\underline{H}$, J = 16.0 Hz), 7.27 (t, 3H, H^{ar}, J = 8.0 Hz), 7.63 (d, 3H, H^{ar}, J = 8.0 Hz), 7.84 (d, 3H, -C$\underline{H}$, J = 16.0 Hz). ^{13}C-NMR (Acetone-d_6) δ, ppm: 63.1, 116.2, 120.1, 121.4, 124.8, 128.2, 129.5, 132.1, 141.6, 156.6, 156.9, 192.7; IR cm^{-1} (ATR mode): 3153(O-H st), 1737 (C=O st). MS: [M+H^{+}]; m/z = 607.11

2.3.4 Synthesis of 1-(3-hydroxycinnamoyl)-3,5-diacetyl-2,4,6-trimethoxy-benzene (339), 1,3-bis(3-hydroxycinnamoyl)-5-acetyl-2,4,6-trimethoxybenzene (340) and 1,3,5-tris(3-hydroxycinnamoyl)-2,4,6-trimethoxybenzene (341)

According to the general procedure A, 1,3,5-triacetyl-2,4,6-trimethoxybenzene **335** (588.0 mg, 2.0 mmol) and 3-hydroxybenzaldehyde (488.0 mg, 4.0 mmol) in methanol (20 mL) were added dropwise into a well stirred suspension of 80% aq KOH (5 mL). The mixture was stirred at room temperature for 1 day to give a crude product which were separated by gradient chromatography on silica gel column (hexane/ethyl acetate, 70:30, 60:40 and 20:80) to obtain pure **339** (242.0 mg, 28% yield), **340** (148.0 mg, 14% yield) and **341** (43.0 mg, 3% yield), respectively (**Scheme 2.4**).

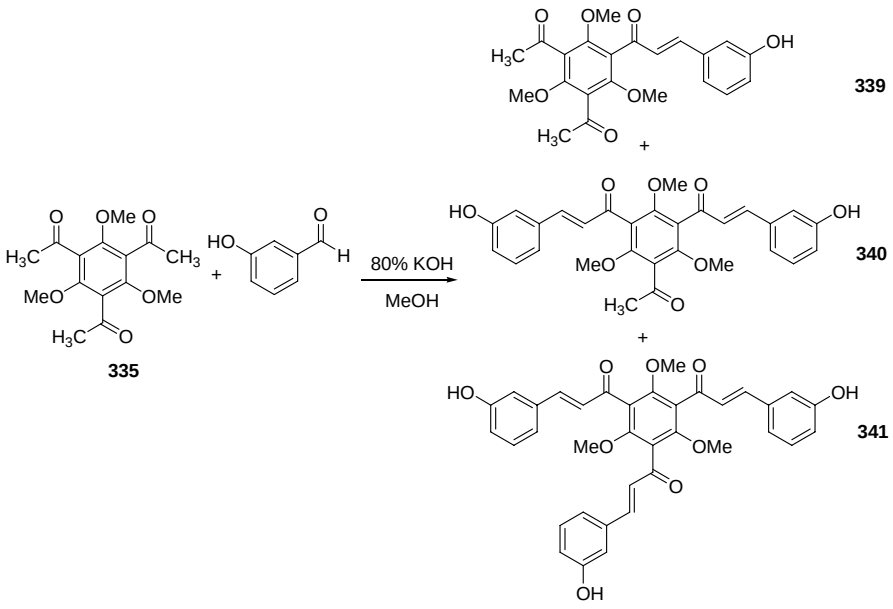

Scheme 2.4 Synthesis of compounds **339**, **340** and **341**

339: ^{1}H-NMR (Acetone-d_6) δ, (ppm): 2.53 (s, 6H, -COC<u>H</u>$_3$), 3.73 (s, 6H, -OC<u>H</u>$_3$), 3.79 (s, 3H, -OC<u>H</u>$_3$), 6.96 (d, 1H, H^{ar}, *J* = 8.0 Hz), 7.07 (d, 1H, -C<u>H</u>, *J* = 16.0 Hz), 7.17 (s, 1H, H^{ar}), 7.20 (d, 1H, H^{ar}, *J* = 8.0 Hz), 7.29 (t, 1H, H^{ar}, *J* = 8.0 Hz), 7.46 (d, 1H, -C<u>H</u>, *J* = 16.0 Hz), ^{13}C-NMR (Acetone-d_6) δ, (ppm): 32.6, 64.2, 64.5, 115.8, 118.9, 121.2, 125.5, 127.5, 128.9, 130.9, 136.8, 146.9, 156.1, 156.8, 158.7, 192.9,

200.6; IR cm^{-1} (ATR mode): 3202 (O-H st), 1694 and 1617 (C=O st); MS: $[M+H^+]$; m/z = 399.85

340: ^{1}H-NMR (Acetone-d_6) δ, (ppm): 2.55 (s, 3H, -COC<u>H</u>$_3$), 3.70 (s, 3H, -OC<u>H</u>$_3$), 3.77 (s, 6H, -OC<u>H</u>$_3$), 6.95 (d, 2H, H^{ar}, *J* = 16.0 Hz), 7.08 (d, 2H, -C<u>H</u>, *J* = 16.0 Hz), 7.19 (s, 2H, H^{ar}), 7.20 (d, 2H, H^{ar}, *J* = 8.0 Hz), 7.28 (t, 2H, H^{ar}, *J* = 8.0 Hz), 7.51 (d, 2H, -C<u>H</u>, *J* = 16.0 Hz); ^{13}C-NMR (Acetone-d_6) δ, (ppm): 32.6, 63.9, 64.2, 115.7, 118.9, 121.2, 122.2, 125.4, 127.5, 128.9, 130.9, 136.8, 146.9, 156.9, 157.5, 158.8, 193.1, 200.7; IR cm^{-1} (ATR mode): 3292 (O-H st), 1691 and 1642 (C=O st); MS: $[M+H^+]$; m/z = 502.93

341: ^{1}H-NMR (Acetone-d_6) δ, (ppm): 3.74 (s, 9H, -OC<u>H</u>$_3$), 6.95 (d, 3H, H^{ar}, *J* = 8.0 Hz), 7.09 (d, 3H, -C<u>H</u>, *J* = 16.0 Hz), 7.20 (s, 3H, H^{ar}), 7.21 (d, 3H, H^{ar}, *J* = 8.0 Hz), 7.28 (t, 3H, H^{ar}, *J* = 8.0 Hz), 7.56 (d, 3H, -C<u>H</u>, *J* = 16.0 Hz); ^{13}C-NMR (Acetone-d_6) δ, (ppm): 63.9, 115.6, 118.9, 121.3, 125.4, 129.0, 130.9, 136.8, 146.8, 157.9, 158.8, 193.2; IR cm^{-1} (ATR mode): 3246 (O-H) and 1629 (C=O); MS: $[M+H^+]$; m/z = 607.02

2.3.5 Synthesis of 1-(4-hydroxycinnamoyl)-3,5-diacetyl-2,4,6-trimethoxy-benzene (342), 1,3-bis(4-hydroxycinnamoyl)-5-acetyl-2,4,6-trimethoxybenzene (343) and 1,3,5-tris(4-hydroxycinnamoyl)-2,4,6-trimethoxybenzene (344)

According to the general procedure A, 1,3,5-triacetyl-2,4,6-trimethoxybenzene **335** (588.0 mg, 2.0 mmol) and 4-hydroxybenzaldehyde (254.0 mg, 2.0 mmol) in methanol (10.0 mL) were added dropwise into a well stirred suspension of 80% aq KOH (6.0 mL). The mixture was stirred at room temperature for 1 day to give a crude product which were separated by gradient chromatography on silica gel column (hexane/ethyl acetate, 70:30, 60:40 and 20:80) to obtain pure **342** (399.0 mg, 49% yield), **343** (196.0 mg, 19% yield) and **344** (66.0 mg, 5% yield), respectively (**Scheme 2.5**).

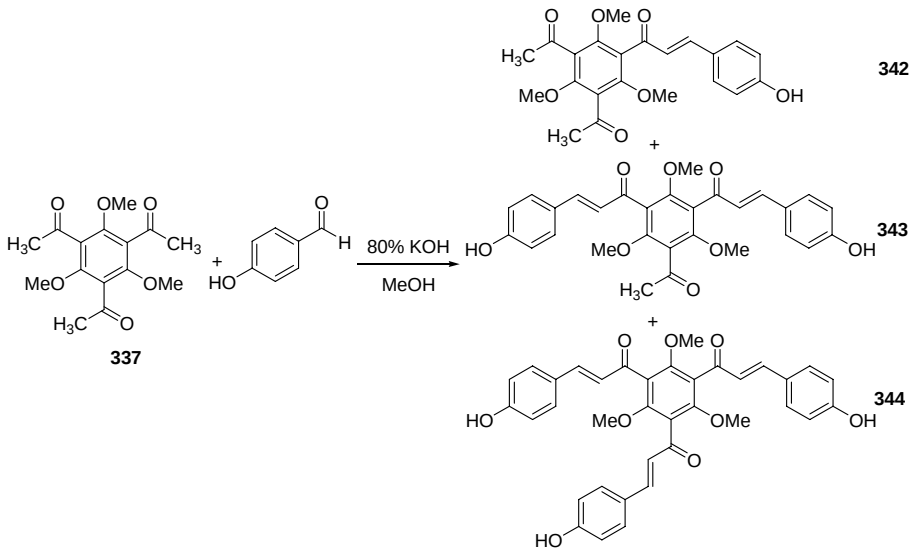

Scheme 2.5 Synthesis of compounds **342**, **343** and **344**

342: ^{1}H-NMR (Acetone-d_6) δ, (ppm): 2.53 (s, 6H, -COC<u>H</u>$_3$), 3.73 (s, 6H, -OC<u>H</u>$_3$), 3.78 (s, 3H, -OC<u>H</u>$_3$), 6.92 (d, 2H, H^{ar}, J = 8.0 Hz), 6.97 (d, 1H, -C<u>H</u>, J = 16.0 Hz), 7.45 (d, 1H, -C<u>H</u>, J = 16.0 Hz), 7.61 (d, 2H, H^{ar}, J = 8.0 Hz); ^{13}C-NMR (Acetone-d_6) δ, (ppm): 31.7, 63.2, 63.6, 116.0, 125.2, 126.0, 126.6, 130.8, 146.4, 154.9, 155.8, 160.4, 191.9, 199.8; IR cm^{-1} (ATR mode): 3394 (O-H st), 1691 and 1626 (C=O st); MS: [M+H$^+$]; m/z = 399.84

343: ^{1}H-NMR (Acetone-d_6) δ, (ppm): 2.52 (s, 6H, -COC<u>H</u>$_3$), 3.66 (s, 3H, -OC<u>H</u>$_3$), 3.74 (s, 6H, -OC<u>H</u>$_3$), 6.90 (d, 4H, H^{ar}, J = 8.0 Hz), 6.95 (d, 2H, -C<u>H</u>, J = 16.0 Hz), 7.47 (d, 4H, H^{ar}, J = 8.0 Hz) 7.60 (d, 2H, -C<u>H</u>, J = 16.0 Hz); ^{13}C-NMR (Acetone-d_6) δ, (ppm): 31.7, 62.9, 63.2, 115.9, 124.8, 125.2, 125.9, 126.6, 130.8, 146.5, 155.6, 156.4, 160.4, 192.2, 199.9; IR cm^{-1} (ATR mode): 3360 (O-H st), 1700 and 1629 (C=O st); MS: [M+H$^+$]; m/z = 502.80

344: ^{1}H-NMR (Acetone-d_6) δ, (ppm): 3.70 (s, 9H, -OC<u>H</u>$_3$), 6.90 (d, 6H, H^{ar}, J = 8.0 Hz), 6.96 (d, 3H, -C<u>H</u>, J = 16.0 Hz), 7.51 (d, 3H, -C<u>H</u>, J = 16.0 Hz), 7.61 (d, 6H, H^{ar}, J = 8.0 Hz); ^{13}C-NMR (Acetone-d_6) δ, (ppm): 62.9, 115.9, 124.8, 125.4, 126.1, 130.8, 146.3, 156.3, 160.2, 192.3; IR cm^{-1} (ATR mode): 3159 (O-H st), 1626 (C=O st); MS: [M+H$^+$]; m/z = 607.02

2.3.6 Synthesis of 1-(4-methoxycinnamoyl)-3,5-diacetyl-2,4,6-trimethoxy-benzene (345), 1,3-bis(4-methoxycinnamoyl)-5-acetyl-2,4,6-trimethoxybenzene (346) and 1,3,5-tris(4-methoxycinnamoyl)-2,4,6-trimethoxybenzene (347)

According to the general procedure A, 1,3,5-triacetyl-2,4,6-trimethoxybenzene **335** (600.0 mg, 2.0 mmol) and 4-hydroxybenzaldehyde (160.0 mg, 1.2 mmol) in methanol (20 mL) were added dropwise into a well stirred suspension of 80% aq KOH (1 mL). The mixture was stirred at room temperature for 4.5 h to give a crude product which were separated by gradient chromatography on silica gel column (hexane/ethyl acetate, 70:30, 60:40 and 20:80) to obtain pure **345** (331.0 mg, 39% yield), **346** (104.0 mg, 10% yield) and **347** (76.0 mg, 6% yield), respectively (**Scheme 2.6**).

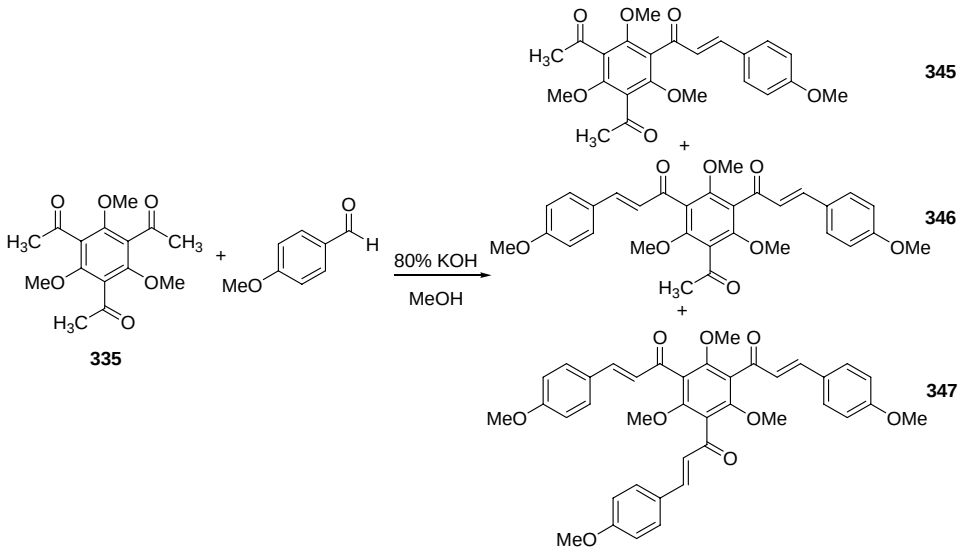

Scheme 2.6 Synthesis of compounds **345**, **346** and **347**

345: ^{1}H-NMR (Acetone-d_6) δ, (ppm): 2.53 (s, 6H, -COC<u>H</u>$_3$), 3.73 (s, 6H, -OC<u>H</u>$_3$), 3.79 (s, 3H, -OC<u>H</u>$_3$), 3.88 (s, 3H, -OC<u>H</u>$_3$), 7.01 (d, 1H, -C<u>H</u>, J = 12.0 Hz), 7.02 (d, 2H, H^{ar}, J = 8.0 Hz), 7.48 (d, 1H, -C<u>H</u>, J = 16.0 Hz), 7.69 (d, 2H, H^{ar}, J = 8.0 Hz); ^{13}C-NMR (Acetone-d_6) δ, (ppm): 31.7, 54.9, 63.2, 63.6, 114.5, 125.8, 127.0, 130.6, 130.9, 133.3, 134.2, 136.4, 138.4, 138.7, 145.9, 155.8, 162.2, 191.9, 199.7; IR cm^{-1} (ATR mode): 1694 and 1632 (C=O st); MS: [M+H^{+}]; m/z = 412.83.

346: ^{1}H-NMR (Acetone-d_6) δ, (ppm): 2.54 (s, 3H, -COC<u>H</u>$_3$), 3.69 (s, 3H, -OC<u>H</u>$_3$), 3.76 (s, 6H, -OC<u>H</u>$_3$), 3.87 (s, 6H, -OC<u>H</u>$_3$), 7.02 (d, 2H, -C<u>H</u>, *J* = 16.0 Hz), 7.03 (d, 4H, H^{ar}, *J* = 8.0 Hz), 7.53 (d, 2H, -C<u>H</u>, *J* = 16.0 Hz), 7.69 (d, 4H, H^{ar}, *J* = 8.0 Hz); ^{13}C-NMR (Acetone-d_6) δ, (ppm): 31.7, 54.9, 62.9, 63.3, 113.4, 114.5, 124.8, 125.8, 125.9, 126.4, 126.6, 127.1, 130.5, 132.5, 145.9, 155.7, 156.5, 163.2, 192.1, 199.9; IR cm^{-1} (ATR mode): 1700 and 1642 (C=O st); MS: [M+H^{+}]; m/z = 530.76.

347: ^{1}H-NMR (Acetone-d_6) δ, (ppm): 3.72 (s, 9H, -OC<u>H</u>$_3$), 3.87 (s, 9H, -OC<u>H</u>$_3$), 7.02 (d, 6H, H^{ar}, *J* = 8.0 Hz), 7.03 (d, 3H, -C<u>H</u>, *J* = 12.0 Hz), 7.56 (d, 3H, -C<u>H</u>, *J* = 16.0 Hz), 7.71 (d, 6H, H^{ar}, *J* = 8.0 Hz); ^{13}C-NMR (Acetone-d_6) δ, (ppm): 54.9, 63.0, 114.5, 124.8, 126.1, 127.1, 130.5, 145.8, 156.4, 162.1, 192.3; IR cm^{-1} (ATR mode): 1638 (C=O st); MS: [M+H^{+}]; m/z = 649.53.

2.3.7 Synthesis of 1-(4-hydroxy-3-methoxycinnamoyl)-3,5-diacetyl-2,4,6-trimethoxybenzene (348), 1,3-bis(4-hydroxy-3-methoxycinnamoyl)-5-acetyl-2,4,6-trimethoxybenzene (349) and 1,3,5-tris(4-hydroxy-3-methoxycinnamoyl)-2,4,6-trimethoxybenzene (350)

According to the general procedure A, 1,3,5-triacetyl-2,4,6-trimethoxybenzene **335** (620.0 mg, 2.1 mmol) and 4-hydroxy-3-methoxybenzaldehyde (640.0 mg, 4.2 mmol) in methanol (30.0 mL) were added dropwise into a well stirred suspension of 80% aq KOH (6.0 mL). The mixture was stirred at room temperature for 2 days to give a crude product which were separated by gradient chromatography on silica gel column (hexane/ethyl acetate, 70:30, 60:40 and 20:80) to obtain pure **348** (430.0 mg, 48% yield), **349** (210.0 mg, 18% yield) and **350** (70.0 mg, 5% yield), respectively (**Scheme 2.7**).

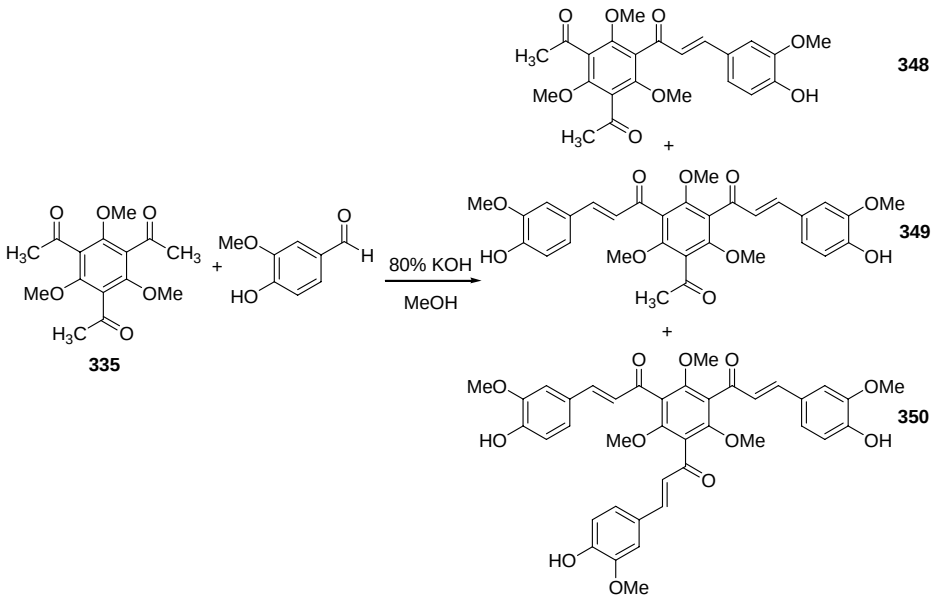

Scheme 2.7 Synthesis of compounds **348**, **349** and **350**

348: ^{1}H-NMR (Acetone-d_6) δ, (ppm): 2.52 (s, 6H, -COC$\underline{H}_3$), 3.73 (s, 6H, -OC$\underline{H}_3$), 3.78 (s, 3H, -OC$\underline{H}_3$), 3.93 (s, 3H, -OC$\underline{H}_3$), 6.89 (d, 1H, H^{ar}, *J* = 8.0 Hz), 7.01 (d, 1H, -C$\underline{H}$, *J* = 16.0 Hz), 7.19 (d, 1H, H^{ar}, *J* = 8.0 Hz), 7.41 (s, 1H, H^{ar}), 7.43 (d, 1H, -C$\underline{H}$, *J* = 16.0 Hz); ^{13}C-NMR (Acetone-d_6) δ, (ppm): 31.7, 55.5, 63.2, 63.6, 110.8, 115.3, 121.7, 124.1, 124.8, 125.1, 125.4, 126.5, 126.6, 146.8, 147.9, 149.8, 152.0, 154.9, 155.7, 191.9, 199.7; IR cm^{-1} (ATR mode): 3416 (O-H st), 1697 and 1632 (C=O st); MS: [M+H^{+}]; m/z = 429.55.

349: ^{1}H-NMR (Acetone-d_6) δ, (ppm): 2.52 (s, 3H, -COC$\underline{H}_3$), 3.66 (s, 3H, -OC$\underline{H}_3$), 3.74 (s, 3H, -OC$\underline{H}_3$), 3.90 (s, 6H, -OC$\underline{H}_3$), 6.87 (d, 2H, H^{ar}, *J* = 8.0 Hz), 6.99 (d, 2H, -C$\underline{H}$, *J* = 16.0 Hz), 7.19 (d, 2H, H^{ar}, *J* = 8.0 Hz), 7.39 (s, 2H, H^{ar}), 7.46 (d, 2H, -C$\underline{H}$, *J* = 16.0 Hz); ^{13}C-NMR (Acetone-d_6) δ, (ppm): 31.7, 55.5, 62.9, 63.2, 110.7, 115.3, 124.1, 124.9, 125.5, 126.5, 146.8, 147.9, 149.8, 155.5, 156.3, 192.2, 199.9; IR cm^{-1} (ATR mode): 3372 (O-H st), 1706 and 1629 (C=O st); MS: [M+H^{+}]; m/z = 563.61.

350: ^{1}H-NMR (Acetone-d_6) δ, (ppm): 3.72 (s, 9H, -OC$\underline{H}_3$), 3.92 (s, 9H, -OC$\underline{H}_3$), 6.89 (d, 6H, H^{ar}, *J* = 8.0 Hz), 7.01 (d, 3H, -C$\underline{H}$, *J* = 16.0 Hz), 7.23 (d, 3H, H^{ar}, *J* = 8.0 Hz), 7.41 (s, 3H, H^{ar}), 7.51 (d, 3H, -C$\underline{H}$, *J* = 16.0 Hz); ^{13}C-NMR (Acetone-d_6) δ, (ppm):

55.5, 62.9, 110.8, 115.3, 124.0, 124.9, 125.7, 126.6, 146.7, 148.0, 149.8, 156.2, 192.4; IR cm^{-1} (ATR mode): 3366 (O-H st), 1632 (C=O st); MS: $[M+H^+]$; m/z = 697.70.

2.3.8 Synthesis of 1-(3,4-dihydroxycinnamoyl)-3,5-diacetyl-2,4,6-trimethoxybenzene (351)

General procedure B, 1-(4-hydroxy-3-methoxycinnamoyl)-3,5-diacetyl-2,4,6-trimethoxybenzene (**348**) (210 mg, 0.4 mmol) was dissolved in dichloromethane (80 mL) and added $AlCl_3$ (450.0 mg, 2.9 mmol). The mixture was stirred at room temperature for 10 min and added pyridine (1.0 mL). After that the reaction was stirred under reflux for 30 h and worked up with 10% HCl. The water layer was extracted with ethyl acetate (3x50 mL). The organic extracts were combined with the previous dichloromethane layer and washed with brine (3x50 mL), and dried by Na_2SO_4 anhydrous. Evaporation of the solvent and purification of the crude product by gradient chromatography on silica gel column (hexane/ethyl acetate, 80:20 and 70:30) obtain the unreacted **348** (60.0 mg, 29% recovered) and pure **351** (34 mg, 18% yield), respectively (**Scheme 2.8**).

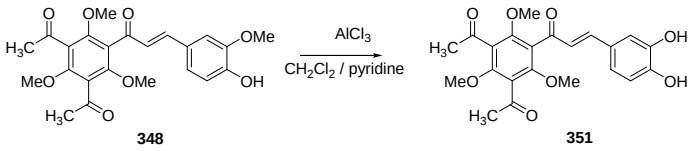

Scheme 2.8 Synthesis of compound **351**

351: ^{1}H-NMR (Acetone-d_6) δ, (ppm): 2.52 (s, 6H, -COC<u>H</u>$_3$), 3.72 (s, 6H, -OC<u>H</u>$_3$), 3.78 (s, 3H, -OC<u>H</u>$_3$), 6.89 (d, 1H, H^{ar}, J = 8.0 Hz), 6.90 (d, 1H, -C<u>H</u>, J = 16.0 Hz), 7.09 (d, 1H, H^{ar}, J = 8.0 Hz), 7.22 (s, 1H, H^{ar}), 7.38 (d, 1H, -C<u>H</u>, J = 16.0 Hz); ^{13}C-NMR (Acetone-d_6) δ, (ppm): 32.6, 64.1, 64.5, 115.6, 116.5, 123.5, 125.9, 126.1, 127.5, 146.4, 147.7, 149.5, 155.8, 156.7, 192.8, 200.7.

2.3.9 Synthesis of 1-(3,4-dihydroxycinnamoyl)-3-(4-hydroxy-3-methoxy-cinnamoyl)-5-acetyl-2,4,6-trimethoxybenzene (352) and 1,3-bis(3,4-dihydroxy-cinnamoyl)-5-acetyl-2,4,6-trimethoxybenzene (353)

According to the general procedure B, 1,3-bis(4-hydroxy-3-methoxycinnamoyl)-5-acetyl-2,4,6-trimethoxybenzene (**349**) (240.0 mg, 0.4 mmol) dissolved in dichloromethane (30.0 mL) was added $AlCl_3$ (400 mg, 2.9 mmol). The mixture was stirred at room temperature for 10 min and added pyridine (1.5 mL). After that the reaction was stirred under reflux condition for 10 h and was worked up with 10% HCl to give a crude product which were separated by gradient chromatography on silica gel column (hexane/ethyl acetate, 60:40 and 40:60) to obtain unreacted **349** (47.0 mg, 19% recovered), **352** (30.0 mg, 12% yield) and **353** (20.0 mg, 8% yield), respectively (**Scheme 2.9**).

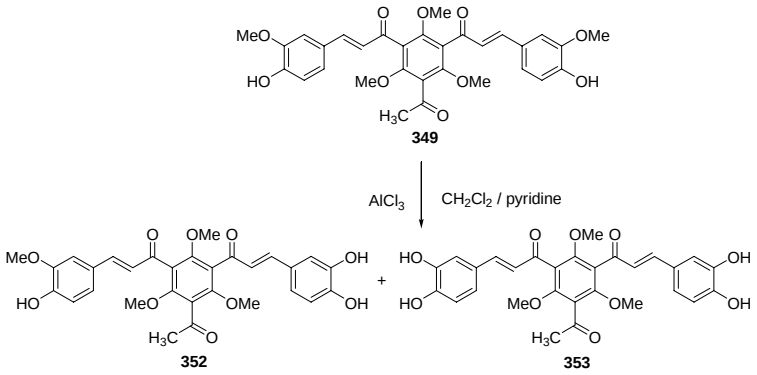

Scheme 2.9 Synthesis of compounds **352** and **353**

352: ^{1}H-NMR (Acetone-d_6) δ, (ppm): 2.53 (s, 3H, -COC<u>H</u>$_3$), 3.67 (s, 3H, -OC<u>H</u>$_3$), 3.76 (s, 6H, -OC<u>H</u>$_3$), 3.92 (s, 3H, -OC<u>H</u>$_3$), 6.89 (d, 2H, H^{ar}, J = 8.0 Hz), 6.90 (d, 1H, -C<u>H</u>, J = 12.0 Hz), 7.00 (d, 1H, -C<u>H</u>, J = 16.0 Hz), 7.10 (d, 1H, H^{ar}, J = 8.0 Hz), 7.20 (d, 1H, H^{ar} J = 12 Hz), 7.24 (s, 1H, H^{ar}), 7.40 (s, 1H, H^{ar}), 7.42 (d, 1H, -C<u>H</u>, J = 16.0 Hz), 7.46 (d, 1H, -C<u>H</u>, J = 20.0 Hz); ^{13}C-NMR (Acetone-d_6) δ, (ppm): 32.6, 56.4, 63.8, 64.1, 111.7, 115.5, 116.2, 116.5, 123.5, 124.9, 125.8, 126.2, 126.5, 127.4, 127.6, 146.5, 147.6, 147.7, 148.9, 149.5, 150.7, 156.6, 157.3, 193.1, 200.8.

353: ^{1}H-NMR (Acetone-d_6) δ, (ppm): 2.51 (s, 3H, -COC<u>H</u>$_3$), 3.65 (s, 3H, -OC<u>H</u>$_3$), 3.73 (s, 6H, -OC<u>H</u>$_3$), 6.87 (d, 2H, H^{ar}, J = 8.0 Hz), 6.88 (d, 2H, -C<u>H</u>, J = 12.0 Hz),

7.08 (d, 2H, H^{ar}, *J* = 8.0 Hz), 7.22 (s, 2H, H^{ar}), 7.39 (d, 2H, -C<u>H</u>, *J* = 16.0 Hz); ^{13}C-NMR (Acetone-d_6) δ, (ppm): 32.6, 63.8, 64.1, 115.4, 115.5, 116.5, 123.5, 123.7, 124.8, 126.3, 127.4, 146.4, 146.9, 147.4, 147.6, 149.4, 156.5, 163.5, 168.3, 192.9, 201.0.

2.3.10 Synthesis of 1-(3,4-dihydroxycinnamoyl)-3,5-bis(4-hydroxy-3-methoxycinnamoyl)-2,4,6-trimethoxybenzene (354), 1,3-bis(3,4-dihydroxycinnamoyl)-5-(4-hydroxy-3-methoxycinnamoyl)-2,4,6-trimethoxybenzene (355) and 1,3,5-tris(3,4-dihydroxycinnamoyl)-2,4,6-trimethoxybenzene (356)

According to the general procedure B, 1,3,5-tris(4-hydroxy-3-methoxycinnamoyl)-2,4,6-trimethoxybenzene (**350**) (400.0 mg, 0.5 mmol) dissolved in dichloromethane (30.0 mL) was added $AlCl_3$ (540 mg, 4.0 mmol) The mixture was stirred at room temperature for 10 min and added pyridine (1.5 mL). After that the reaction was stirred under reflux condition for 10 h. The reaction was worked up with 10% HCl to give a crude product which were separated by using gradient preparative chromatography on TLC plate (dichloromethane/methanol, 99:1) to obtain unreacted compounds **350** (37.0 mg, 9% recovered), **354** (31.0 mg, 7.4% yield), **355** (27.0 mg, 6.5% yield) and **356** (10.0 mg, 2.4% yield) (**Scheme 2.10**).

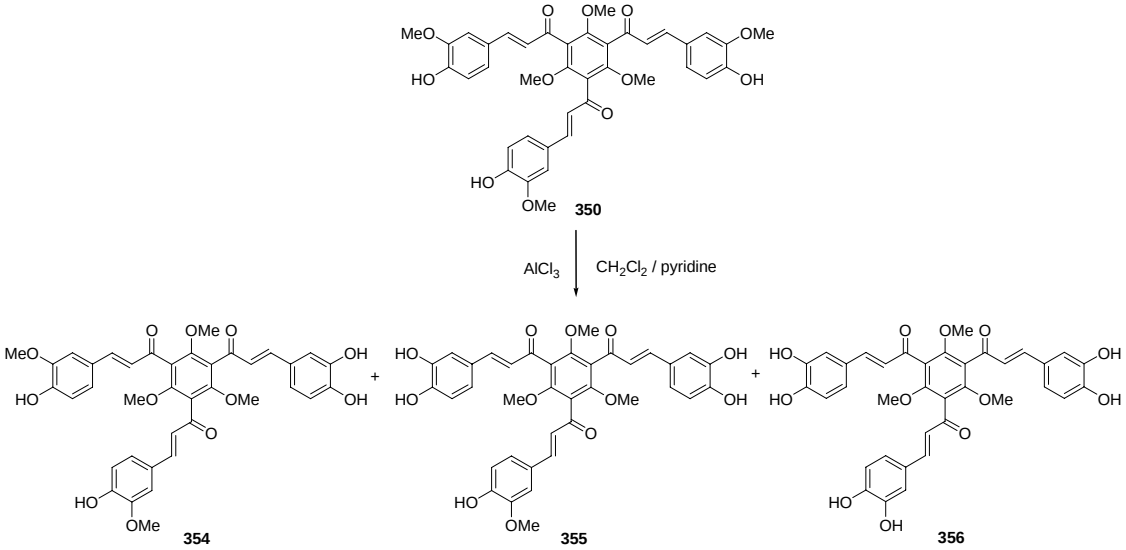

Scheme 2.10 Synthesis of compounds **354**, **355** and **356**

354: ^{1}H-NMR (Acetone-d_6) δ, (ppm): 3.71 (s, 9H, -OC<u>H</u>$_3$), 3.91 (s, 6H, -OC<u>H</u>$_3$), 6.83 (d, 1H, H^{ar}, *J* = 4.0 Hz), 6.86 (d, 1H, -C<u>H</u>, *J* = 16.0 Hz), 6.88 (d, 2H, H^{ar}, *J* = 4.0 Hz), 6.99 (d, 2H, -C<u>H</u>, *J* = 16.0 Hz), 7.06 (d, 1H, H^{ar}, *J* = 8.0 Hz), 7.21 (s, 1H, H^{ar}), 7.28 (d, 2H, H^{ar}, *J* = 8.0 Hz), 7.38 (s, 2H, H^{ar}), 7.44 (d, 1H, -C<u>H</u>, *J* = 16.0 Hz), 7.49 (d, 2H, -C<u>H</u>, *J* = 16.0 Hz); ^{13}C-NMR (Acetone-d_6) δ, (ppm): 56.4, 63.8, 63.9, 111.8, 115.1, 116.3, 116.6, 123.6, 124.8, 125.5, 125.8, 125.9, 126.5, 127.3, 147.4, 147.7, 148.9, 150.9, 151.6, 157.0, 157.1, 193.1, 193.4.

355: ^{1}H-NMR (Acetone-d_6) δ, (ppm): 3.71 (s, 9H, -OC<u>H</u>$_3$), 3.90 (s, 3H, -OC<u>H</u>$_3$), 6.84 (d, 2H, H^{ar}, *J* = 4.0 Hz), 6.87 (d, 2H, -C<u>H</u>, *J* = 16.0 Hz), 6.88 (d, 1H, H^{ar}, *J* = 4.0 Hz), 6.99 (d, 1H, -C<u>H</u>, *J* = 16.0 Hz), 7.08 (d, 2H, H^{ar}, *J* = 8.0 Hz), 7.22 (d, 1H, H^{ar}, *J* = 8.0 Hz), 7.23 (s, 2H, H^{ar}), 7.39 (d, 2H, -C<u>H</u>, *J* = 20 Hz), 7.42 (s, 1H, H^{ar}), 7.48 (d, 1H, -C<u>H</u>, *J* = 16.0 Hz); ^{13}C-NMR (Acetone-d_6) δ, (ppm): 56.4, 63.9, 111.8, 115.5, 116.3, 116.5, 123.3, 124.8, 125.8, 125.9, 126.5, 126.9, 127.4, 147.1, 147.6, 148.0, 148.9, 150.7, 150.8, 157.1, 157.2, 193.2, 193.4.

356: ^{1}H-NMR (Acetone-d_6) δ, (ppm): 3.57 (s, 9H, -OC<u>H</u>$_3$), 6.70 (d, 3H, -C<u>H</u>, *J* = 16.0 Hz), 6.70 (d, 3H, H^{ar}, *J* = 8 Hz), 7.05 (d, 3H, H^{ar}, *J* = 8 Hz), 7.06 (d, 3H, -C<u>H</u>, *J* = 16.0 Hz), 7.11 (s, 3H, H^{ar})

2.3.11 Synthesis of 1-(4-hydroxycinnamoyl)-3,5-diacetyl-2,4,6-trihydroxy-benzene (357), 1,3-bis(4-hydroxycinnamoyl)-5-acetyl-2,4,6-trihydroxybenzene (358) and 1,3,5-tris(4-hydroxycinnamoyl)-2,4,6-trihydroxybenzene (359)

In the second method, attempt synthesized the compound **334** was directly condensed with 4-hydroxybenzaldehyde using KOH or NaOEt as the initiated base. The reaction did not yield the desired products, after work up reaction with 10% HCl. Only the starting **334** and 4-hydroxybenzaldehyde were recovered (**Scheme 2.11**).

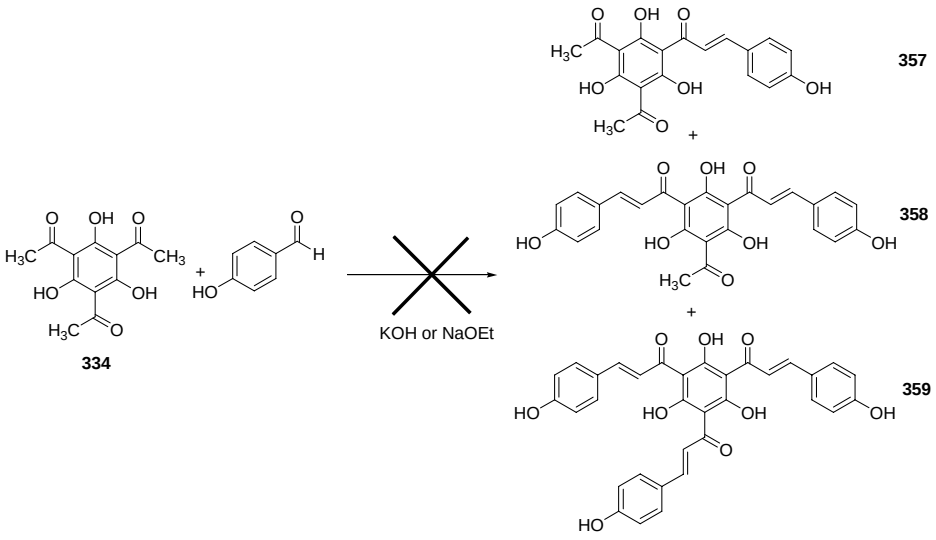

Scheme 2.11 Attempted synthesized of compounds **357**, **358** and **359**

2.4 Assay of HIV-1 IN inhibitory activity

2.4.1 Enzyme

HIV-1 IN protein was kindly provided by Dr. Robert Craigie (the National Institute of Health, Bethesda, Maryland, USA), and stored at -80 °C before use.

2.4.2 Oligonucleotide substrates

Oligonucleotides of long terminal repeated bases from donor DNA (LTRD) and from target substrate (TS) DNA were purchased from QIAGEN Operon, USA and stored at -25 °C before use. The sequence of biotinylated LTR donor DNA and its unlabelled complement were 5′-biotin-ACCCTTTTAGTCAGTGTGGAAAATCTCT AGCAGT-3′(LTR-D1) and 3′-GAAAATCAGTCACACCTTTTAGAGATCGTCA-5′ (LTR-D2), respectively. While those of the target substrate DNA (digoxigenin-labelled target DNA, TS-1) and its 3′-labelled complement were 5′-TGACCAAGGG CTAATTCACT-digoxigenin and digoxigenin-ACTGGTTCCCGATTAAGTGA-5′ (TS-2), respectively.

2.4.3 Annealing of the substrate DNA

Firstly, LTR-D1 and LTR-D2, TS-1 and TS-2 were mixed separately and then the former solution was diluted to a concentration of 2 pmol/mL, while the later one was made to 5 pmol/mL by diluting with KTE (a buffer solution containing 10 mM Tris-HCl (pH 8.0), 1mM EDTA and 100 mM KCl). Both solutions were heated at 85 °C for 15 min in water bath. After heating, cool each sample solution gradually to room temperature in water bath (for about 3 h) and was stored both of them at -20 °C until using.

2.4.4 Pretreatment of the multiplate

To a 96-well plate was added 50 μL of a steptavidin solution containing 40 μg/mL steptavidin, 90 mM Na_2CO_3 and 10 mM KCl. After that cover the microplate with plastic seal and put it gently overnight at 4 °C (for coating). After discarding steptavidin coating solution, wash coated microplate with phosphate buffer saline (PBS) solution (300 μL) in two times. The blocking buffer (300 μL) contain 1% skin milk in PBS was added into each well and the plate was kept at room temperature for 30 minutes (for blocking). After discarding blocking buffer, wash each well with PBS solution (300 μL) two times and then the PBS solution was completely removed. A biotinylated LTR donor DNA (50 μL) solution containing 10 mM tris-HCl (pH 8.0), 1mM NaCl and 40 mol/mL of LTR donor DNA was added into each well and mixed them gently at room temperature for 30 minutes (for adsorption). After discarding the LTR donor solution, wash microplate with PBS solution (300 μL) two times and then fill each well with 300 μL of PBS (If necessary, store at 4 °C). Just before the integration reaction, discard PBS solution of each well and then rinse with 300 μL of distilled water (one or two times).

2.4.5 Multiplate integration assay (MIA)

The integration reaction was evaluated according to the method previously described [71, 72]. A mixture (45 μL) composed of 12 μL of IN buffer [containing 150 mM 3-(*N*-morpholino) propanesulfonic acid, pH 7.2 (MOPS), 75 mM $MnCl_2$, 5 mM dithiothritol (DTT), 25% glycerol and 500 μg/mL bovine serum albumin], 1 μL of 5 pmol/mL digoxigenin-labelled target DNA and 32 μL of sterilized water were added into each well of a 96-well plate. Subsequently, 6 μL of a sample solution and 9 μL of 1/5 dilution of integrase enzyme were added to the mixture in the well and incubated at 37 °C for 80 min. The content in each well was washed with PBS four times, and added 100 μL of 500 mU/mL alkaline phosphatase (AP) labelled anti-digoxigenin antibody and further incubated at 37 °C for 1 h. The mixture was washed again with washing buffer containing 0.05% Tween 20 in PBS four times and with plain PBS four times. Then, AP buffer (150 μL) containing 100 mM Tris-HCl (pH 9.5), 100 mM NaCl, 5 mM $MgCl_2$ and 10 mM *p*-nitrophenyl phosphate was added to each well and incubated at 37 °C for 1 h. Finally, each solution on the plate was measured the absorbance with a microplate reader at the wavelength of 405 nm. A control composed of the similar reaction mixture with 50% DMSO in place of the sample solution while a blank was buffer-E containing 20 mM MOPS (pH 7.2), 400 mM potassium glutamate, 1 mM ethylenediaminetetraacetate disodium salt (EDTA·2Na), 0.1% Nonidet-P 40 (NP-40), 20% glycerol, 1 mM DTT and 4 M urea without the integrase enzyme. Suramin, a known polyanionic HIV-1 IN inhibitor was used as a positive control. % Inhibition against HIV-1 IN could be calculated from the equation below:

$$\% \text{ Inhibition against HIV-1 IN} = \left[\frac{OD_{control} - OD_{sample}}{OD_{control}} \right] x100$$

where OD = absorbance detected from each well

The results of anti-HIV-1 IN activity were expressed as mean±S.D. from four determinations. The IC_{50} values were calculated using the Microsoft excel program.

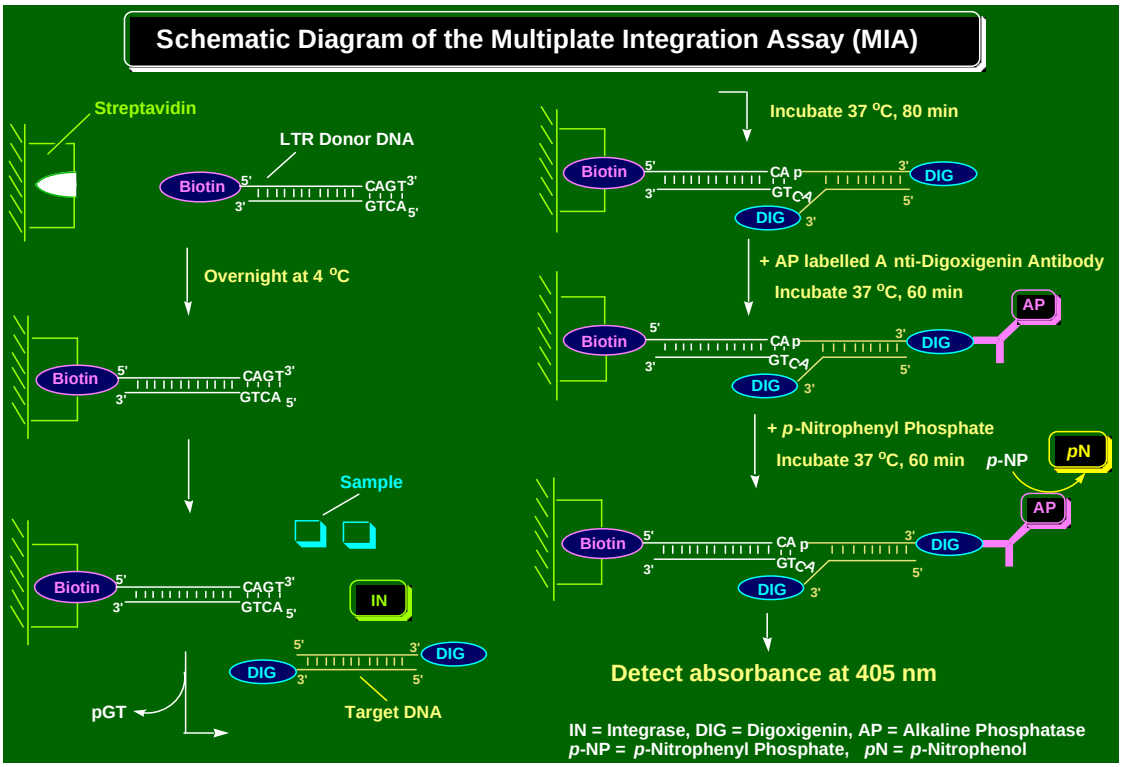

Figure 2.1 Diagram of the multiplate integration assay using the 96-well plate

2.5 Molecular Modeling

2.5.1 Structure of inhibitor

The studied inhibitors are a series of multi-cinnamoyl compounds **336-356**. The 3D structures of IN inhibitor were generated using GaussView 3.09. Since hexasubstituted benzene can have their substituents arranged into eight possible conformations [73, 74] based on their positions relative to the benzene ring whether it is “above” or “below” a plane of the benzene ring. Therefore, compound **341** was selected as a model to identify the lowest energy conformation by quantum mechanical method at B3LYP/6-31G(d) level of theory using Gaussian 03 program. All eight conformations are listed in **Table 2.1**. The obtained lowest energy conformation of **341** was then used as a guideline to build conformer for all compounds (**336-356**). Subsequently, geometry optimization at the B3LYP/6-31G(d) level was performed for each compound. Finally, the resulting structures were applied for docking calculations.

Table 2.1 Structure of all eight possible conformations of compound **341**

Notation[1]	**Structure**
ababab	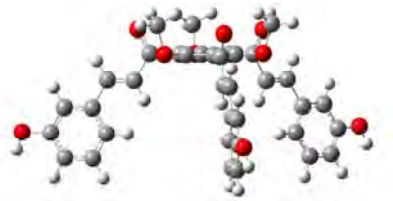
ababbb	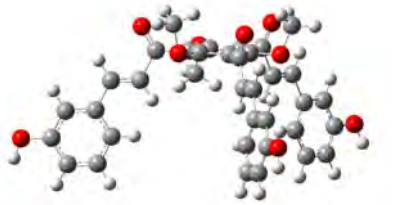
ababaa	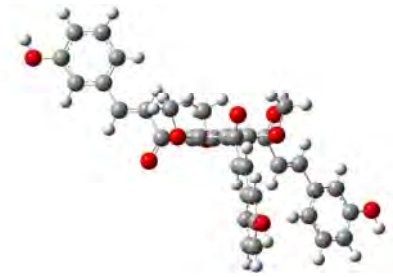
abaaba	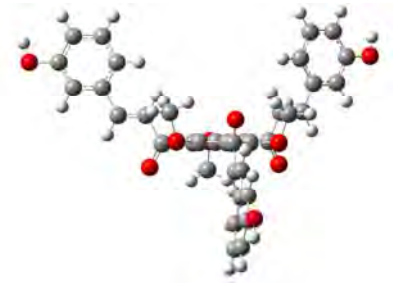
abaaaa	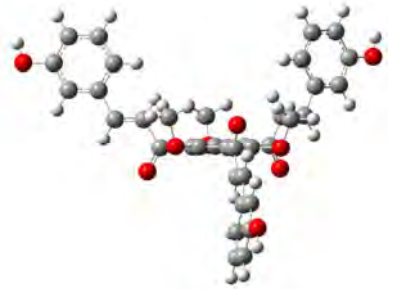

Table 2.1 Continued

Notation[1]	Structure
aabbba	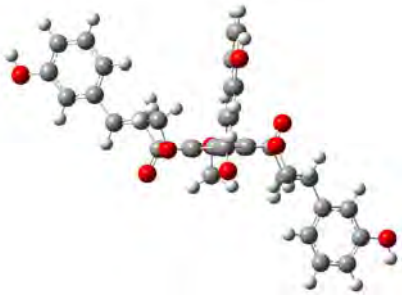
abbaab	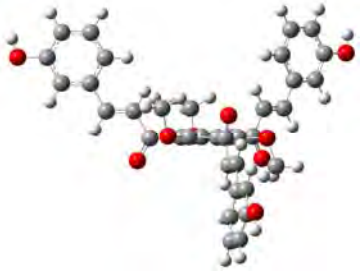
aaaaaa	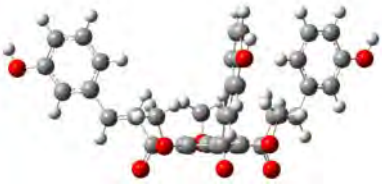

[1]"*a*" and "*b*" denote position of substituent as "above" and "below" the benzene plane, respectively.

2.5.2 Structure of enzyme

As it is well known that an inhibitor binds to HIV-1 IN at the catalytic core domain, the only available X-ray structure of IN core domain complex with 5CITEP [14] was used in our studies. The structure was obtained from the protein data bank with PDB code 1QS4 [75]. It contains three chains but 5CITEP is bound to chain A. Therefore, only chain A was selected. All water molecules and 5CITEP were removed while a magnesium ion at the active site was maintained. Finally, missing residues and hydrogen atoms were added.

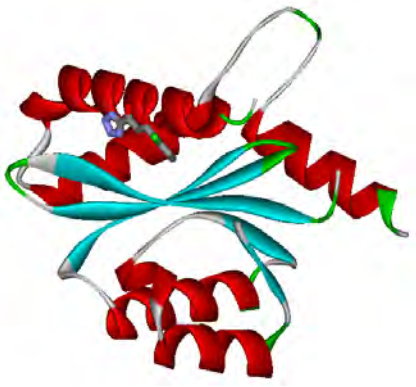

Figure 2.2 The X-ray crystallographic structure of HIV-1 IN core domain (only chain A) complex with the inhibitor 5CITEP (PDB code 1QS4)

2.5.3 Molecular docking

Molecular docking calculations were performed using AutoDock 4.0 software package. The structures of IN proteins were set up for docking as follows: Polar hydrogens were added using the PROTONATE utility distributed with AutoDock 4.0. The Kollman united atom charges and salvation parameters were added to the final protein file. For the ligands, the Gasteiger charges were used. The grid maps representing the protein in the actual docking process were calculated with AutoGrid. The grids were chosen to be sufficiently large to include not only the active site but also significant portions of the surrounding surface. The dimensions of the grids for HIV-1 IN (1QS4) protein docking were thus 50 x 50 x 50 $Å^3$, with a spacing of 0.375 Å. The Lamarckian genetic search algorithm was chosen for all dockings. The maximum number of energy evaluations was increased to 2,500,000 per run; the maximum number of generations in the genetic algorithm was increased to 100,000; and the number of GA run was 100. All other parameters were maintained at their default settings. 5CITEP was re-docked in order to validate our docking protocol. Finally, all the compounds were docked into the active site of IN using the established setting.

CHAPTER III

RESULTS AND DISCUSSION

3.1 Synthesis

3.1.1 Synthesis of 1,3,5-triacetyl-2,4,6-trihydroxybenzene (334)

Compound **334** was selected as the starting material for two strategies of the synthesis of multi-cinnamoyl analogs. In the first strategy, all hydroxyl groups of compound **334** were first protected by methylations using dimethyl sulfate followed by condensations with various substituted benzaldehydes. The other strategy involved the direct condensations of compound **334** with various substituted benzaldehydes without protection. This key precursor **334** was easily synthesized in 76% yield from phloroglucinol dihydrate **333** through one-pot esterifications and Fries rearrangements following the reported procedure [64, 65]. The mechanism of the reaction is shown in **Scheme 3.1**.

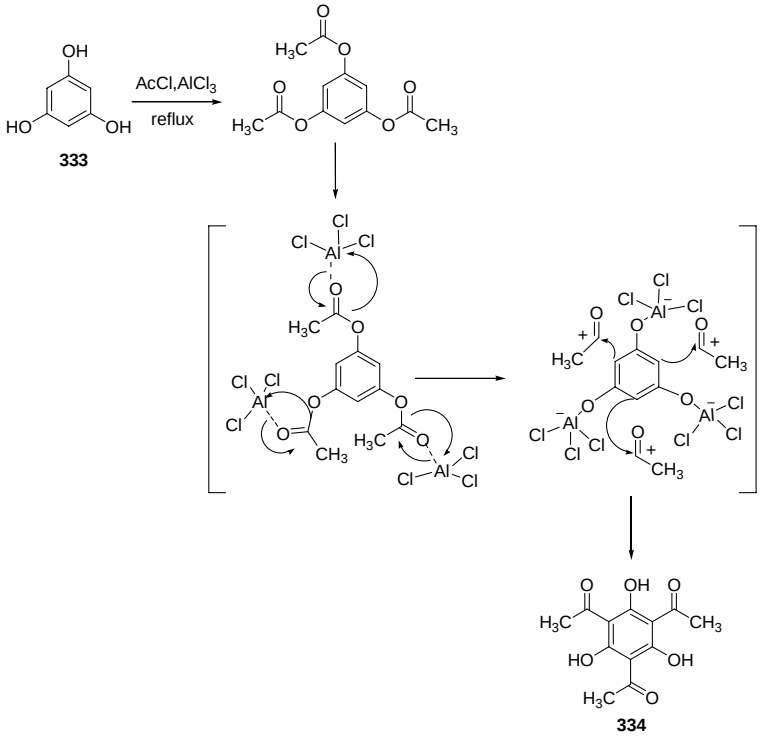

Scheme 3.1 Synthesis of 1,3,5-triacetyl-2,4,6-trihydroxybenzene (**334**)

^{1}H-NMR spectrum of the product **334** showed a singlet signal at δ 17.16 ppm (**Figure A.1** in Appendix) corresponding to the hydroxyl protons at 2, 4 and 6 positions forming strong intramolecular hydrogen bonds with the adjacent carbonyl groups of the three acetyl substituents at 1, 3 and 5 positions of the benzene ring (**Figure 3.1**).

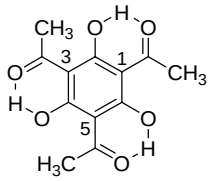

Figure 3.1 Intramolecular hydrogen bonds of compound **334**

3.1.2 Synthesis of 1,3,5-triacetyl-2,4,6-trimethoxybenzene (335)

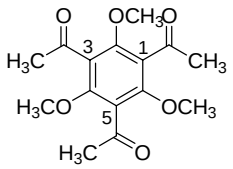

335

Figure 3.2 Structure of 1,3,5-triacetyl-2,4,6-trimethoxybenzene (**335**)

Compound **335** was prepared in 88% yield by excessive methylations at all phenolic hydroxyl groups using excess dimethyl sulfate and base (K_2CO_3) [64, 65]. ^{1}H NMR spectrum of **335** exhibited the singlet signal of three methoxy groups at δ 3.75 ppm, with the absence of the hydrogen bonding hydroxyl protons at the 2, 4 and 6 positions (**Figure A.3** in Appendix).

3.1.3 Synthesis of various multicinnamoyl analogs 336-350

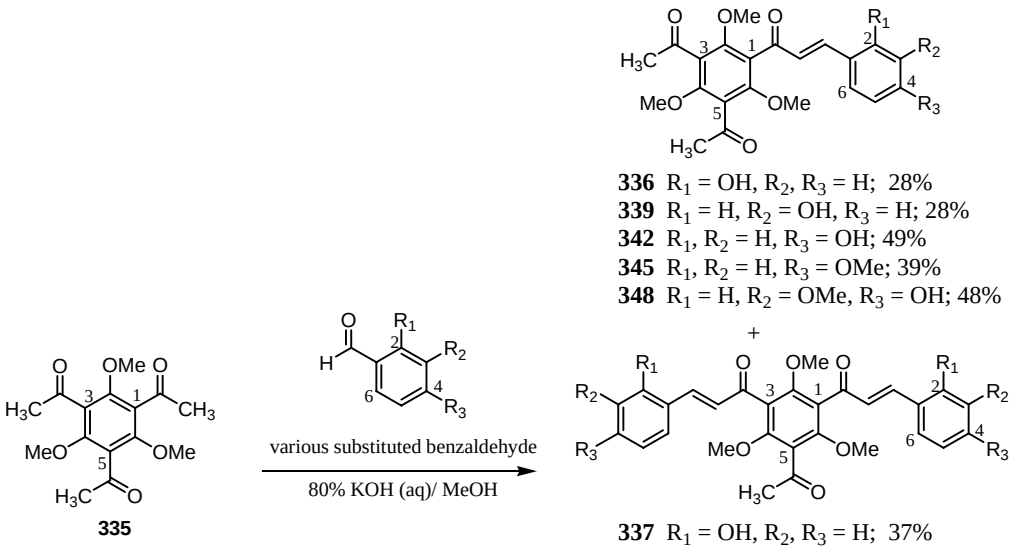

various substituted benzaldehyde	R_1	R_2	R_3
1	OH	H	H
2	H	OH	H
3	H	H	OH
4	H	H	OCH_3
5	H	OCH_3	OH

Scheme 3.2 Synthesis of new multicinnamoyl analogs and synthesis yields of mono-, bis-, tris-cinnamoyl analogs

3.1.4 Synthesis of 1-(2-hydroxycinnamoyl)-3,5-diacetyl-2,4,6-trimethoxy-benzene (336), 1,3-bis(2-hydroxycinnamoyl)-5-acetyl-2,4,6-trimethoxybenzene (337) and 1,3,5-tris(2-hydroxycinnamoyl)-2,4,6-trimethoxybenzene (338)

Compounds **336**, **337** and **338** were synthesized from compound **335**. The hexasubstituted benzene platform **335** was dissolved in methanol and condensed with

2-hydroxybenzaldehyde using 80% aqueous of KOH under Claisen-Schmidt condensation procedure. The crude product was purified by chromatographic gradient system to obtain compounds **336**, **337** and **338** in 28%, 37% and 13% yields, respectively (**Scheme 3.2**). All compounds were fully characterized by spectroscopic techniques. The ^{1}H-NMR spectra of compounds **336**, **337** and **338** showed quite similar aromatic and olefinic proton signals. The main differences that could help differentiate these compounds were the signal ratios of the methoxy groups based on symmetry of the molecules and the signals at chemical shift around 2.5 ppm that corresponded to two acetyl groups in compound **336** (**Figure A**.**5** in Appendix), one acetyl group in compound **337** (**Figure A**.**7** in Appendix) and none in compound **338** (**Figure A**.**9** in Appendix).

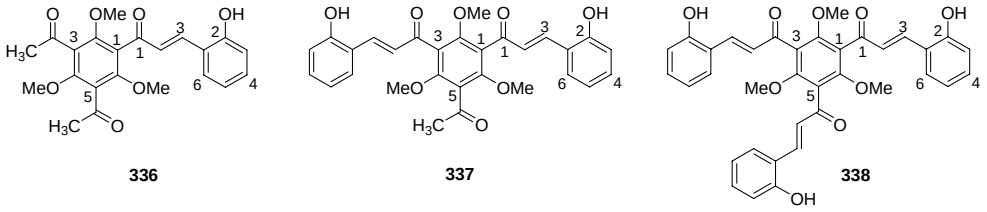

Figure 3.3 Structure of compounds **336**, **337** and **338**

3.1.5 Synthesis of 1-(3-hydroxycinnamoyl)-3,5-diacetyl-2,4,6-trimethoxy-benzene (339), 1,3-bis(3-hydroxycinnamoyl)-5-acetyl-2,4,6-trimethoxybenzene (340) and 1,3,5-tris(3-hydroxycinnamoyl)-2,4,6-trimethoxybenzene (341)

The synthesis method and structural characterizations for compounds **339**, **340** and **341** were similar to that of compounds **336**, **337** and **338**. In this case, compound **335** was condensed with 3-hydroxybenzaldehyde under strong basic condition. The crude product was purified by chromatographic gradient system to obtain compounds **339**, **340** and **341** in 28%, 14% and 3% yields, respectively (**Scheme 3.2**). All structures of the synthesized compounds were in good agreement with their spectroscopic data (**Figure A**.**11-25** in Appendix).

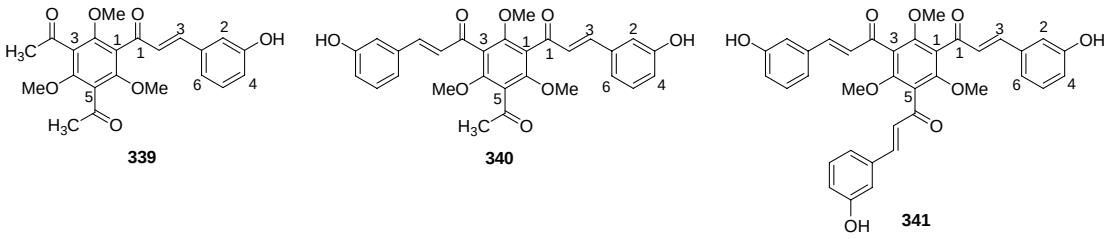

Figure 3.4 Structure of compounds **339**, **340** and **341**

3.1.6 Synthesis of 1-(4-hydroxycinnamoyl)-3,5-diacetyl-2,4,6-trimethoxy-benzene (342), 1,3-bis(4-hydroxycinnamoyl)-5-acetyl-2,4,6-trimethoxybenzene (343) and 1,3,5-tris(4-hydroxycinnamoyl)-2,4,6-trimethoxybenzene (344)

Following the same route as the synthesis of compounds **336**, **337** and **338**, compounds **342**, **343** and **344** were synthesized from compound **335** by condensation with 4-hydroxybenzaldehyde under Claisen-Schmidt condensation procedure. The crude product was purified by chromatographic gradient system to obtain compounds **342**, **343** and **344** in 49%, 19% and 5% yields, respectively (**Scheme 3.2**). All structures of the synthesized compounds were consistent with their spectroscopic data (**Figure A**.**26-31** in Appendix).

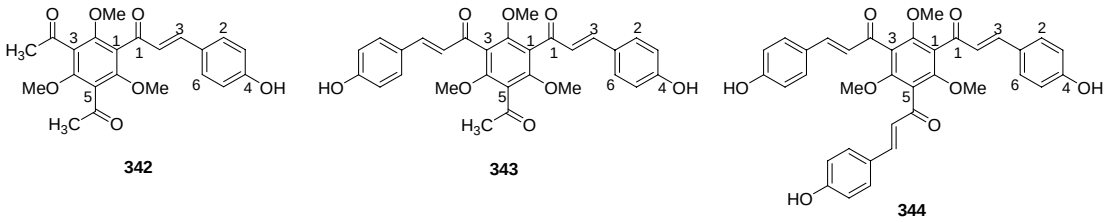

Figure 3.5 Structure of compounds **342**, **343** and **344**

3.1.7 Synthesis of 1-(4-methoxycinnamoyl)-3,5-diacetyl-2,4,6-trimethoxy-benzene (345), 1,3-bis(4-methoxycinnamoyl)-5-acetyl-2,4,6-trimethoxybenzene (346) and 1,3,5-tris(4-methoxycinnamoyl)-2,4,6-trimethoxybenzene (347)

Compounds **345**, **346** and **347** were synthesized from compound **335** condensed with 4-methoxybenzaldehyde by Claisen-Schmidt condensation method. The crude product was purified by chromatographic gradient system to obtain compounds **345**, **346** and **347** in 39%, 10% and 6% yields, respectively (**Scheme 3.2**).

All compounds were fully characterized by spectroscopic techniques (**Figure A.32-37** in Appendix).

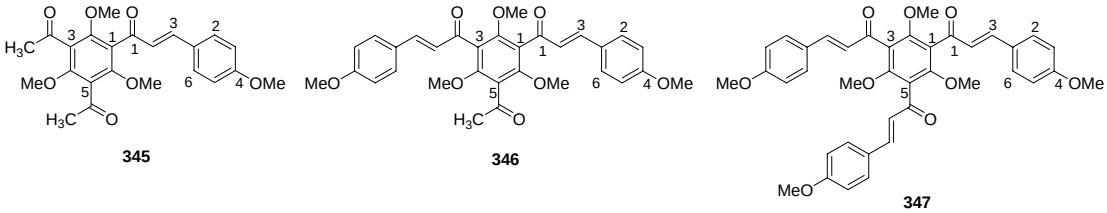

Figure 3.6 Structure of compounds **345**, **346** and **347**

3.1.8 Synthesis of 1-(4-hydroxy-3-methoxycinnamoyl)-3,5-diacetyl-2,4,6-trimethoxybenzene (348), 1,3-bis(4-hydroxy-3-methoxycinnamoyl)-5-acetyl-2,4,6-trimethoxybenzene (349) and 1,3,5-tris(4-hydroxy-3-methoxycinnamoyl)-2,4,6-trimethoxybenzene (350)

Compounds **348**, **349** and **350** were synthesized from compound **335** condensing with 3-methoxy-4-hydroxybenzaldehyde (vanillin) by Claisen-Schmidt condensation method. The crude product was purified by chromatographic gradient system to obtain compounds **348**, **349** and **350** in 48%, 18% and 5% yields, respectively (**Scheme 3.2**). All compounds were fully characterized by spectroscopic techniques (**Figure A**.**38-43** in Appendix).

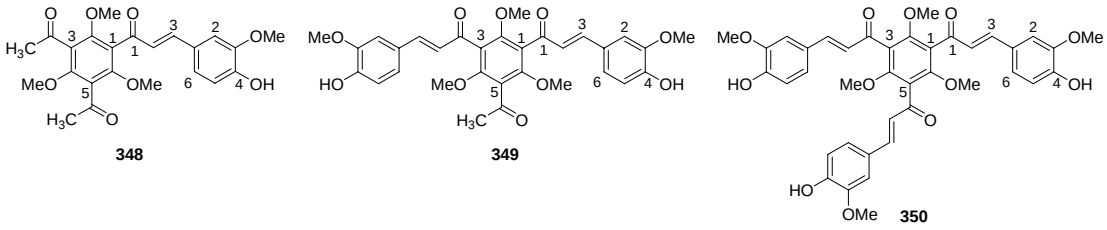

Figure 3.7 Structure of compounds **348**, **349** and **350**

3.1.9 Synthesis of 1-(3,4-dihydroxycinnamoyl)-3,5-diacetyl-2,4,6-trimethoxybenzene (351)

Compound **351** was prepared from compound **348** upon treatment with $AlCl_3$ as the catalyst. The crude product was purified by chromatographic gradient system to

obtain compounds **351** in 18% yielded and 29% recovered starting material. The ^{1}H-NMR spectrum of compound **351** showed two methoxy groups of the core structure remained at the same positions, and the signal of the methoxy group on the flanking phenyl ring was absent (**Figure A.44-48** in Appendix).

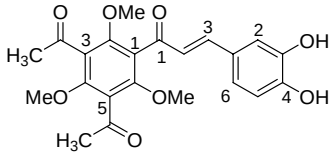

351

Figure 3.8 Structure of compound **351**

3.1.10 Synthesis of 1-(3,4-dihydroxycinnamoyl)-3-(4-hydroxy-3-methoxy-cinnamoyl)-5-acetyl-2,4,6-trimethoxybenzene (352) and 1,3-bis(3,4-dihydroxy-cinnamoyl)-5-acetyl-2,4,6-trimethoxybenzene (353)

Compounds **352** and **353** were demethylated from compound **349** using $AlCl_3$ as catalyst. The crude product was purified by chromatographic gradient system to obtain compounds **352** and **353** in 12% and 8% yields respectively, together with 19% recovered starting material. All structures of the synthesized compounds **352** and **353** were consistent with their spectroscopic data in appendix (**Figure A.49-58**). The ^{1}H-NMR spectrum of compound **353** in acetone-d_6 (δ; ppm) showed one methoxy group at chemical shift 3.52 ppm, two methoxy groups at the same chemical shift 3.60 ppm for compound **352** (**Figure A.49** in Appendix) and the absence of the methoxy group on the flanking phenyl ring for compound **353** (**Figure A.54** in Appendix).

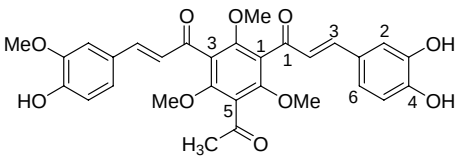

352

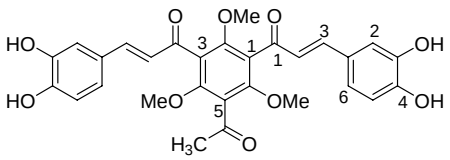

353

Figure 3.9 Structure of compounds **352** and **353**

3.1.11 Synthesis of 1-(3,4-dihydroxycinnamoyl)-3,5-bis(4-hydroxy-3-methoxycinnamoyl)-2,4,6-trimethoxybenzene (354), 1,3-bis(3,4-dihydroxycinnamoyl)-5-(4-hydroxy-3-methoxycinnamoyl)-2,4,6-trimethoxybenzene (355) and 1,3,5-tris(3,4-dihydroxycinnamoyl)-2,4,6-trimethoxybenzene (356)

Compounds **354, 355** and **356** were demethylated from compound **350** using $AlCl_3$ as catalyst. The crude product was purified by using isocratic on TLC plate (dichloromethane/methanol, 99:1) to obtain compounds **354**, **355** and **356** in 7.4%, 6.5% and 2.4% yields respectively, together with 8.6% recovered starting material **350**. All structures of the synthesized compounds were consistent with their spectroscopic data. (**Figure A.59-63** in Appendix for compound **354**, and **Figure A.64-68** in Appendix for compound **355)**.

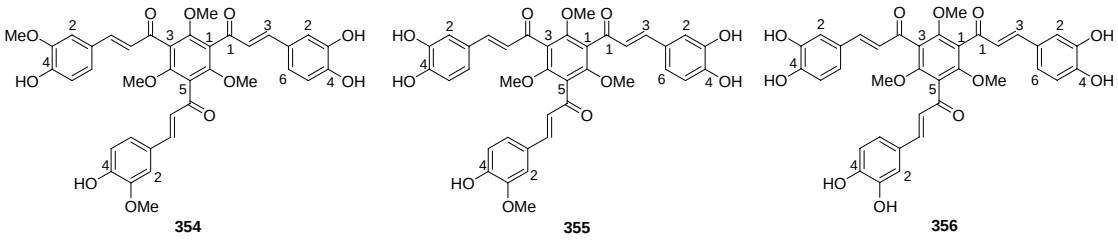

Figure 3.10 Structure of compounds **354**, **355** and **356**

3.1.12 Synthesis of 1-(4-hydroxycinnamoyl)-3,5-diacetyl-2,4,6-trihydroxybenzene (357), 1,3-bis(4-hydroxycinnamoyl)-5-acetyl-2,4,6-trihydroxybenzene (358) and 1,3,5-tris(4-hydroxycinnamoyl)-2,4,6-trihydroxybenzene (359)

In the second method, compound **334** was directly condensed with 4-hydroxybenzaldehyde using KOH or NaOEt as the initiated base. The reaction did not yield the desired product, possibly because both starting materials form only salts of compound **334** and 4-hydroxybenzaldehyde were recovered after worked up reaction (**Scheme 3.3**).

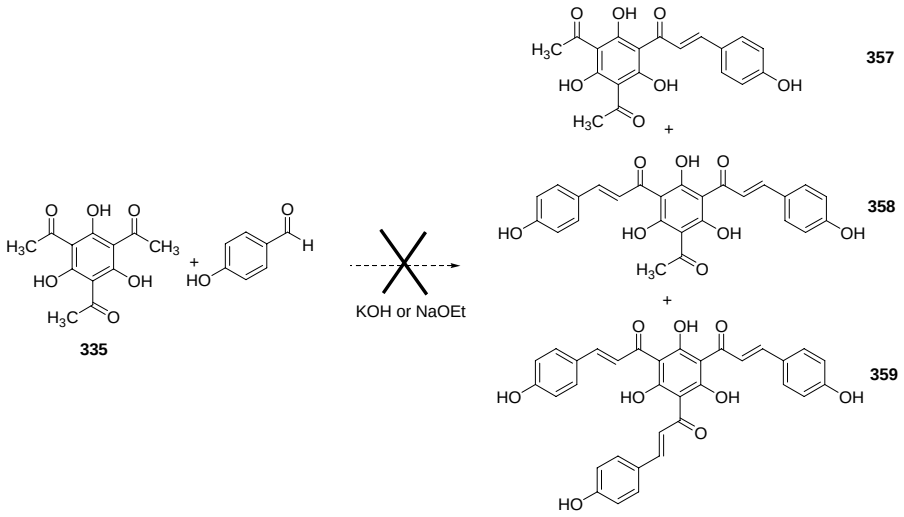

Scheme 3.3 Attempted synthesis of compounds **357**, **358** and **359**

3.2 Bioactivities

Assay of HIV-1 IN inhibitory activity

The bioassay studies on HIV-1 IN inhibitory activity were carried out using the method reported by Tewtrakul and coworkers [71, 72]. The multiplate integration assay (MIA) results on the newly synthesized compounds **334-356** indicated positive inhibition against HIV-1 integrase at concentrations of 100, 30 and 10 μM. %Inhibition and IC_{50} (μM) values are shown in **Table 3.1**. The core structure compounds **334** and **335** showed only mild activity without the cinnamoyl groups. After compound **335** was condensed with various benzaldehyde derivatives to create the number of cinnamoyl groups, the activity had much improved especially when the flanking aromatic rings of the cinnamoyl moieties carrying free hydroxyl groups at *meta*- positions such as compound **339** (mono-) was active (17.91%) at concentration 100 μM. Then, the cinnamoyl groups were added on core structure such as compounds **340** (bis-) and **341** (tris-) were increased activity 36.12% and 79.96% respectively. The result also suggested the importance of multiple *meta*- hydroxyl groups on the cinnamoyl moieties. The compound **341** was more active (IC_{50} = 9.5 μM) than the compounds with less number of these groups as in mono-cinnamoyl: **336**, **339**, **342**, **345** and **348**; bis-cinnamoyl: **337**, **340**, **343**, **346** and **349**. Other

phenolic derivatives **336-340** and **342-350** showed only moderate activity in comparison with that of curcumin **165** [40]. Their IC_{50} values in MIA method were found to be >100 μM**.**

Table 3.1 %Inhibition of HIV-1 IN enzyme at 100 (μM) and IC_{50} (μM) by compounds **334-356**

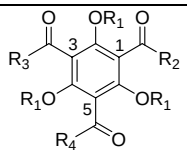

					% Inhibition of IN enzyme at various concentrations (μM)			IC_{50} (μM)
					100	**30**	**10**	
	R_1	R_2	R_3	R_4				
334	H	CH_3	CH_3	CH_3	21.02±3.73	-	-	>100
335	CH_3	CH_3	CH_3	CH_3	11.74±3.80	-	-	>100
336	CH_3		CH_3	CH_3	13.75±2.53	-	-	>100
337	CH_3		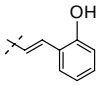	CH_3	38.27±2.19	-	-	>100
338	CH_3				28.16±3.09	-	-	>100
339	CH_3	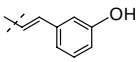	CH_3	CH_3	17.91±1.61	-	-	>100
340	CH_3	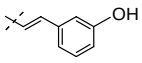	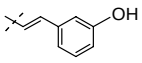	CH_3	36.12±4.08	-	-	>100
341	CH_3	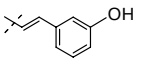	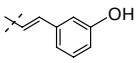	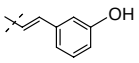	79.96±2.13	68.24±1.09	49.15±2.33	9.5
342	CH_3	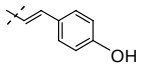	CH_3	CH_3	-10.58±3.23	-	-	>100
343	CH_3	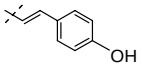	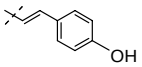	CH_3	26.24±2.56	-	-	>100
344	CH_3	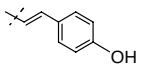	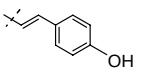	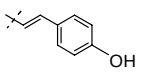	40.45±1.27	-	-	>100
345	CH_3	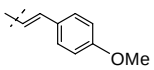	CH_3	CH_3	12.51±3.67	-	-	>100
346	CH_3	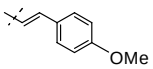	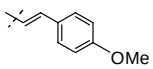	CH_3	14.18±6.41	-	-	>100
347	CH_3	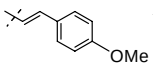	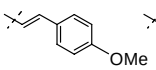	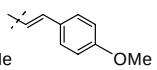	-18.90±4.21	-	-	>100
348	CH_3	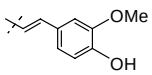	CH_3	CH_3	25.63±4.89	-	-	>100

Table 3.1 Continued

	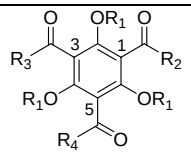			% Inhibition of IN enzyme at various concentrations (μM)			IC_{50} (μM)
				100	**30**	**10**	
	R_1	R_2	R_3	R_4			
349	CH_3	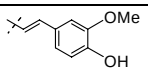	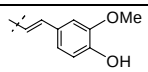	CH_3	33.07±0.05	-	-	>100
350	CH_3	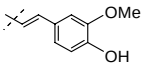	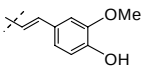	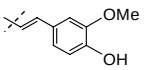	35.75±4.98	-	-	>100
351	CH_3	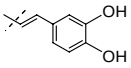	CH_3	CH_3	24.94±3.16	-	-	>100
352	CH_3	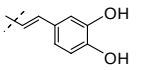	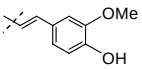	CH_3	55.95±1.02	16.25±1.20	2.74±4.32	89.4
353	CH_3	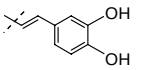	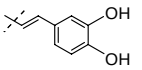	CH_3	90.30±0.03	86.88±1.60	59.46±1.91	3.5
354	CH_3	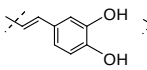	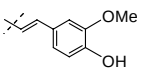	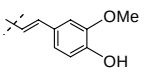	44.36±3.30	-	-	>100
355	CH_3	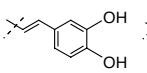	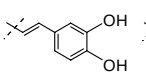	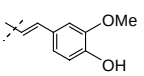	74.78±2.61	56.58±1.39	44.01±2.70	16.5
356	CH_3	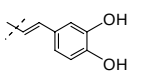	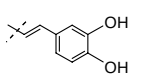	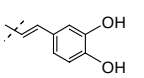	93.60±0.94	81.03±0.31	75.75±1.65	7.0
	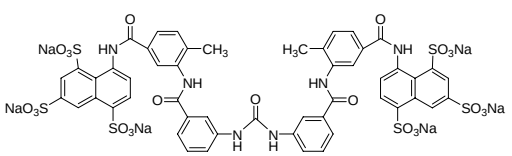				99.89±0.41	89.40±1.73	69.72±1.56	2.7
	143							
	Suramin (positive control)							

Compounds **348**, **349** and **350** have methoxyl groups at *meta*- positions, which decreased activity (IC_{50} >100 μM). When, **348**, **349** and **350** were demethylated to give the catechol on benzene ring such as compound **352** which has catechol on one of flanking phenyl ring, showed weak activity (IC_{50} = 89.4 μM) whereas **353** (IC_{50} = 3.5 μM) which has catechols both flanking phenyl rings showed highest activities than all synthesized compounds. Compound **355** which has catechols both flanking phenyl rings of tris-cinnamoyl groups showed IC_{50} value of 16.5 μM, then compound **356** which has catechols three flanking phenyl rings, increased activity (IC_{50} = 7.0 μM). Catechol groups of the cinnamoyl side chain seemed to help increase the activity especially when both of them were presented in the same molecule. The four active compounds and one weak activities compound showed in **Figure 3.11**.

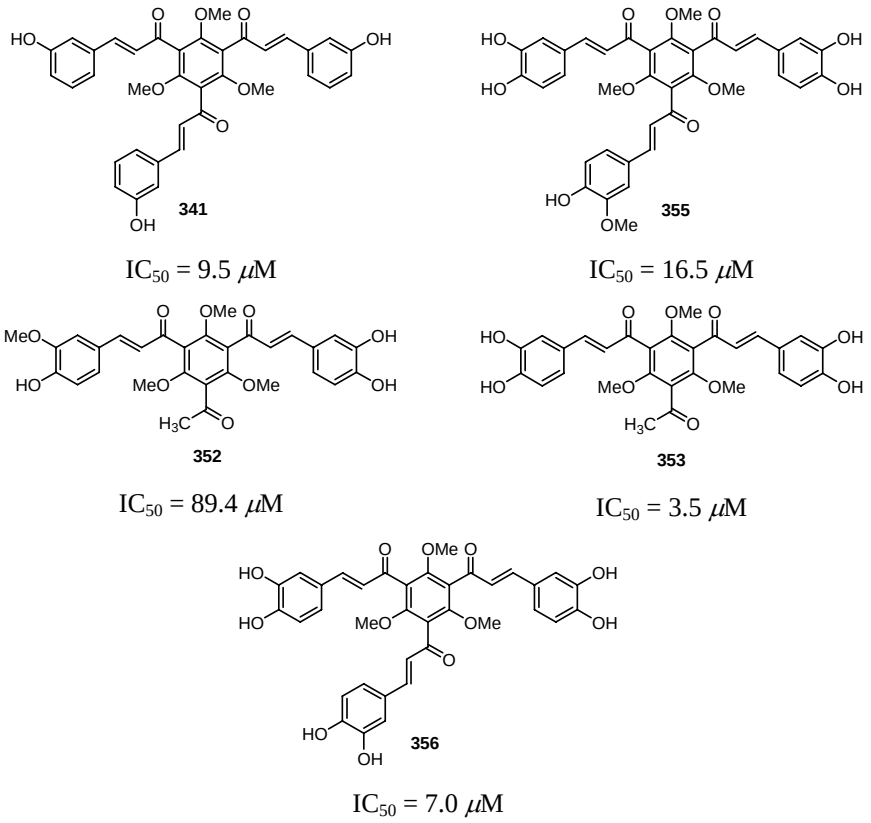

Figure 3.11 Structures and IC_{50} values of active compounds **341**, **355**, **352**, **353** and **356**

3.3 Molecular Modeling

Energies of all 8 possible conformations of compound **341** optimized at B3LYP/6-31G(d) level were given in **Table 3.2**. As expected, conformation *ababab* has the lowest energy. This is because the repulsive interactions between adjacent groups around the benzene ring forced the substituents to arrange alternately above (*a*) and below (*b*) the central benzene ring in trigonally symmetric pattern (*ababab*). The torsion angles relative to the central ring plane of the three cinnamoyl (τ_1) and three methoxy (τ_2) groups were 58.2° and -94.4° respectively (**Figure 3.12**). Interestingly, the *abaaaa* conformation is not stable because it was turned into *abaaba* conformation after optimization. This is probably due to strong steric effect of the four neighboring groups (*aaaa*) and asymmetric molecule.

Table 3.2 Theoretical optimizations of the eight possible conformers of **341**

Conformation		Energy (a.u.)	Relative energy (kcal/mol)
Starting	**Final**		
ababab	*ababab*	-2053.57442731	0.00
ababbb	*ababbb*	-2053.56808621	3.98
ababaa	*ababaa*	-2053.56427878	6.37
abaaba	*abaaba*	-2053.56426385	6.38
abaaaa	*abaaba*	-2053.56424969	6.39
aabbba	*aabbba*	-2053.55869477	9.87
abbaab	*abbaab*	-2053.55839594	10.06
aaaaaa	*aaaaaa*	-2053.53644233	23.84

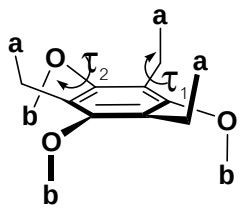

a = above and *b* = below the benzene plane

Figure 3.12 The pictorial structure of a conformer of hexasubstituted benzene scaffold with the substituents arranged in *ababab* conformation

From these data, the *ababab* conformation was used as a starting conformation for all compounds (**336**-**356**). Energy of the optimized structures at B3LYP/6-31G(d) level was shown in **Table 3.3**.

Table 3.3 Optimization energy of 21 multi-cinnamoyl analogs (**336**-**356**)

compound	Energy (a.u.)	Compound	Energy (a.u.)
336	-1369.31431674	**347**	-2170.59166692
337	-1711.44304328	**348**	-1483.14433591
338	-2053.57482086	**349**	-1939.08632989
339	-1369.31394499	**350**	-2395.03776455
340	-1711.44258618	**351**	-1444.13862200
341	-2053.57442733	**352**	-1900.08359901
342	-1369. 31537738	**353**	-1861.09184697
343	-1711.44552030	**354**	-2356.04139249
344	-2053.57836237	**355**	-2317.04501118
345	-1408.31988936	**356**	-2278.04862059
346	-1789.45447569		

3.3.1 Molecular docking of compounds 336, 337 and 338

The results showed hydrogen bonding between ligand and two amino acid residues for compound **336**, four amino acid residues for compound**s 337** and **338** (**Figure 3.13** and **Table 3.4**). Compound **337** has the lowest binding energy (-3.61 kcal/mol) compared to the other two compounds (**336** and **338**) and this is in agreement with experimental biological activity. Although the IC_{50} of three compounds is higher than 100 μM, compound **337** exhibited higher activity than the two compounds (38%) at concentration of 100 μM. The free 2-hydroxyl groups on 1,3-bis(phenyl flanking ring) of compound **337** were bonded with Lys159, His67 and Glu152. Moreover carbonyl group of cinnamoyl group was bonded with Asn155.

Table 3.4 The active site amino acid residues interacting with the cinnamoyl analogs **336**, **337** and **338** reported from docking experiment

Compound	Lowest energy (kcal/mol)	%Inhibition against HIV-1 IN (100 μM)	IC_{50} (μM)	Hydrogen bonding (Å) and interacting amino acid residues						
				Asp 64	Glu 152	Asn 155	Cys 65	His 67	Lys 156	Lys 159
336	-3.37	14	>100	-	-	-	-	-	2.31	2.05
337	-3.61	38	>100	-	2.03	2.01, 2.81	-	1.91, 2.08	-	2.04
338	-3.27	28	>100	2.26	2.01, 2.32	2.87	2.32	-	-	-

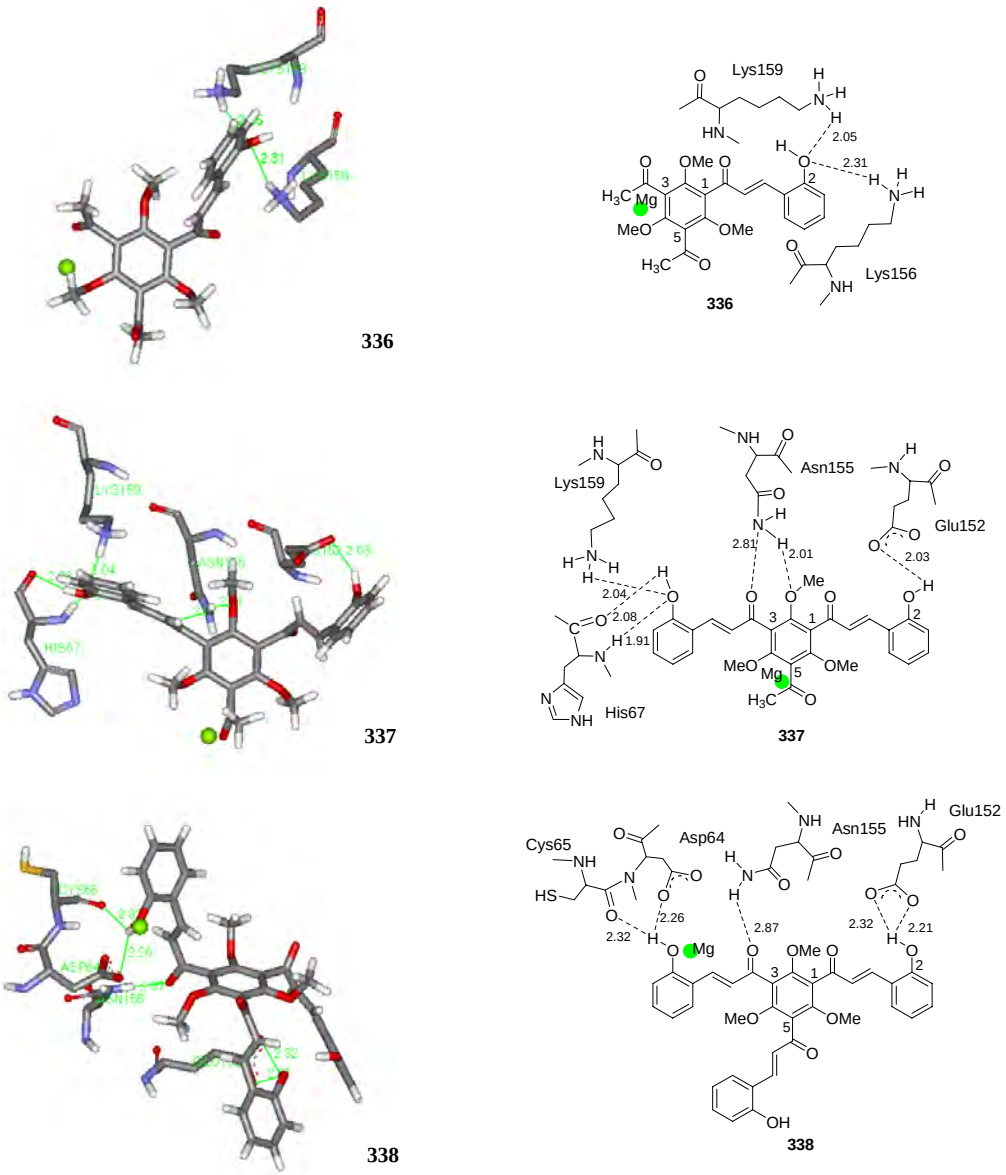

Figure 3.13 Predicted binding conformations of compounds **336**, **337** and **338** inside the HIV-1 integrase active site (modified PDB code 1QS4)

3.3.2 Molecular docking of compounds 339, 340 and 341

The results showed hydrogen bonding between ligand and four amino acid residues for compound **339**, three amino acid residues for compound **340** and six amino acid residues for compound **341** (**Figure 3.14** and **Table 3.5**). The compound **341** gave the highest activity with an IC_{50} value of 9.5 μM**.** This compound contains more hydrogen bonding than the two compounds **339** and **340** that showed IC_{50} in

MIA method to be higher than 100 μM. All free hydroxyl groups on phenyl flanking ring of compound **341** was bonded with Lys156, Glu152, Ser147, and Thr66. Moreover the carbonyl groups were bonded with Gln148.

Table 3.5 The active site amino acid residues interacting with the cinnamoyl analogs **339**, **340** and **341** reported from docking experiment

Compound	Lowest energy (kcal/mol)	%Inhibition against HIV-1 IN (100 μM)	IC_{50} (μM)	Hydrogen bonding (Å) and interacting amino acid residues					
				Glu 152	Asn 155	Gln 148	Thr 66	Ser 147	Lys 156
339	-3.46	17.91	>100	2.04, 3.02	1.84	-	-	-	-
340	-3.94	36.12	>100	-	-	1.95, 1.99	3.05	-	1.95
341	-3.62	79.96	9.5	2.09	-	2.95	1.86	2.02	1.85

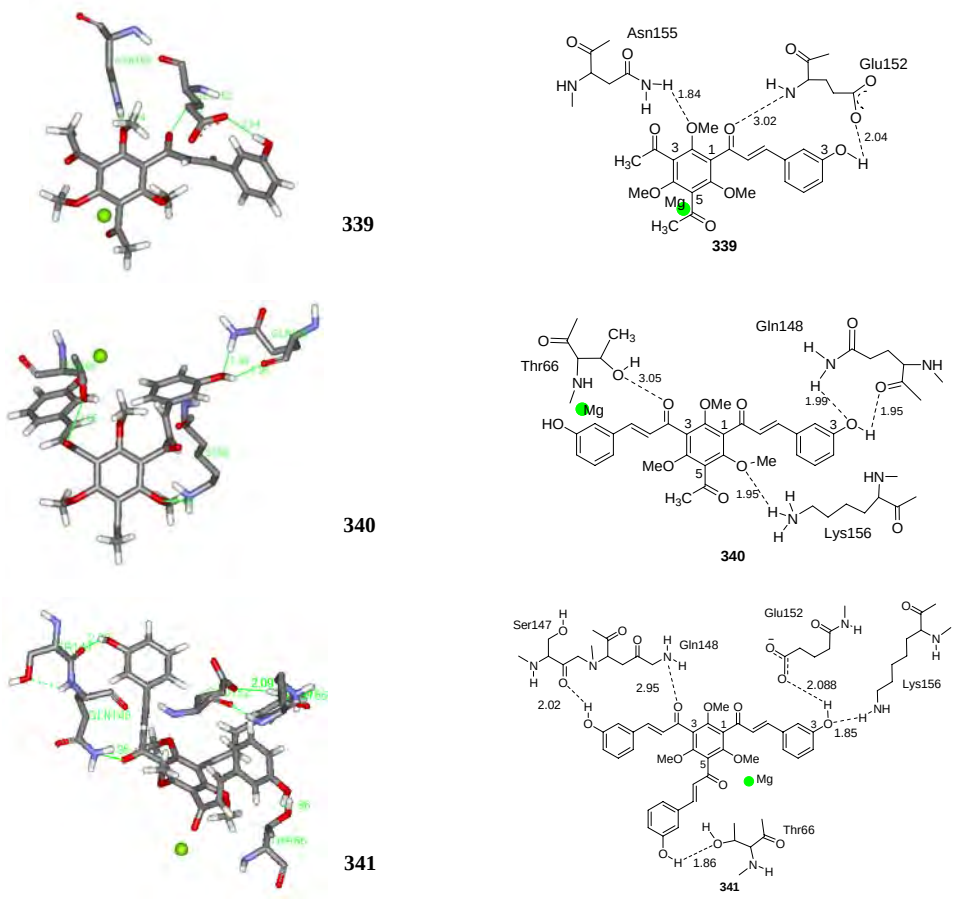

Figure 3.14 Predicted binding conformations of compounds **339**, **340** and **341** inside the HIV-1 integrase active site (modified PDB code 1QS4)

3.3.3 Molecular docking of compounds 342, 343 and 344

The results showed hydrogen bonding between ligand and five amino acid residues for compound **342**, three amino acid residues for compound **343** and one amino acid residues for **344** (**Figure 3.15** and **Table 3.6**). The bioactivity of these three compounds showed IC_{50} at >100 µM**.** However, at concentration of 100 µM, compound **344** exhibited higher activity than two compounds (40%). In this series, no relationship between docking results and bioactivity was found. The 4-hydroxylcinnamoyl group at first position of compounds **342, 343** and **344** were bonded with Gln148. The carbonyl of acetyl group at third position (**342**) and 4-hydroxylcinnamoyl group at third position (**343**) were bonded with similarly His67 and the methoxy group on core structure of benzene ring at sixth position of two compounds (**342** and **343**) were bonded with Lys156. The carbonyl group of 4-hydroxycinnamoyl group at first position of compound **342** was bonded with Asn155.

Table 3.6 The active site amino acid residues interacting with the cinnamoyl analogs **342**, **343** and **344** reported from docking experiment

Compound	Lowest energy (kcal/mol)	%Inhibition against HIV-1 IN (100 μM)	IC_{50} (μM)	Hydrogen bonding (Å) and interacting amino acid residues				
				Asn 155	Gln 148	Thr 66	His 67	Lys 156
342	-2.91	-10.58	>100	2.95	2.12	2.83	3.02	2.13, 2.44
343	-3.20	26.24	>100	-	1.89, 2.02	-	3.02	2.49
344	-2.99	40.45	>100	-	1.88, 2.07	-	-	-

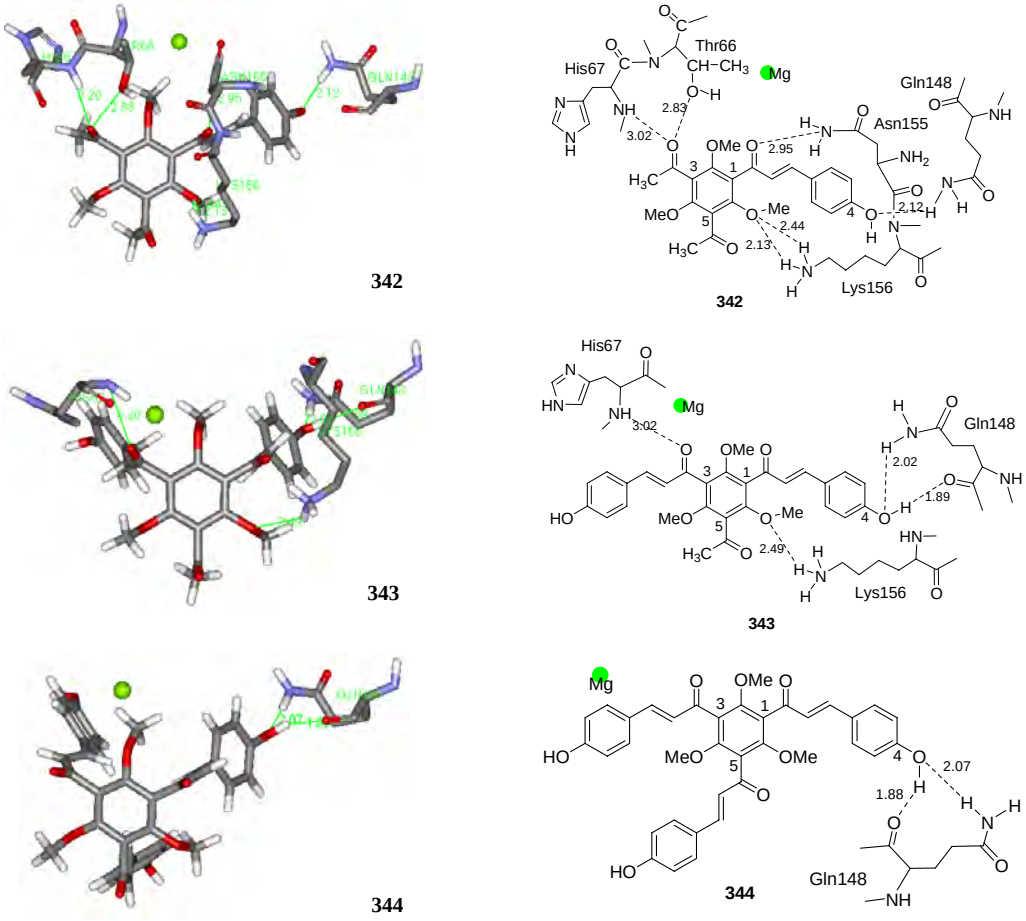

Figure 3.15 Predicted binding conformations of **342**, **343** and **344** inside the HIV-1 integrase active site (modified PDB code 1QS4)

3.3.4 Molecular docking of compounds 345, 346 and 347

The results showed hydrogen bonding between ligand and four amino acid residues for compounds **345**, three amino acid residues for **346** and one amino acid residues for compound **347** (**Figure 3.16** and **Table 3.7**). The result of docking predicted compound **347** has the lowest activity compared to two compounds (**345** and **346**) but it formed only one hydrogen bond with the enzyme. The anti-HIV-1 IN activity of compound **347** was the lowest percentage at 100 μM (-18.90%) compared to two compounds **345** (12.51%) and **346** (14.18%) but three compounds showed similar activity in MIA method with IC_{50} values > 100 µM. The 4-methoxylcinnamoyl group at first position of compounds **345**, **346** and **347** were bonded with Gln148.

Compounds **345** and **346** showed more activity than **347** maybe because they have more hydrogen bonding than compound **347**.

Table 3.7 The active site amino acid residues interacting with the cinnamoyl analogs **345**, **346** and **347** reported from docking experiment

Compound	Lowest energy (kcal/mol)	%Inhibition against HIV-1 IN (100 μM)	IC_{50} (μM)	Hydrogen bonding (Å) and interacting amino acid residues			
				Gln 148	Thr 66	His 67	Lys 156
347	-2.75	12.51	>100	1.90	2.83	3.14	1.97
348	-2.03	14.18	>100	1.81	3.19	-	2.01
349	-2.65	-18.90	>100	2.23	-	-	-

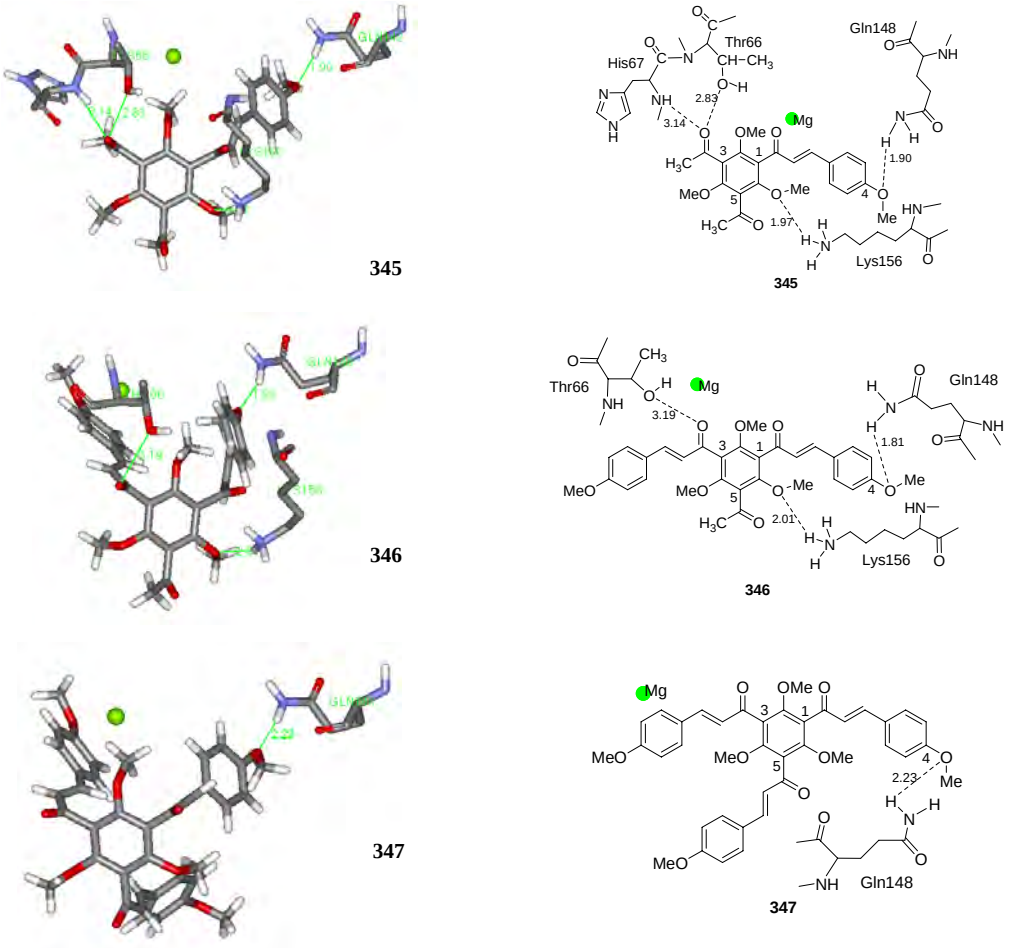

Figure 3.16 Predicted binding conformations of **345**, **346** and **347** inside the HIV-1 integrase active site (modified PDB code 1QS4)

3.3.5 Molecular docking of compounds 348, 349 and 350

The results showed hydrogen bonding between ligand and four amino acid residues for compound **348** and two amino acid residues for **349** and **350** (**Figure 3.17**-**3.18** and **Table 3.8**). The docking results predicted that **349** and **350** possessed similar activity because they were bound with the same amino acid residues. Three compounds showed similar activity in MIA method with IC_{50} > 100 μM. However, at concentration of 100 μM, compounds **349** and **350** exhibited activity at 33 and 35 %inhibition, respectively. The 4-hydroxycinnamoyl of first position of compounds **348**, **349** and **350** were bonded with Gln148. The compounds **349** and **350** exhibited %inhibition more than **348** could be described from stronger of hydrogen bonding between methoxyl group and amino acid residues.

Table 3.8 The active site amino acid residues interacting with the cinnamoyl analogs **348**, **349** and **350** reported from docking experiment

Compound	Lowest energy (kcal/mol)	%Inhibition against HIV-1 IN (100 μM)	IC_{50} (μM)	Hydrogen bonding (Å) and interacting amino acid residues		
				Gln 148	Lys 156	Lys 159
348	-2.89	25.63	>100	2.88	2.17	2.23, 2.41, 2.43
349	-3.19	33.07	>100	1.88, 1.92	2.07	-
350	-2.87	35.75	>100	1.83, 1.98	2.38	-

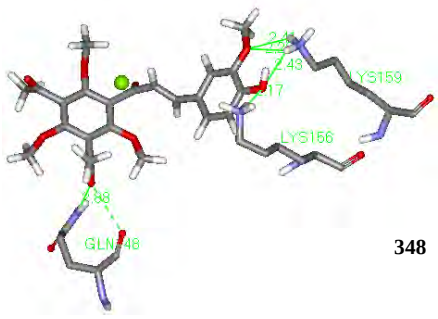

348

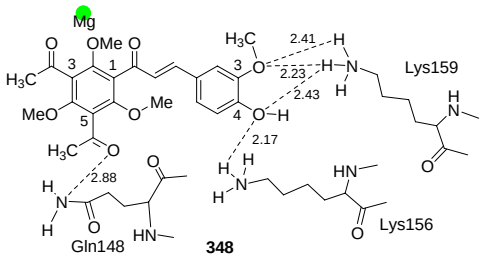

348

Figure 3.17 Predicted binding conformations of compound **348** inside the HIV-1 integrase active site (modified PDB code 1QS4)

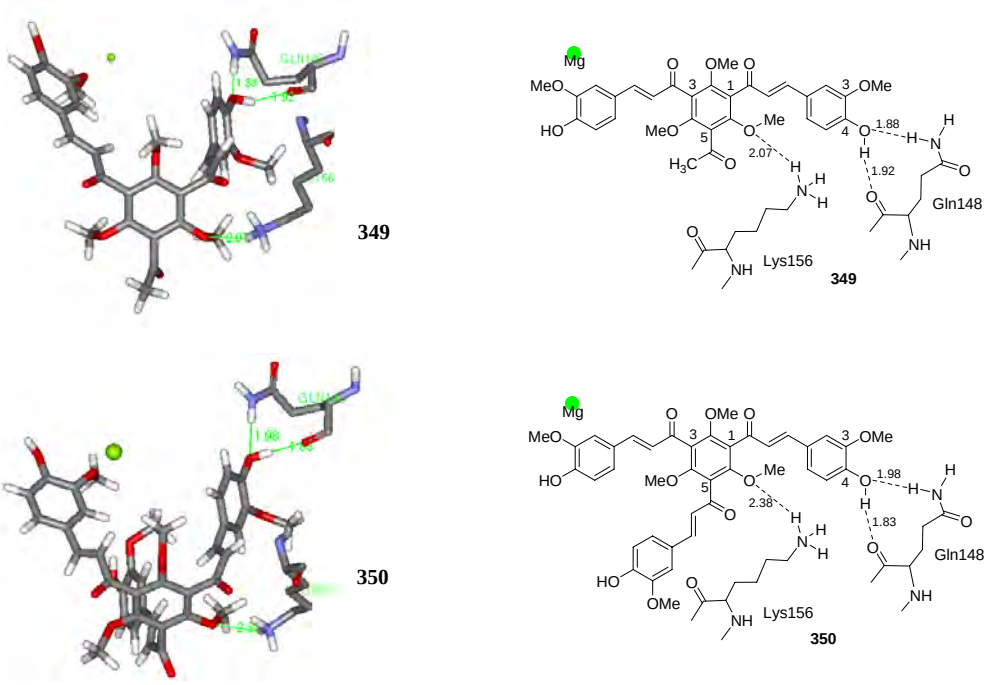

Figure 3.18 Predicted binding conformations of compounds **349** and **350** inside the HIV-1 integrase active site (modified PDB code 1QS4)

3.3.6 Molecular docking of compounds 351, 352, 353, 354, 355 and 356

The result of catechol series showed hydrogen bonding between ligand and four amino acid residues for compounds **353** and **356**, three amino acid residues for compounds **351** and **352**, two amino acid residues for compounds **354** and **355** (**Figure 3.19-3.20**). In **Table 3.9**, high activity of compounds **353** and **356** (IC_{50} = 3.5 and 7.0 μM respectively) can be explained from their stronger hydrogen bonding and more amino acid residues than the other compounds (**351**, **352**, **354** and **355**). The methoxyl group at sixth position and the carbonyl group at third position of core structure of compounds **353** and **356** were bonded similarly with Lys156 and Thr66. Moreover, the carbonyl group of **353** was bonded with His67. The catechol at the first position of 3,4-dihydroxycinnamoyl **353** was bonded three hydrogen bonding with Gln148 whereas, the 3-hydroxyl groups of 3,4-dihydroxycinnamoyl at first and third positions of **356** were bonded with Asp116 and Glu92, respectively.

Table 3.9 The active site amino acid residues interacting with the cinnamoyl analogs **351**, **352**, **353**, **354**, **355** and **356** reported from docking experiment

Compound	Lowest energy (kcal/mol)	% Inhibition against HIV-1 IN (100 μM)	IC_{50} (μM)	Hydrogen bonding (Å) and interacting amino acid residues								
				Gln 148	Thr 66	His 67	Glu 92	Asp 116	Asn 117	Glu 152	Asn 155	Lys 156
351	-3.25	24.94	>100	-	3.05	-	-	-	-	2.22, 2.98	1.78, 3.14	-
352	-3.07	55.95	89.4	-	-	-	1.85	-	1.94	-	1.88	-
353	-3.75	90.30	3.5	1.97, 2.17, 2.38	2.73	3.07	-	-	-	-	-	2.17
354	-4.54	44.36	>100	-	-	-	-	1.75	-	-	-	1.92, 2.46
355	-3.86	74.78	16.5	1.93, 2.27	-	-	-	-	-	-	-	1.96
356	-3.96	93.60	7.0	-	2.89	-	1.92	1.65	-	-	-	2.10

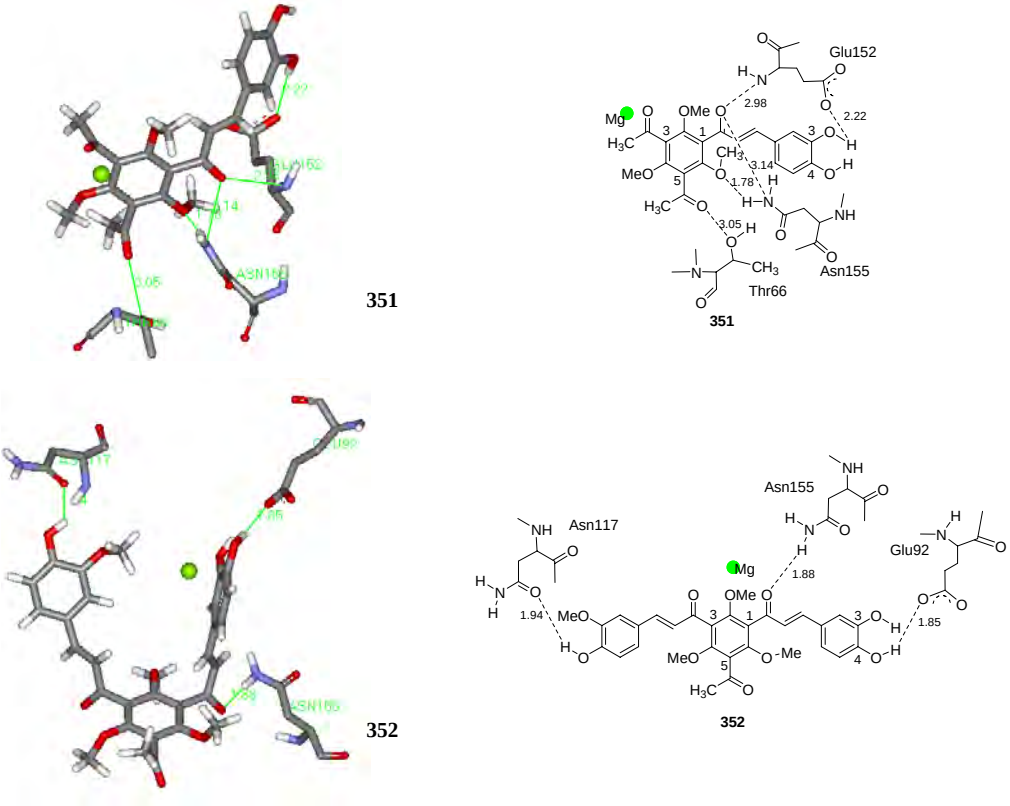

Figure 3.19 Predicted binding conformations of compounds **351** and **352** inside the HIV-1 integrase active site (modified PDB code 1QS4)

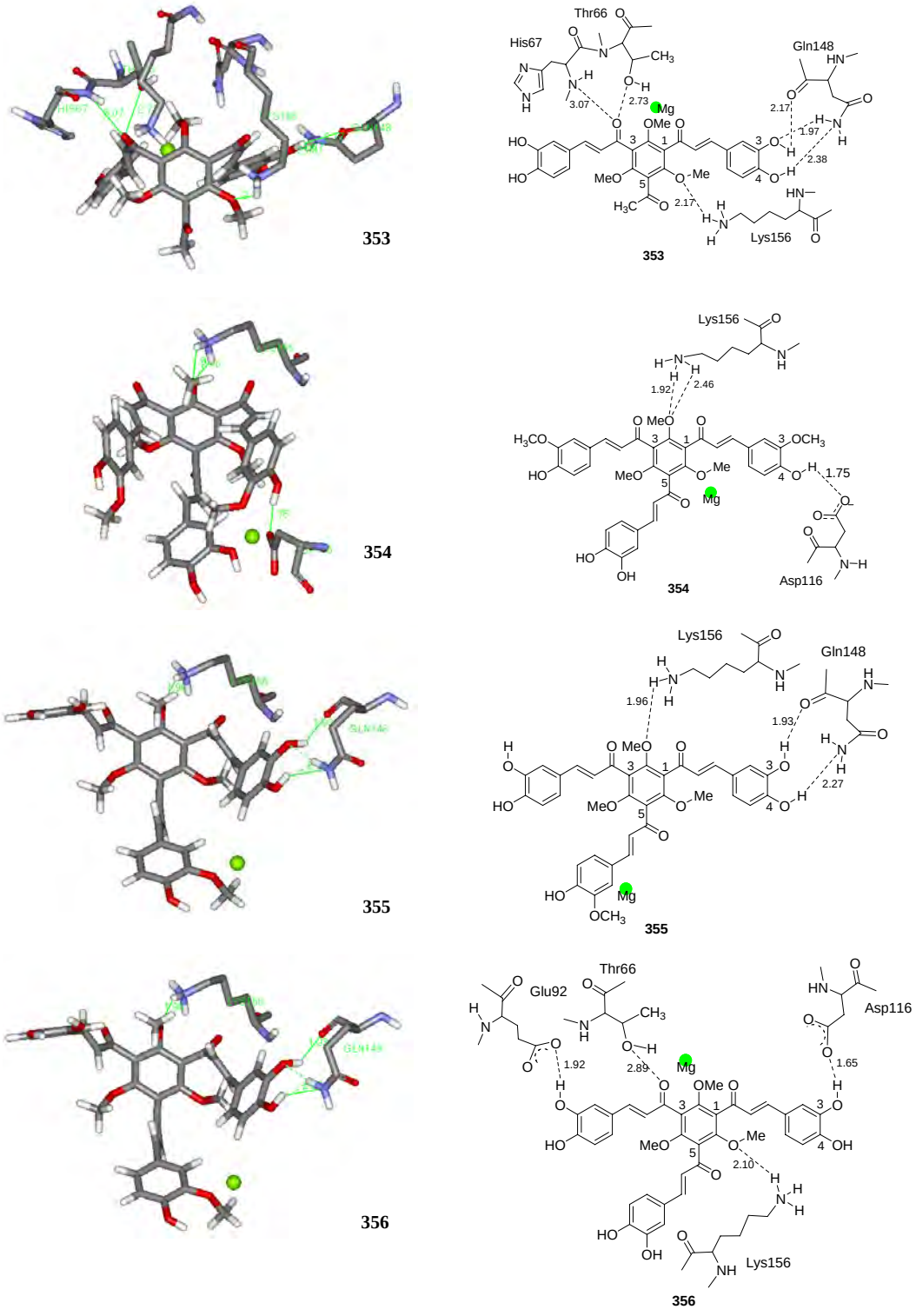

Figure 3.20 Predicted binding conformations of compounds **353**, **354**, **355** and **356** inside the HIV-1 integrase active site (modified PDB code 1QS4)

3.3.7 Superimposition of compound 351 with 353

Compound **351** was superimposed with compound **353** (**Figure 3.21**), in which compound **351** has only one cinnamoyl group while compound **353** has two groups. The results showed that one additional cinnamoyl group of compound **353** formed strong hydrogen bond with carbonyl donor and amide accepter groups of Gln148 whereas *para*-hydroxyl on cinnamoyl group of compound **351** was hydrogen accepter and hydrogen donor with carbonyl and amide groups of Glu152 respectively. The methoxyl group at fifth position on core structure of compound **353** was hydrogen donor with Lys156 while this position in compound **351** formed H-bond with amide accepter of Asn 155. The carbonyl of acetyl group at third position on core structure of compound **351** was hydrogen donor with hydroxyl group of Thr66. When acetyl group of compound **351** was replaced by cinnamoyl group (**353)**, in which carbonyl at the similarly position was hydrogen donor with hydroxyl group of Thr66 and amide group of His67. Compound **353** has more hydrogen bonding than compound **351**. This is a reason for higher activity of compound **353** compared to compound **351** (IC_{50} of 3.5 μM for **353** vs. IC_{50} > 100 μM for **351**).

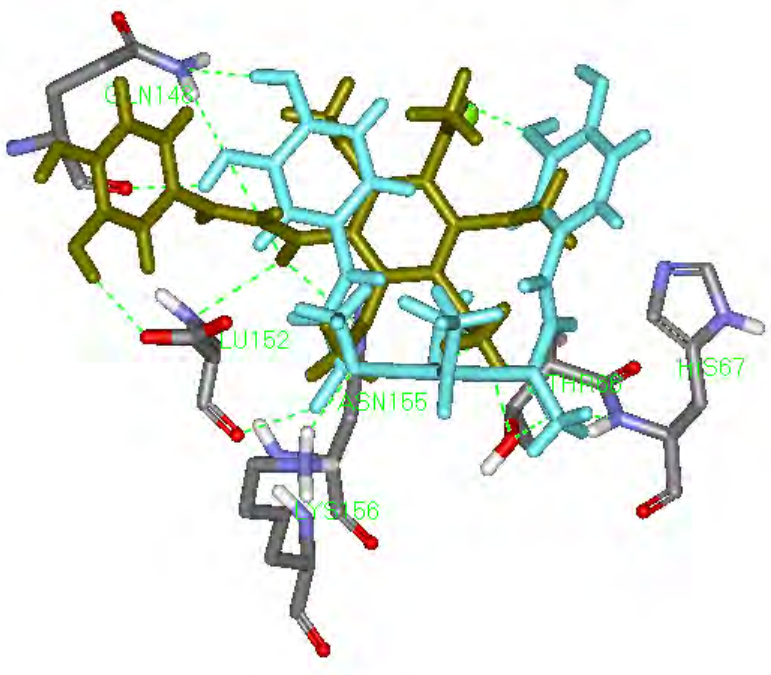

Figure 3.21 Superimposition of predicted binding conformation of compounds **351** and **353** inside the HIV-1 integrase active site

3.3.8 Superimposition of compound 352 with 353

Compound **352** is structurally very similar to compound **353**. The only difference is that the *meta*-hydroxyl group of cinnamoyl group in compound **353** was replaced with methoxyl group in compound **352**. Therefore, the two compounds were superimposed to each other (**Figure 3.22**). The results showed that the catechol of cinnamoyl group in compound **353** and the only one *para*-hydroxyl on cinnamoyl group in compound **352** were hydrogen bond with carbonyl donor and amide accepter groups of Gln148. The methoxyl group at fifth position on core structure of both compounds was hydrogen donor at the same position of Lys156. The carbonyl of acetyl group at third position on core structure of compound **353** was hydrogen donor with hydroxyl group of Thr66 and amide group of His67 while compound **352** has no hydrogen bonding with these amino acid residues. Compound **352** has less hydrogen bonding than compound **353**. Thus it is predicted that compound **352** has lower activity than compound **353** (IC_{50} of 3.5 μM for **353** vs. IC_{50} of 89.4 μM for **352**).

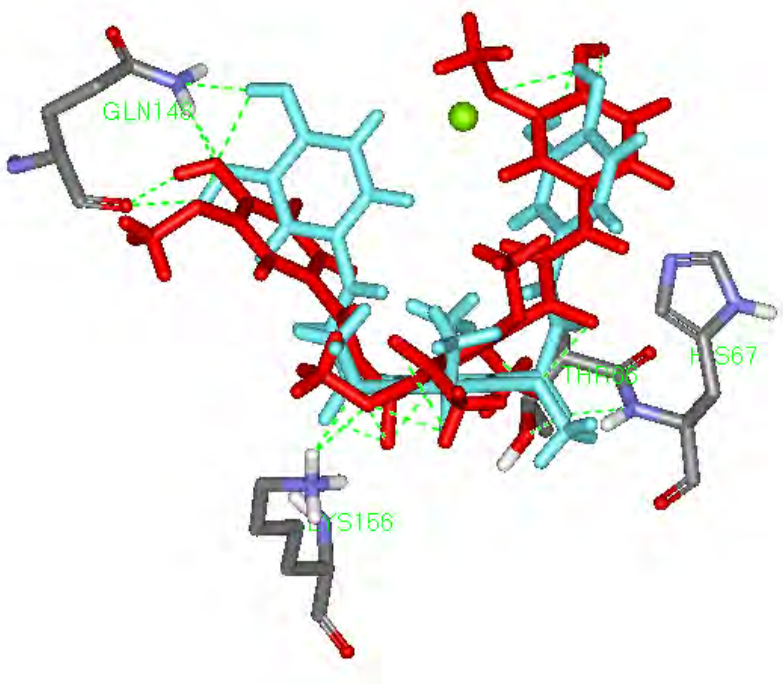

Figure 3.22 Superimposition of predicted binding conformation of compounds **352** and **353** inside the HIV-1 integrase active site

3.3.9 Superimposition of compound 355 with 353

Compound **355** was superimposed with compound **353** (**Figure 3.23**), in which both compounds have two cinnamoyl groups with catechol. But one acetyl group of compound **353** was replaced with one meta-methoxyl of catechol on cinnamoyl group in compound **355**. The results showed that one catechol of cinnamoyl group in compounds **353** and **355** were hydrogen bond with carbonyl donor and amide accepter groups of Gln148. The methoxyl group at fifth position on core structure of both compounds were hydrogen donor at the similarly position of Lys156. The carbonyl of acetyl group at third position on core structure of compound **353** was hydrogen donor with hydroxyl group of Thr66 and amide group of His67 while compound **355** has no hydrogen bonding with these amino acid residues. Compound **355** has less hydrogen bonding than compound **353**. This is in agreement with experimental data which compound **355** is less active than compound **353** (IC_{50} of 3.5 μM for **353** vs. IC_{50} of 16.5 μM for **355**).

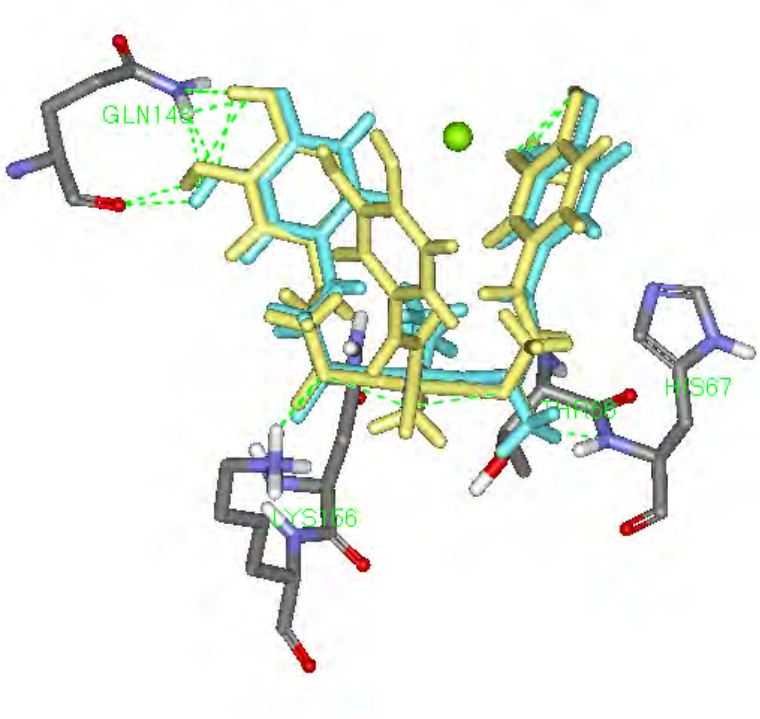

Figure 3.23 Superimposition of predicted binding conformation of compounds **355** and **353** inside the HIV-1 integrase active site

3.3.10 Superimposition of compound 356 with 353

Compound **356** was superimposed with compound **353** (**Figure 3.24**), in which compound **353** has only two cinnamoyl groups with catechol while compound **356** has three such groups. The results showed that a cetachol in one cinnamoyl group of compound **353** was hydrogen bond with carbonyl donor and amide accepter groups of Gln148 whereas *meta*-hydroxyl of cinnamoyl group at first and third position of compound **356** were hydrogen bond with carbonyl donor of Asp116 and carbonyl donor of Glu92. The methoxyl group at fifth position on core structure of both compounds was hydrogen donor at the same position of Lys156. The carbonyl of acetyl group at third position on core structure of compound **353** was hydrogen donor with hydroxyl group of Thr66 and amide group of His67 but compound **356** was hydrogen donor with hydroxyl group of Thr66. Compounds **353** and **356** have equal number of hydrogen bonding but with different amino acid residues. However, compound **353** was bond with important amino acid residue (Gln 148) than compound **356** (Glu92). Therefore, compound **356** has slightly less activity than compound **353** (IC_{50} of 3.5 μM for **353** vs. IC_{50} of 7.0 μM for **356**).

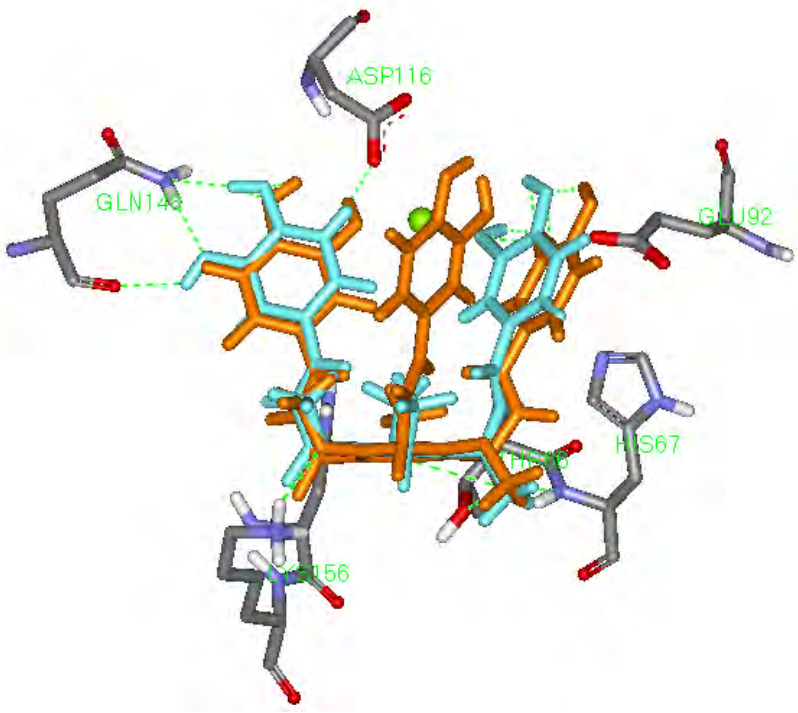

Figure 3.24 Superimposition of predicted binding conformation of compounds **356** and **353** inside the HIV-1 integrase active site

CHAPTER IV

CONCLUSION

This work was divided into three parts that included synthesis, bioassay on HIV-1 integrase and molecular docking of multi-cinanamoyl analogs. The first part was synthesis of starting material compound **334** from phloroglucinol dihydrate **333** was acetylated to obtain compound **334** (76% yield) and followed by methylation to give compound **335** (88% yield) using the reported procedures [64-65]. Compound **335** provided the *ababab* geometric platform in which the later functionalized substituents on 1, 3, 5 positions would point toward the same direction and augment the property of each other. Spectroscopic characterizations were consistent with those of the previous reports [64, 65].

The cinnamoyl moieties bearing compounds were constructed by extending from the acetyl substituents of the obtained hexasubstituted benzene platform. Compounds **336**-**350** were synthesized by using aqueous 80% KOH between the platform **335** and various substituted benzaldehydes such as 2-hydroxybenzaldehyde, 3-hydroxybenzaldehyde, 4-hydroxybenzaldehyde, 4-methoxybenzaldehyde and 3-methoxy-4-hydroxybenzaldehyde, initiated by high concentration of hydroxide base. The condensations gave the mono-cinnamoyl analogs **336**, **339**, **342**, **345** and **348** as the major products in the range of 28-49% yield along with sequentially less amount of bis-cinnamoyl compounds **337**, **340**, **343**, **346** and **349** (10-19% yield) and tris-cinnamoyl compounds **338**, **341**, **344**, **347** and **350** (3-6 %yield).

The catechol moieties on phenyl flanking ring in **351** was synthesized in 18 % yield from demethylation of the methoxy group on the flanking phenyl ring of compound **350** using $AlCl_3$ as the catalyst. Compounds **352** and **353** were similarly synthesized from partial and fully demethylations of the methoxy groups on flanking phenyl rings of compound **349** in 12 and 8 %yields, respectively. In addition, compounds **354**, **355** and **356** were also synthesized in 7.4, 6.5, 2.4% yields respectively from the same process of demethylations of the methoxy groups on flanking phenyl rings of compound **350**. All synthesized compounds were characterized by various methods such as NMR, IR and MS to be consistent with the

expected structures. The syntheses of these products appeared to have rather low yields because the intentional relatively mild demethylating condition and limited reaction time was used to prevent further reaction at the methoxy groups of the core structure. The products could probably be obtained in higher amount with longer reaction time.

Next, anti-HIV-1 IN activity assay of nineteen cinnamoyl analogs **336-355** were carried out using the multiplate integration assay (MIA) method reported by Tewtrakul and coworkers [71, 72]. The multiplate integration assay (MIA) results on some of these newly synthesized compounds indicated position sign of inhibition against HIV-1 integrase. The result suggested that the activity could arise from multiple free hydroxyl groups at *meta*- positions (**341**) and catechol moieties (**352, 353** and **355**) on the flanking aromatic rings of the cinnamoyl moieties, which was more active than other related compounds including curcumin **164**. The five relatively active compounds, **341**, **352**, **353**, **355** and **356** showed IC_{50} values against HIV-1 integrase at 9.5, 89.4, 3.5, 16.5 and 7 μM, respectively. Other twelve phenolic, four methoxybenzene and two catechol derivatives showed only moderate or inactive.

The docking calculations of the tested compounds placed inside the catalytic core of HIV-1 integrase enzyme were performed using Autodock 4.0 program. The studies revealed that the conformationally constrained *meta*-hydroxy group on three flanking phenyl ring of tris-cinnamoyl analogs **341** and dihydroxy groups on flanking phenyl rings of **353** were properly placed inside the binding pocket of IN to establish the relatively strong interactions with the active site Mg^{2+} and five amino acid residues, Glu152, Gln148, Lys156 Ser147 and Thr66 for compound **341,** four amino acid residues, His67, Lys156, Gln148 and Thr66 for **353** and four amino acid residues**,** Asp116, Glu92, Lys156 and Thr66 for **356** within the catalytic core domain of the IN enzyme. This result supported the hypothesis of the importance of multiple *meta*-hydroxy groups and catechol moieties on flanking phenyl ring of hexasubstituted benzene ring that worked together upon binding inside the integrase enzyme active site, rendering the compounds carrying these moieties relatively active and becoming an attractive group of potential anti-HIV drugs.

REFERENCES

[1]. Gottlieb, M. S. AIDS-Past and Future. N. Engl. J. Med. 344 (23) (2001): 1788-1791.

[2]. Gallo, R. C., and Montagnier, L. The discovery of HIV as the cause of AIDS. N. Engl. J. Med. 349 (2003): 2283-2285.

[3]. WHO and UNAIDS. AIDS epidemic update [online] 2010. Available from: http://www.unaids.org/en/media/unaids/contentassets/documents/unaidspublication/2010/20101123_globalreport_en%5B1%5D.pdf [2011, January 29].

[4]. Cotelle, P. Patented HIV-1 Integrase Inhibitors (1998-2005). Recent Patents on Anti-Infective Drug Discover. 1 (2006): 1-15.

[5]. De Clercq, E. New developments in anti-HIV chemotherapy. Curr. Med. Chem. 8 (2001): 1543-1572.

[6]. De Clercq, E. Toward improved anti-HIV chemotherapy: therapeutic strategies for intervention with HIV infections. J. Med. Chem. 38 (1995): 2491-2517.

[7]. Artico, M. Non-nucleoside anti-HIV-1 reverse transcriptase inhibitors (NNRTIs): a chemical survey from lead compounds to selected drugs for clinical trials. Farmaco. 51 (1996): 305-331.

[8]. Martin, J. A., Redshaw, S., and Thomas, G. J. Inhibitors of HIV protease. Prog. Med. Chem. 32 (1995): 239-287.

[9]. Kilby, J. M., et al. Potent suppression of HIV-1 replication in humans by T-20, a peptide inhibitor of gp41-mediated virus entry. Nat. Med. 4 (1998): 1302-1307.

[10]. La Femina, R. L., et al. Requirement of active human immunodeficiency virus type I integrase enzyme for productive infection of human T-lymphoid cells. J. Virol. 66 (1992): 7414-7419.

[11]. Sakai, H., et al. Integration is essential for efficient gene expression of human immunodeficiency virus type I. J. Virol. 67 (1993): 1169-1174.

[12]. Asante-Appiah, E., and Skalka, A. M. Molecular mechanisms in retrovirus DNA integration. Antiviral Res. 36 (1997): 139-156.

[13]. Kukolj, G., and Skalka, A. M. Enhanced and coordinated processing of synapsed viral DNA ends by retroviral integrases *in vitro*. Genes Dev. 9 (1995): 2556-2567.

[14]. Goldgur, Y., et al. Structure of the HIV-1 integrase catalytic domain complexed with an inhibitor: a platform for antiviral drug design. Proc. Natl. Acad. Sci. U.S.A. 96 (1999): 13040-13043.

[15]. Reinke, R., Lee, D. J., and Robinson, W. E. Inhibition of human immuno-deficiency virus type 1 isolates by the integrase inhibitor L-731,988, a diketo acid. Antimicrob. Agents Chemother. 46 (2002): 3292-3297.

[16]. Debyser, Z., Cherepanov, P., Van Maele, B., De Clercq, E., and Witvrouw, M. In search of authentic inhibitors of HIV-1 integrase. Antiviral Chem. Chemother. 13 (2002): 1-15.

[17]. Neamati, N., Sunder, S., and Pommier, Y. Design and discovery of HIV-1 integrase inhibitors. DDT. 2 (11) (1997): 487-498.

[18]. Mazumder, A., Cooney, D., Agbaria, R., Gupta, M., and Pommier, Y. Inhibition of human immunodeficiency virus type 1 integrase by 3'-azido-3'-deoxythymidylate. Proc. Natl. Acad. Sci. USA 91 (1994): 5771-5775.

[19]. Mazumder, A., et al. Effects of nucleotide analogs on hyman immunodeficiency virus type 1 integrase. Mol. Pharmacol. 49 (4) (1996): 621-628.

[20]. Mazumder, A., et al. Probing interactions between viral DNA and human immunodeficiency virus type 1 integrase using dinucleotides. Mol. Pharmacol. 51 (4) (1997): 567-575.

[21]. Mazumder, A., Neamati, N., Ojwang, J. O., Sunder, S., Rando, R. F., and Pommier, Y. Inhibition of the Human Immunodeficiency virus type 1 integrase by guanosine quartet structures. Biochemistry 35 (1996): 13762-13771.

[22]. Fesen, M. R., Kohn, K. W., Leteurtre, F., and Pommier, Y. Inhibitors of human immunodeficiency virus integrase. Proc. Natl. Acad. Sci. USA 90 (1993): 2399-2403.

[23]. Neamati, N., et al. Highly potent synthetic polyamide, bistamycins and lexitropsins as inhibitors of human immunodeficiency virus type 1 integrase. Mol. Pharmacol. 54 (2) (1998): 280-290.

[24]. Eich, E., et al. (-)-Arctigenin as a lead structure for inhibitors of human immunodeficiency virus type-1 integrase. J. Med. Chem. 39 (1) (1996): 86-95.

[25]. LaFemina, R. L., et al. Inhibition of human immunodeficiency virus integrase by bis-caechols. Antimicrob. Agents Chemother. 39 (2) (1995): 320-324.

[26]. Fesen, M. R., Pommier, Y., Leteurtre, F., Hiroguchi, S., Yung, J., and Kohn, K. W. Inhibition of HIV-1 integrase by flavones, caffeic acid phenethyl ester (CAPE) and related compounds. Biochem. Pharmacol. 48 (3) (1994): 595-608.

[27]. Burke, T. R., et al. Hydroxylated aromatic inhibitors of HIV-1 integrase. J. Med. Chem. 38 (1995): 4171-4178.

[28]. Mazumder, A., et al. Effects of tyrphostin, protein kinase inhibitors, on human immunodeficiency virus type 1 integrase. Biochemistry 34 (1995): 15111-15122.

[29]. Robinson, W. E. Jr., Reinecke, M. G., Abdel-Malek, S., Jia, Q., and Chow, S. A. Inhibitors of HIV-1 replication that inhibit HIV integrase. Proc. Natl. Acad. Sci. USA. 93 (1996): 6326-6331.

[30]. Neamati, N., et al. Depsides and depsidones as inhibitors of HIV-1 integrase: discovery of novel inhibitors through 3D database searching. J. Med. Chem. 40 (1997): 942-951.

[31]. Zhao, H., Neamati, N., Mazumder, A., Sunder, S., Pommier, Y., and Burke, Jr. T. R. Arylamide inhibitors of HIV-1 integrase. J. Med. Chem. 40 (1997): 1186-1194.

[32]. Zhao, H., et al. Hydrazide-containing inhibitors of HIV-1 integrase. J. Med. Chem. 40 (1997): 937-941.

[33]. Mazumder, A., et al. Antiretroviral agents as inhibitors of both human immunodeficiency virus type 1 integrase and protease. J. Med. Chem. 39 (1996): 2472-2481.

[34]. Zhao, H., et al. Coumarin-based inhibitors of HIV integrase. J. Med. Chem. 40 (1997): 242-249.

[35]. Cushman, M., and Sherman, P. Inhibition of HIV-1 integration protein by aurintricarboxylic acid monomers, monomer analogs, and polymer fractions. Biochem. Biophys. Res. Commun. 185 (1) (1992): 85-90.

[36]. Cushman, M., et al. Cosalane analogues with enhanced potencies as inhibitors of HIV-1 protease and integrase. J. Med. Chem. 38 (1995): 443-452.

[37]. Carteau, S., Mouscadet, J. F., Goulaouic, H., Subra, F., and Auclair, C. Inhibitory effect of the polyanionic drug suramin on the *in vitro* HIV DNA integration reaction. Arch. Biochem. Biophys. 305 (2) (1993): 606-610.

[38]. Nicklaus, M. C., et al. HIV-1 integrase pharmacophore: discovery of inhibitors through three-dimensional database searching. J. Med. Chem. 40 (1997): 920-929.

[39]. Neamati, N., et al. Diarylsulfones, a novel class of human immunodeficiency virus type 1 integrase inhibitors. Antimicrob. Agents Chemother. 41 (2) (1997): 385-393.

[40]. Mazumdar, A., et al. Curcumin analogs with altered potencies against HIV-1 integrase as probes for biochemical mechanisms of drug action. J. Med. Chem. 40 (1997): 3057-3063.

[41]. Pabon, H. J. J. A synthesis of curcumin and related compounds. Recl. Trav. Chim. Pays-Bas. 83 (1964): 379-386.

[42]. Artico, M., et al. Geometrically and conformationally restrained cinnamoyl compounds as inhibitors of HIV-1 integrase: synthesis, biological evaluation, and molecular modeling. J. Med. Chem. 41 (21) (1998): 3948-3960.

[43]. Costi, R., et al. 2,6-Bis(3,4,5-trihydroxybenzy-lydene) derivatives of cyclohexanone: novel potent HIV-1 integrase inhibitors that prevent HIV-1 multiplication in cell-based assays. Bioorg. Med. Chem. 12 (2004): 199-215.

[44]. Sui, Z., Salto, R., Li, J., Craik, C., and de Montellano, P. R. O. Inhibition of the HIV-1 and HIV-2 proteases by curcumin and curcumin boron complexes. Bioorg. Med. Chem. 6 (1) (1993): 415-422.

[45]. Ramkumar, K., et al. Discovery of 3-acetyl-4-hydroxy-2-pyranone derivatives and their difluoridoborate complexes as a novel class of HIV-1 integrase inhibitors. Bioorg. Med. Chem. 16 (2008): 8988-8998.

[46]. d′ Angelo, J., Mouscadet, J. F., Desmaële, D., Zouhiri, F., and Leh, H. HIV-1 integrase: the next target for AIDS therapy?. Pathol. Biol. 49 (2001): 237-46.

[47]. Marchand, C., et al. Structural determinants for HIV-1 integrase inhibition by β-diketo acids. J. Biol. Chem. 277 (2002): 12596-12603.

[48]. Hazuda, D. J., et al. Inhibitors of strand transfer that prevent integration and inhibit HIV-1 replication in cell. Science. 287 (5453) (2000): 646-650.

[49]. Embrey, M. W., et al. A series of 5-(5-6)-dihydrouracil substituted 8-hydroxy-[1,6]naphthyridine-7-carboxylic acid 4-fluorobenzylamide inhibitors of HIV-1 integrase and viral replication in cells. Bioorg. Med. Chem. Lett. 15 (20) (2005): 4550-4554.

[50]. Miller, M., et al. Biochemical and antiviral activity of MK-0518, a potent HIV integrase inhibitor. XVI International AIDS Conference. August 13-18 (2006): Toronto,Canada.

[51]. Summa, V., et al. Discovery of raltegravia, a potent, selective orally bioavailable HIV-integrase inhibitor for the treatment of HIV-AIDS infection. J. Med. Chem. 51 (2008): 5843-5855.

[52]. Al-Mawsawi, L. Q., Al-Safi, R. I., and Neamati, N. Anti-infectives clinical progress of HIV-1 integrase inhibitors. Expert Opin. Emerg. Drugs 13 (2008): 213-225.

[53]. Iwamoto, M., et al. Safety, tolerability, and pharmacokinetics of raltegravir after single and multiple doses in healthy subjects. Clin. Pharmacol. Ther. 83 (2008): 293-299.

[54]. Braun, J. F., Cronje, R. J., and Henderson, M. G. HIV-1 integrase inhibitors. The PRN Notebook. 13 (2008): 1-9.

[55]. Robinson, T. P., Hubbard IV, R. B., Ehlers, T. J., Arbiser, J. L., Goldsmith, D. J., and Bowen, J. P. Synthesis and biological evaluation of aromatic eneones related to curcumin. Bioorg. Med. Chem. 13 (2005): 4007-4013.

[56]. Jin, F., et al. Structural requirements of 2',4',6'-tris(methoxymethoxy) chalcone derivatives for anti-inflammatory activity: the importance of 2'-hydroxy moiety. Arch. Pharm. Res. 30 (11) (2007) 1359-1367.

[57]. Aponte, J. C., et al. Synthesis, Cytotoxicity, and anti-*Trypanosoma cruzi* activity of new chalcones. J. Med. Chem. 51 (2008): 6230-6234.

[58]. Boumendjel, A., et al. Antimitotic and antiproliferative activities of chalcones: forward structure-activity relationship. J. Med. Chem. 51 (2008): 2307 2310.

[59]. Kavvadias, D., et al. The flavone hispidulin, a benzodiazepine receptor ligand with positive allosteric properties, traverses the blood-brain barrier and exhibits anticonvulsive effects. Br. J. Pharmacol. 142 (2004): 811-820.

[60]. Xu, B., Pelish, H., Kirchhausen, T., and Hammond, G. B. Large scale synthesis of the Cdc42 inhibitor secramine A and its inhibition of cell spreading. Org. Biomol. Chem. 4 (2006): 4149-4157.

[61]. Vutukuri, D. R., Bharathi, P., Yu, Z., Rajasekaran, K., Tran, M. H., and Thayumanavan, S. A mild deprotection strategy for allyl-protecting groups and its implications in sequence specific dendrimer synthesis. J. Org. Chem. 68 (2003): 1146-1149.

[62]. Smith, A. B., Rivero, R. A., Hale, K. J., and Vaccaro, H. A. Phyllanthoside-phyllanthostatin synthetic studies. 8. Total synthesis of (+)-phyllanthoside. Development of the Mitsunobu glycosyl ester protocol. J. Am. Chem. Soc. 113 (1991): 2092-2112.

[63]. Maria, K., Dimitra, H. L., and Maria, G. Synthesis and anti-inflammatory activity of chalcones and related mannich bases. Medicinal Chemistry 4 (2008): 586-596.

[64]. Saowanaporn Choksakulporn. Synthesis of hexasubstituted benzene derivatives from phloroglucinol. M.Sc. Thesis, Department of Chemistry, Chulalongkorn University, Bangkok 2005.

[65]. Simaan, S., Siegel, J. S., and Biali, S. E. Tris(arylmethyl) derivatives of 1,3,5-trimethoxy and 1,3,5-triethylbenzene. J. Org. Chem. 68 (2003): 3699-3670.

[66]. Vajragupta, O., Boonchoong, P., Morris, G. M., and Olson, A. J. Active site binding modes of curcumin in HIV-1 protease and integrase. Bioorg. Med. Chem. Lett. 15 (2005): 3364-3368.

[67]. Healy, E. F., Sanders, J., King, P. J., and Robinson, W. E. Jr. A docking study of L-chicoric acid with HIV-1 integrase. J. Mol. Graph. Model. 27 (2009): 584-589.

[68]. Lee, D. J., and Robinson, W. E. Jr. Preliminary mapping of a putative inhibitor-bindingpocket for HIV-1 integrase inhibitors. Antimicrob. Agents Chemother. 50 (2006): 134-142.

[69]. Lin, Z., et al. Chicoric acid analogues as HIV-1 integrase inhibitors. J. Med. Chem. 42 (1999): 1401-1414.

[70]. Chang, Y. C., Ching, T. T., and Syu, W. J. Assaying the activity of HIV-1 integrase with DNA-coated plates. J. Virol. Methods. 59 (1996): 135-140.

[71]. Tewtrakul, S., et al. HIV-1 integrase inhibitory substances from *Coleus parvifolius*. Phytother. Res. 17 (2003): 232-239.

[72]. Tewtrakul, S., Itharat, A., and Rattanasuwan, P. Anti-HIV-1 protease and HIV-1 integrase activities of Thai medicinai piants known as Hua-Khao-Yen. J. Ethnopharmacol. 105 (2006): 312-315.

[73]. Hou, Z., Stack, T. D. P., Sunderland, C. J., and Raymond, K. Enhanced iron (III) chelation through ligand predisposition: syntheses, structures and stability of tris-catecholate enterobactin analogs. Inorg. Chem. Acta 263 (1997): 341-355.

[74]. Marks, V., Gottlieb, H. E., and Biali, S. E. Stereochemistry of polyethylated aromatic systems. Eur. J. Org. Chem. (2003): 1825-1835.

[75]. CSB PDB Protein DATA BANK [online] 2011. Available from: http://www.rcsb.org/pdb/home/home.do [2009, October 7].

APPENDIX

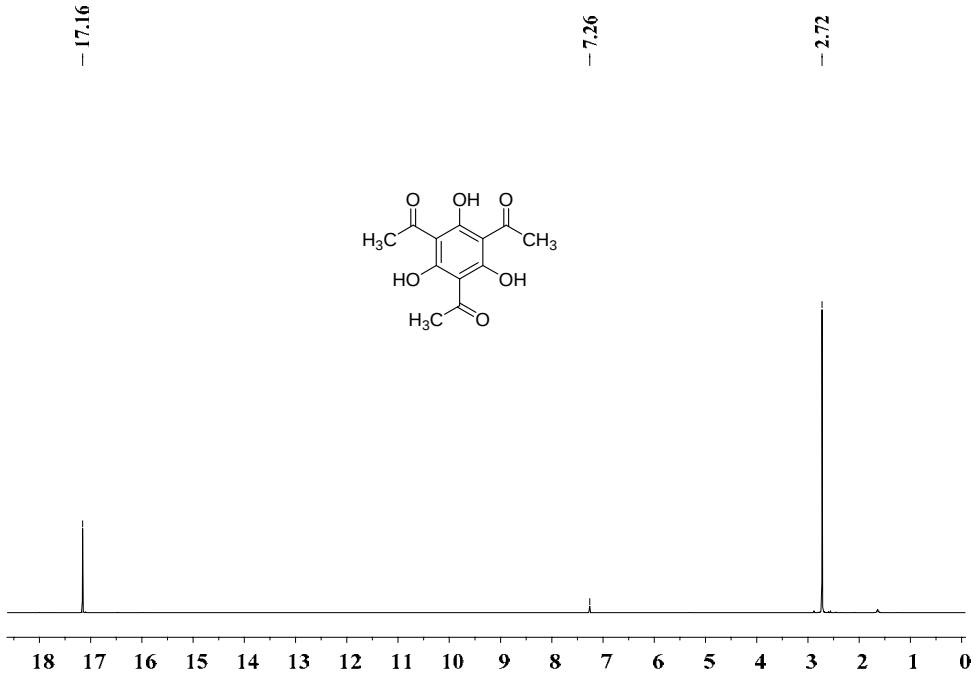

Figure A.1 ^{1}H-NMR ($CDCl_3$) spectrum of 1,3,5-triacetyl-2,4,6-trihydroxybenzene (**334**)

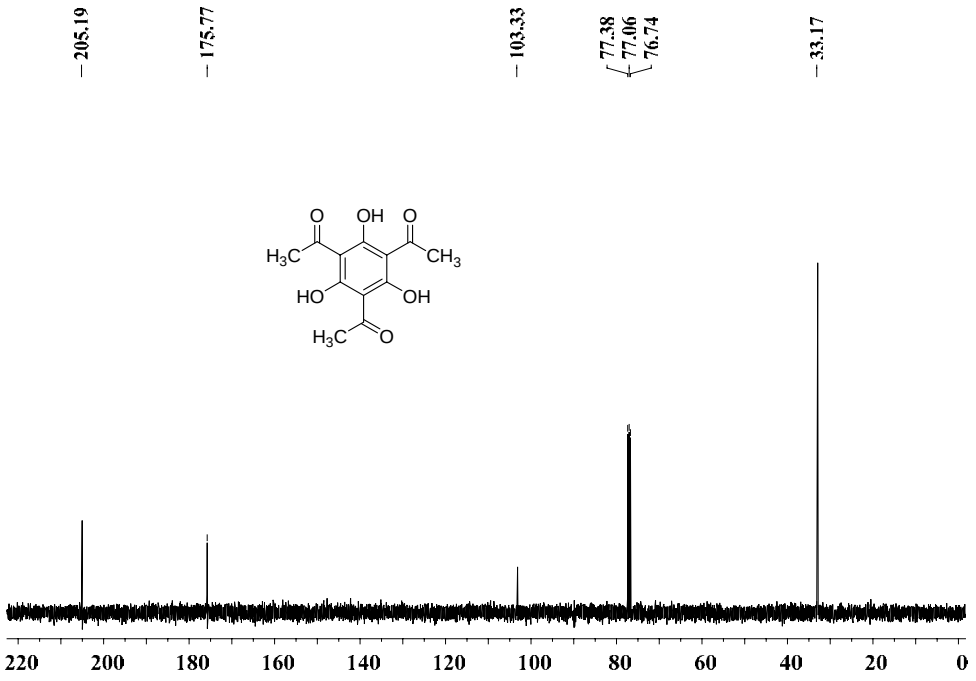

Figure A.2 ^{13}C-NMR ($CDCl_3$) spectrum of 1,3,5-triacetyl-2,4,6-trihydroxybenzene (**334**)

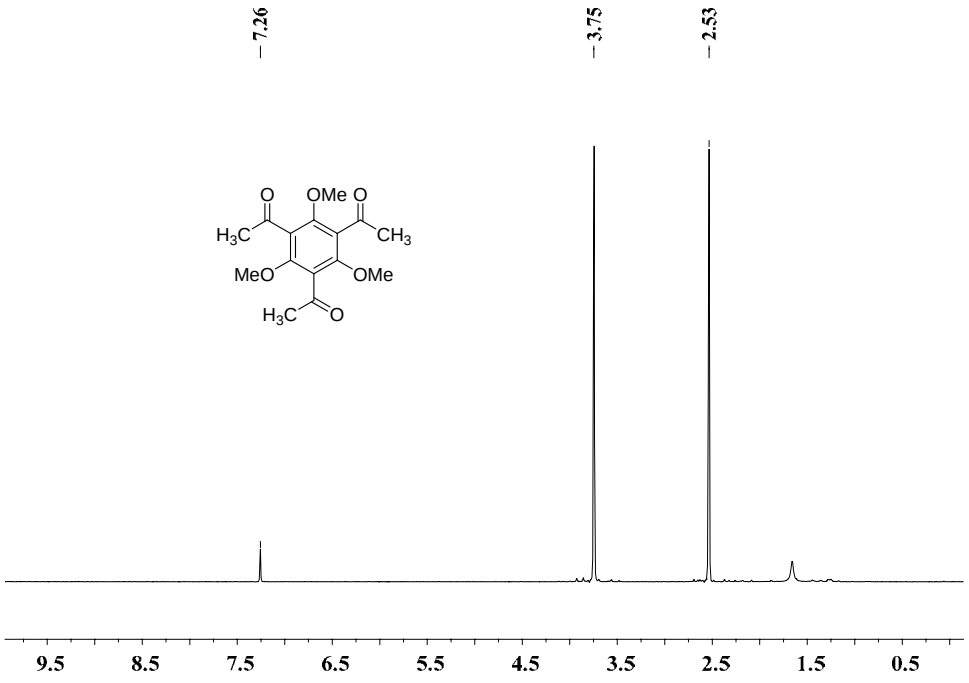

Figure A.3 ^{1}H-NMR ($CDCl_3$) spectrum of 1,3,5-triacetyl-2,4,6-trimethoxybenzene (**335**)

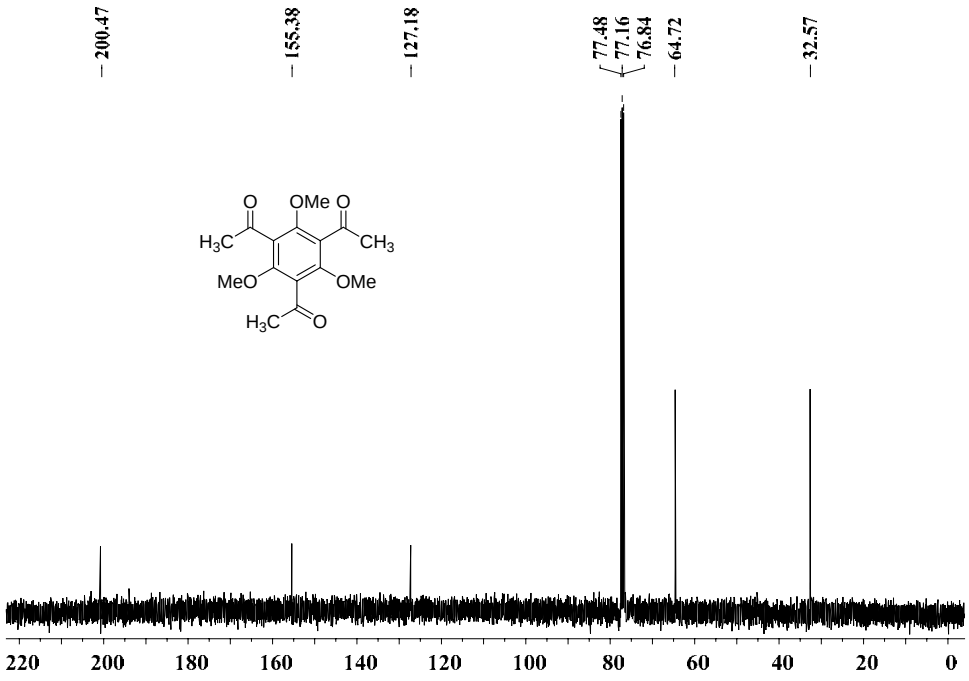

Figure A.4 ^{13}C-NMR ($CDCl_3$) spectrum of 1,3,5-triacetyl-2,4,6-trimethoxybenzene (**335**)

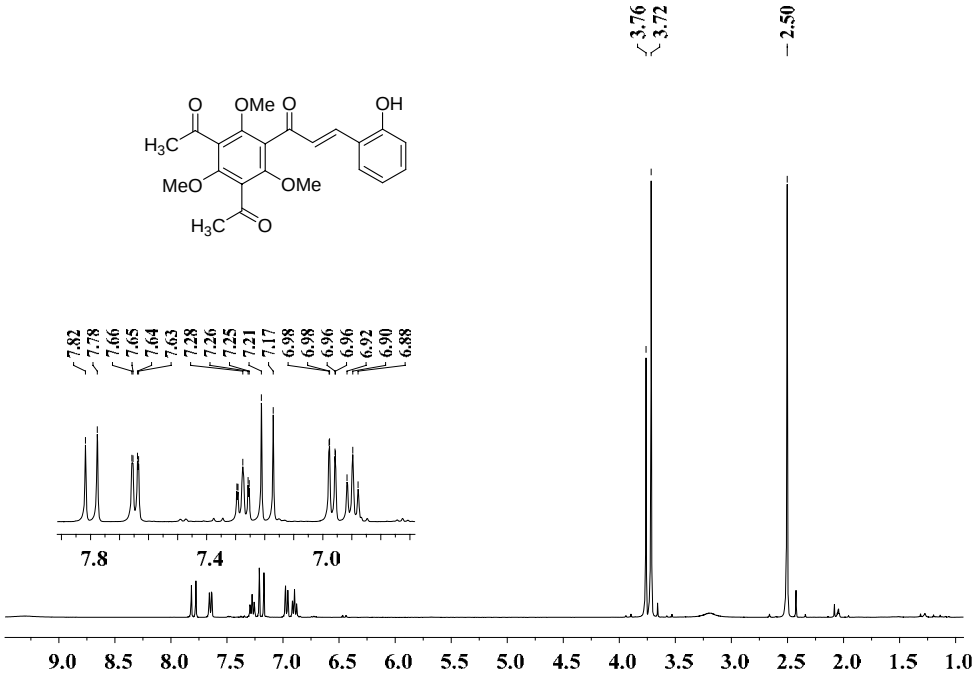

Figure A.5 ^{1}H-NMR (Acetone-d_6) spectrum of 1-(2-hydroxycinnamoyl)-3,5-diacetyl-2,4,6-trimethoxybenzene (**336**)

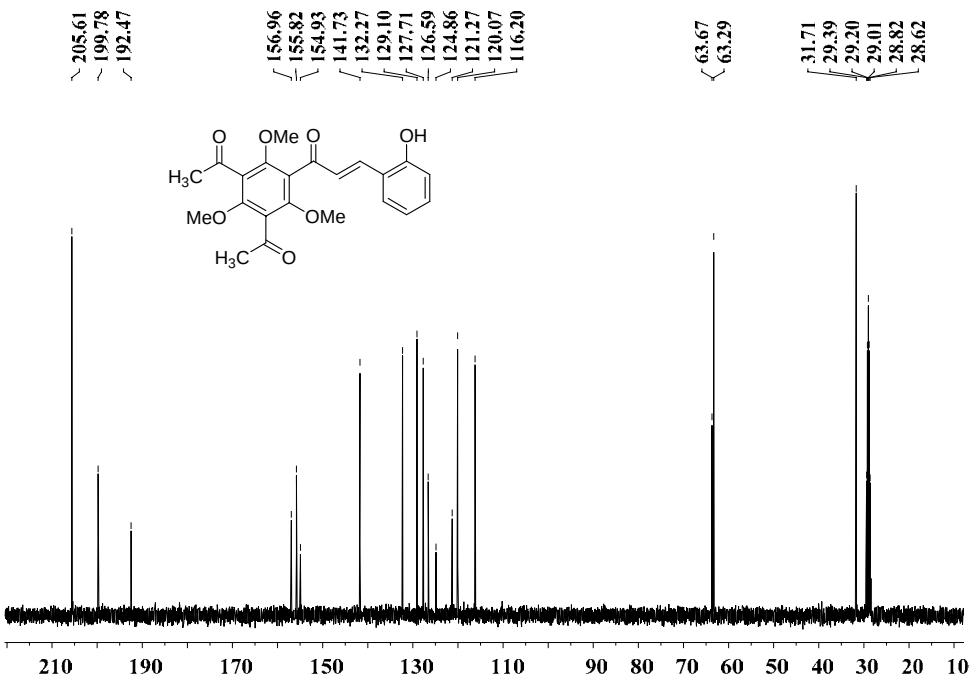

Figure A.6 ^{13}C-NMR (Acetone-d_6) spectrum of 1-(2-hydroxycinnamoyl)-3,5-diacetyl-2,4,6-trimethoxybenzene (**336**)

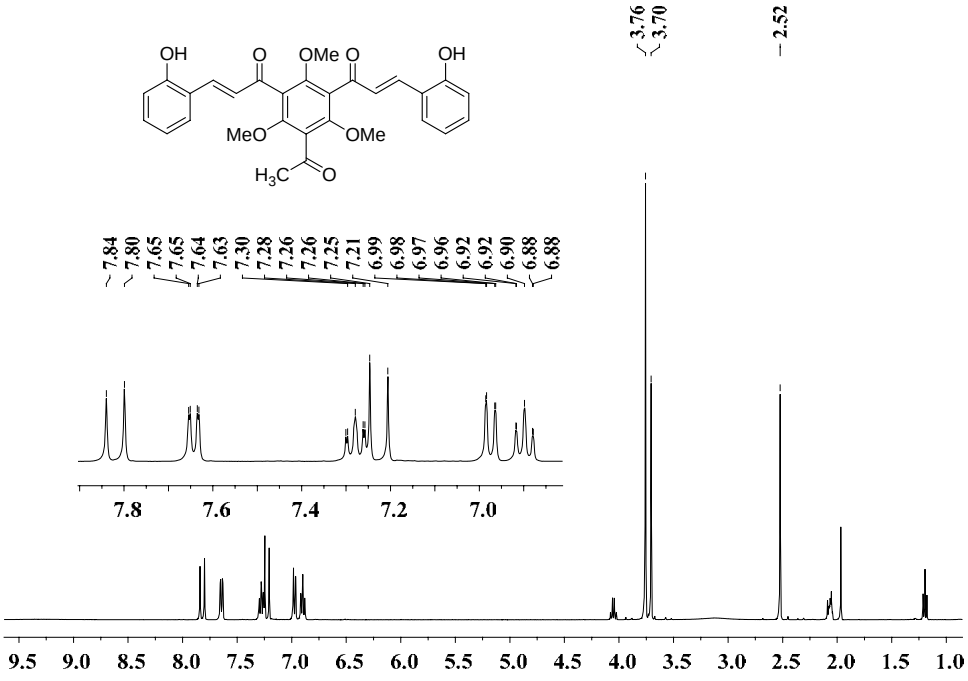

Figure A.7 ^{1}H-NMR (Acetone-d_6) spectrum of 1,3-bis(2-hydroxycinnamoyl)-5-acetyl-2,4,6-trimethoxybenzene (**337**)

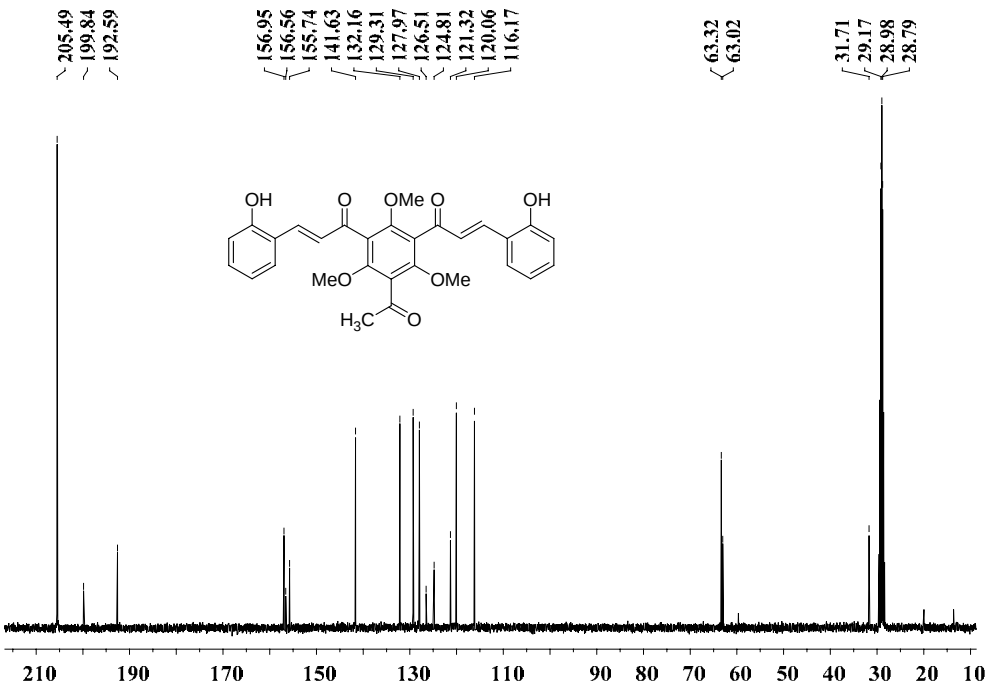

Figure A.8 ^{13}C-NMR (Acetone-d_6) spectrum of 1,3-bis(2-hydroxycinnamoyl)-5-acetyl-2,4,6-trimethoxybenzene (**337**)

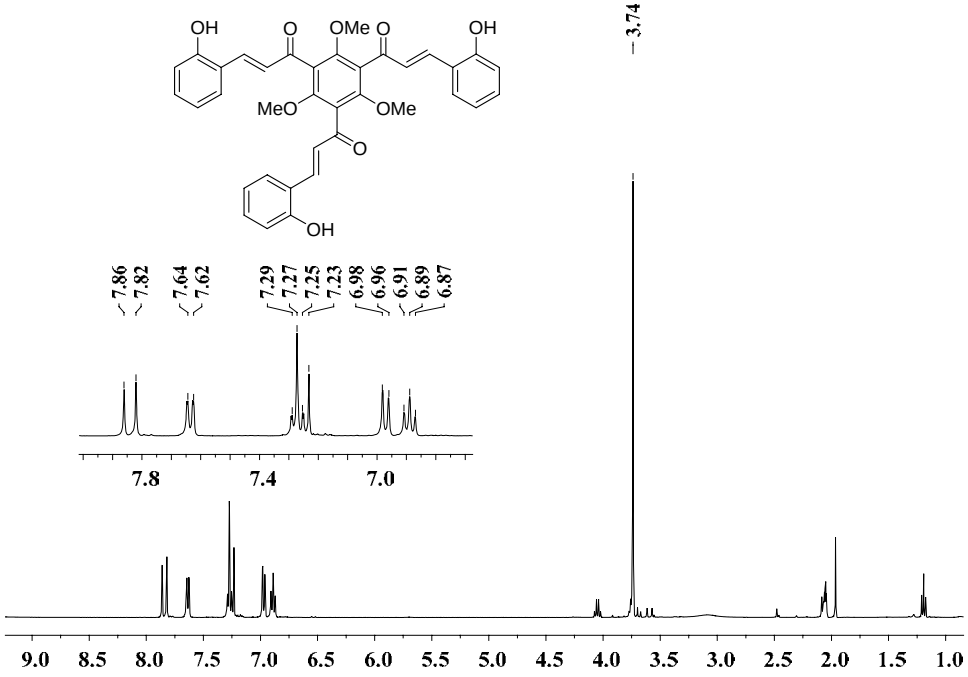

Figure A.9 ^{1}H-NMR (Acetone-d_6) spectrum of 1,3,5-tris(2-hydroxycinnamoyl)-2,4,6-trimethoxybenzene (**338**)

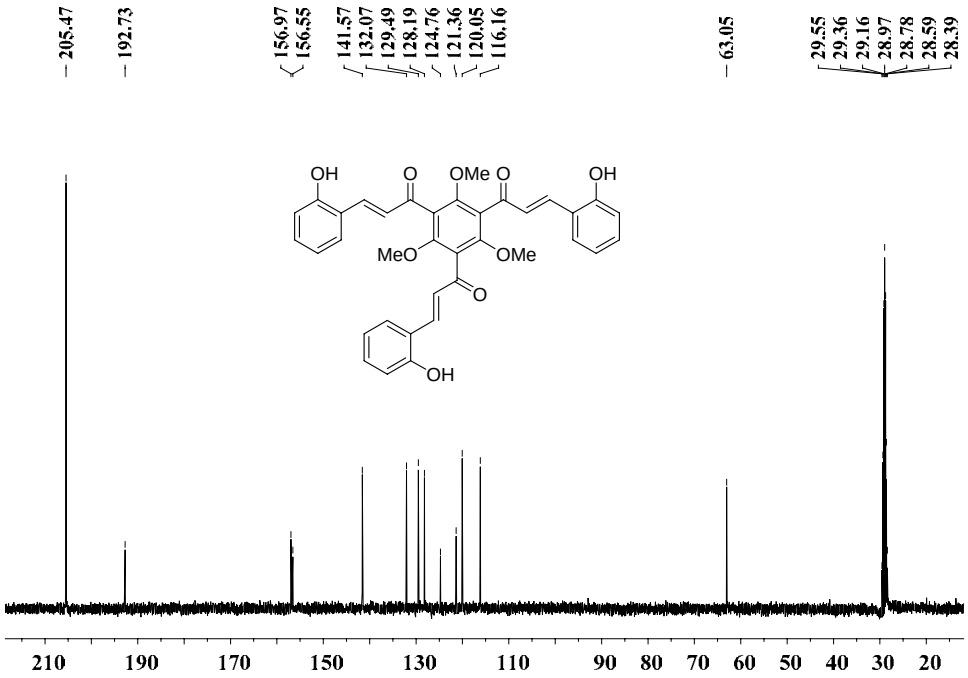

Figure A.10 ^{13}C-NMR (Acetone-d_6) spectrum of 1,3,5-tris(2-hydroxycinnamoyl)-2,4,6-trimethoxybenzene (**338**)

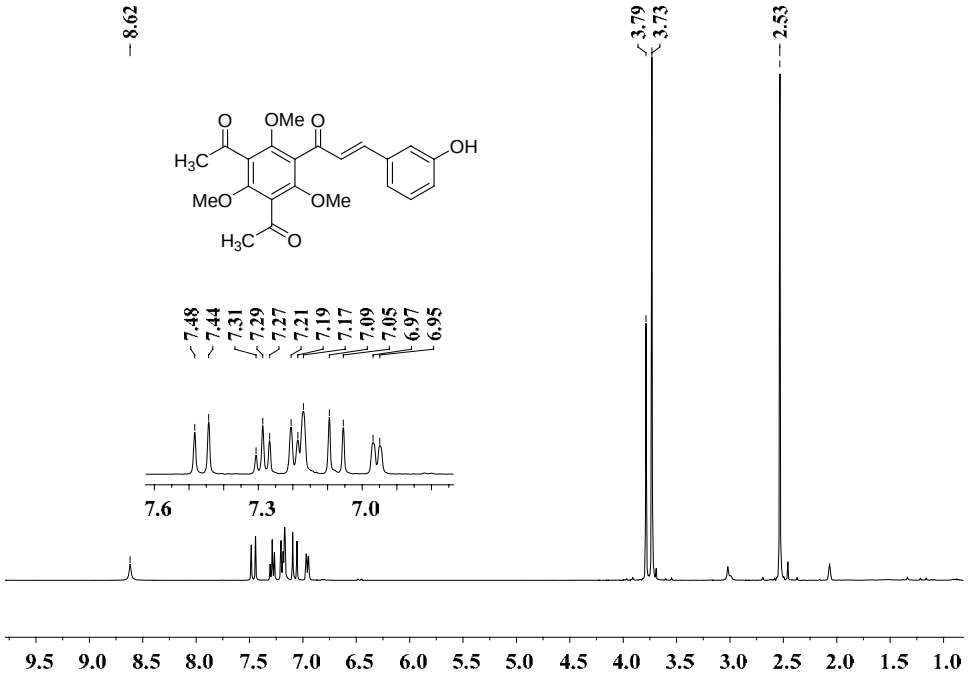

Figure A.11 ^{1}H-NMR (Acetone-d_6) spectrum of 1-(3-hydroxycinnamoyl)-3,5-diacetyl-2,4,6-trimethoxyenzene (**339**)

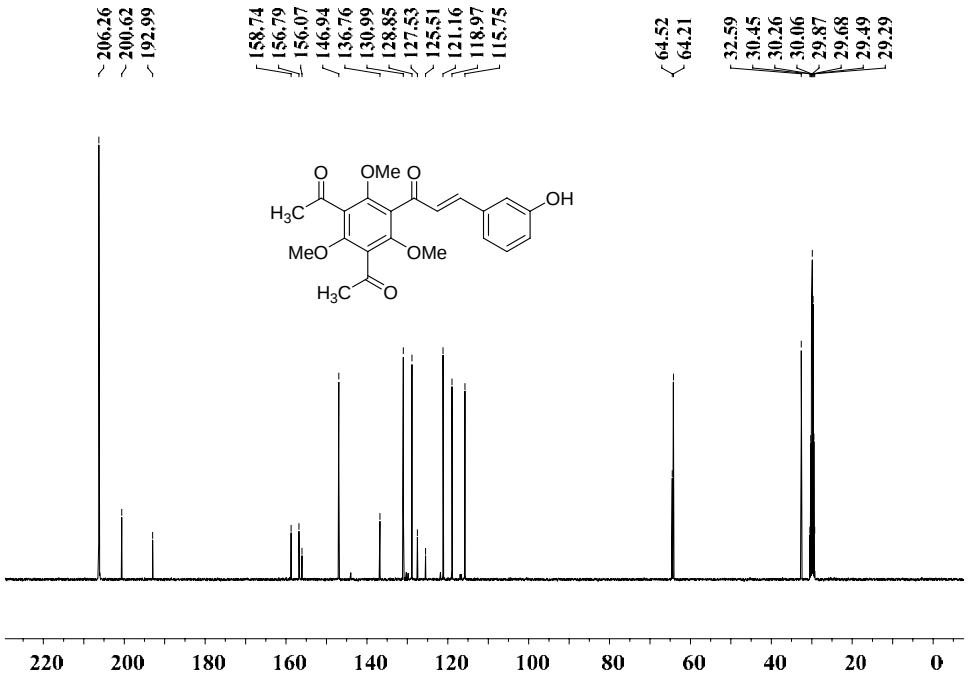

Figure A.12 ^{13}C-NMR (Acetone-d_6) spectrum of 1-(3-hydroxycinnamoyl)-3,5-diacetyl-2,4,6-trimethoxyenzene (**339**)

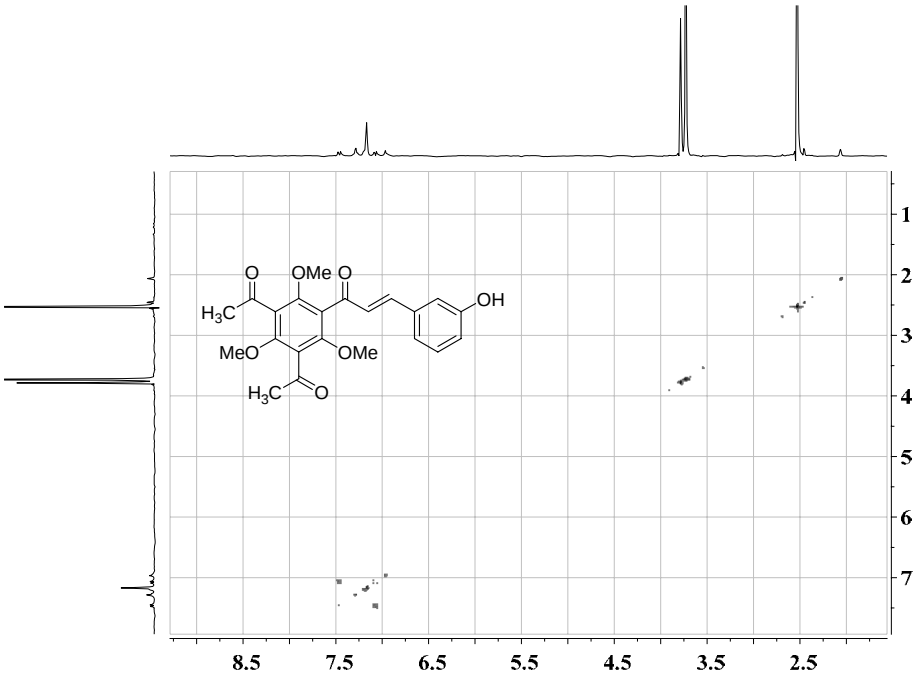

Figure A.13 COSY NMR (Acetone-d_6) spectrum of 1-(3-hydroxycinnamoyl)-3,5-diacetyl-2,4,6-trimethoxyenzene (**339**)

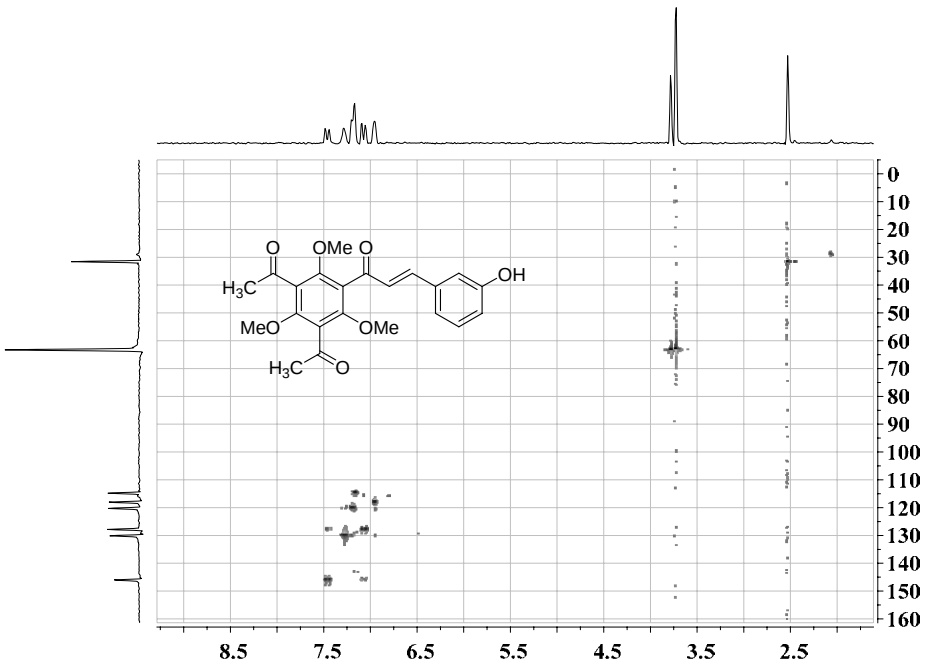

Figure A.14 HMQC NMR (Acetone-d_6) spectrum of 1-(3-hydroxycinnamoyl)-3,5-diacetyl-2,4,6-trimethoxyenzene (**339**)

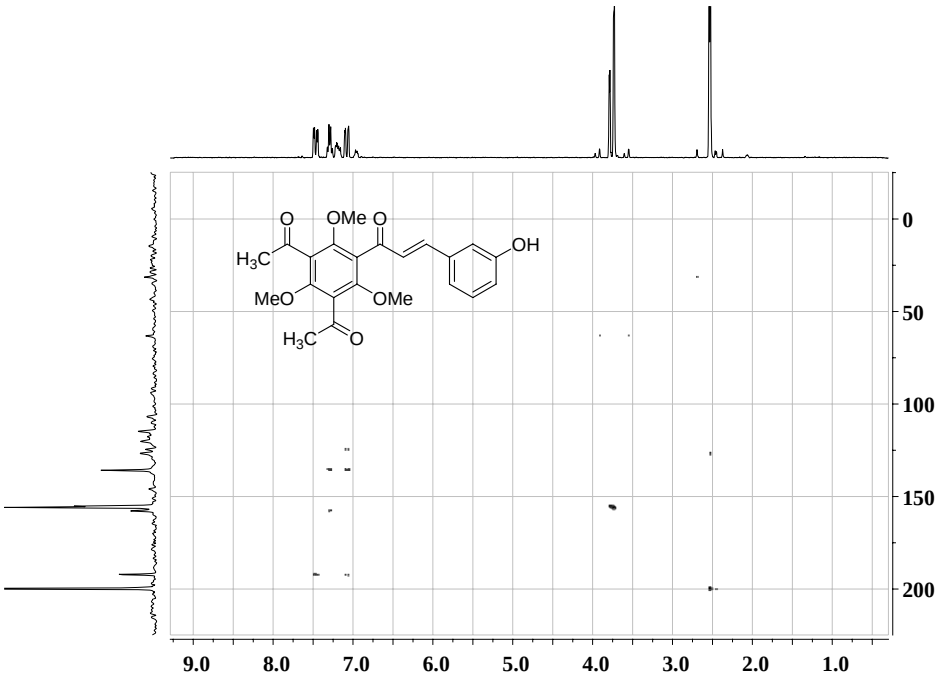

Figure A.15 HMBC NMR (Acetone-d_6) spectrum of 1-(3-hydroxycinnamoyl)-3,5-diacetyl-2,4,6-trimethoxyenzene (**339**)

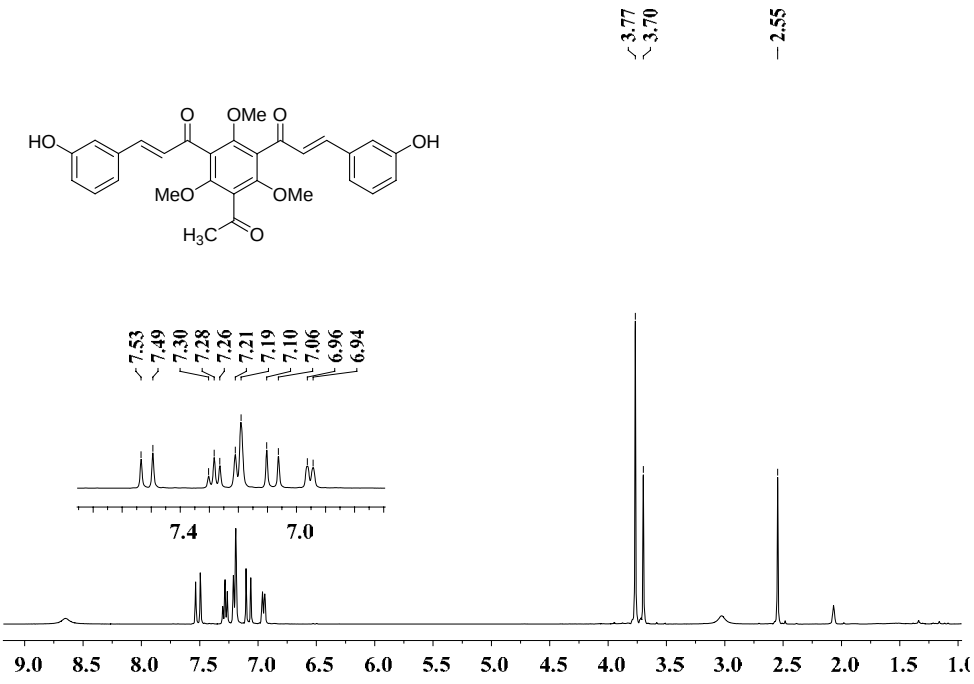

Figure A.16 ^{1}H-NMR (Acetone-d_6) spectrum of 1,3-bis(3-hydroxycinnamoyl)-5-acetyl-2,4,6-trimethoxybenzene (**340**)

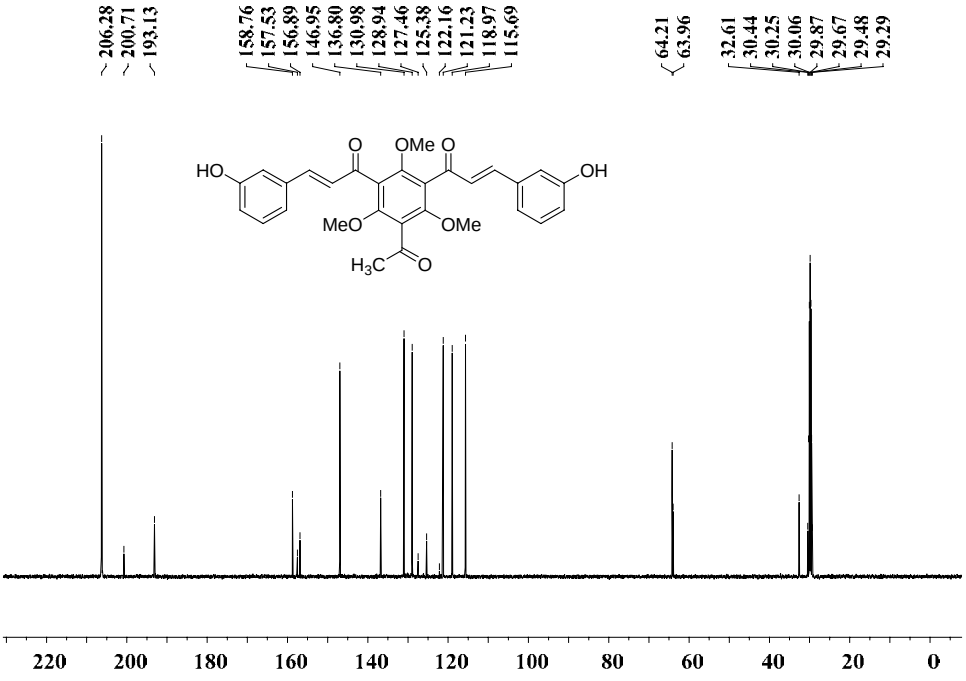

Figure A.17 ^{13}C-NMR (Acetone-d_6) spectrum of 1,3-bis(3-hydroxycinnamoyl)-5-acetyl-2,4,6-trimethoxybenzene (**340**)

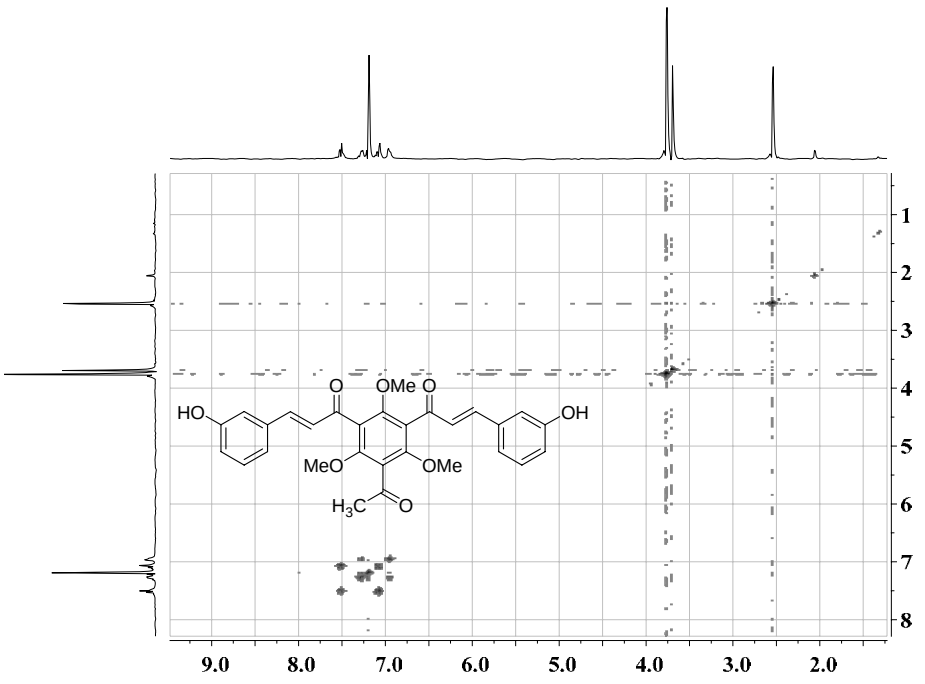

Figure A.18 COSY NMR (Acetone-d_6) spectrum of 1,3-bis(3-hydroxycinnamoyl)-5-acetyl-2,4,6-trimethoxybenzene (**340**)

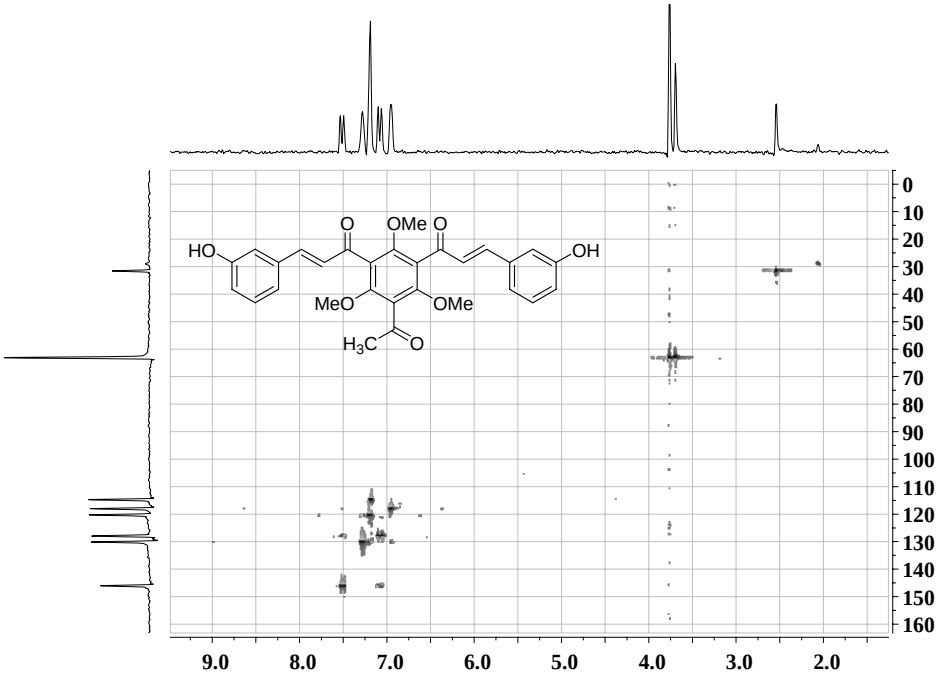

Figure A.19 HMQC NMR (Acetone-d_6) spectrum of 1,3-bis(3-hydroxycinnamoyl)-5-acetyl-2,4,6-trimethoxybenzene (**340**)

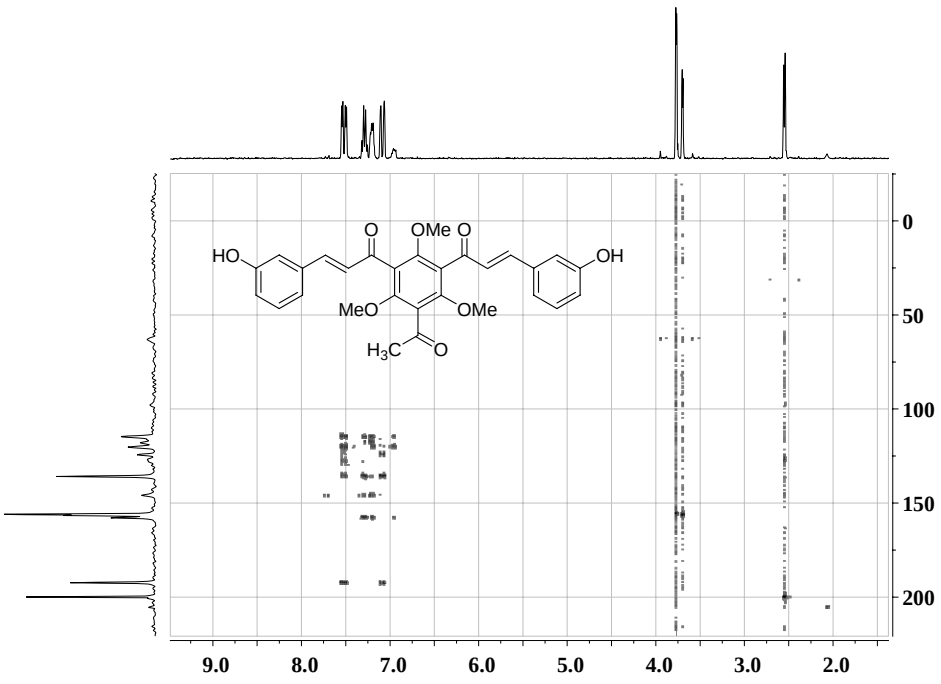

Figure A.20 HMBC NMR (Acetone-d_6) spectrum of 1,3-bis(3-hydroxycinnamoyl)-5-acetyl-2,4,6-trimethoxybenzene (**340**)

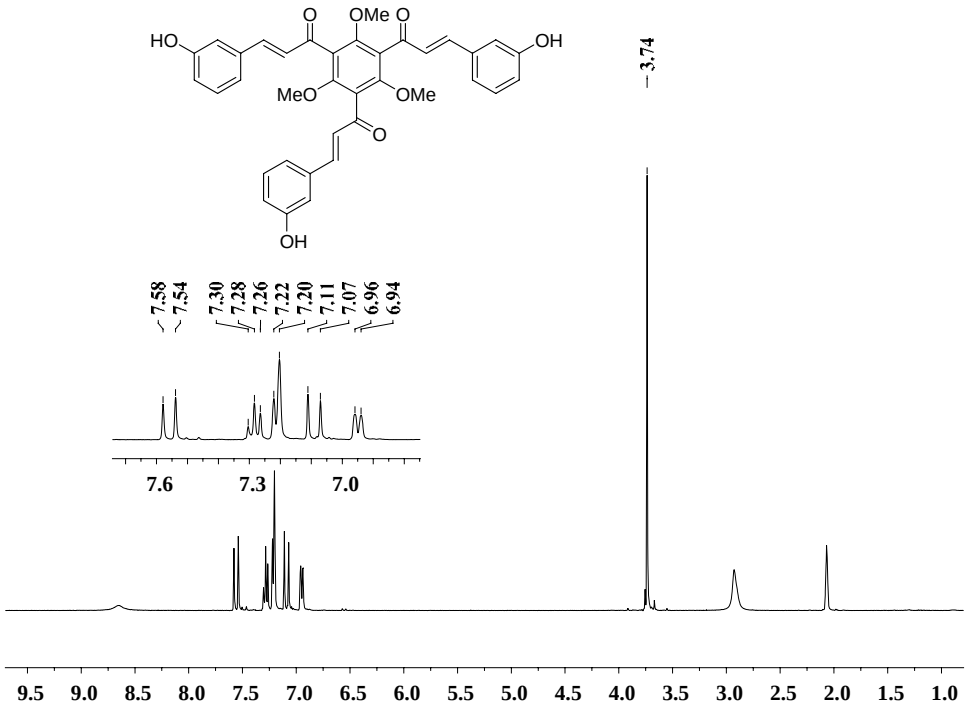

Figure A.21 ^{1}H-NMR (Acetone-d_6) spectrum of 1,3,5-tris(3-hydroxycinnamoyl)-2,4,6-trimethoxybenzene (**341**)

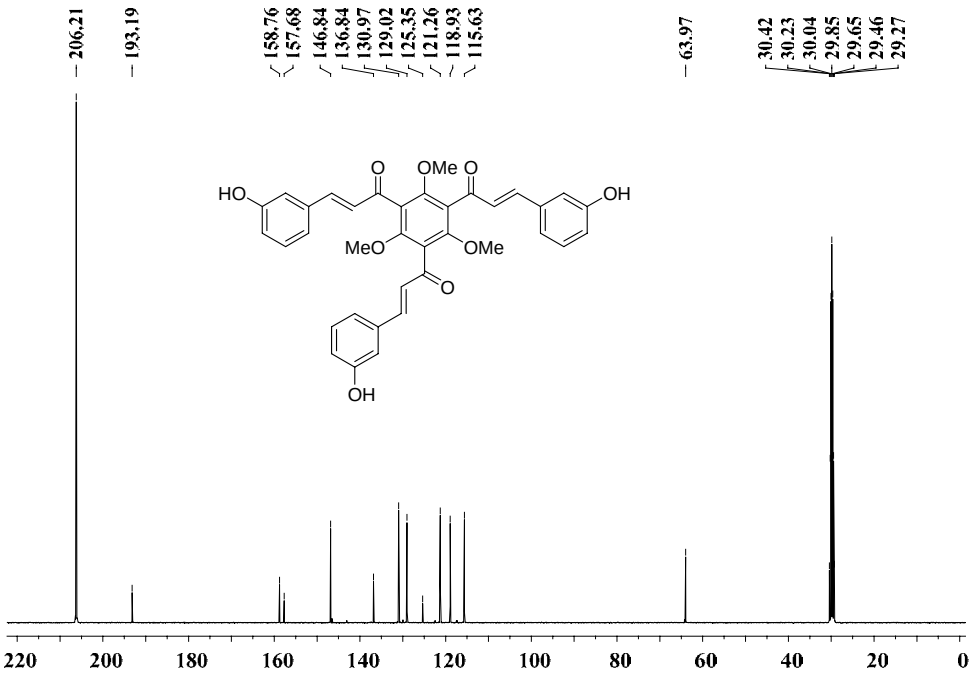

Figure A.22 ^{13}C-NMR (Acetone-d_6) spectrum of 1,3,5-tris(3-hydroxycinnamoyl)-2,4,6-trimethoxybenzene (**341**)

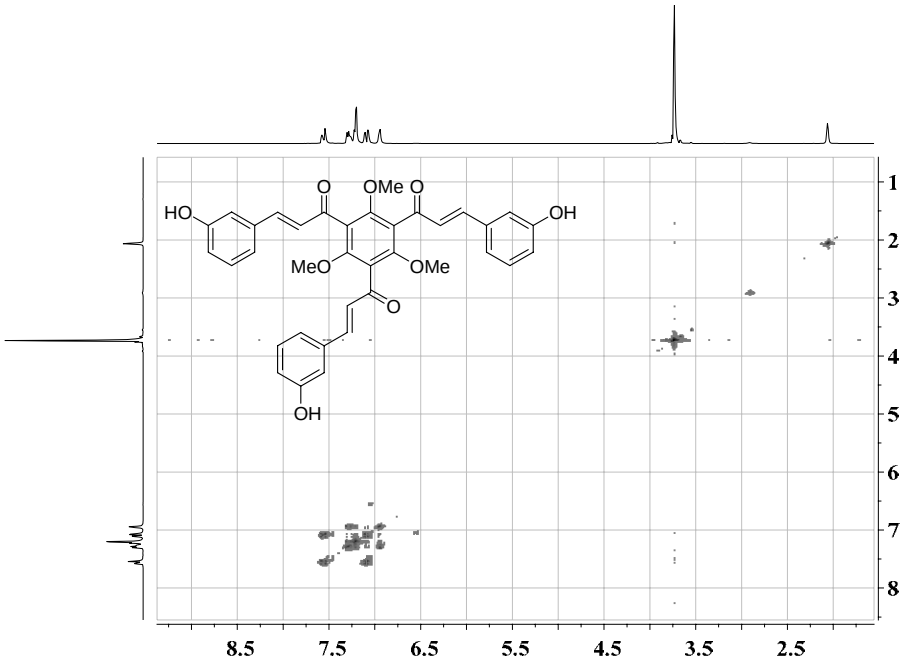

Figure A.23 COSY (Acetone-d_6) spectrum of 1,3,5-tris(3-hydroxycinnamoyl)-2,4,6-trimethoxybenzene (**341**)

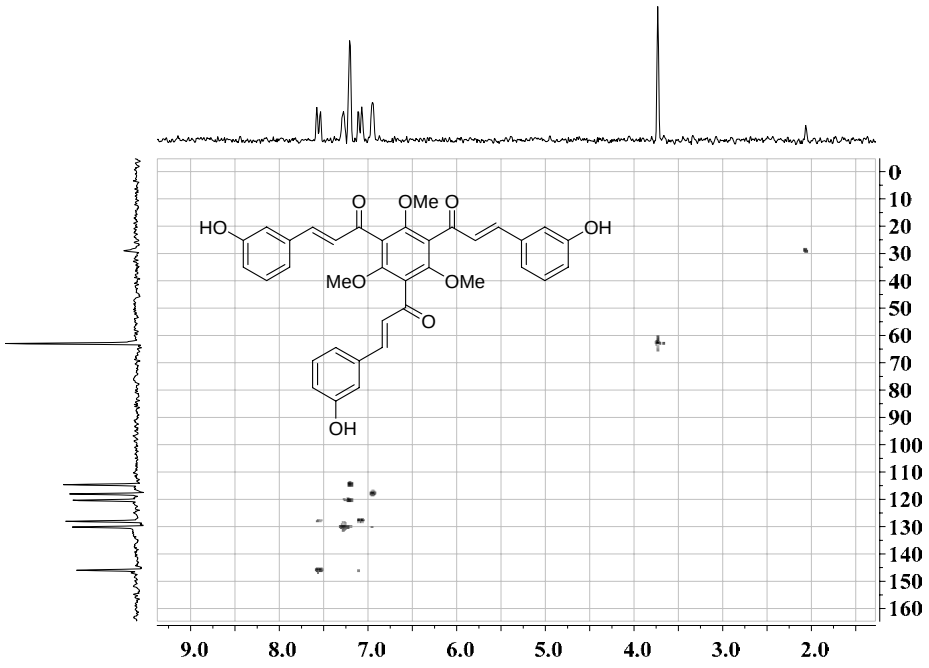

Figure A.24 HMQC (Acetone-d_6) spectrum of 1,3,5-tris(3-hydroxycinnamoyl)-2,4,6-trimethoxybenzene (**341**)

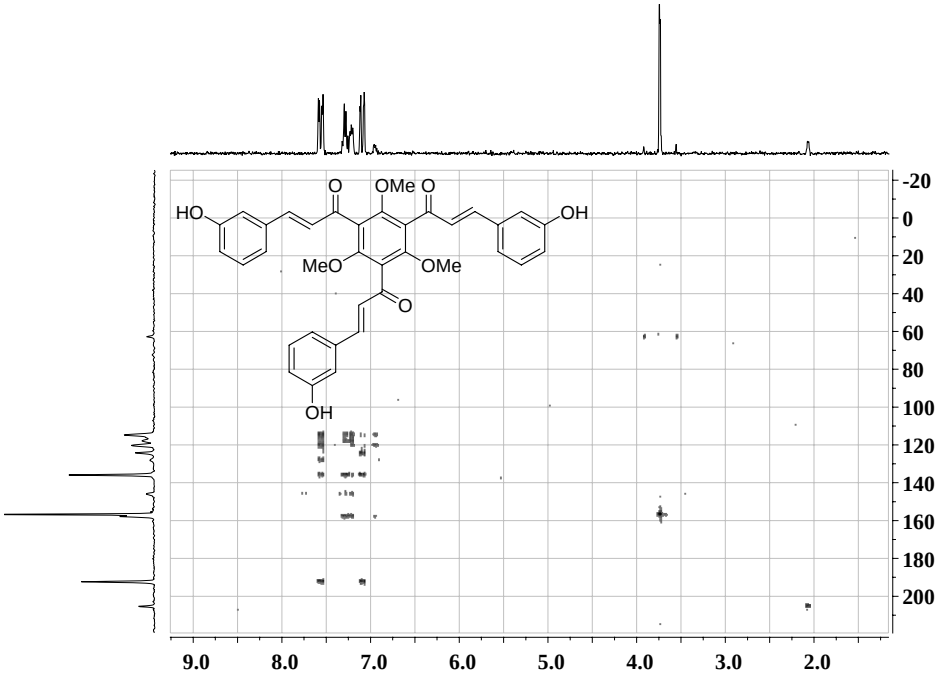

Figure A.25 HMBC NMR (Acetone-d_6) spectrum of 1,3,5-tris(3-hydroxycinnamoyl)-2,4,6-trimethoxybenzene (**341**)

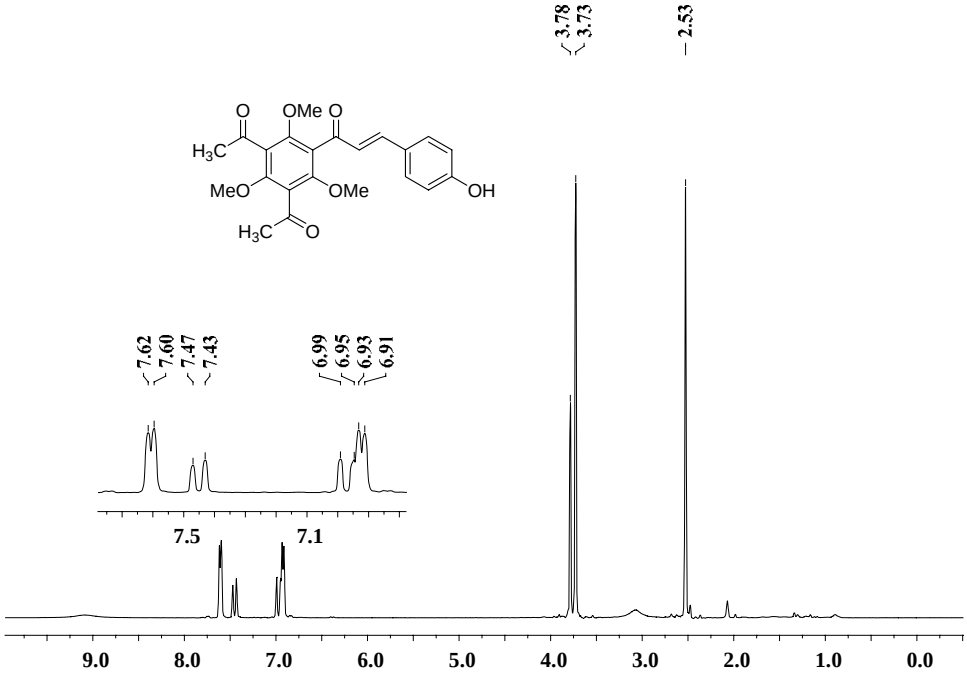

Figure A.26 ^{1}H-NMR (Acetone-d_6) spectrum of 1-(4-hydroxycinnamoyl)-3,5-diacetyl-2,4,6-trimethoxybenzene (**342**)

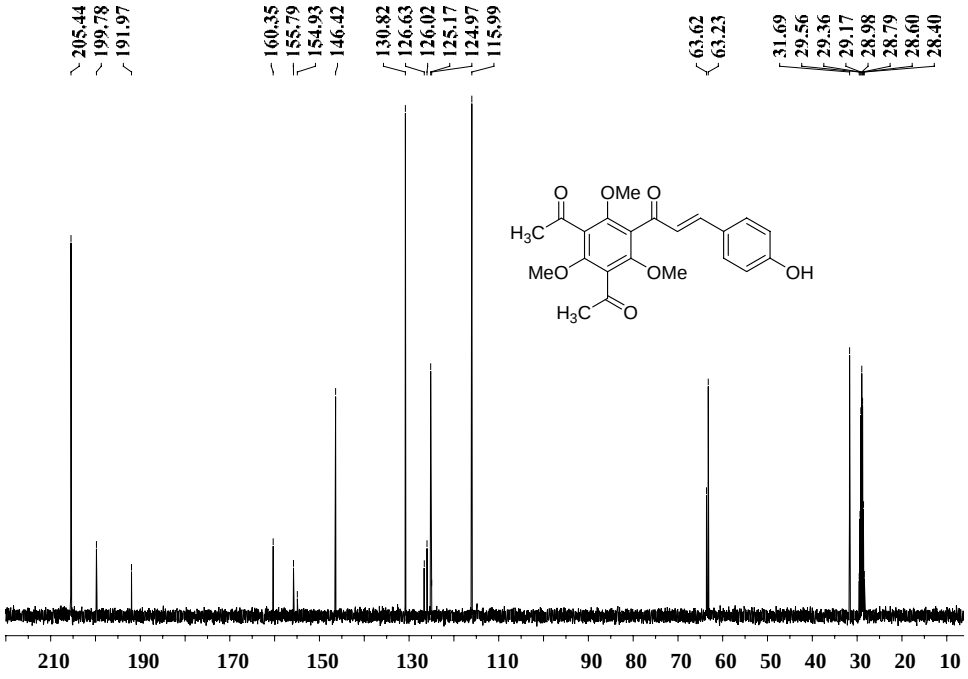

Figure A.27 ^{13}C-NMR (Acetone-d_6) spectrum of 1-(4-hydroxycinnamoyl)-3,5-diacetyl-2,4,6-trimethoxybenzene (**342**)

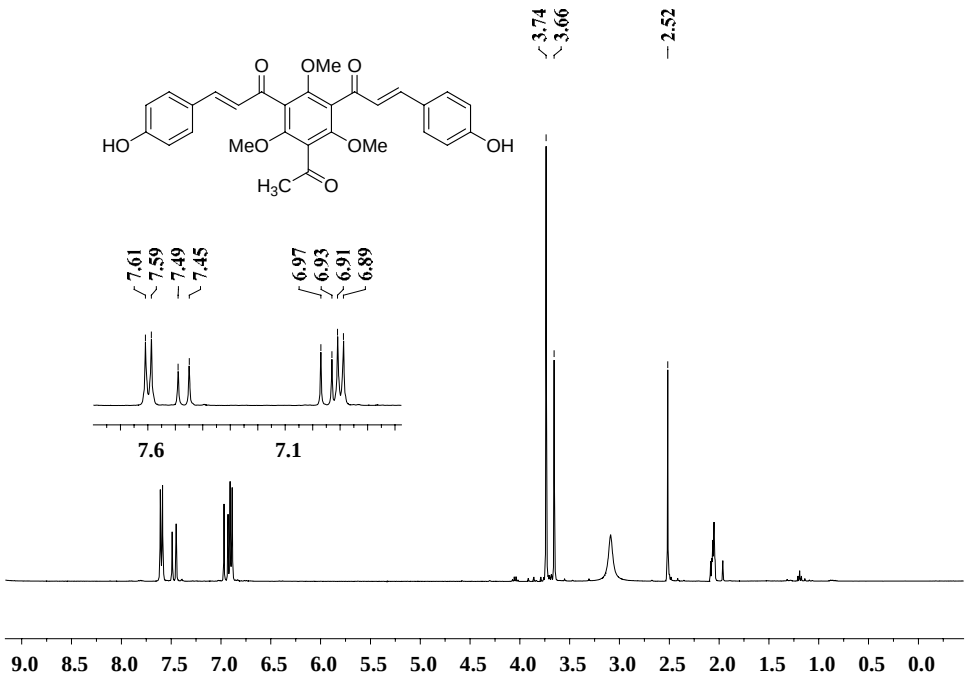

Figure A.28 ^{1}H-NMR (Acetone-d_6) spectrum of 1,3-bis(4-hydroxycinnamoyl)-5-acetyl-2,4,6-trimethoxybenzene (**343**)

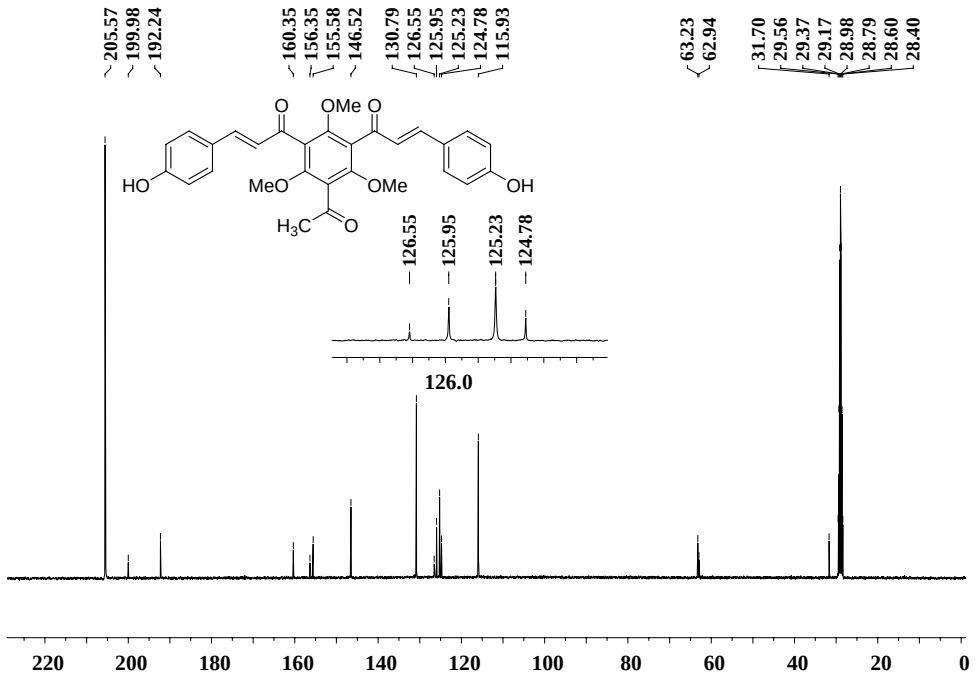

Figure A.29 ^{13}C-NMR (Acetone-d_6) spectrum of 1,3-bis(4-hydroxycinnamoyl)-5-acetyl-2,4,6-trimethoxybenzene (**343**)

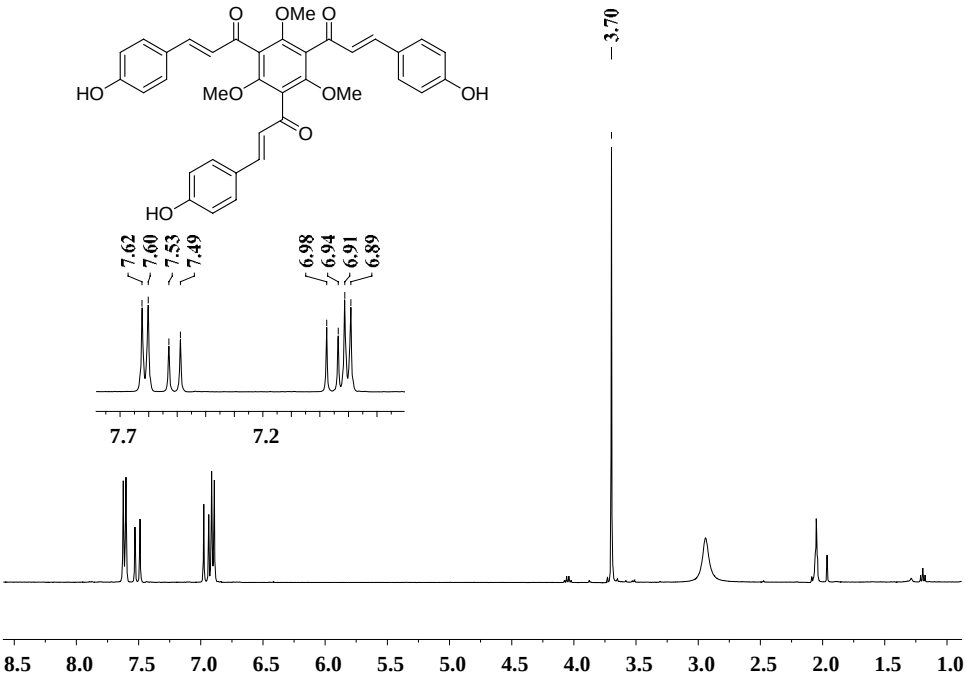

Figure A.30 ^{1}H-NMR (Acetone-d_6) spectrum of 1,3,5-tris(4-hydroxycinnamoyl)-2,4,6-trimethoxybenzene (**344**)

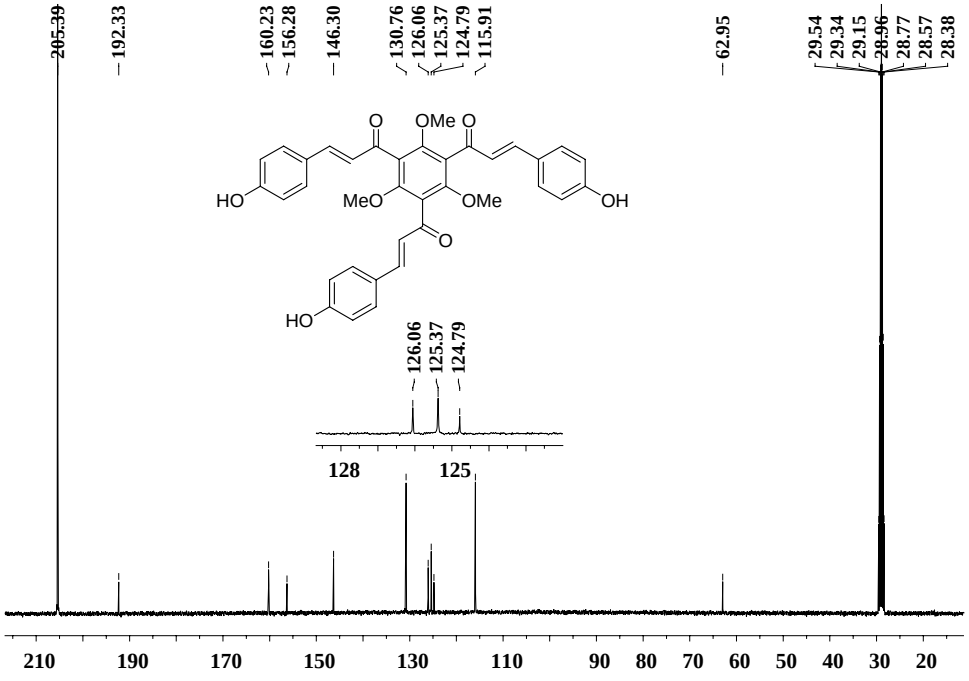

Figure A.31 ^{13}C-NMR (Acetone-d_6) spectrum of 1,3,5-tris(4-hydroxycinnamoyl)-2,4,6-trimethoxybenzene (**344**)

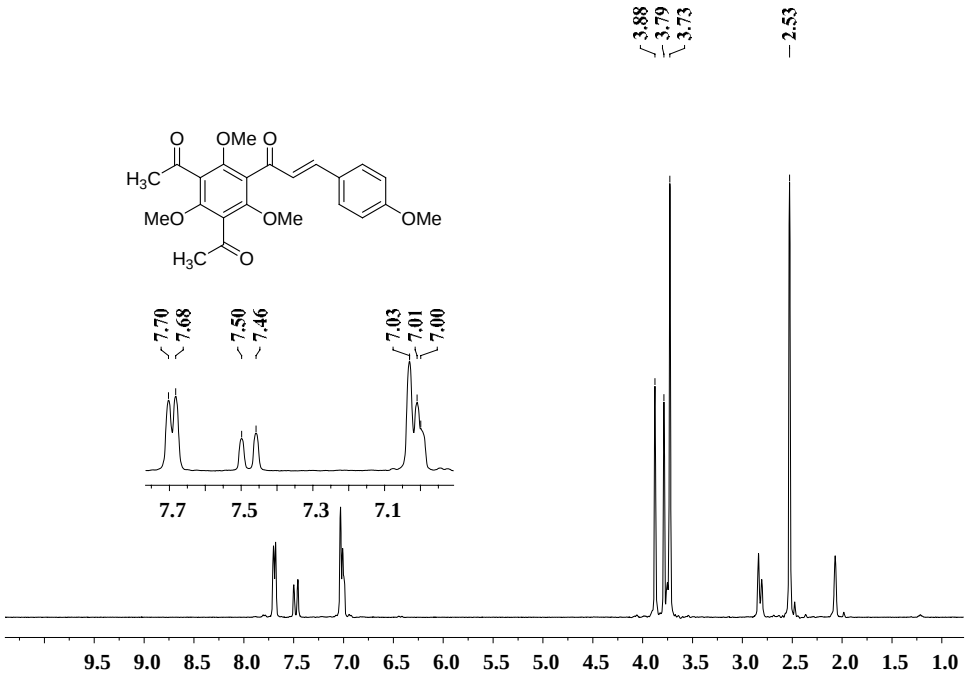

Figure A.32 ^{1}H-NMR (Acetone-d_6) spectrum of 1-(4-methoxycinnamoyl)-3,5-diacetyl-2,4,6-trimethoxybenzene (**345**)

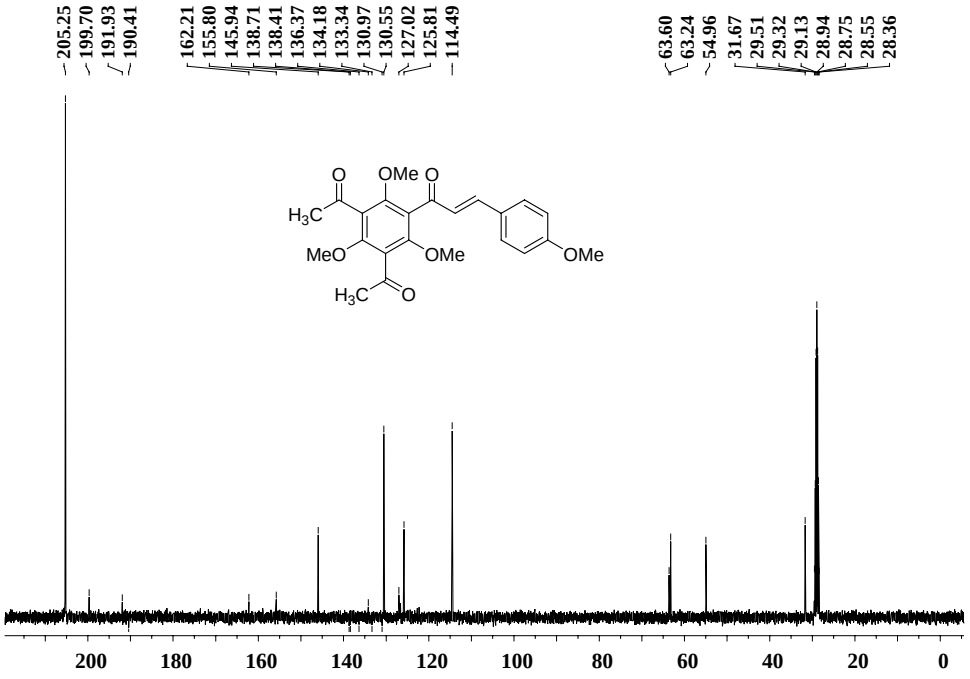

Figure A.33 ^{13}C-NMR (Acetone-d_6) spectrum of 1-(4-methoxycinnamoyl)-3,5-diacetyl-2,4,6-trimethoxybenzene (**345**)

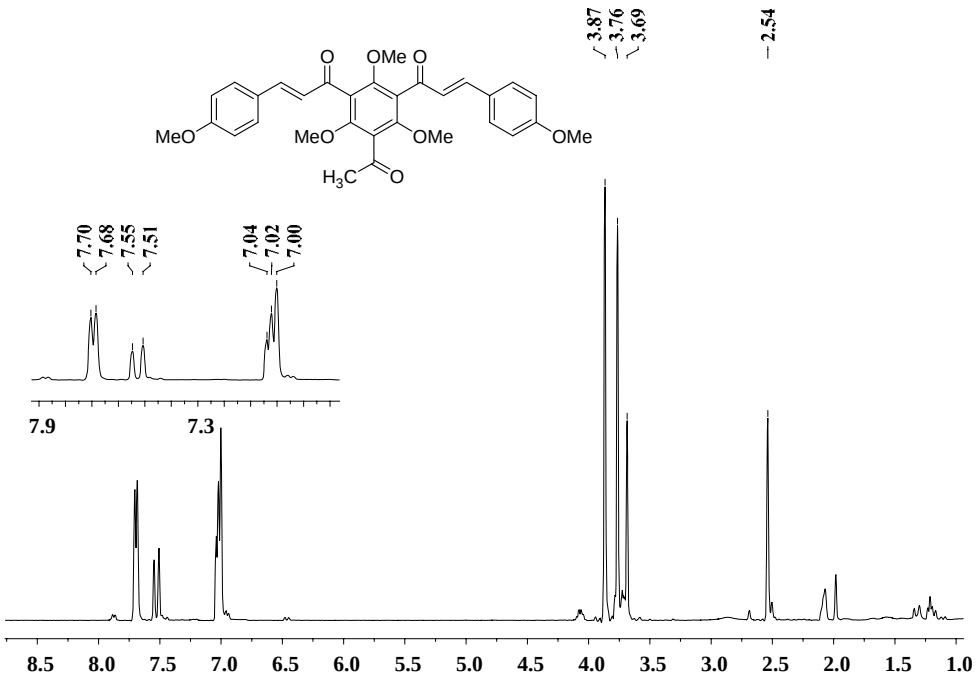

Figure A.34 ^{1}H-NMR (Acetone-d_6) spectrum of 1,3-bis(4-methoxycinnamoyl)-5-acetyl-2,4,6-trimethoxybenzene (**346**)

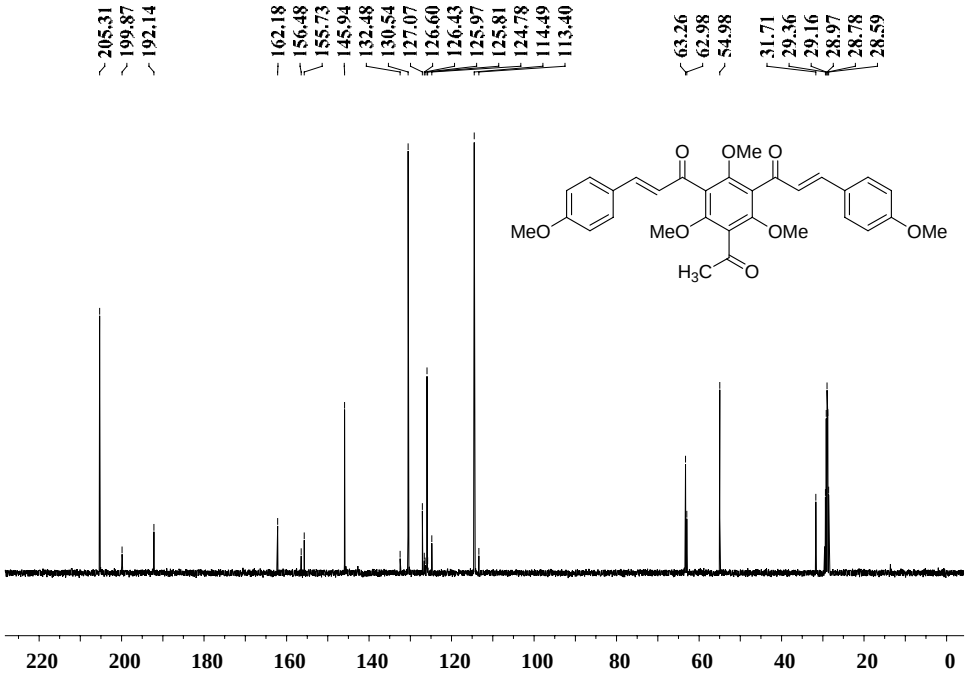

Figure A.35 ^{13}C-NMR (Acetone-d_6) spectrum of 1,3-bis(4-methoxycinnamoyl)-5-acetyl-2,4,6-trimethoxybenzene (**346**)

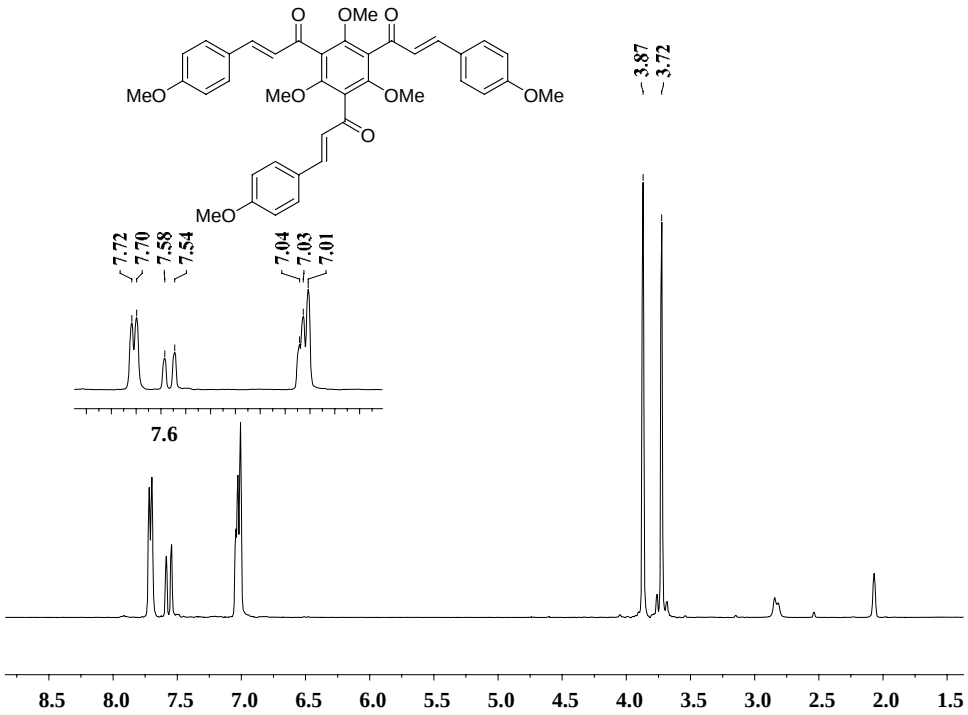

Figure A.36 ^{1}H-NMR (Acetone-d_6) spectrum of 1,3,5-tris(4-methoxycinnamoyl)-2,4,6-trimethoxybenzene (**347**)

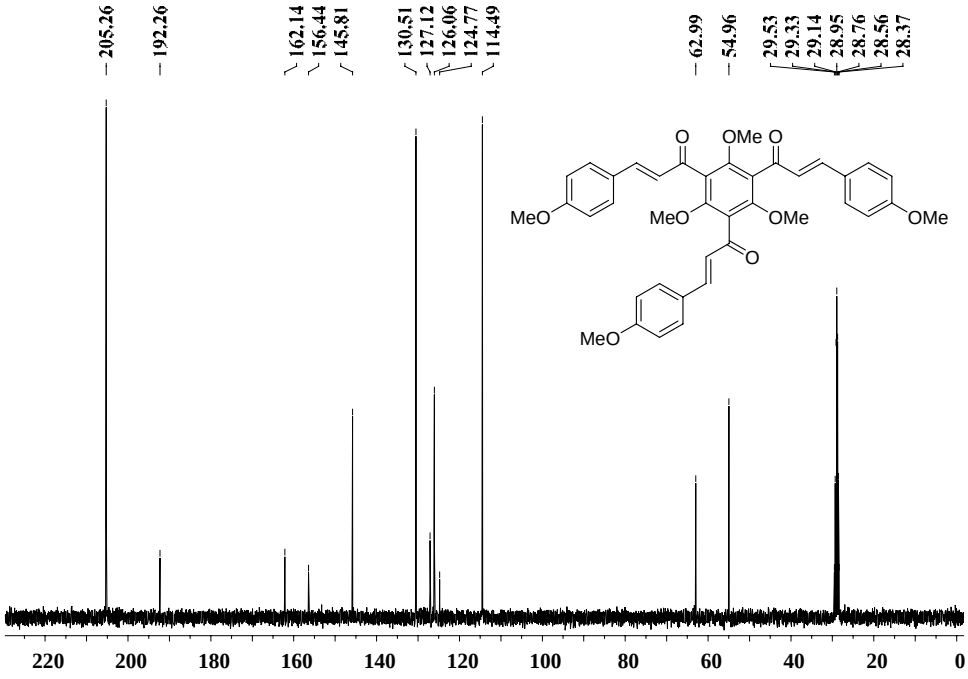

Figure A.37 ^{13}C-NMR (Acetone-d_6) spectrum of 1,3,5-tris(4-methoxycinnamoyl)-2,4,6-trimethoxybenzene (**347**)

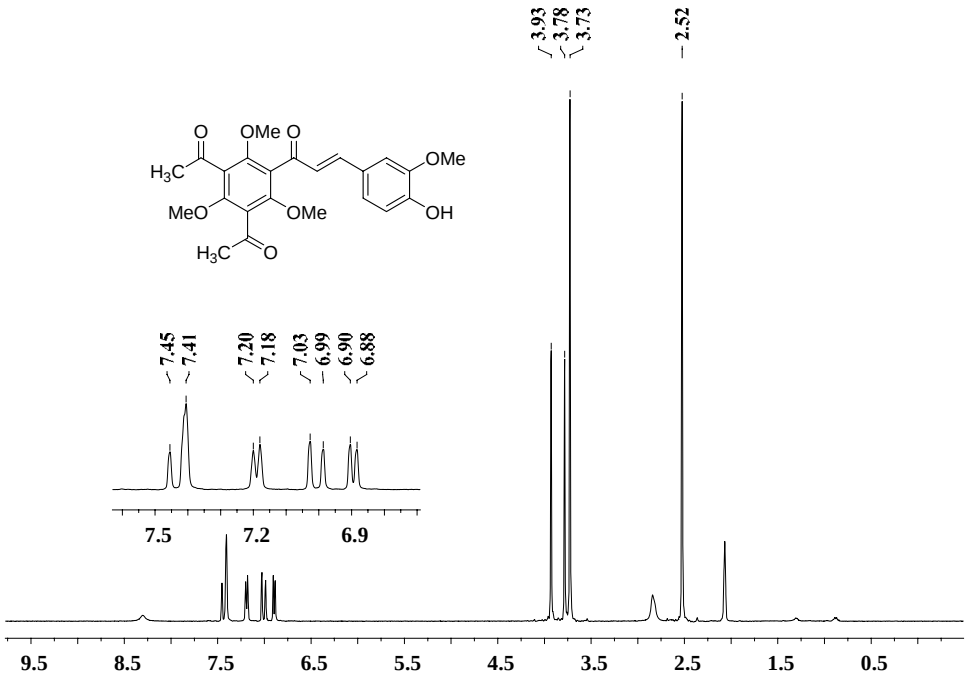

Figure A.38 ^{1}H-NMR (Acetone-d_6) spectrum of 1-(4-hydroxy-3-methoxycinnamoyl)-3,5-diacetyl-2,4,6-trimethoxybenzene (**348**)

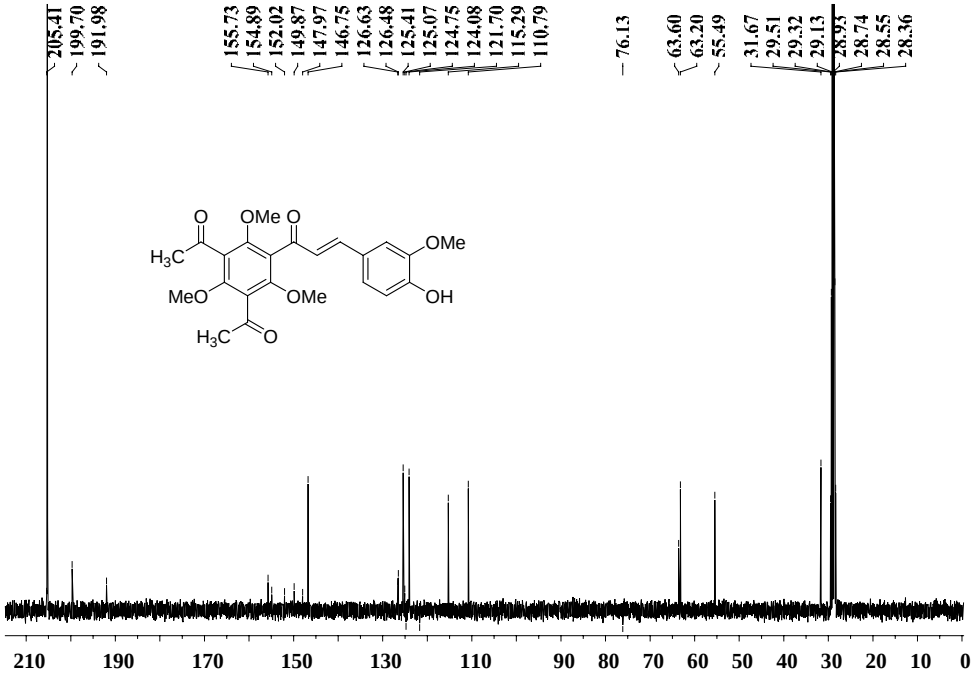

Figure A.39 ^{13}C-NMR (Acetone-d_6) spectrum of 1-(4-hydroxy-3-methoxycinnamoyl)-3,5-diacetyl-2,4,6-trimethoxybenzene (**348**)

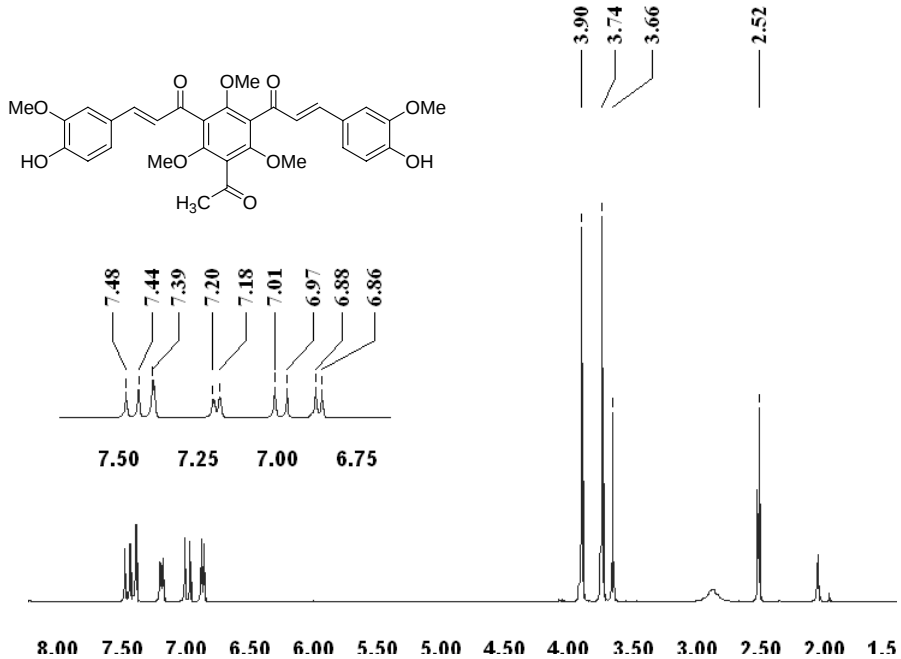

Figure A.40 ^{1}H-NMR (Acetone-d_6) spectrum of 1,3-bis(4-hydroxy-3-methoxycinnamoyl)-5-acetyl-2,4,6-trimethoxybenzene (**349**)

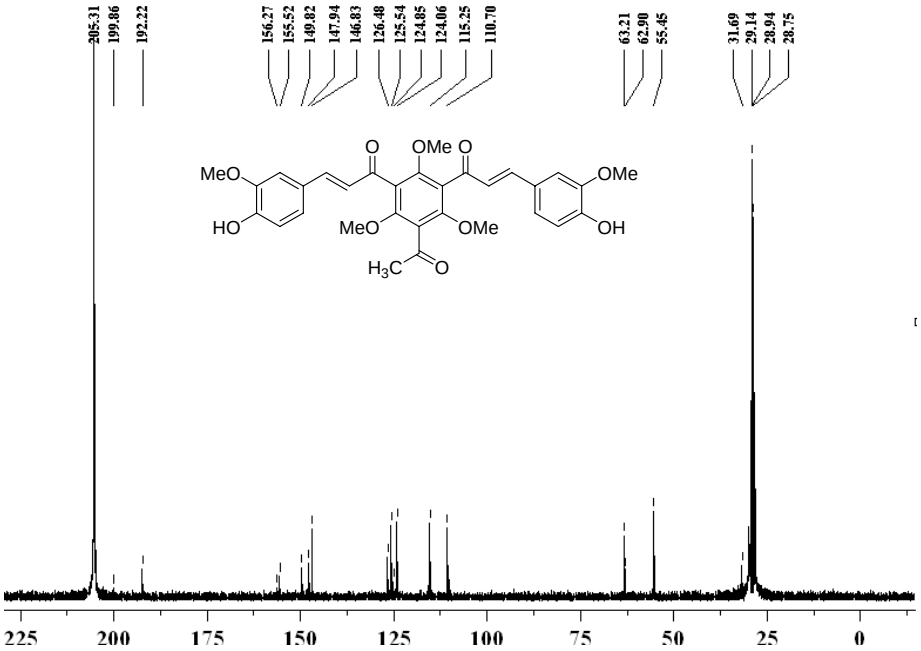

Figure A.41 ^{13}C-NMR (Acetone-d_6) spectrum of 1,3-bis(4-hydroxy-3-methoxycinnamoyl)-5-acetyl-2,4,6-trimethoxybenzene (**349**)

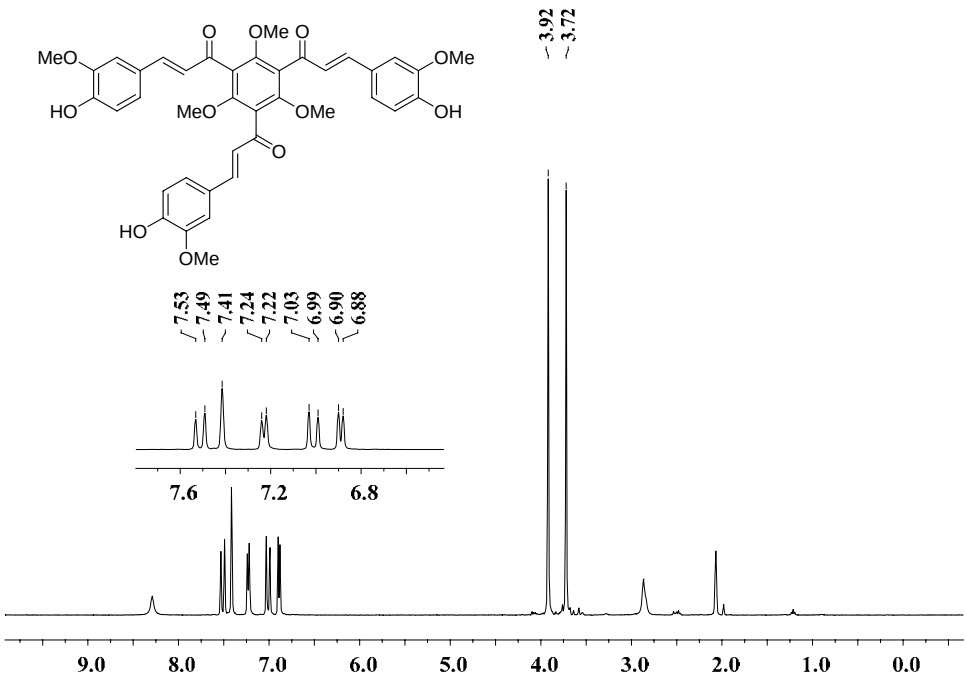

Figure A.42 ^{1}H-NMR (Acetone-d_6) spectrum of 1,3,5-tris(4-hydroxy-3-methoxycinnamoyl)-2,4,6-trimethoxybenzene (**350**)

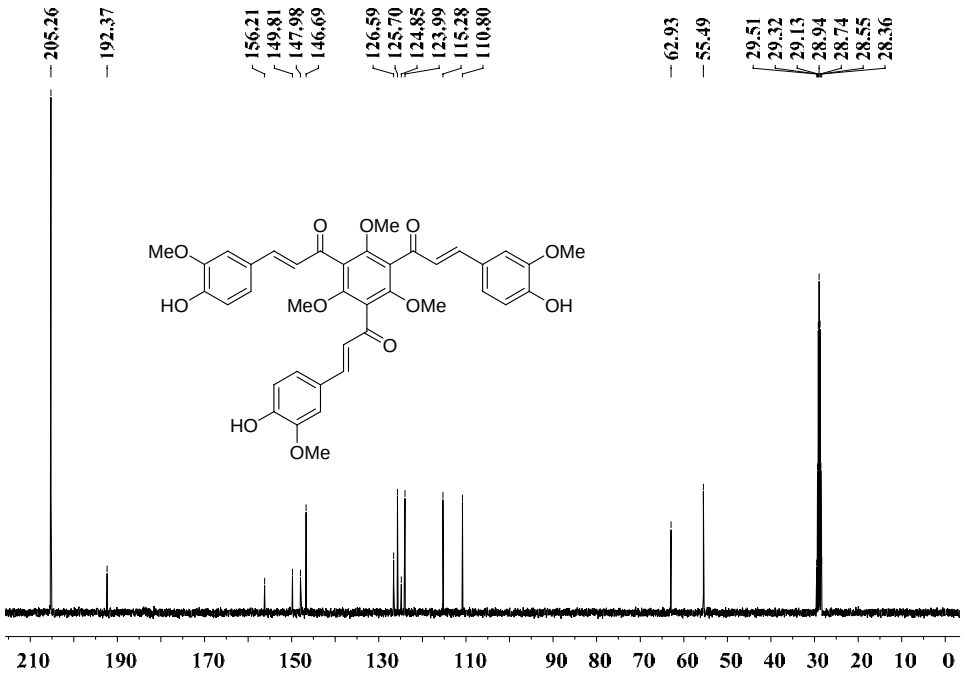

Figure A.43 ^{13}C-NMR (Acetone-d_6) spectrum of 1,3,5-tris(4-hydroxy-3-methoxycinnamoyl)-2,4,6-trimethoxybenzene (**350**)

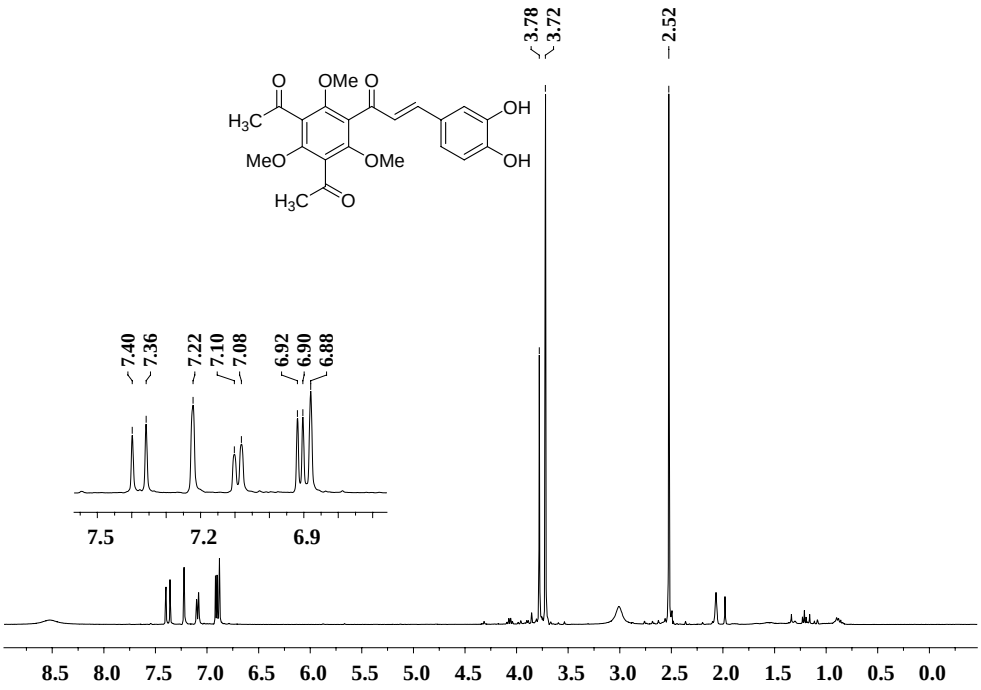

Figure A.44 ^{1}H-NMR (Acetone-d_6) spectrum of 1-(3,4-dihydroxycinnamoyl)-3,5-diacetyl-2,4,6-trimethoxybenzene (**351**)

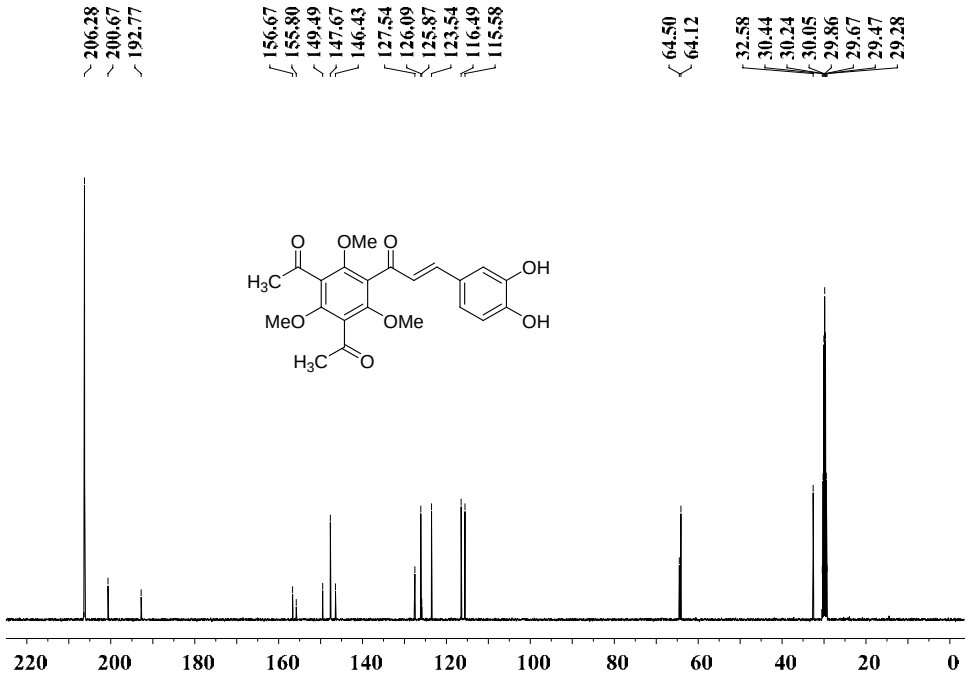

Figure A.45 ^{13}C-NMR (Acetone-d_6) spectrum of 1-(3,4-dihydroxycinnamoyl)-3,5-diacetyl-2,4,6-trimethoxybenzene (**351**)

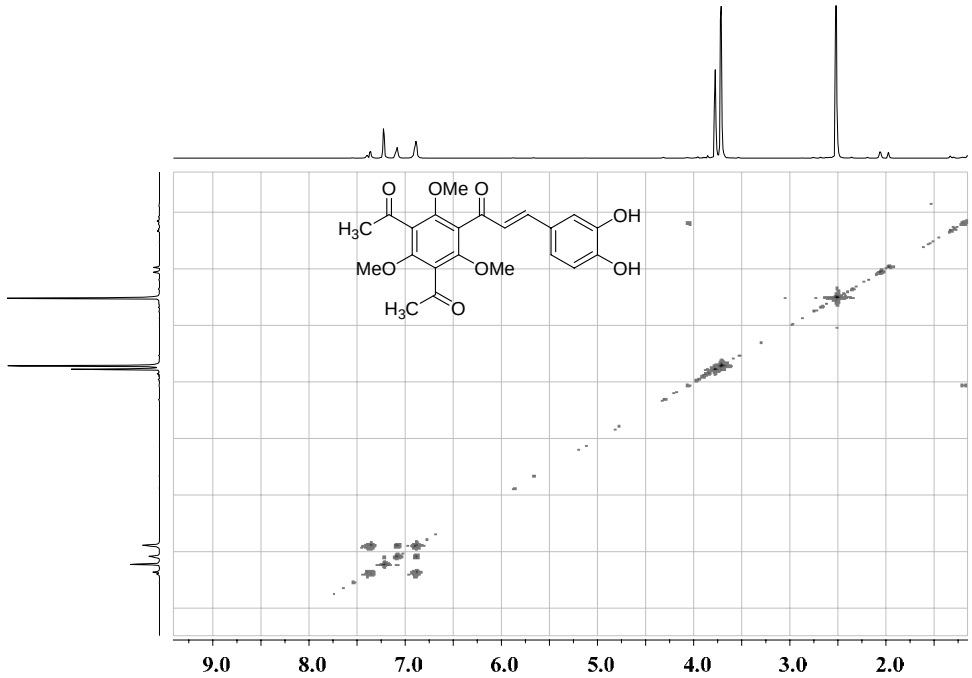

Figure A.46 COSY NMR (Acetone-d_6) spectrum of 1-(3,4-dihydroxycinnamoyl)-3,5-diacetyl-2,4,6-trimethoxybenzene (**351**)

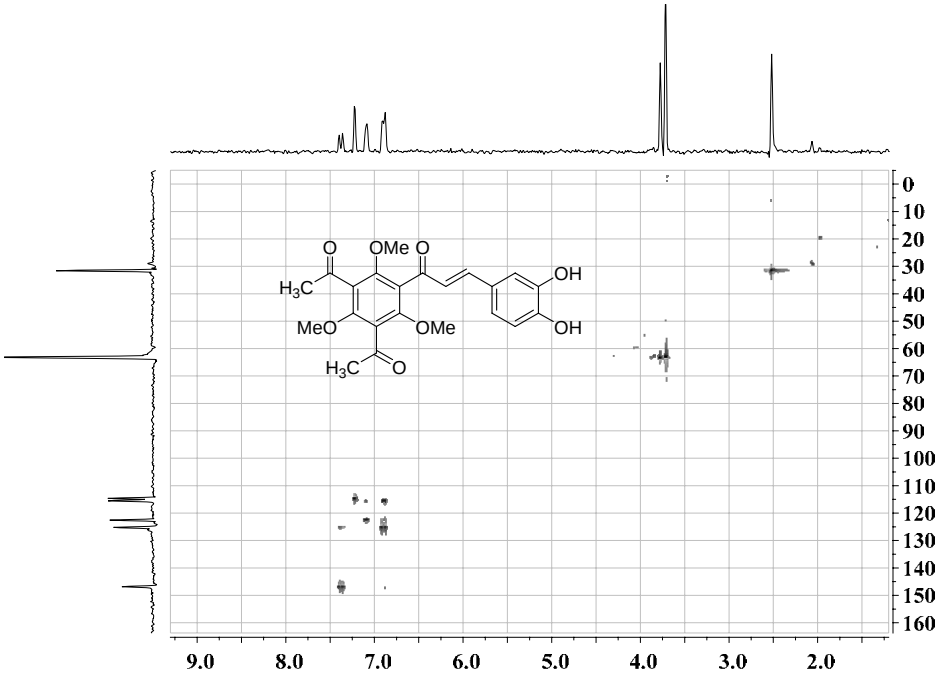

Figure A.47 HMQC NMR (Acetone-d_6) spectrum of 1-(3,4-dihydroxycinnamoyl)-3,5-diacetyl-2,4,6-trimethoxybenzene (**351**)

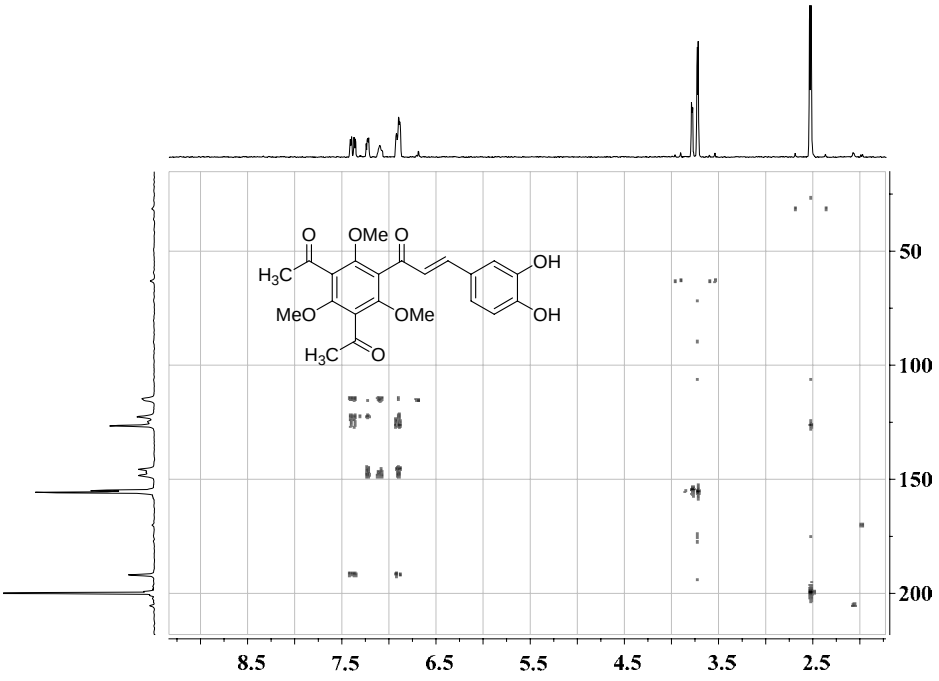

Figure A.48 HMBC NMR (Acetone-d_6) spectrum of 1-(3,4-dihydroxycinnamoyl)-3,5-diacetyl-2,4,6-trimethoxybenzene (**351**)

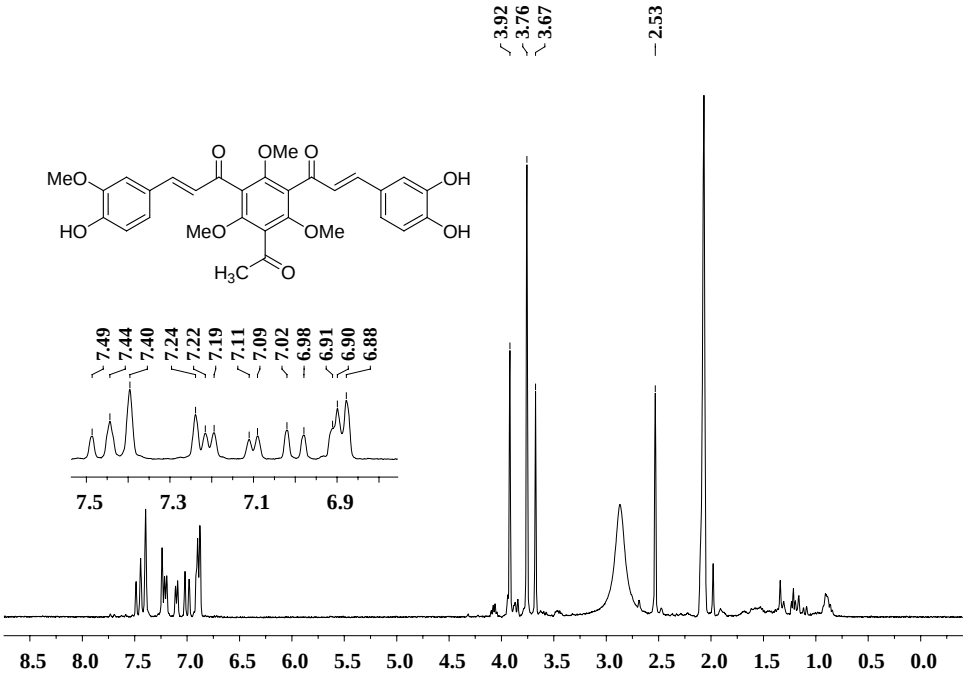

Figure A.49 ^{1}H-NMR (Acetone-d_6) spectrum of 1-(3,4-dihydroxycinnamoyl)-3-(4-hydroxy-3-methoxycinnamoyl)-5-acetyl-2,4,6-trimethoxybenzene (**352**)

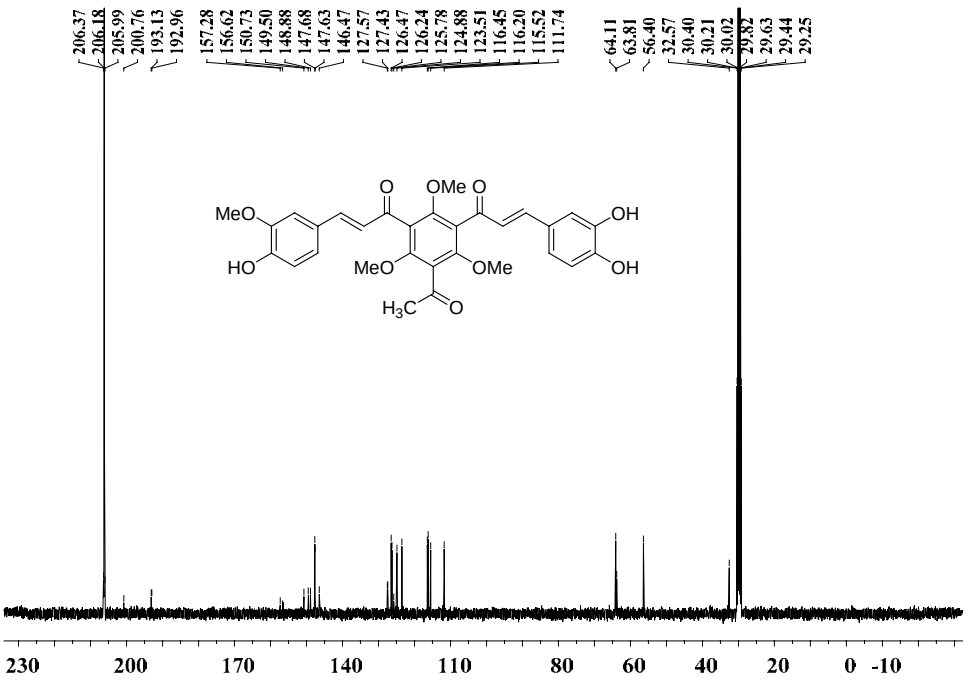

Figure A.50 ^{13}C-NMR (Acetone-d_6) spectrum of 1-(3,4-dihydroxycinnamoyl)-3-(4-hydroxy-3-methoxycinnamoyl)-5-acetyl-2,4,6-trimethoxybenzene (**352**)

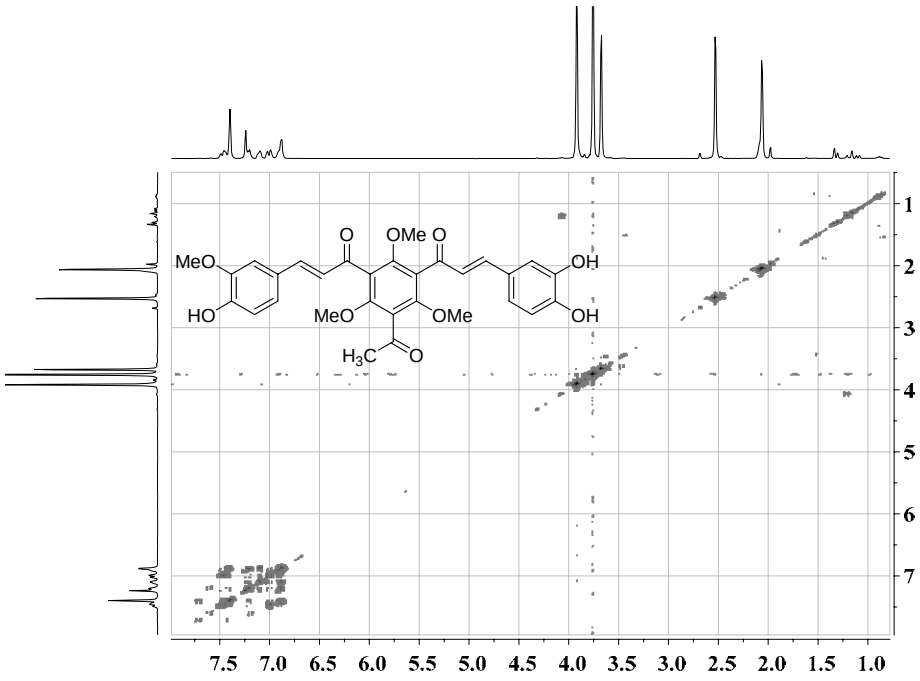

Figure A.51 COSY NMR (Acetone-d_6) spectrum of 1-(3,4-dihydroxycinnamoyl)-3-(4-hydroxy-3-methoxycinnamoyl)-5-acetyl-2,4,6-trimethoxybenzene (**352**)

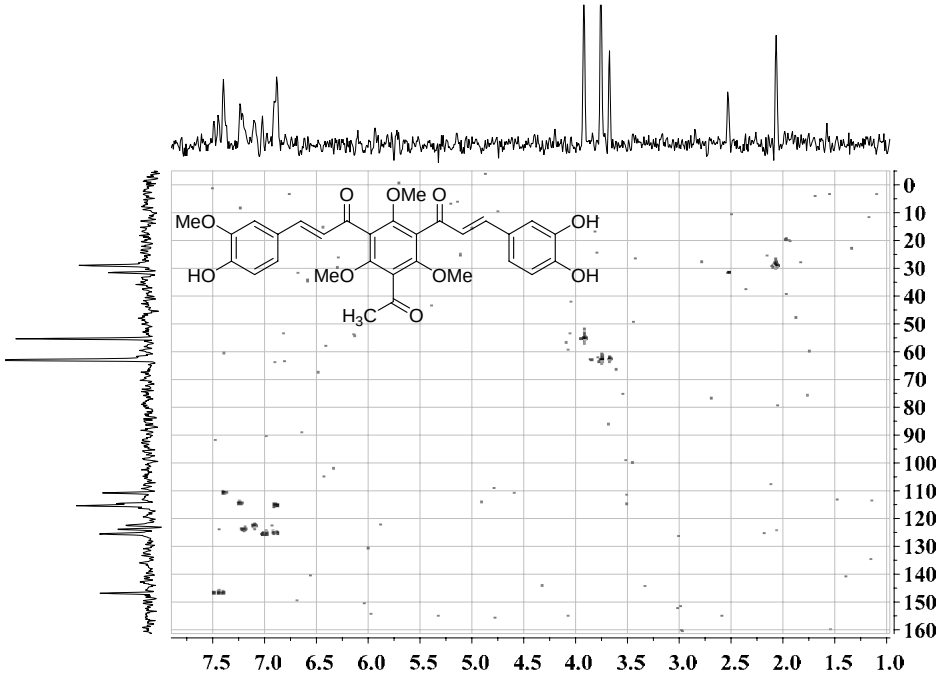

Figure A.52 HMQC NMR (Acetone-d_6) spectrum of 1-(3,4-dihydroxycinnamoyl)-3-(4-hydroxy-3-methoxycinnamoyl)-5-acetyl-2,4,6-trimethoxybenzene (**352**)

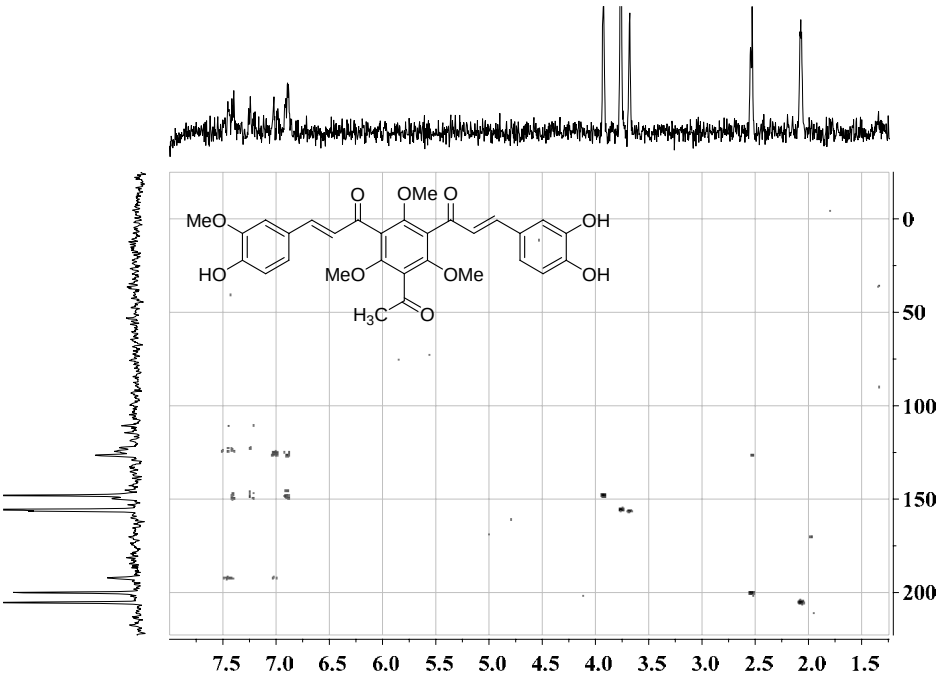

Figure A.53 HMBC NMR (Acetone-d_6) spectrum of 1-(3,4-dihydroxycinnamoyl)-3-(4-hydroxy-3-methoxycinnamoyl)-5-acetyl-2,4,6-trimethoxybenzene (**352**)

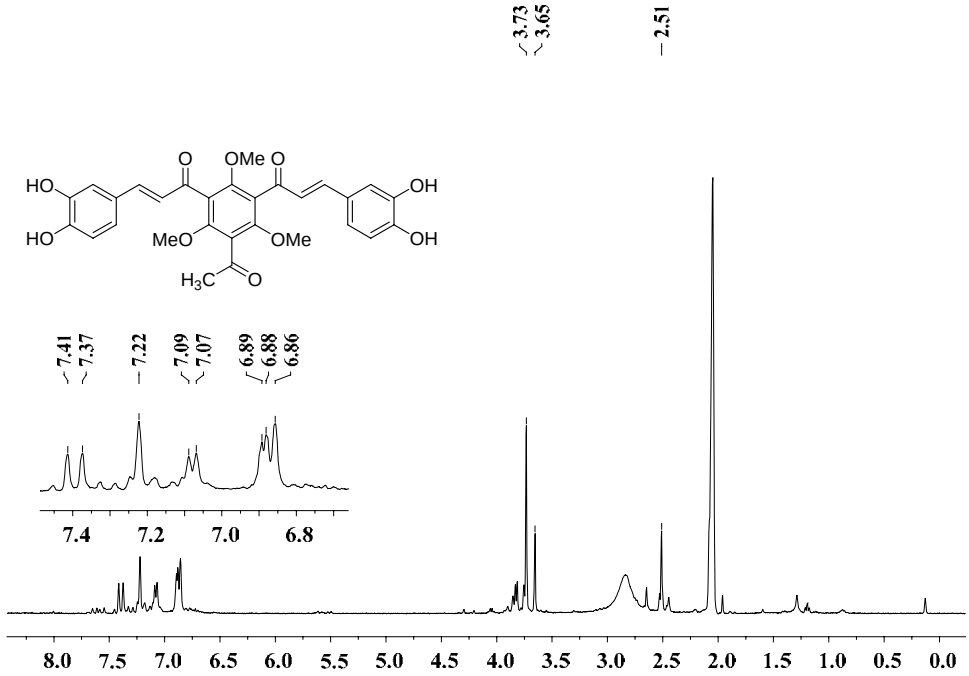

Figure A.54 ^{1}H-NMR (Acetone-d_6) spectrum of 1,3-bis(3,4-dihydroxycinnamoyl)-5-acetyl-2,4,6-trimethoxybenzene (**353**)

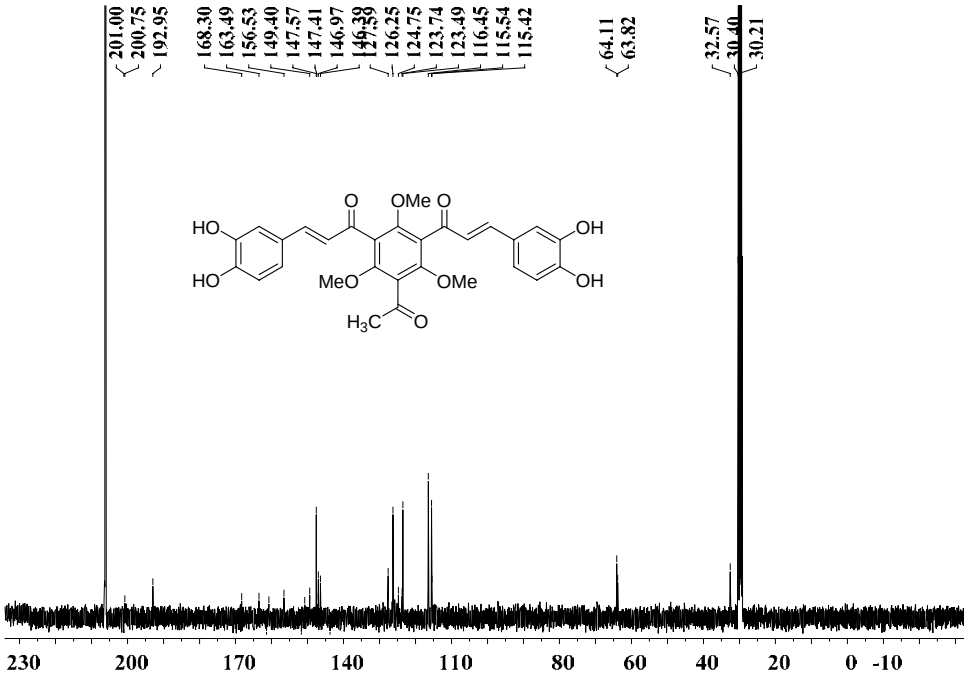

Figure A.55 ^{13}C-NMR (Acetone-d_6) spectrum of 1,3-bis(3,4-dihydroxycinnamoyl)-5-acetyl-2,4,6-trimethoxybenzene (**353**)

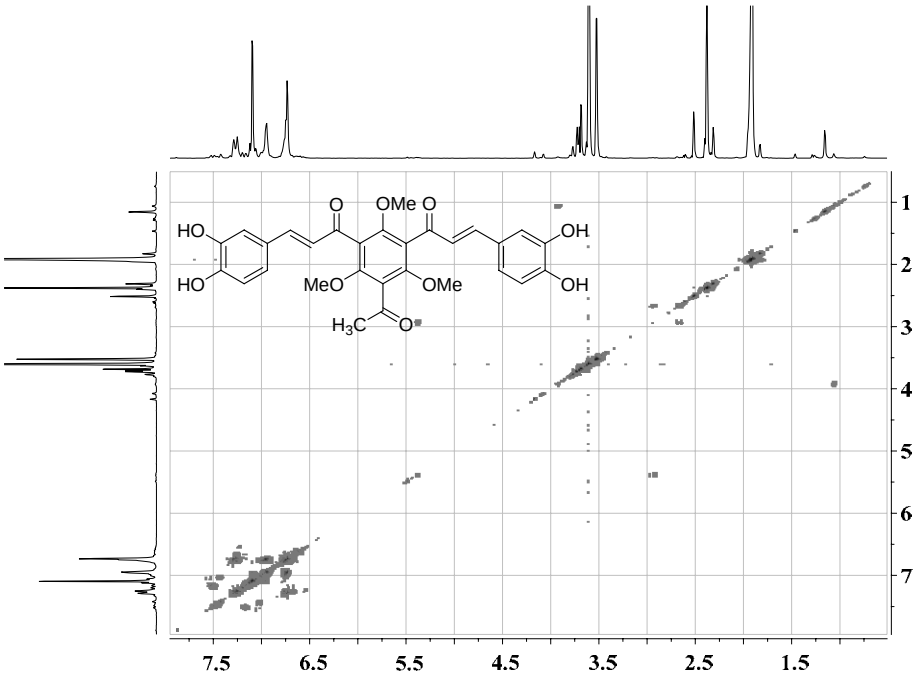

Figure A.56 COSY NMR (Acetone-d_6) spectrum of 1,3-bis(3,4-dihydroxycinnamoyl)-5-acetyl-2,4,6-trimethoxybenzene (**353**)

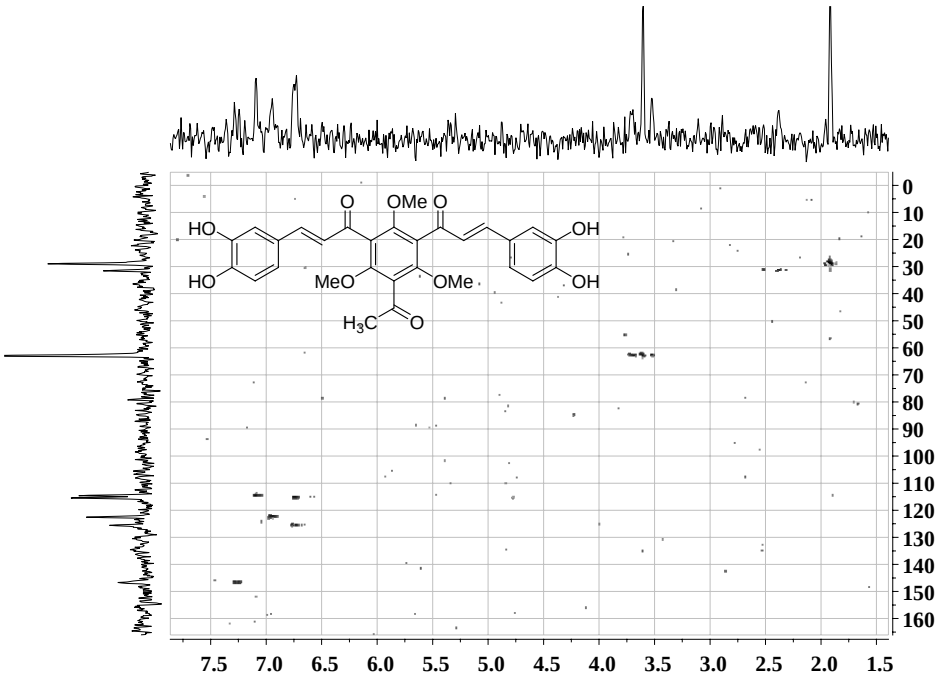

Figure A.57 HMQC NMR (Acetone-d_6) spectrum of 1,3-bis(3,4-dihydroxycinnamoyl)-5-acetyl-2,4,6-trimethoxybenzene (**353**)

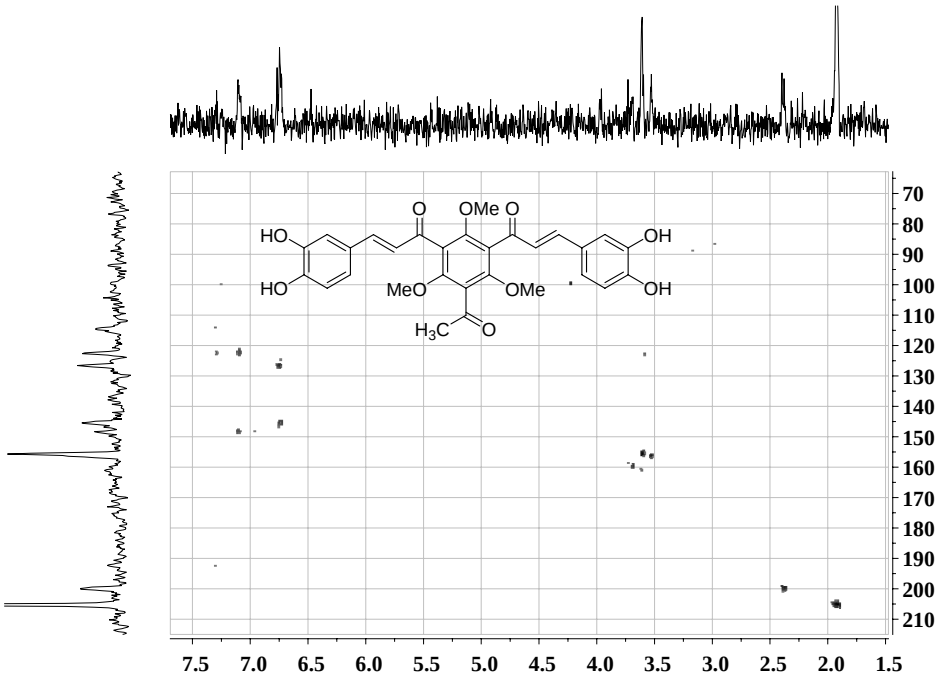

Figure A.58 HMBC NMR (Acetone-d_6) spectrum of 1,3-bis(3,4-dihydroxycinnamoyl)-5-acetyl-2,4,6-trimethoxybenzene (**353**)

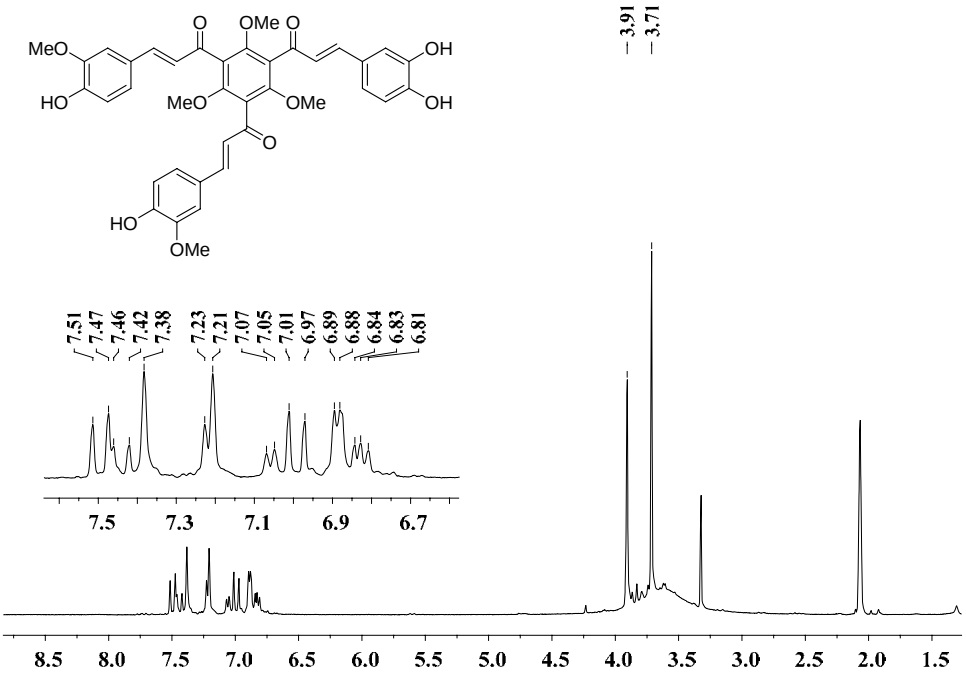

Figure A.59 ^{1}H-NMR (Acetone-d_6) spectrum of 1-(3,4-dihydroxycinnamoyl)-3,5-bis(4-hydroxy-3-methoxycinnamoyl)-2,4,6-trimethoxybenzene (**354**)

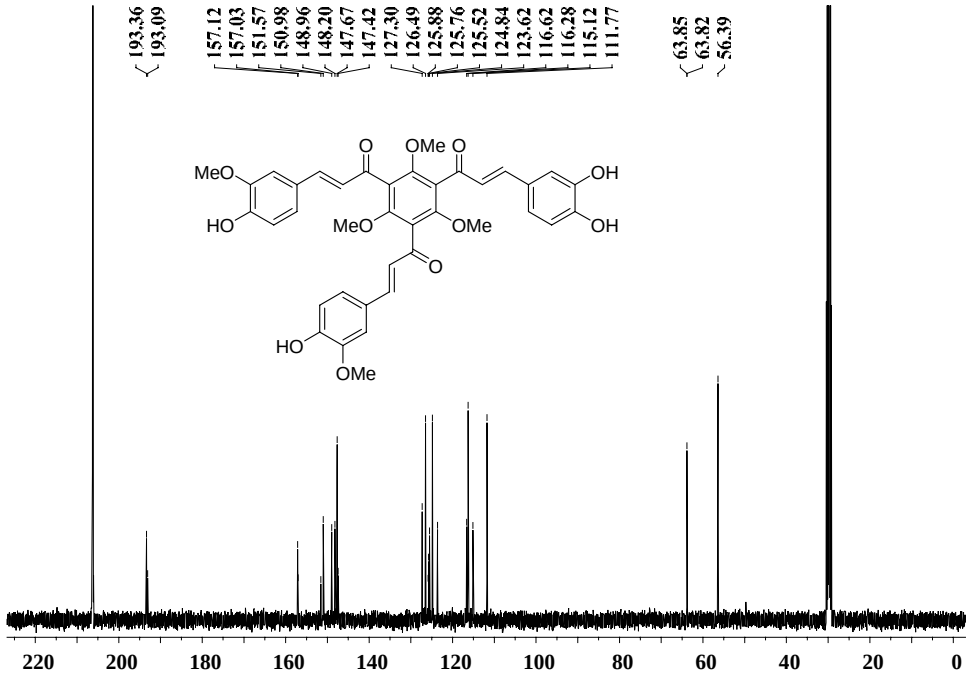

Figure A.60 ^{13}C-NMR (Acetone-d_6) spectrum of 1-(3,4-dihydroxycinnamoyl)-3,5-bis(4-hydroxy-3-methoxycinnamoyl)-2,4,6-trimethoxybenzene (**354**)

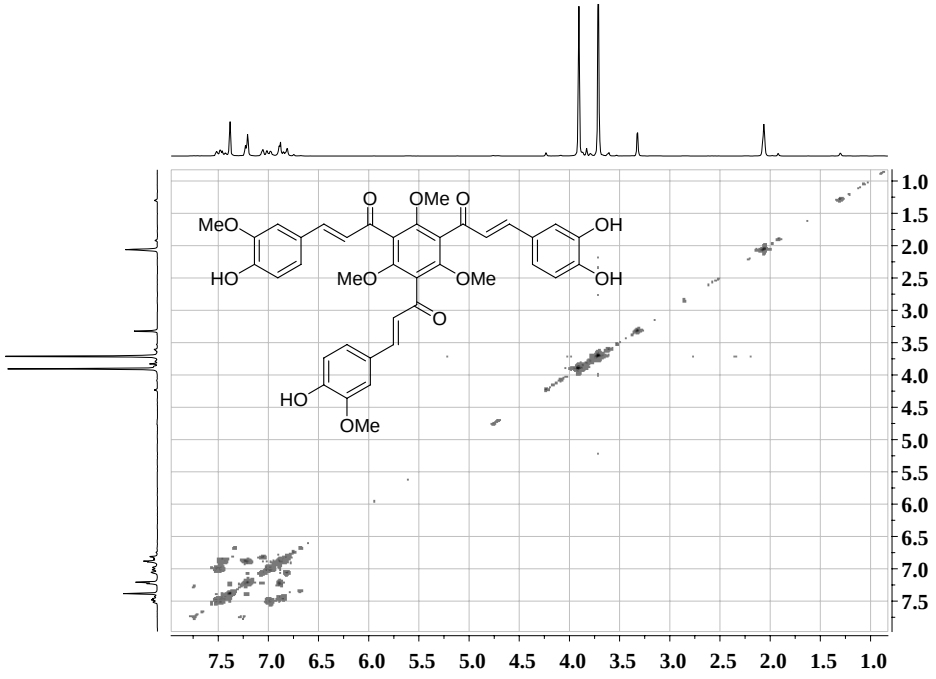

Figure A.61 COSY NMR (Acetone-d_6) spectrum of 1-(3,4-dihydroxycinnamoyl)-3,5-bis(4-hydroxy-3-methoxycinnamoyl)-2,4,6-trimethoxybenzene (**354**)

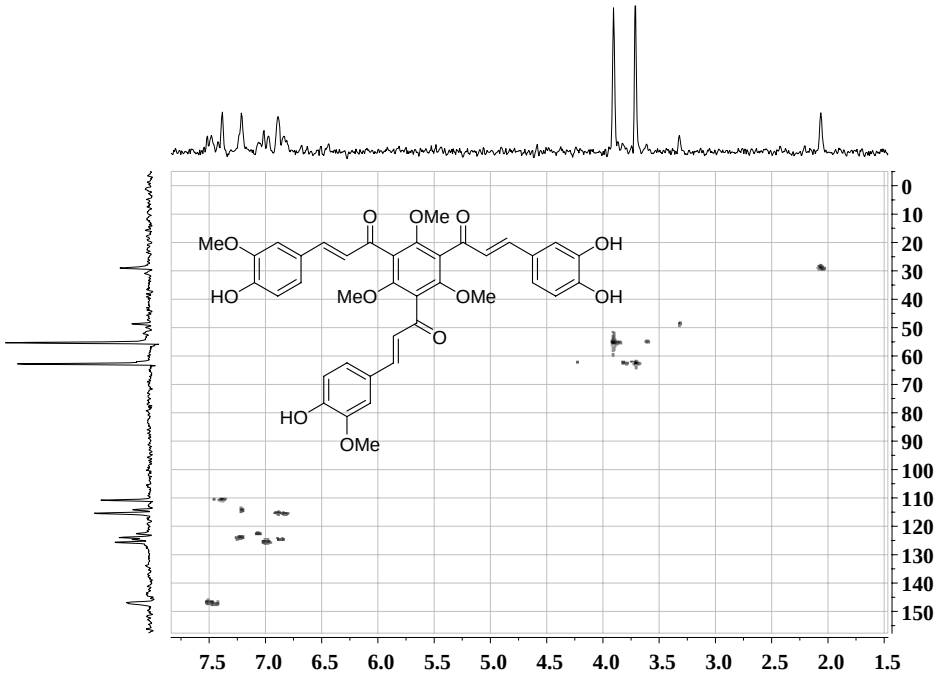

Figure A.62 HMQC NMR (Acetone-d_6) spectrum of 1-(3,4-dihydroxycinnamoyl)-3,5-bis(4-hydroxy-3-methoxycinnamoyl)-2,4,6-trimethoxybenzene (**354**)

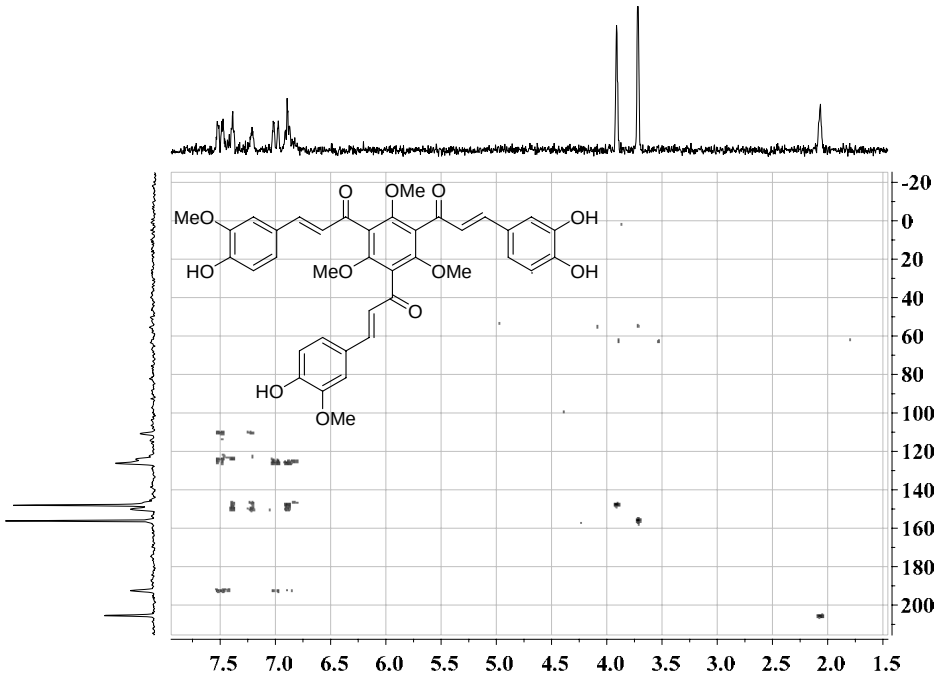

Figure A.63 HMBC NMR (Acetone-d_6) spectrum of 1-(3,4-dihydroxycinnamoyl)-3,5-bis(4-hydroxy-3-methoxycinnamoyl)-2,4,6-trimethoxybenzene (**354**)

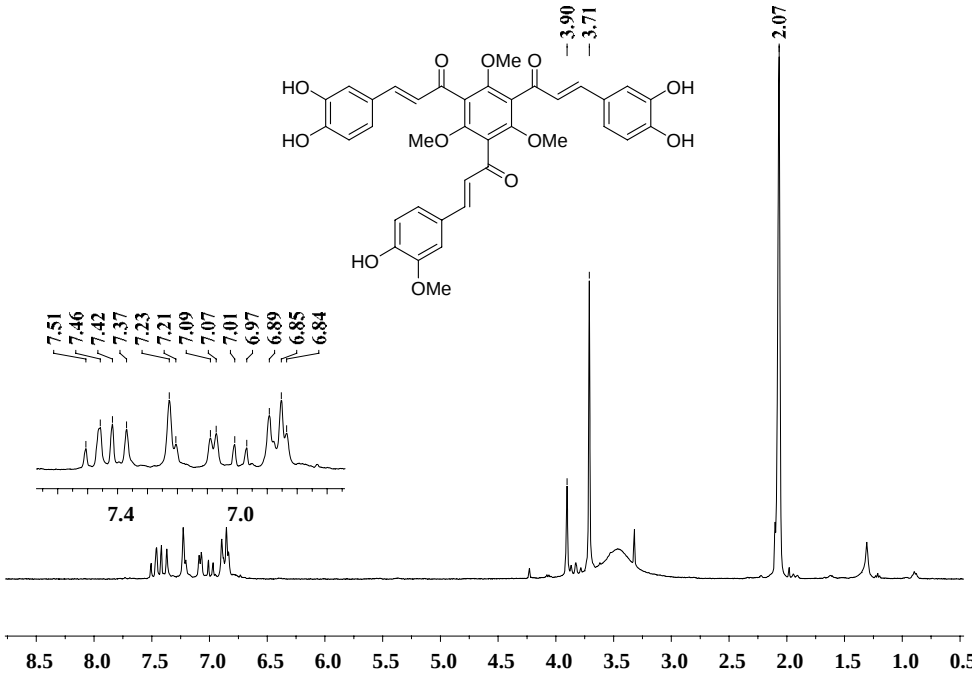

Figure A.64 ^{1}H-NMR (Acetone-d_6) spectrum of 1,3-bis(3,4-dihydroxycinnamoyl)-5-(4-hydroxy-3-methoxycinnamoyl)-2,4,6-trimethoxybenzene (**355**)

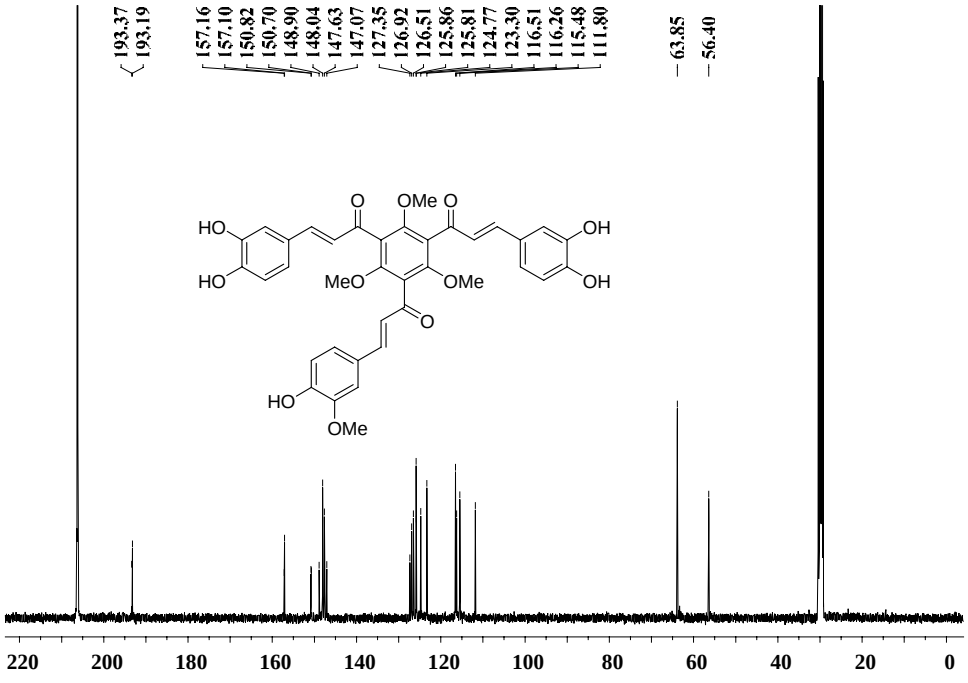

Figure A.65 ^{13}C-NMR (Acetone-d_6) spectrum of 1,3-bis(3,4-dihydroxycinnamoyl)-5-(4-hydroxy-3-methoxycinnamoyl)-2,4,6-trimethoxybenzene (**355**)

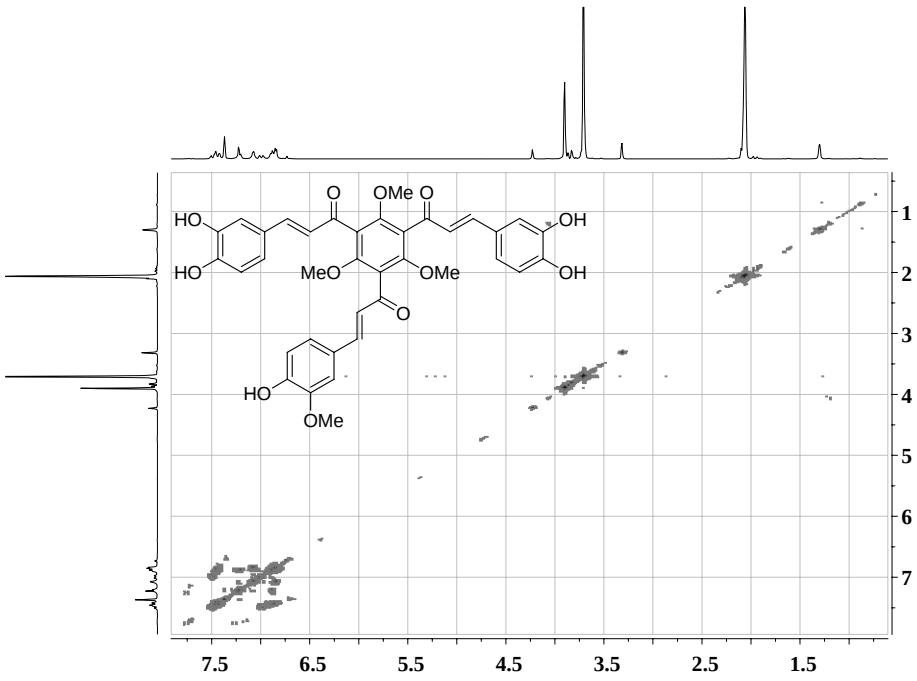

Figure A.66 COSY NMR (Acetone-d_6) spectrum of 1,3-bis(3,4-dihydroxycinnamoyl) -5-(4-hydroxy-3-methoxycinnamoyl)-2,4,6-trimethoxybenzene (**355**)

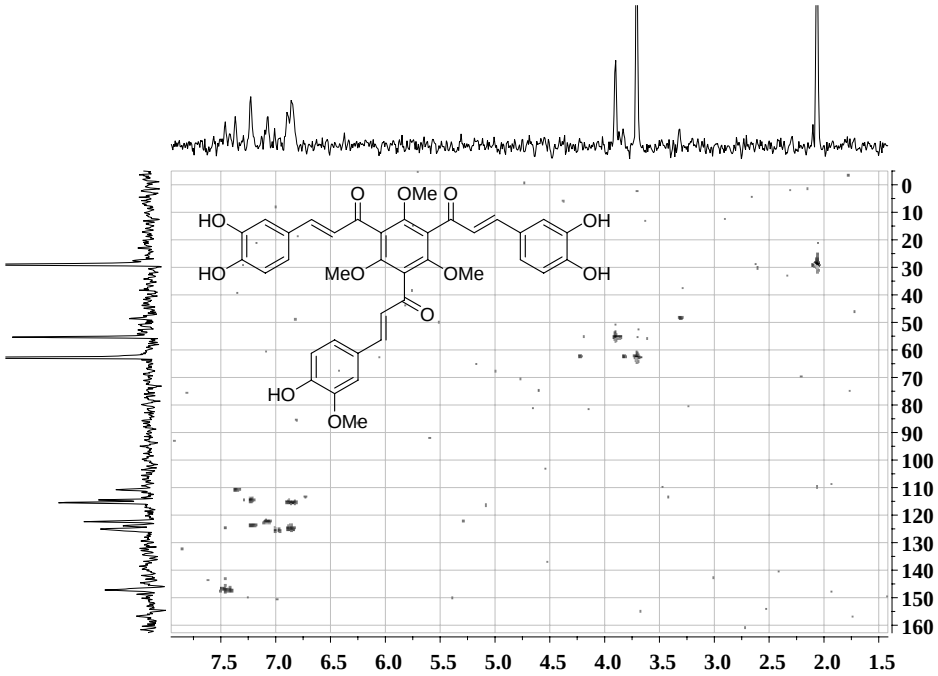

Figure A.67 HMQC NMR (Acetone-d_6) spectrum of 1,3-bis(3,4-dihydroxycinnamoyl)-5-(4-hydroxy-3-methoxycinnamoyl)-2,4,6-trimethoxybenzene (**355**)

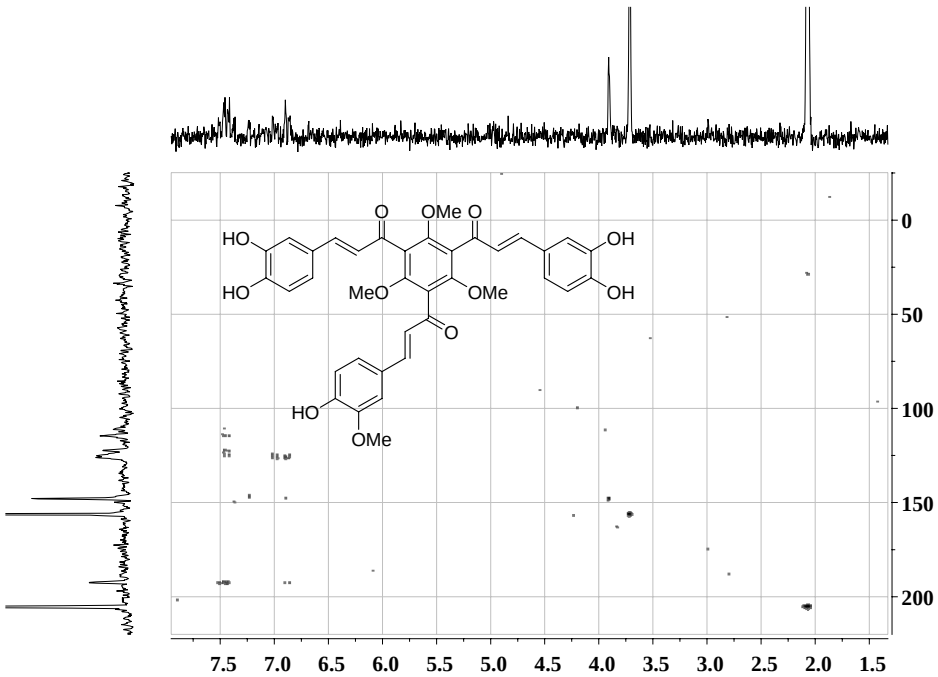

Figure A.68 HMBC NMR (Acetone-d_6) spectrum of 1,3-bis(3,4-dihydroxycinnamoyl)-5-(4-hydroxy-3-methoxycinnamoyl)-2,4,6-trimethoxybenzene (**355**)

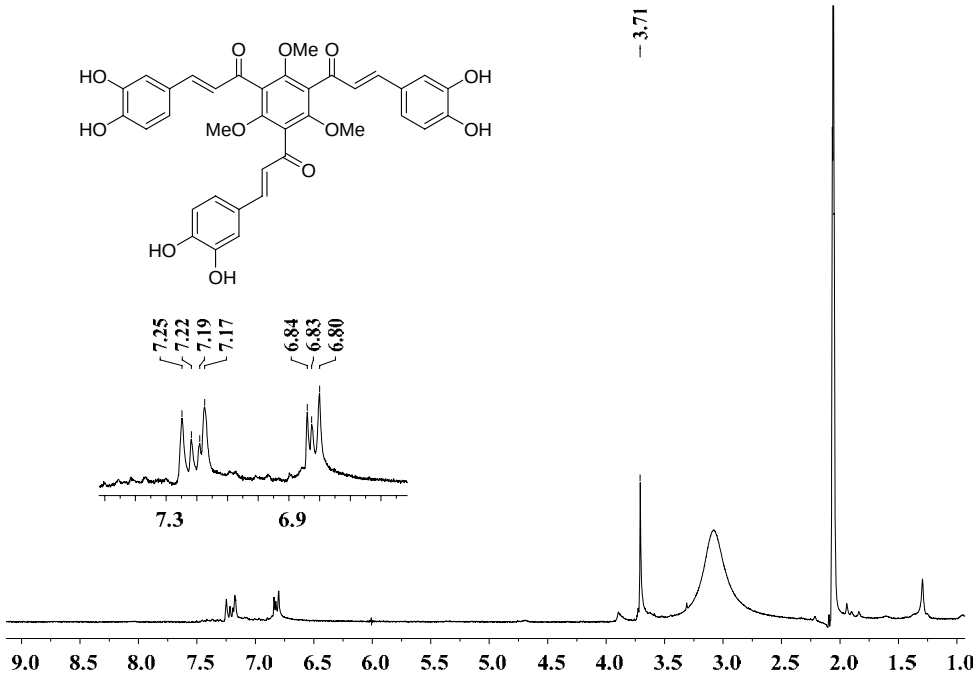

Figure A.69 ^{1}H-NMR (Acetone-d_6) spectrum of 1,3,5-tris(3,4-dihydroxycinnamoyl)-2,4,6-trimethoxybenzene (**356**)

VITAE

Name: Miss Wipa Tupchiangmai

Date of Birth: May 17th, 1970

Address: 200/43 Moo 1, Tambon Bang Phriang, Aumper Bang Bo, Samut Prakan 10560

Email: w_chingmai@hotmail.com

Education:

YEAR	INSTITUTION	DEGREE
1988	Bangbo Vittayakom	High School
1993	Ramkhamhaeng Univ.	B.Sc. (Chemistry)
2000	Ramkhamhaeng Univ.	M.Sc. (Applied chemistry)
2011	Chulalongkorn Univ.	Ph.D. (Chemistry)